STRUCTURAL AND OBSERVATIONAL ASPECTS OF ASYMPTOTICALLY SAFE QUANTUM GRAVITY

CHRIS RIPKEN

Structural and observational aspects of asymptotically safe Quantum Gravity

This thesis has been financially supported by the Netherlands organization for Scientific Research (NWO) within the Foundation for Fundamental Research on Matter (FOM) grant 13VP12.

ISBN 978-94-028-1986-1

Structural and observational aspects of asymptotically safe Quantum Gravity

Due to the corona pandemic the public defense of this thesis had to be postponed from May 11, 2020 to September 18, 2020. Printed theses bearing the date of May 11 had already been brought into circulation prior to this postponement.

Printed by Ipskamp, Enschede
Cover design by Studio 0404, Nijmegen

Structural and observational aspects of asymptotically safe Quantum Gravity

Proefschrift ter verkrijging van de graad van doctor
aan de Radboud Universiteit Nijmegen
op gezag van de rector magnificus prof. dr. J.H.J.M. van Krieken,
volgens besluit van het college van decanen
in het openbaar te verdedigen op

vrijdag 18 september 2020

om 11.30 uur precies

door

Anton Christiaan Ripken

geboren op 31 maart 1993

te Drunen

Promotor: prof. dr. R. Loll
Copromotor: dr. F.S. Saueressig

Manuscriptcommissie:
prof. dr. R.H.P Kleiss (voorzitter)
prof. dr. B. Dittrich (University of Waterloo, Canada)
prof. dr. T.R. Morris (University of Southampton, Verenigd Koninkrijk)
prof. dr. M. Reuter (Johannes Gutenberg-Universität Mainz, Duitsland)
prof. dr. N.P. Landsman

Structural and observational aspects of asymptotically safe Quantum Gravity

Doctoral thesis to obtain the degree of doctor
from Radboud University Nijmegen
on the authority of the Rector Magnificus prof. dr. J.H.J.M. van Krieken,
according to the decision of the Council of Deans
to be defended in public on

Friday, September 18, 2020,

at 11.30 hours

by

Anton Christiaan Ripken

born on March 31, 1993

in Drunen

Supervisor: prof. dr. R. Loll
Co-supervisor: dr. F.S. Saueressig

Manuscript committee:
prof. dr. R.H.P Kleiss (chairman)
prof. dr. B. Dittrich (University of Waterloo, Canada)
prof. dr. T.R. Morris (University of Southampton, United Kingdom)
prof. dr. M. Reuter (Johannes Gutenberg-Universität Mainz, Germany)
prof. dr. N.P. Landsman

SAMENVATTING

De hedendaagse theoretische natuurkunde is gestoeld op twee paradigma's. Enerzijds geeft Algemene Relativiteitstheorie een uitstekende beschrijving van zwaartekracht en het universum op grote lengteschalen. Anderzijds vormt kwantumveldentheorie (QFT) de basis voor ons begrip van de elementaire deeltjes op lengteschalen van ongeveer 10^{-20} m. Hoewel beide theorieën binnen hun eigen domein van toepassing experimenteel overtuigend zijn bevestigd, is een formulering van zwaartekracht als een kwantumtheorie (kwantumgravitatie) vooralsnog een onopgeloste uitdaging gebleken.

Eén van de problemen die daarbij overkomen dienen te worden is renormaliseerbaarheid. In een kwantumtheorie zijn de koppelingsconstanten afhankelijk van de energieschaal waarbij ze worden gemeten. Vanuit een Wilsoniaans standpunt is deze schaalafhankelijkheid het gevolg van het momentumschilsgewijs uitintegreren van kwantumfluctuaties. Dit geeft een stroomveld door de ruimte van koppelingsconstanten, die de renormalisatiegroepstroom (*RG flow*) wordt genoemd. Door een stroomlijn langs dit veld te volgen verkrijgen we de effectieve actie, waar alle kwantumfluctuaties zijn uitgeïntegreerd.

Wanneer we storingstheorie gebruiken in de kwantisatie van Algemene Relativiteitstheorie, vinden we dat de negatieve massadimensie van Newtons constante leidt tot onfysische oneindigheden van observabelen. Om deze divergenties te compenseren, dienen we oneindig veel nieuwe vrije parameters in te voeren. Hierdoor verliest de theorie zijn voorspellende waarde. Deze problemen kenmerken de (perturbatieve) niet-renormaliseerbaarheid van Algemene Relativiteitstheorie.

In het Asymptotische Veiligheidsscenario, geformuleerd door Weinberg, wordt renormaliseerbaarheid van zwaartekracht gerealiseerd door een interagerend vast punt (NGFP) van de renormalisatiegroep. Vanwege het interagerende karakter is dit punt lastig te bestuderen middels storingstheorie. Dankzij functionele methoden zijn er nu sterke aanwijzingen dat een dergelijk vast punt bestaat. Een dergelijk vast punt geeft een mogelijkheid voor een UV-completering van de theorie, alsmede een herstel van de voorspellende kracht.

Hoewel Asymptotische Veiligheid een veelbelovende kandidaat is voor een theorie van kwantumgravitatie, dient het nog verscheidene tests te doorstaan. Ten eerste levert een

goede theorie voorspellingen die experimenteel getest kunnen worden. In Asymptotische Veiligheid levert de voorwaarde dat een RG-stroomlijn voortkomt uit het NGFP in het UV een elegant mechanisme voor experimentele voorspellingen. Ten tweede moet de theorie een aantal structurele eigenschappen hebben. Eén daarvan is unitariteit, die essentieel is voor de waarschijnlijkheidsinterpretatie van kwantumtheorie. Het is een open probleem om te bepalen of unitariteit compatibel is met Asymptotische Veiligheid. Vanwege aanwezige interacties van het NGFP is dit een delicate kwestie.

In dit proefschrift zullen we beide vraagstukken nader bestuderen. We beginnen met een kort overzicht van Asymptotische Veiligheid en unitariteit. Vervolgens presenteren we de technieken die ten grondslag liggen aan de functionele renormalisatiegroepvergelijking (FRGE) die de Wilsoniaanse RG flow van zwaartekracht beschrijft.

Als een eerste test bestuderen we oplossingen van de FRGE in de context van de kosmologie. Kosmologische waarnemingen, met name die van de kosmische achtergrondstraling, leggen strenge restricties op aan modellen voor de evolutie van het universum. We construeren een fenomenologisch gemotiveerd kosmologisch model dat in overeenstemming is met Asymptotische Veiligheid. Hiervoor projecteren we de FRGE op R^2-zwaartekracht, en bestuderen haar oplossingen. Dit model bevat het Starobinsky-inflatiemodel, één van de meest succesvolle modellen voor inflatie. We construeren een asymptotisch veilige RG-stroomlijn dat voortkomt uit het NGFP, en bovendien overeenkomt met de observationele data over het vroege- en late-tijdperk in de geschiedenis van het universum.

Vervolgens onderzoeken we structurele eigenschappen van de RG flow van zwaartekracht. We bekijken de expansie van de effectieve gemiddelde actie in termen van vormfactoren. Deze momentum-afhankelijke functies beschrijven de schaalafhankelijkheid van interacties. We classificeren de vormfactorenvoor de laagste orde interacties in pure zwaartekracht en zwaartekracht-materiesystemen. In het bijzonder generaliseren vormfactoren propagatoren tot algemene functies van het momentum.

In het algemeen zijn hogere-afgeleidetheorieën onfysisch vanwege zogeheten Ostrogradski-ghosts. Deze spookdeeltjes komen voor uit polen in de propagator met negatief residue, en schenden unitariteit. We bestuderen de hogere-afgeleidepropagator van een scalair veld gekoppeld aan zwaartekracht. De RG zou op twee manieren een oplossing kunnen bieden voor Ostrogradski-ghosts.

Ten eerste beperken we ons tot (inverse) propagatoren die polynomiaal zijn in het momentum. Door deze truncatie bevat de propagator onvermijdelijk extra polen. Er zitten hierdoor Ostrogradski-ghosts in de propagator, waarbij de schending van unitariteit gecodeerd wordt door de massa van de ghost. In de renormalisatiegroep wordt deze massa schaalafhankelijk. We ontdekken dat deze schaalafhankelijkheid de mogelijkheid geeft de schending van unitariteit op te heffen door de ghosts oneindig zwaar te maken.

Ten tweede bestuderen we de propagator door middel van de volledige vormfactor. Dit

biedt de mogelijkheid de schending van unitariteit op een tweede manier te verwijderen: een dergelijke vormfactor staat hogere afgeleiden toe zonder extra polen te introduceren. We construeren de stroomvergelijking waaraan deze vormfactor voldoet en bestuderen de eigenschappen van het vaste punt. We vinden dat het deeltjesspectrum geen Ostrogradski-ghost bevat.

Ten slotte komen we terug op de Ostrogradski-instabiliteit met de vraag welke hogere-afgeleide-theorieën gevaarlijk zijn voor unitariteit. Hiertoe gebruiken we een axiomatische benadering voor (Euclidische) kwantumveldentheorie. Als uitgangspunt nemen we de eis dat de theorie voldoet aan de Osterwalder-Schraderaxioma's. Deze geven condities voor een Euclidische QFT zodat deze equivalent is aan een unitaire theorie in Minkowskiruimte. Centraal in de Osterwalder-Schraderaxioma's is reflectie-positiviteit, die voorwaarden oplegt voor het bestaan van een Euclidische tijdsrichting. We bewijzen voor een grote klasse van hoger-orde-afgeleide-theorieën de noodzakelijke en voldoende voorwaarden voor reflectie-positiviteit.

In dit proefschrift behandelen we zowel observationele en structurele aspecten van asymptotisch veilige kwantumgravitatie. Enerzijds relateren we de RG flow van zwaartekracht aan kosmologische waarnemingen, anderzijds bestuderen we the eigenschappen van unitariteit in hogere-afgeleidetheorieën. In beide gevallen kunnen vormfactoren een belangrijke rol spelen. Zo bieden ze de mogelijkheid tot observeerbare kwantumgravitationele effecten, en geven ze structurele informatie over de propagerende vrijheidsgraden. Deze prominente rol in ons begrip van zwaartekracht op een fundamenteel niveau geeft een duidelijke motivatie voor verdere studie van deze objecten, volgend op de eerste stappen in dit proefschrift.

SUMMARY

Present-day theoretical physics is based on two paradigms. On the one hand, General Relativity gives an excellent description of gravity and the universe at large length scales. On the other hand, quantum field theory (QFT) forms the basis of our understanding of elementary particles on scales of approximately 10^{-20} m. While both theories have seen impressive experimental confirmation within their domains of application, a formulation of gravity as a quantum theory (quantum gravity) has been elusive so far.

One of the problems to overcome is renormalizability. In a quantum theory, the coupling constants acquire a dependence on the energy scale at which they are measured. From the Wilsonian point of view, the energy dependence is obtained from integrating out quantum fluctuations momentum shell by momentum shell. This gives rise to a flow through the space of coupling constants, called the renormalization group (RG) flow. Following a particular RG trajectory along the flow, one obtains the effective action where all quantum fluctuations are integrated out.

When we use perturbation theory to quantize General Relativity, we find that the negative mass dimension of Newton's constant leads to unphysical infinities in observables. In order to compensate for these divergences, one needs to introduce an infinite number of new free parameters. Therefore, the predictive power of the theory is lost. This demonstrates the (perturbative) non-renormalizability of General Relativity.

In the Asymptotic Safety scenario, formulated by Weinberg, renormalizability of gravity is realized by an interacting fixed point (NGFP) of the renormalization group. Due to its interacting character, this point is difficult to study perturbatively. However, functional methods have provided strong evidence for the existence of such a fixed point. This fixed point opens up the possibility of a UV-completion of the theory, as well as a restoration of predictive power.

Although Asymptotic Safety is a promising candidate for a theory of quantum gravity, it still needs to pass several tests. First, a viable theory should provide predictions that can be experimentally tested. In Asymptotic Safety, the requirement that an RG trajectory emanates from the NGFP in the UV provides an elegant mechanism that gives rise to predictions. Secondly, the theory should satisfy certain structural properties, such as unitarity. Unitarity is a key ingredient in the probabilistic interpretation of a quantum

theory. It is an open problem to determine whether Asymptotic Safety is compatible with unitarity. Owed to the interactions present in the NGFP, this is an intricate question.

In this PhD thesis, we investigate both problems. We start with an overview of Asymptotic Safety and unitarity. Next, we present the methods underlying the functional renormalization group equation (FRGE) encoding the Wilsonian RG flow of gravity.

As a first test, we study solutions to the FRGE in the context of cosmology. Cosmological observations, in particular those of the cosmic microwave background, impose severe restrictions on models for the evolution of the universe. We construct a phenomenologically valid cosmological model compatible with Asymptotic Safety. For this purpose, we explicitly solve the FRGE projected to R^2-gravity. This naturally incorporates Starobinsky inflation, which is one of the most successful inflationary models. We explicitly construct an asymptotically safe RG trajectory that emanates from the NGFP, and in addition agrees with the observational data describing the early and late time evolution of the universe.

We then study structural properties of the RG flow of gravity. We examine the approximation of the effective average action including form factors. These momentum-dependent functions encode the scale dependence of interactions. We classify the form factors for the lowest order interactions in pure gravity and in gravity-matter systems. In particular, form factors generalize propagators to general functions of the momentum.

Generically, higher derivative theories are unphysical because of so-called Ostrogradski ghosts. These ghost particles are associated to poles in the propagator that have negative a residue and violate unitarity. In the context of the renormalization group, we study the higher-derivative propagator of a scalar field coupled to gravity. The RG may provide a cure for the Ostrogradski ghosts in two ways.

First, we restrict ourselves to (inverse) propagators which are polynomial in the momentum. Due to the polynomial truncation, the propagator necessarily contains additional poles. Thus, such propagators contain Ostrogradski ghosts, where the unitarity violation is encoded in the ghost mass. In the renormalization group, the mass becomes scale dependent. We discover that this scale dependence provides the possibility to remove the unitarity violation by making the ghosts infinitely heavy.

Secondly, we study the propagator using a proper form factor. This allows for another possibility to lift unitarity violation: such a form factor may admit higher derivatives without introducing additional poles. We construct the flow equation satisfied by this form factor and study its fixed point properties. We find that the particle spectrum of the form factor appears to be free of Ostrogradski ghosts.

Ultimately, we return to the Ostrogradski instability with the question which higher-order derivative theories are dangerous for unitarity. For this we use an axiomatic approach for (Euclidean) quantum field theory. As a starting point, we require that the theory satisfies the Osterwalder-Schrader axioms. These give conditions for a Euclidean QFT being equivalent to a unitary theory in Minkowski space. Central in the Osterwalder-Schrader

axioms is reflection positivity, that gives conditions for the existence of a Euclidean time direction. We prove for a large class of theories of higher-derivative theories the necessary and sufficient requirements for reflection positivity.

In this thesis, we discuss both observational and structural aspects of asymptotically safe quantum gravity. On the one hand we link the RG flow of gravity to cosmological observations, on the other hand we study the properties of unitarity in higher derivative theories. In either case, form factors may play an important role, opening up possibilities for observable corrections due to quantum gravity, as well as providing structural information about the propagating degrees of freedom. This prominent role in understanding gravity at the quantum level provides a clear motivation for studying these objects beyond the first steps taken in this thesis.

CONTENTS

ACRONYMS

CMB	cosmic microwave background	24
EAA	effective average action	4
FRG	functional renormalization group	7
FRGE	functional renormalization group equation	7
GFP	Gaussian fixed point	6
GR	general relativity	1
IDE	integro-differential equation	17
IR	infrared	4
NGFP	non-Gaussian fixed point	6
ODE	ordinary differential equation	17
PDE	partial differential equation	17
QFT	quantum field theory	1
QG	quantum gravity	2
RG	renormalization group	4
UV	ultraviolet	4

CHAPTER 1

INTRODUCTION

1.1 The need for quantum gravity

From everyday experience, gravity is the most prominent of the forces of Nature. It was the first of the four fundamental forces to be identified, first described by Newton [6], long before the unification of electromagnetism by Maxwell [7], or even before humanity had an inkling about the existence of the strong and weak nuclear forces (see [8] for a history of the discovery of the nuclear forces). However, despite its ubiquity, it remains in many ways the most elusive of the four fundamental forces.

With the development of quantum field theory (QFT) (see [9–11] for textbook treatments), the strong interaction and the electroweak interactions were described in a common framework, known as the Standard Model of particle physics. Extensive experimental tests have confirmed the predictions of the Standard Model, culminating in the discovery of the Higgs particle at the Large Hadron Collider (LHC) in 2012 [12, 13].

On the other hand, Einstein's theory of general relativity (GR) provides the modern description of gravity (for textbook expositions, refer to [14–18]). Also general relativity's predictions have been put to the test, with the spectacular observation of gravitational waves at LIGO and Virgo as recent highlight [19].

Despite their incredible success, the Standard Model and general relativity differ in a fundamental way. The Standard Model is a quantum theory, where particles are represented as operators on a Hilbert space. Inherent to the quantum formalism is its probabilistic interpretation, where fluctuations of the particle fields occur with a certain probability. GR is in that respect a classical theory: the dynamics of space and time are (at least locally) completely determined by its equations of motion.

Various attempts have been made to formulate general relativity as a quantum theory [20]; prominent examples include string theory [21–23], Loop Quantum Gravity [24, 25], Causal Dynamical Triangulations [26, 27], and Asymptotic Safety [28, 29]. Although

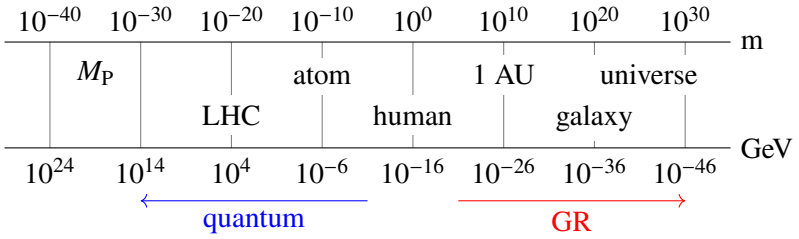

Figure 1.1: *Distance scales in Nature. Quantum effects have been observed at distances smaller than 1 meter, whereas GR effects are measured at larger scales.*

each approach has proven itself as a rich source of theoretical models, each program comes with its own specific challenges, such as providing a unique realization of the theory (e.g. the vacuum problem in String Theory), the construction of a classical limit recovering the degrees of freedom of GR (featured in discrete approaches such as Loop Quantum Gravity and Causal Dynamical Triangulations), or resolving dependence of an artifical background metric (key in the Asymptotic Safety approach). There is as yet no conclusive evidence as to which program will provide a satisfactory description of Nature.

There are several reasons why the search for quantum gravity (QG) is a nontrivial task. So far, there are few experimental clues on what to expect for such a theory. Non-gravitational quantum effects of matter have been observed on small length scales, ranging from 10^{-20} m probed by subatomic collider experiments at the LHC up to the everyday meter scale in molecular physics (see Figure 1.1). As an extreme case, quantum effects have to be taken into account in the description of neutron stars, which are typically of kilometer size. On the other hand, general relativity has been proven to be successful on large length scales, starting at the very largest cosmic scales (10^{26} m) down to solar system tests at 1 astronomical unit (AU) $\approx 10^{10}$ m. In fact, Newtonian gravity has been tested experimentally to sub-millimeter length scales [30]. The connection between this separation of scales motivates the approach taken in this thesis.

A first glimpse on what a theory of Quantum Gravity should involve is provided by the Planck mass M_P. This is given by the unique combination of the (reduced) Planck constant $\hbar$, the speed of light c, and Newton's constant G that has the units of a mass,

$$M_P = \sqrt{\frac{\hbar c}{8\pi G}} = 2.4 \times 10^{27} \text{ eV} . \tag{1.1}$$

This energy scale can be interpreted as the scale where both quantum effects, signaled by the occurrence of $\hbar$, relativistic effects, marked by c, and gravitational physics denoted by G become relevant. Comparing the Planck energy to other energy scales in Figure 1.1, we see that the Planck scale is far beyond any scale accessible by present-day experiments.

A second motivation for a theory of quantum gravity is given by the limitation of general relativity. Inherent to the formalism, GR predicts its own breakdown with the occurrence of spacetime singularities, such as in the Schwarzschild metric describing a black hole

$$\mathrm{d}s^2 = -\left(1 - \frac{2GM}{r}\right)\mathrm{d}t^2 + \left(1 - \frac{2GM}{r}\right)^{-1}\mathrm{d}r^2 + r^2\mathrm{d}\Omega^2\,, \tag{1.2}$$

where M denotes the black hole mass, t the time coordinate, r the radial coordinate and $\mathrm{d}\Omega$ the spherical volume element. Clearly, this metric is singular at the locus $r = 0$, and general relativity gives no prediction for the fate of spacetime at this point.

Finally, incorporating gravity into quantum field theory turns out to be far from straightforward. Taking a conventional approach, one could try to quantize the Einstein-Hilbert action

$$S_{\mathrm{EH}} = \frac{1}{16\pi G}\int \mathrm{d}^4x\sqrt{|-g|}\,R\,, \tag{1.3}$$

where g denotes the determinant of the metric $g_{\mu\nu}$, and R the Ricci scalar. Using standard perturbation techniques, one finds that a scattering amplitude calculated from this action yields a divergent momentum integral [31, 32]. A possibility to cure this is to introduce an extra term in the action as a counterterm for the divergences. In the case of (1.3), this is the infamous Goroff-Sagnotti counterterm [32]. Quantizing this counterterm introduces new divergences, that have to be cured by new counterterms, and so on. This yields an infinite tower of counterterms, each coming with its own coupling constant. Since all couplings need to be measured, one would need an infinite number of experiments to make a prediction from this theory. In this way, predictivity of the theory is lost. A theory suffering from this property is called non-renormalizable.

In this thesis, we study the Asymptotic Safety approach to quantum gravity. Rather than introducing new degrees of freedom or additional symmetries, the Asymptotic Safety program takes the conventional approach that the spacetime metric encodes the correct quantum mechanical degrees of freedom. The key difference to standard QFT methods is the use of non-perturbative techniques. In the discussion above, we found that a perturbative study of the renormalization of the Einstein-Hilbert action resulted in a non-renormalizable theory. However, if one is able to treat the renormalization of gravity *non-perturbatively*, it may turn out that the resulting QFT is actually in good shape. This scenario, first conjectured by Weinberg in the 1970s [33–36], goes by the name of Asymptotic Safety. In the next section, we discuss renormalization in a more general setting, as well as the non-perturbative techniques necessary to study renormalization. We then apply the developed framework in the context of quantum gravity.

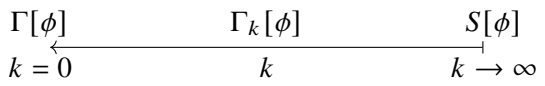

Figure 1.2: *The effective average action interpolates between the classical action S and the quantum effective action Γ, while integrating out fluctuations with energy larger than an energy scale k.*

1.2 The renormalization group

At the heart of renormalization lies the scale-dependence of physics. Following Wilson's modern view [37], we regard renormalization as "integrating out" degrees of freedom at a given scale. The remaining degrees of freedom then correspond to different effective physics.

This is formalized by introducing a scale-dependent effective average action (EAA), denoted by $\Gamma_k[\phi]$ [38–40]. The scale k denotes the energy scale up to which degrees of freedom have been integrated out (see Figure 1.2). For $k \to \infty$, we obtain the classical action S for the fundamental degrees of freedom. As this corresponds to high energies, this regime is called ultraviolet (UV). For $k \to 0$, referred to as infrared (IR), all degrees of freedom have been integrated out and we retrieve the full quantum effective action Γ. The family of actions traced out by Γ_k forms an renormalization group (RG) trajectory; together they form the same theory at different effective scales.

In order to study the flow of the effective average action, we expand Γ_k in a basis of operators $\{\mathcal{O}_i[\phi]\}$, spanning the theory space $\mathcal{T}$. This basis contains all monomials of ϕ that satisfy the symmetries of the theory:

$$\Gamma_k[\phi] = \sum_i \bar{u}_i(k)\, \mathcal{O}_i[\phi]\,. \tag{1.4}$$

The coefficients $\bar{u}_i(k)$, referred to as the running couplings of the system, are the coordinates of Γ_k with respect to this basis.

Introducing the logarithmic RG scale $t = \log(k/k_0)$, where k_0 is an arbitrary reference scale, taking a derivative with respect to t defines a flow equation on theory space $\mathcal{T}$. In general, the couplings $\bar{u}_i(k)$ have a canonical mass dimension d_i. Defining the dimensionless couplings $u_i(k) \equiv k^{-d_i}\bar{u}_i(k)$ and expressing the flow equation in terms of the u_i, the flow equation becomes autonomous (i.e. independent of any explicit k) and the scaling of the theory is captured by the β-functions of the couplings

$$\partial_t u_i(k) = \beta_{u_i}\left(\{u_j\}\right)\,. \tag{1.5}$$

The solution to these first-order differential equations are exactly the RG trajectories. Methods for calculating the β-functions are for instance perturbation theory [11], or functional methods [38–41].

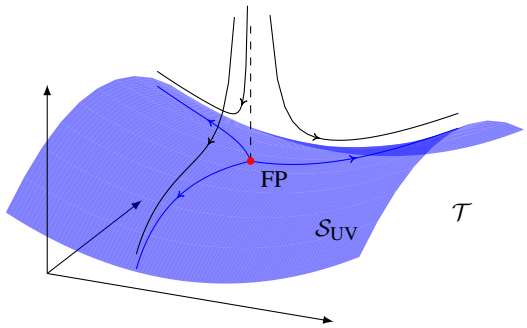

Figure 1.3: *The UV-critical hypersurface $\mathcal{S}_{\rm UV}$ embedded in theory space $\mathcal{T}$. Trajectories emanating from the fixed point (blue lines) span the UV-critical hypersurface, whereas trajectories approaching from an irrelevant direction (dashed line) are driven away from the fixed point (black lines).*

1.2.1 Renormalizability

A complete theory should satisfy the condition that the couplings $u_i(k)$ remain finite at all scales. In addition, one should be able to characterize the theory completely by a finite number of measurements. If the latter would not be satisfied, the theory would fail to be predictive. A theory that satisfies both conditions is called renormalizable.

At first glance, providing a predictive theory is problematic in the light of the infinite sum in (1.4), since it seems that an infinite number of couplings should be measured. However, there is a way to cure both problems in a single stroke. By the first condition, the couplings should remain finite at all scales. This implies that the RG trajectory must have an endpoint where the couplings remain constant. This is satisfied for a simultaneous root of the β-functions

$$\beta_{u_i}\big|_{u_j=u_j^*} = 0\,, \quad \forall i\,. \tag{1.6}$$

The point $\{u_j^*\}$ is therefore a fixed point of the RG flow.

The fixed point also provides an elegant solution to the problem of predictivity. The family of RG trajectories attracted to a fixed point forms the UV-critical hypersurface $\mathcal{S}_{\rm UV}$ in theory space; see Figure 1.3. If this surface is finite-dimensional, a trajectory is identified exactly by specifying a finite number of parameters. Thus, the condition that a trajectory lies within such a surface restores predictivity. If this condition is satisfied, the theory is called renormalizable.

The RG flow near the fixed point is conveniently characterized by linearizing the

β-functions. Expanding the flow around the fixed point, we obtain up to first order

$$\beta_{u_i} \simeq \sum_j \mathbf{M}_{ij} \left(u_j - u_j^*\right) . \tag{1.7}$$

The matrix $\mathbf{M} = \partial\beta_{u_i}/\partial u_j$ is referred to as the stability matrix. Diagonalizing the stability matrix, we can solve the flow equation in terms of the right-eigenvectors V_I and eigenvalues $\lambda_I = -\theta_I$ of $\mathbf{M}$, satisfying $\mathbf{M}V_I = -\theta_I V_I$:

$$u_i(t) = u_i^* + C_I V_{Ii} \exp\left(-\theta_I t\right) . \tag{1.8}$$

The numbers C_I determine the initial conditions of the RG flow, and are a priori not fixed. The θ_I, known as the critical exponents, determine the direction of the flow. If $\mathrm{Re}\,(\theta_I) > 0$, the RG flow is automatically attracted to the fixed point as $t \to \infty$, and C_I is a free parameter of the theory that is not fixed by the asymptotic safety condition. The corresponding eigendirection V_I is then called UV-relevant. If $\mathrm{Re}\,(\theta_I) < 0$, the RG flow is attracted to the fixed point only if $C_I = 0$. This fixes the initial condition, and the eigendirection V_I is called UV-irrelevant. In the case where $\theta_I = 0$, a linear approximation does not suffice to determine whether the direction is relevant or irrelevant. The direction V_I is then called marginal. A higher-order expansion of the β-function is then needed to determine whether V_I is UV-attractive or not. The dimension of the UV-critical hypersurface is thus given by the number of relevant directions, plus the number of UV-attractive marginal couplings.

The critical exponents can be used to classify a fixed point. A fixed point whose critical exponents are equal to the canonical mass dimension is named Gaussian fixed point (GFP). If an RG trajectory is attracted to the Gaussian fixed point (GFP) at high energies, the theory is called asymptotically free. If the critical exponents are not equal to the canonical mass dimension, the fixed point is referred to as a non-Gaussian fixed point (NGFP). The fixed point theory is then interacting, and trajectories attracted by the non-Gaussian fixed point (NGFP) are asymptotically safe.

1.2.2 Asymptotically safe quantum gravity

We are now in a position to review the non-renormalizability of gravity. From an RG perspective, the Newton coupling becomes scale-dependent, denoted by $G(k)$. Since it has mass dimension $2 - d$, where d denotes the spacetime dimension, we define its dimensionless counterpart g_k by the relation

$$g_k = k^{d-2} G(k) . \tag{1.9}$$

Taking the derivative with respect to t, we find

$$\partial_t g = (d - 2 + \eta_N) g , \tag{1.10}$$

where we have captured quantum corrections to the running of G by the anomalous dimension

$$\eta_N = G^{-1}\partial_t G\,. \tag{1.11}$$

We observe that the value $g = 0$ is indeed a fixed point of the RG flow. We can then study the RG flow of g in perturbation theory. In $d = 4$ spacetime dimensions, the β-function of g up to first order in g is given by

$$\partial_t g = 2g + \mathcal{O}(g^2)\,. \tag{1.12}$$

From the stability analysis explained in the previous section, we therefore conclude that the Newton coupling is irrelevant. Thus, if the RG trajectory realized in nature were to end at the fixed point $g = 0$, the value of g is fixed, and is given by $g = 0$ at all scales. Since we observe a nonzero value of the Newton coupling, this is clearly excluded. Therefore, gravity is not perturbatively renormalizable.[1]

However, from (1.10) we infer that there is a second possibility to obtain a fixed point for β_g, namely if $\eta_N = 2 - d$. As this is at a nonzero value of g, this would be a NGFP. As was first conjectured by Weinberg in the seventies [33–36], such a fixed point may render gravity asymptotically safe.

Using a perturbative expansion around $d = 2 + \epsilon$ dimensions, hints for such a NGFP were already available when Weinberg formulated his conjecture [43–46], for later works see [47–50]. However, a non-perturbative treatment at finite ϵ only became available with the advent of functional methods [38–40], that opened the avenue to study the Asymptotic Safety scenario in $d = 4$ dimensions [51–112] and its phenomenological implications [106–173] in a systematic way.

1.3 The functional renormalization group equation

The central tool in studying the non-perturbative RG flow of gravity is the functional renormalization group equation (FRGE), also referred to as the Wetterich equation [38]:

$$\partial_t \Gamma_k[\phi] = \frac{1}{2}\,\mathrm{Tr}\left[\left(\Gamma_k^{(2)}[\phi] + \mathcal{R}_k\right)^{-1}\partial_t \mathcal{R}_k\right]\,. \tag{1.13}$$

The right-hand side of this equation consists of a trace over all fluctuation fields. The flow of the effective propagator $\left(\Gamma_k^{(2)}\right)^{-1}$ is modified by a regulator $\mathcal{R}_k$, which suppresses IR modes of momentum $p^2 \ll k^2$. The UV is regulated by the derivative $\partial_t \mathcal{R}_k$, which

[1] Extending General Relativity by including higher-order curvature terms in the action will yield a perturbatively renormalizable quantum theory [42]. However, such a higher-derivative theory is non-unitary since it contains a ghost (see section 1.4).

suppresses modes of momentum $p^2 \gg k^2$. In section 2.1, we give a derivation of the FRGE via a path integral approach.

In practice, the FRGE cannot be solved exactly. A method of approximating a solution is given by truncating the series (1.4) to include operators $\mathcal{O}_i$ that are of interest. These operators are retained in an ansatz for Γ_k, which is substituted into the FRGE. The approximate flow of the couplings $\{u_i\}$ are given by projecting the right-hand side of the FRGE onto the $\mathcal{O}_i$.

Since this prescription does not make any assumption on the size of the u_i, this method can be applied to the non-perturbative regime. In particular, this setup has proven fruitful in the context of gravity. Starting with the seminal work [102], there is by now substantial evidence for the existence of a NGFP for gravity in $d = 4$ spacetime dimensions [51–112].

1.4 Unitarity

The asymptotic safety scenario provides a mechanism for removing UV divergences from the theory, as well as for rendering the number of free parameters finite. A viable quantum theory, however, should satisfy additional constraints. One of these constraints is that the effective action $\Gamma = \Gamma_{k=0}$ yields a unitary quantum field theory at $k = 0$.

Since the effective action includes in principle all possible interaction monomials that are compatible with the symmetry of the theory, one should be careful which terms in the action are generated along an RG trajectory. Potentially dangerous terms in the effective action are higher-derivative terms contributing to propagators of matter fields. These are typically associated to Ostrogradski instabilities or violation of unitarity, see [174, 175] for reviews.

It was shown by Ostrogradski in the 1850s that non-degenerate classical systems containing time derivatives of finite degree larger than two give rise to Hamiltonians whose kinetic term is not bounded from below [176]. Irrespective of the exact form of the action, the unbounded Hamiltonian will yield several unwanted phenomena, related to the instability of the system. At the classical level, the presence of degrees of freedom coming with a wrong-sign kinetic term allows to accelerate particles to infinite velocity while keeping the total energy of the system constant.

This type of instability also appears in the corresponding quantum system. While the presence of higher-derivative terms in the propagators lowers the degrees of divergencies arising in loop computations, the presence of positive and negative energy states may trigger an instantaneous decay of the vacuum. Naively, a way out may be to reinterpret the negative-energy creation and annihilation operators as positive-energy annihilation and creation operators, respectively. Although this seems to cure the instability of the vacuum state, this procedure yields states with negative norm. Removing these states from the physical spectrum, however, yields a non-unitary S-matrix. Thus, these higher-

derivative interactions violate unitarity of the theory.

In the case of a non-interacting scalar field theory, the Ostrogradski instability can be nicely illustrated by the Kallén-Lehmann representation [10]. This representation expresses the dressed propagator $G(x-y)$ as a superposition of freely propagating particles with mass $\mu \geq 0$ and propagator

$$G_{\text{free}}\left(x;\mu^2\right) = \int \frac{\mathrm{d}^d p}{(2\pi)^d} \frac{1}{p^2+\mu^2} \mathrm{e}^{ipx}\,, \tag{1.14}$$

such that

$$G(x-y) = \int_0^\infty \mathrm{d}\mu^2\, \rho\left(\mu^2\right) G_{\text{free}}\left(x-y;\mu^2\right)\,. \tag{1.15}$$

For a unitary theory, the spectral density $\rho\left(\mu^2\right)$ is a sum over states with positive coefficients, thus $\rho\left(\mu^2\right) \geq 0$. If $\rho\left(\mu^2\right) < 0$ for some μ^2 in the physical sector of the theory, then unitarity issues arise.

In particular, a system containing scalar fields ϕ where the propagator contains a fourth-order kinetic term will prove to be dangerous:

$$S = \frac{Z}{2} \int \frac{\mathrm{d}^d p}{(2\pi)^d} \phi \left[p^2 + Y p^4\right] \phi\,, \tag{1.16}$$

where Z denotes a wave-function renormalization and Y is the coupling associated to the higher-derivative term. Expanded in a Fourier basis, the propagator is given by

$$G(p) = \frac{1}{Z} \frac{1}{p^2 + Y p^4}\,. \tag{1.17}$$

Using partial fraction decomposition, this can be expanded in terms of free propagators:

$$G(p) = \frac{1}{Z}\left(\frac{1}{p^2} - \frac{1}{p^2 + \frac{1}{Y}}\right)\,. \tag{1.18}$$

We see that the Kallén-Lehmann spectrum contains a massless state with positive density, and a state of mass

$$\mu^2 = Y^{-1} \tag{1.19}$$

with negative density. The latter state is called a (Ostrogradski) ghost. It is easy to see that the spectral density is not positive. Therefore, the theory will generically be unstable.

Generically, gravitational interactions will generate propagators with higher derivative terms such as (1.16). This puts additional constraints on which RG trajectory is regarded as physically viable. The interplay between unitarity and the renormalization group is one of the main topics in this thesis.

1.5 Setup of this thesis

The remainder of this thesis is organized in six chapters. In chapter 2, we give a detailed introduction to the functional methods used in studying the FRG. We start by a derivation of the FRGE in section 2.1. Next, we discuss the construction of an RG flow for gravity. This involves the background field method, which allows to fix redundant gauge degrees of freedom and define a regulator. This has important consequences for diffeomorphism symmetry.

In chapter 3, we apply the RG machinery developed in this introduction to cosmology, and see the implications of scale dependence on astrophysical observables. We will first study observational data on inflation and the late-time evolution of the universe. We then construct an RG flow for a gravitational truncation, and investigate the compatibility of the resulting RG trajectories with observations.

Chapter 4 is dedicated to the interplay between asymptotic safety and unitarity, in the context of scalar fields coupled to gravity. Specifically, we study the effects of metric fluctuations on the generation of a p^4-propagator in the effective action. As explained above, these higher-derivative terms may prove to be dangerous for unitarity. We consider the possibility of using the renormalization group as a cure for these Ostrogradski instabilities.

In chapter 5, we discuss so-called form factors. These combine infinitely many couplings into a momentum-dependent function, allowing for a systematic expansion of Γ_k in the number of fields. We study the generalization of the system discussed in chapter 4, from a p^4-dependent propagator to a full function of the momentum.

Higher derivative propagators can be dangerous for unitarity, or its Euclidean equivalent, which goes under the name of reflection positivity. For flat spacetime, one can write down strict requirements for a theory obeying reflection positivity in terms of its partition function. However, an explicit condition on e.g. the propagator of the theory is less clear. In chapter 6, we present a theorem that gives necessary and sufficient conditions for a large class of higher-derivative propagators for being reflection positive.

We conclude the thesis in chapter 7 with a summary and an outlook on further developments building on the results in this thesis. In particular, we will focus on future prospects related to the question of unitarity in asymptotically safe quantum gravity, and possible observable consequences.

CHAPTER 2

FUNCTIONAL METHODS IN RENORMALIZATION

In this chapter, we review some general properties of the FRG. We begin with a derivation of the FRGE in section 2.1 via a path integral approach. We then discuss truncation schemes of the effective average action in section 2.2, yielding different types of differential equations for the RG flow. In section 2.3, we apply the developed FRG framework to the case of gravity. We conclude this chapter with some remarks about the applications of the functional RG in this thesis in section 2.4.

Section 2.2 and section 2.3 are based on:

> B. Knorr, C. Ripken, and F. Saueressig. *Form Factors in Asymptotic Safety: conceptual ideas and computational toolbox*. *Class. Quant. Grav.* (2019) [arXiv:1907.02903].

2.1 Derivation of the FRGE

We kick off with a derivation of the FRGE à la Wetterich [38] that was introduced in (1.13) and plays a central role throughout this thesis. The derivation of the FRGE is based on the path integral formalism. In many cases, the path integral is not a well-defined object in the sense that it is extremely hard to construct an integration measure on the desired space of configuration. In this chapter, however, we assume that the path integral measure has been constructed. In this way, we can derive an exact equation that can serve as a starting point for setting up a QFT.

The derivation of the Wetterich equation can be found in many works (see [38–40, 177] for original research papers, or [28, 29, 178, 179] for reviews). In these works,

the space over which the path integral is taken is assumed to consist of functions over spacetime. With this assumption comes a lot of additional structure, such as an inner product constructed from a spacetime integral, or linearity from addition and multiplication of functions. In this section, we will try to reconstruct the Wetterich equation from a minimal set of assumptions.

2.1.1 The Schwinger functional

We start out our construction with a measure space $(\mathfrak{F}, \Sigma, \mu)$, consisting of a set $\mathfrak{F}$ equipped with a σ-algebra Σ and a measure μ. We assume the measure μ to be positive and finite. The measure space induces the path integral $\mathcal{Z} = \int \mathrm{d}\mu(\varphi)$. From this integral, we can construct for $p \in [1, \infty]$ the Banach spaces $\mathrm{L}^p(\mu)$ of p-integrable functions, including the extremal case $\mathrm{L}^\infty(\mu)$ of bounded μ-integrable functions.

We then define the *partition function* $Z\colon \mathrm{L}^\infty(\mu) \to \mathbb{R}$ as the generating functional

$$Z[J] = \int \mathrm{d}\mu\, \mathrm{e}^J \,. \tag{2.1}$$

Since the measure μ is finite, and $J \in \mathrm{L}^\infty(\mu)$ is a bounded function, we conclude that $Z[J]$ is finite, and furthermore positive. We note that $\mathcal{Z} = Z[0]$. At this stage, we notice that we have not assumed any linear structure on $\mathfrak{F}$ in order to define H. In particular, there is no reference to a spacetime structure that allows for a construction of a pairing such as $J \cdot \varphi = \int \mathrm{d}^d x\, j(x)\varphi(x)$. This is in contrast to usual definitions of Z in the literature.

Now let $H \subseteq \mathrm{L}^\infty(\mu)$ be a Hilbert space equipped with an inner product $\langle \cdot\,, \cdot \rangle$ and induced norm $\| \cdot \|$. In addition, we assume that

$$\int \mathrm{d}\mu\, |J|^2 < C \qquad \text{for all} \qquad J \in H\,, \qquad \|J\| = 1 \tag{2.2}$$

for some bounding constant $C > 0$.

We now realize the renormalization group as follows. Let $\{\Delta S_k\} \subset \mathrm{L}^\infty(\mu)$ be a 1-parameter family of bounded μ-integrable functions parameterized by k. We define the k-dependent Schwinger functional $W_k\colon H \to \mathbb{R}$ by

$$W_k[J] = \log Z[J - \Delta S_k] = \log \int \mathrm{d}\mu\, \mathrm{e}^{J - \Delta S_k} \,. \tag{2.3}$$

For the moment, we do not specify any specific form for ΔS_k.

The inner product structure provides a functional derivative. Given a differentiable function $f\colon H \to \mathbb{R}$ and $J \in H$, we define the derivative $\frac{\delta f}{\delta J}[J] \in H$ implicitly by the relation

$$\left\langle \frac{\delta f}{\delta J}[J], \phi \right\rangle = \delta_\phi f[J] \equiv \lim_{\varepsilon \to 0} \frac{1}{\varepsilon} \left(f[J + \varepsilon\phi] - f[J] \right) \,, \tag{2.4}$$

for any $\phi \in H$. Since H is a Hilbert space, this completely characterizes $\frac{\delta f}{\delta J}[J]$. Note that the J appearing in the denominator of $\frac{\delta f}{\delta J}$ is a dummy variable. Taking a second derivative, one obtains the Hessian operator, given by

$$\left\langle \phi, f^{(2)}[J]\psi \right\rangle = \left\langle \phi, \frac{\delta^2 f}{\delta J^2}[J]\psi \right\rangle = \delta_\phi \delta_\psi f[J] \,. \tag{2.5}$$

Combining the integration measure μ and the inner product structure, we can define multiplication operators. For $J \in \mathrm{L}^\infty(\mu)$, we characterize the operator $m(J)$ by the matrix elements

$$\langle \phi, m(J)\,\psi \rangle = \int \mathrm{d}\mu\, \phi J \psi \,. \tag{2.6}$$

Because of the bound (2.2), it is straightforward to see that the operator $m(1)$ is bounded. From that, it follows that for all $J \in \mathrm{L}^\infty(\mu)$ the operator $m(J)$ is bounded.

In the following, we assume that the Schwinger functional W_k is at least twice differentiable. We can now use the structures discussed above to calculate derivatives of the Schwinger functional W_k:

Lemma 2.1. *The first two derivatives of W_k are given by*

$$\begin{aligned} \left\langle \frac{\delta W_k}{\delta J}[J], \phi \right\rangle &= \mathrm{e}^{-W_k[J]} \int \mathrm{d}\mu\, \mathrm{e}^{J-\Delta S_k}\phi \,, \\ \left\langle \phi, W_k^{(2)}[J]\,\psi \right\rangle &= \left\langle \phi, \left(m\left(\mathrm{e}^{-W_k[J]+J-\Delta S_k}\right) - \left|\frac{\delta W_k}{\delta J}[J]\right\rangle \left\langle \frac{\delta W_k}{\delta J}[J]\right| \right)\psi \right\rangle \,, \end{aligned} \tag{2.7}$$

where we defined the 1-dimensional projector $|\phi\rangle\langle\phi|$ by $|\phi\rangle\langle\phi|\,\psi = \langle\phi,\psi\rangle\,\phi$.

Proof. The first derivative follows from applying the chain rule on (2.3) Taking a second derivative of this expression, we obtain the matrix element

$$\begin{aligned} \left\langle \phi, W_k^{(2)}[J]\psi \right\rangle &= \mathrm{e}^{-W_k[J]} \int \mathrm{d}\mu\, \phi \mathrm{e}^{J-\Delta S_k}\psi \\ &\quad - \mathrm{e}^{-2W_k[J]} \left(\int \mathrm{d}\mu \mathrm{e}^{J-\Delta S_k}\phi \right)\left(\int \mathrm{d}\mu \mathrm{e}^{J-\Delta S_k}\psi \right) \\ &= \left\langle \phi, \left(m\left(\mathrm{e}^{-W_k[J]+J-\Delta S_k}\right) - \left|\frac{\delta W_k}{\delta J}[J]\right\rangle \left\langle \frac{\delta W_k}{\delta J}[J]\right| \right)\psi \right\rangle \,, \end{aligned} \tag{2.8}$$

which proves the lemma. □

2.1.2 The effective average action

Diagrammatically, the Schwinger functional is the generating functional of connected Feynman diagrams. Taking a Legendre transform, gives a generating functional for one-particle irreducible (1PI) diagrams. In order for the Legendre transform to be well-defined,

we assume that the functional W_k is strictly convex for all k. The Legendre transform is now uniquely defined and invertible and defined as the function $\tilde{\Gamma}_k : H \to \mathbb{R}$ given by

$$\tilde{\Gamma}_k[\phi] = \sup_{J \in H} \gamma_\phi[J] \equiv \sup_{J \in H} \langle \phi, J \rangle - W_k[J] \,. \tag{2.9}$$

The functional derivatives of W_k and $\tilde{\Gamma}_k$ satisfy the following properties:

Lemma 2.2. *Let $\phi \in H$ and $k \geq 0$. Then W_k and $\tilde{\Gamma}_k$ satisfy the following relations:*

$$\phi = \frac{\delta W_k}{\delta J}\left[\frac{\delta \tilde{\Gamma}_k}{\delta J}[\phi]\right] \tag{2.10}$$

and

$$W_k^{(2)}\left[\frac{\delta \tilde{\Gamma}_k[\phi]}{\delta J}\right] = \left(\tilde{\Gamma}_k^{(2)}[\phi]\right)^{-1} . \tag{2.11}$$

Proof. We begin with the observation that if W_k is strictly convex, there is a unique element $\mathcal{J}[\phi, k] \in H$ that exhausts the supremum. Thus, the functional γ_ϕ has a stationary point at $\mathcal{J}[\phi, k]$. This gives the condition for all $\psi \in H$

$$0 = \left\langle \frac{\delta \gamma_\phi}{\delta J}\left[\mathcal{J}[\phi, k]\right], \psi \right\rangle = \langle \phi, \psi \rangle - \left\langle \frac{\delta W_k}{\delta J}\left[\mathcal{J}[\phi, k]\right], \psi \right\rangle , \tag{2.12}$$

for all $\psi \in H$, which gives the relation $\phi = \frac{\delta W_k}{\delta J}\left[\mathcal{J}[\phi, k]\right]$. Taking a derivative of $\tilde{\Gamma}_k$, we find

$$\begin{aligned} \left\langle \frac{\delta \tilde{\Gamma}_k}{\delta J}[\phi], \psi \right\rangle &= \delta_\psi \tilde{\Gamma}_k[\phi] = \delta_\psi \left(\langle \phi, \mathcal{J}[\phi, k] \rangle - W_k\left[\mathcal{J}[\phi, k]\right] \right) \\ &= \langle \psi, \mathcal{J}[\phi, k] \rangle + \left\langle \phi, \delta_\psi \mathcal{J}[\phi, k] \right\rangle - \delta_\psi W_k\left[\mathcal{J}[\phi, k]\right] \\ &= \langle \psi, \mathcal{J}[\phi, k] \rangle + \left\langle \phi, \delta_\psi \mathcal{J}[\phi, k] \right\rangle - \delta_{\delta_\psi \mathcal{J}[\phi,k]} W_k\left[\mathcal{J}[\phi, k]\right] \\ &= \langle \psi, \mathcal{J}[\phi, k] \rangle \,, \end{aligned} \tag{2.13}$$

which shows that $\mathcal{J}[\phi, k] = \frac{\delta \tilde{\Gamma}_k}{\delta J}[\phi]$. Furthermore, combining this with (2.10) gives

$$\phi = \frac{\delta W_k}{\delta J}\left[\frac{\delta \tilde{\Gamma}_k}{\delta J}[\phi]\right] , \tag{2.14}$$

which proves the first claim. Using the chain rule, taking a derivative of this expression gives the relation

$$\psi = W_k^{(2)}\left[\frac{\delta \tilde{\Gamma}_k}{\delta J}[\phi]\right] \tilde{\Gamma}_k^{(2)}[\phi]\psi \tag{2.15}$$

for all $\psi \in H$. This shows that the Hessian of W_k is related to the inverse of the Hessian of $\tilde{\Gamma}_k$:

$$W_k^{(2)}\left[\frac{\delta \tilde{\Gamma}_k}{\delta J}[\phi]\right] = \left(\tilde{\Gamma}_k^{(2)}[\phi]\right)^{-1} . \tag{2.16}$$

This completes the proof of the lemma. □

2.1.3 Proof of the Wetterich equation

We are now in a position to derive the FRGE. It provides an RG equation in the sense that it gives an expression for the k-derivative of the effective average action. One of the special features of the Wetterich equation is that it is a closed equation for the effective average action Γ_k, in the sense that it makes no direct reference to the path integral measure.

Before we define the EAA and complete the proof of the Wetterich equation, we need the following result:

Lemma 2.3. *The k-derivative of $\tilde{\Gamma}_k$ is given by the path integral*

$$\partial_k \tilde{\Gamma}_k[\phi] = \mathrm{e}^{-W_k\left[\frac{\delta\tilde{\Gamma}_k}{\delta J}[\phi]\right]} \int \mathrm{d}\mu\, \mathrm{e}^{\frac{\delta\tilde{\Gamma}_k}{\delta J}[\phi]-\Delta S_k}\, \partial_k \Delta S_k \,. \tag{2.17}$$

Proof. We use the chain rule to obtain

$$\begin{aligned} \partial_k \tilde{\Gamma}_k[\phi] &= \partial_k \left(\left\langle \phi, \tfrac{\delta\tilde{\Gamma}_k}{\delta J}[\phi] \right\rangle - W_k\left[\tfrac{\delta\tilde{\Gamma}_k}{\delta J}[\phi]\right] \right) \\ &= \left\langle \phi, \partial_k \tfrac{\delta\tilde{\Gamma}_k}{\delta J}[\phi] \right\rangle - (\partial_k W_k)\left[\tfrac{\delta\tilde{\Gamma}_k}{\delta J}[\phi]\right] - \delta_{\partial_k \frac{\delta\tilde{\Gamma}_k}{\delta J}[\phi]} W_k\left[\tfrac{\delta\tilde{\Gamma}_k}{\delta J}[\phi]\right] \\ &= -(\partial_k W_k)\left[\tfrac{\delta\tilde{\Gamma}_k}{\delta J}[\phi]\right] , \end{aligned} \tag{2.18}$$

where we used Lemma 2.2 to cancel the first and third term in the second line. Using the chain rule once more, this can be written as

$$\partial_k \tilde{\Gamma}_k[\phi] = \delta_{\partial_k \Delta S_k} W_k\left[\tfrac{\delta\tilde{\Gamma}_k}{\delta J}[\phi]\right] = \mathrm{e}^{-W_k\left[\frac{\delta\tilde{\Gamma}_k}{\delta J}[\phi]\right]} \int \mathrm{d}\mu\, \mathrm{e}^{\frac{\delta\tilde{\Gamma}_k}{\delta J}[\phi]-\Delta S_k}\, \partial_k \Delta S_k \,. \tag{2.19}$$

This was to be proven. □

In order to prove the Wetterich equation, we make a particular choice for ΔS_k. This is fixed by choosing a 1-parameter family of trace-class operators $\mathcal{R}_k$ on H. We then define the EAA as

$$\Gamma_k[\phi] = \tilde{\Gamma}_k[\phi] - \frac{1}{2}\langle \phi, \mathcal{R}_k \phi \rangle \,. \tag{2.20}$$

We now fix ΔS_k by noting that the space $\mathrm{L}^2(\mu)$ of square-integrable functions is a Hilbert space with inner product $\langle f, g\rangle_{\mathrm{L}^2(\mu)} = \int \mathrm{d}\mu\, fg$. We then define $\Delta S_k \in \mathrm{L}^\infty(\mu) \subseteq \mathrm{L}^2(\mu)$ implicitly by

$$\langle \Delta S_k, J\rangle_{\mathrm{L}^2(\mu)} = \frac{1}{2}\,\mathrm{Tr}\left[m(J)\,\mathcal{R}_k\right] , \tag{2.21}$$

for all $J \in \mathrm{L}^\infty(\mu)$. Here, the trace Tr denotes the trace over the Hilbert space H. The expression (2.21) completely characterizes ΔS_k, since $\mathrm{L}^\infty(\mu) \subseteq \mathrm{L}^2(\mu)$ is dense. Moreover, the trace is finite since $m(J)$ is bounded and $\mathcal{R}_k$ is trace-class.

We remark here that in contrast to conventional derivations of the FRGE, we make no reference to an inner product structure on $\mathfrak{F}$. Usually, one uses the spacetime structure to define $\Delta S_k[\varphi] = \frac{1}{2}\int \mathrm{d}^{\mathrm{d}}x\, \varphi(x)\mathcal{R}_k\varphi(x)$. In the construction presented here, such an assumption is not necessary.

We can now complete the proof of the Wetterich equation.

Theorem 2.4. *Let Γ_k and ΔS_k be defined as above. Then the Wetterich equation holds:*

$$\partial_k \Gamma_k[\phi] = \frac{1}{2}\,\mathrm{Tr}\left[\left(\Gamma_k^{(2)}[\phi] + \mathcal{R}_k\right)^{-1}\partial_k\mathcal{R}_k\right]. \tag{2.22}$$

Proof. We recognize in (2.17) the $\mathrm{L}^2(\mu)$-inner product

$$\begin{aligned}\partial_k\tilde{\Gamma}_k[\phi] &= \left\langle \mathrm{e}^{-W_k\left[\frac{\delta\tilde{\Gamma}_k}{\delta J}[\phi]\right]+\frac{\delta\tilde{\Gamma}_k}{\delta J}[\phi]-\Delta S_k}, \partial_k\Delta S_k\right\rangle_{\mathrm{L}^2(\mu)} \\ &= \frac{1}{2}\,\mathrm{Tr}\left[m\left(\mathrm{e}^{-W_k\left[\frac{\delta\tilde{\Gamma}_k}{\delta J}[\phi]\right]+\frac{\delta\tilde{\Gamma}_k}{\delta J}[\phi]-\Delta S_k}\right)\partial_k\mathcal{R}_k\right],\end{aligned} \tag{2.23}$$

where we have used (2.21) to write this as a trace over H. Combining this with (2.20), we find for the k-derivative of the EAA:

$$\begin{aligned}\partial_k\Gamma_k[\phi] &= \frac{1}{2}\,\mathrm{Tr}\left[m\left(\mathrm{e}^{-W_k\left[\frac{\delta\tilde{\Gamma}_k}{\delta J}[\phi]\right]+\frac{\delta\tilde{\Gamma}_k}{\delta J}[\phi]-\Delta S_k}\right)\partial_k\mathcal{R}_k\right] - \frac{1}{2}\,\mathrm{Tr}\left[|\,\phi\rangle\langle\phi\,|\,\partial_k\mathcal{R}_k\right] \\ &= \frac{1}{2}\,\mathrm{Tr}\left[W_k^{(2)}\left[\frac{\delta\tilde{\Gamma}_k}{\delta J}[\phi]\right]\partial_k\mathcal{R}_k\right] = \frac{1}{2}\,\mathrm{Tr}\left[\left(\tilde{\Gamma}_k^{(2)}[\phi]\right)^{-1}\partial_k\mathcal{R}_k\right] \\ &= \frac{1}{2}\,\mathrm{Tr}\left[\left(\Gamma_k^{(2)}[\phi] + \mathcal{R}_k\right)^{-1}\partial_k\mathcal{R}_k\right].\end{aligned} \tag{2.24}$$

In the first line, we have noted that we can write the inner product $\langle\phi, \partial_k\mathcal{R}_k\phi\rangle$ as a trace over the projection operator $|\phi\rangle\langle\phi|\,\partial_k\mathcal{R}_k$. In going to the second line, we have applied Lemma 2.2 and Lemma 2.1 to relate this to the Hessian of W_k. We then use Lemma 2.2 again to insert the Hessian of $\tilde{\Gamma}_k$, which can then be related to Γ_k in the last line. This proves the FRGE. □

2.2 Truncation schemes in the EAA

Although the Wetterich equation is exact, it is difficult to construct exact solutions. One method is to use a truncated ansatz for Γ_k to obtain an approximate solution. Such an approximation includes a subset of monomials $\{\mathcal{O}_i\}$ of the set of all possible monomials that are compatible with the field content and symmetries of the theory.

approximation of Γ_k	structure of RG flow	fixed points
finite number of $\mathcal{O}_i$	ODEs	algebraic
field-dependent functions $f(R_1, \cdots, R_n; t)$	PDEs ($n+1$ var.)	PDEs (n var.)
momentum-dependent form factors $f(p_1, \cdots, p_n; t)$	IDEs ($n+1$ var.)	IDEs (n var.)

Table 2.1: *Summary of the mathematical structures capturing the flow of Γ_k in different classes of approximations. Depending on the scale-dependent terms retained in Γ_k, the projected flow equations are nonlinear ordinary differential equations (ODEs), partial differential equations (PDEs), or (partial) integro-differential equations (IDEs). Since fixed functionals are k-stationary solutions, their structure is governed by differential equations that contain one variable less than the corresponding flow equation.*

The cardinality of the set $\{\mathcal{O}_i\}$ has important consequences for the type of equation obtained from the truncated FRGE. An overview of the different cases and their RG flow structure can be found in Table 2.1.

In chapter 1, we have discussed the case of approximations where the ansatz for Γ_k retains a finite number of running couplings. In this case, the flow equations are (nonlinear) ordinary differential equations (ODEs), and the fixed point equations are algebraic. Around a fixed point, the RG flow can be studied using the linearized flow equation. The stability of the fixed point is captured by the (finite-dimensional) stability matrix $\mathbf{M}_{ij} = \partial\beta_{u_i}/\partial u_j$, and the critical exponents θ_I.

In special cases, the truncation has been extended to include an infinite number of monomials. An example is the $f(R)$-truncation [53, 64, 65, 67, 70, 75, 85, 90, 106, 110], which contains an ansatz for an action of the metric $g_{\mu\nu}$ of the form

$$\Gamma_k[g] \simeq \frac{1}{16\pi G_k}\int \mathrm{d}^d x\sqrt{g}\, f_k(R)\,, \tag{2.25}$$

where R denotes the Ricci scalar. In this truncation, the function f_k includes an infinite number of couplings. For a general action, such a coupling function may contain several arguments. The flow and fixed point equations now become partial differential equations (PDEs).

The discussion of the stability of the fixed point extends straightforwardly to an infinite number of couplings. The stability matrix $\mathbf{M}$ gets promoted to an operator whose eigenfunctions V_I depend on the arguments of the function f, such that the expansion

around the fixed point reads

$$f\left(R_1,\cdots,R_n;t\right)=f^*\left(R_1,\cdots,R_n\right)+C_I V_{Ii}\left(R_1,\cdots,R_n\right)\mathrm{e}^{-\theta_i t}\,. \tag{2.26}$$

Here f is the dimensionless coupling function and the R_i are the field arguments such as the Ricci scalar.

When studying the propagation of degrees of freedom at the quantum level, a finite truncation may lead to spurious results. An example will be discussed in chapter 4, where we study the propagator of a scalar field of the form

$$\Gamma_k^{\text{scalar}}[\phi,g]\simeq\frac{1}{2}Z_k\int \mathrm{d}^dx\sqrt{g}\,\phi\left(\Delta+Y_k\Delta^2\right)\phi\,. \tag{2.27}$$

Such a truncation automatically leads to spurious poles in the propagator of the scalar field, which suggest the presence of unphysical ghost fields.

The action (2.27) can be generalized to include operators of higher order in Δ by an ansatz of the form

$$\Gamma_k^{\text{scalar}}[\phi,g]\simeq\frac{1}{2}Z_k\int \mathrm{d}^dx\sqrt{g}\,\phi f_k(\Delta)\phi\,. \tag{2.28}$$

This ansatz tracks the full momentum dependence of the propagator. When evaluating the FRGE for this truncation, the inclusion of this so-called *form factor* leads to an integro-differential equation (IDE) determining the admissible $f\left(p^2\right)$. Conceptually, this may be understood by noticing that besides the external momentum the argument of the form factor may also include the loop momentum integrated over in the trace. This entails that a consistent solution requires knowing the form factor on the entire positive real axis. Thus approximating the form factor by a Taylor series (possibly with finite radius of convergence) is not suitable and new computational methods for solving such equations are required. Form factors will be studied in more detail in chapter 5.

2.3 The EAA for gravity

Up to now, we have been abstract about the organization of the action monomials $\mathcal{O}_i$. In order to construct a basis of monomials in gauge theories and gravity, one has to deal with redundant gauge degrees of freedom that have to be removed. A method to fix these gauge degrees to freedom is provided by the background field formalism.

In this framework, one decomposes the physical metric $g_{\mu\nu}$ into a fixed but arbitrary background field $\bar{g}_{\mu\nu}$ and a fluctuation field $h_{\mu\nu}$. Conceptually, the background metric provides the metric structure that is used to discriminate high-momentum modes from low-momentum modes. Its simplest incarnation is by means of a linear split:

$$g_{\mu\nu}=\bar{g}_{\mu\nu}+h_{\mu\nu}\,. \tag{2.29}$$

Alternatively, other parameterizations can be considered, such as the exponential split $g_{\mu\alpha}\left[\mathrm{e}^{h}\right]^{\alpha}{}_{\nu}$, e.g. in [48, 79, 94, 98, 107, 163, 180, 181].[1]

The background field formalism provides a convenient way to gauge-fix the freedom of performing coordinate transformations, $\delta g_{\mu\nu} = \mathcal{L}_v g_{\mu\nu}$, where $\mathcal{L}_v$ denotes the Lie derivative along the vector v. The linear split (2.29) entails that a transformation of $g_{\mu\nu}$ under diffeomorphisms may be implemented either by quantum gauge transformations,

$$\delta^{\mathrm{Q}}\bar{g}_{\mu\nu} = 0\,, \qquad \delta^{\mathrm{Q}} h_{\mu\nu} = \mathcal{L}_v g_{\mu\nu}\,, \tag{2.30}$$

keeping the background metric fixed, or by background gauge transformations,

$$\delta^{\mathrm{B}}\bar{g}_{\mu\nu} = \mathcal{L}_v \bar{g}_{\mu\nu}\,, \qquad \delta^{\mathrm{B}} h_{\mu\nu} = \mathcal{L}_v h_{\mu\nu}\,, \tag{2.31}$$

where each quantity transforms as a tensor of the corresponding rank.

Gauge-fixing is now implemented via the Faddeev-Popov method. In the present context, this entails supplementing the EAA by a suitable gauge-fixing and ghost action:

$$\Gamma_k[g, c, \bar{c}; \bar{g}] = \Gamma_k^{\mathrm{grav}}[g; \bar{g}] + \Gamma^{\mathrm{gf}}[g; \bar{g}] + S^{\mathrm{gh}}[g, c, \bar{c}; \bar{g}] \tag{2.32}$$

Throughout this thesis, we will use the following gauge-fixing action:

$$\Gamma_k^{\mathrm{gf}}[g; \bar{g}] = \frac{1}{16\pi G_k}\frac{1}{\alpha}\int \mathrm{d}^d x\sqrt{\bar{g}}\,\bar{g}^{\mu\nu} F_\mu F_\nu\,, \tag{2.33}$$

where F_μ is defined as

$$F_\mu[g; \bar{g}] = \bar{\nabla}^\nu g_{\mu\nu} - \frac{1+\beta}{d}\bar{\nabla}_\mu g^\nu{}_\nu\,, \tag{2.34}$$

The associated ghost action then reads

$$S^{\mathrm{gh}}[g, c, \bar{c}; \bar{g}] = -\int \mathrm{d}^d x\sqrt{\bar{g}}\,\bar{c}_\mu \mathcal{M}^\mu{}_\nu c^\nu\,, \tag{2.35}$$

with the Faddeev-Popov operator given by

$$\mathcal{M}^\mu{}_\nu = \bar{g}^{\mu\beta}\bar{\nabla}^\alpha \nabla_\alpha g_{\beta\nu} + \bar{g}^{\mu\beta}\bar{\nabla}^\alpha \nabla_\beta g_{\alpha\nu} - 2\frac{1+\beta}{d}\bar{g}^{\alpha\beta}\bar{\nabla}^\mu \nabla_\alpha g_{\beta\nu}\,. \tag{2.36}$$

In these expressions, the parameters α and β are gauge-fixing parameters. Tuning these parameters to specific values yields computational simplifications. In particular, the case $\beta = \frac{d}{2} - 1$ will be used throughout this thesis and is known as harmonic gauge. Special cases for α are Feynman gauge $\alpha = 1$ and Landau limit $\alpha \to 0$.

[1] In the exponential split, fluctuations cannot alter the signature of the physical metric, i.e. $g_{\mu\nu}$ and $\bar{g}_{\mu\nu}$ have the same signature. The underlying conformal field theories arising from the exponential and linear split possess different central charges [95]. This suggests that the linear and exponential parameterization lead to gravitational theories in different universality classes. For an exploration of the most general local parameterization up to second order in the fluctuation field see [79].

2.3.1 Restoration of diffeomorphism invariance

By construction, the gauge-fixing sector is breaking the symmetry under quantum gauge transformations. At the same time, the gauge-fixing (and regulator terms) may be constructed in such a way that the background gauge transformations are realized explicitly and maintained along the RG flow. The background gauge transformations may then be used to obtain a manifestly diffeomorphism-invariant effective action depending on a single metric g by setting $\Gamma[g] = \Gamma_{k=0}[h;\bar{g}]|_{h=0}$.

Due to the gauge-fixing and regulator terms, Γ_k depends on two independent arguments, which may be chosen as either $\Gamma_k[h;\bar{g}]$ or as $\Gamma_k[g,\bar{g}]$. The former formulation has the natural interpretation of considering graviton fluctuations in a fixed but arbitrary background, whereas the second one emphasizes the "bi-metric" character of the EAA.

While the two formulations are equivalent on the exact level, in typical approximations they correspond to different projections in theory space and therefore yield complementary information. Both formulations allow for practical calculations; in the fluctuation language, calculations have been done resolving vertices up to four graviton legs [57–59, 61, 62, 68, 82, 110], and first results on the all-orders fluctuation field dependence to lowest order in the momentum have been presented in [81]. In the bi-metric language, the most advanced calculations resolve both background and full metric Einstein-Hilbert structures [51, 88]. Since the object driving the flow in the Wetterich equation is the fluctuation two-point function $\Gamma_k^{(2,0)}[h;\bar{g}]$, where the $(2,0)$ denotes that the second derivative has been taken with respect to h rather than $\bar{g}$. Therefore, we will resort to the $(h;\bar{g})$-setup throughout the rest of this chapter.

The extra metric dependence is controlled by a split-Ward or Nielsen identity. It arises from the observation that the decomposition (2.29) is invariant under local split-symmetry transformations

$$\bar{g}_{\mu\nu} \mapsto \bar{g}_{\mu\nu} + \epsilon_{\mu\nu}\,, \qquad h_{\mu\nu} \mapsto h_{\mu\nu} - \epsilon_{\mu\nu}\,. \tag{2.37}$$

This transformation results in a (modified) split-Ward identity that relates functional derivatives of Γ_k with respect to the background to derivatives with respect to the fluctuation field. Schematically, it reads

$$\frac{\delta\Gamma_k[h;\bar{g}]}{\delta\bar{g}} - \frac{\delta\Gamma_k[h;\bar{g}]}{\delta h} = \mathcal{N}[h;\bar{g}]\,. \tag{2.38}$$

The $\mathcal{N}[h;\bar{g}]$ carries the information about the non-trivial behavior of diffeomorphism transformations of the gauge-fixing sector and regulator [56, 69, 72, 83, 87, 89–91, 93, 100, 105, 111, 178, 182–185].

The bi-metric structure of the EAA can be approached in two different ways, schematically depicted in Figure 2.1. The first approach is to solve the Nielsen identity (2.38) by calculating the fluctuation two-point function in terms of background correlators. Structurally, the relation involves all background correlators and background derivatives of the

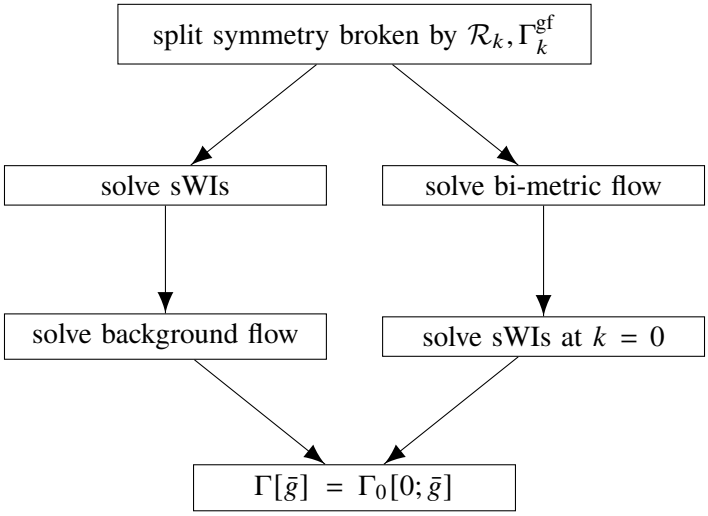

Figure 2.1: *Setup to obtain the effective action using the two schemes outlined in the main text.*

regulator, as well as the gauge-fixing and ghost action,

$$\Gamma_k^{(2,0)} = \Gamma_k^{(2,0)}\left[\Gamma_k^{(0,n)}\left[h;\bar{g}\right], \frac{\delta^n}{\delta\bar{g}^n}\mathcal{R}_k, \Gamma_k^{\rm gf}, S^{\rm gh}\right]. \tag{2.39}$$

To lowest order, the background and fluctuation correlators agree. The corrections to this can be organized in an expansion in the number of loops. Once the approximation of the fluctuation propagator is obtained, the actual flow equation can be solved.

The second way is to employ a vertex expansion of Γ_k,

$$\Gamma_k\left[h;\bar{g}\right] = \sum_m \frac{1}{m!}\int \mathrm{d}^d x\sqrt{\bar{g}}\left[\Gamma_k^{(m)}\left[\bar{g}\right]\right]^{\mu_1\nu_1\cdots\mu_m\nu_m} h_{\mu_1\nu_1}\cdots h_{\mu_m\nu_m}. \tag{2.40}$$

The vertices $\Gamma_k^{(m)}\left[\bar{g}\right]$ depend on both background curvatures and the momenta of the fluctuation fields in terms of covariant background derivatives. With this ansatz, both background and fluctuation correlators are resolved individually. Because this does not respect split symmetry, this in a sense enlarges theory space by monomials that violate split symmetry. However, these correlators are clearly related by the Nielsen identities. The strategy most often employed is to solve this in a sense over-complete flow, and then to impose the Nielsen identity only in the IR limit $k \to 0$. This is expected to reduce the dimension of theory space back to its original dimension.

Inserting the vertex expansion (2.40) into the FRGE and comparing order by order in h, one infers that the scale-dependence of $\Gamma_k^{(m)}$ is expressed in terms of $\Gamma_k^{(m+1)}$, $\Gamma_k^{(m+2)}$

and lower-order m-point functions. Thus, solving the flow of Γ_k at the level of the m-point vertex requires some closure conditions for the $(m+1)$ and $(m+2)$-point function. The established procedure employed in most works is to retain the tensor structures of the classical action and to identify the couplings of the two highest, non-resolved correlators with couplings from the highest-order resolved vertex. In chapter 5, we will come back to the question of how to close the flow equations in such a way that split symmetry breaking is minimized.

2.4 Conclusion

In this chapter we have investigated some aspects of the functional renormalization group. We have seen that the functional renormalization group equation can be derived on quite general grounds from the path integral. However, as the FRGE makes no direct reference to the path integral, it can be used as a starting point of a well-defined quantum field theory.

Despite the exact nature of the FRGE, finding exact solutions is very hard. One may find approximate solutions by using a truncated ansatz for the effective average action. Depending on the truncation, the truncated FRGE reduces to a set of ordinary differential, partial differential or integro-differential equations.

Since gravity is a gauge theory, we have to deal with redundant gauge degrees of freedom when we apply the RG framework. This is implemented via the background field method. Using the Faddeev-Popov mechanism, we supplement the truncation ansatz for the EAA by a suitable gauge-fixing and associated ghost action. This procedure, however, breaks quantum diffeomorphism invariance. This can be restored by solving the Nielsen identity, either before solving the flow equation or after one has taken the limit $\lim_{k\to 0}\Gamma_k$. This should give an effective action that depends solely on the quantum metric $g_{\mu\nu}$.

At this stage, we have developed the tools necessary to perform an RG computation. In the next chapters, we will put this into action in several truncation schemes. In chapter 3, we study the RG flow of gravity in a cosmological context. Chapter 4 discusses a gravity-matter system including a higher-derivative term of the form (2.27), and its unitarity properties. In chapter 5 we generalize this to (2.28) in our study of form factors.

CHAPTER 3

CONSISTENT COSMOLOGY FROM THE RG FLOW OF GRAVITY

The following chapter is based on:

> G. Gubitosi, R. Ooijer, C. Ripken, and F. Saueressig. *Consistent early and late time cosmology from the RG flow of gravity*. *J. Cosmol. Astropart. Phys.* **1812**.12 (2018) 004. [arXiv:1806.10147].

> G. Gubitosi, F. Saueressig, and C. Ripken. *Scales and hierachies in asymptotically safe quantum gravity: a review*. *Found. Phys.* **49**.9 (2019) 972. [arXiv:1901.01731].

Additional computational details are relegated to Appendix B and Appendix C.

3.1 Introduction

One thing any viable QG theory should do is to accommodate the observed values of the gravitational couplings. Even though measurements of quantum gravity on solar-system scales are notoriously difficult [186], cosmological observations give some constraints on admissible theories of gravity. In particular, QG should give an explanation for the incredibly small value that is measured for the cosmological constant [187]. Furthermore, there are strong indications that the universe has gone through a phase of accelerated expansion, known as inflation [188, 189]. In this chapter, we will study whether the asymptotic safety program supports such phenomena.

3.1.1 The cosmological standard model

By now, there is a well-established and experimentally well-tested phenomenological description of cosmology, known as the ΛCDM model (see [187, 190, 191] for reviews). The ΛCDM model has been very successful in describing the late-time evolution of the universe, from nontrivial predictions such as the cosmic microwave background (CMB), the abundances of elements in the universe, and large-scale structure formation. Observations show that the universe is at large scales approximately homogeneous and isotropic. The evolution of such a universe is captured by a Friedmann-Lemaître-Robertson-Walker (FLRW) geometry, given by the line element

$$\mathrm{d}s^2 = \mathrm{d}t^2 - a^2(t)\left(\frac{\mathrm{d}r^2}{1-kr^2} + r^2\mathrm{d}\Omega^2\right), \tag{3.1}$$

where the scale factor $a(t)$ parameterizes the evolution of the volume of the universe. The factor $k \in \{-1, 0, 1\}$ describes whether the universe is open, static or closed, respectively. The Einstein equations then reduce to the Friedmann equations, that govern the evolution of the scale factor a. Denoting the Hubble rate H by $H \equiv \frac{\dot{a}}{a}$, where the dot denotes a derivative with respect to t, the Friedmann equation reads

$$\frac{k^2}{a^2} = H^2\left(\Omega_{\text{matter}} + \Omega_{\text{radiation}} + \Omega_\Lambda - 1\right). \tag{3.2}$$

Here Ω_i denotes the contribution of different fractions of the contents of the universe. In particular, we have the dark energy contribution Ω_Λ due to the presence of the cosmological constant:

$$\Omega_\Lambda = \frac{\Lambda}{3H_0^2}, \tag{3.3}$$

where H_0 denotes the present-day Hubble rate.

Structure formation is driven by small inhomogeneities that originate from quantum fluctuations. These perturbations are described by the power spectrum $\mathcal{P}_i(k)$, given by the Fourier transform of the 2-point correlation functions. On physical grounds, we can assume that $\mathcal{P}(k)$ is well approximated by a power law:

$$\mathcal{P}_i(k) \simeq A_i\left(\frac{k}{k_0}\right)^{n_i-1}. \tag{3.4}$$

In this expression, k denotes the wave number and k_0 denotes an arbitrary reference scale. The amplitude of the fluctuation is denoted by A_i. The parameter n_i is the so-called *spectral tilt*. For $n_i = 1$, the spectrum is perfectly homogeneous.

Perturbations around the FLRW metric can be decomposed into scalar and tensor fluctuations. This yields the spectral tilts n_s, n_t corresponding to the scalar and tensor

fluctuations, respectively. In addition, one has the ratio $r = A_t/A_s$ of tensor to scalar amplitudes. Observations of the CMB have put severe constraints on the values of n_s and r, see Figure 3.1.[1]

3.1.2 The cosmological constant problem

The cosmological constant enters as a free parameter in the ΛCDM model, and must be fixed by observations. The value of the cosmological constant is often considered as the biggest mismatch between theoretical expectations and astrophysical observations (see [192–195] and references therein). From the vacuum contributions in a QFT with UV cutoff Λ_{UV}, it is expected that

$$\Lambda \propto \Lambda_{\mathrm{UV}}^2 \,, \tag{3.5}$$

where the proportionality constant is of order one. Identifying Λ_{UV} with the Planck scale M_{P}, introduced in (1.1), as the "typical" scale of QG, we expect that the cosmological constant will have a similar value. However, observations from distant supernovae [188, 189] yield

$$\Lambda_{\mathrm{obs}} = 4 \times 10^{-66}\,\mathrm{eV}^2 \simeq 10^{-120}\, M_{\mathrm{P}}^2 \,, \tag{3.6}$$

which is a gigantic 120 orders of magnitude smaller. In order to cure this discrepancy, one may envision starting out with a bare value of the cosmological constant Λ_{bare} that is chosen such that it exactly cancels the quantum contributions from the field modes. However, this would imply the fine-tuning of the value of Λ_{bare} up to 120 digits. In standard QFT, such a mechanism is absent. In that respect, the cosmological constant problem is considered a prototypical example of the naturalness problem [196].

3.1.3 Inflation

Observations from the CMB [197] show that the universe is extremely homogeneous at large scales, with temperature fluctuations of only 10^{-5} times the value of the average CMB temperature. Assuming that this homogeneity has a common causal origin, it must mean that large parts of the universe must have been in causal contact in the past. This suggests that the universe has undergone a period of accelerated expansion, called inflation [198].

The accelerated expansion can be driven by various different physical mechanisms [199]. Each mechanism gives a specific shape of the power spectrum of primordial perturbations, yielding different predictions for the spectral tilt n_s and tensor-to-scalar ratio r. These can be checked against experimental observations. Figure 3.1 shows the observational constraints measured by the Planck satellite [197]. In addition, the

[1] To date, there is no observation of the tensor spectral index n_t.

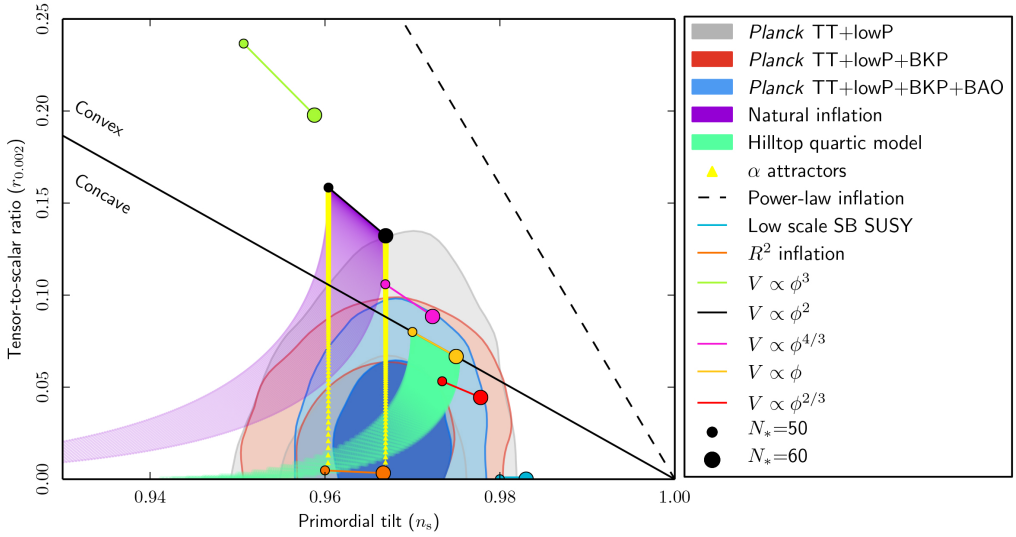

Figure 3.1: *Observational constraints on the tensor-to-scalar ratio r and the scalar spectral tilt n_s from Planck observations. The strongest constraint from observations is denoted by the blue contour. Various models for inflation give different predictions for r and n_s. Note that Starobinsky inflation (R^2-inflation), denoted by the orange line, is in excellent agreement with the observational data.*
Credit: PLANCK collaboration. Planck 2015 results. XX. Constraints on inflation. Astron. Astrophys. ***594*** *(2016) A20. [arXiv:1502.02114], reproduced with permission © ESO.*

predictions for n_s and r are shown for various models. The experimental data rule out a large number of models.

One model that seems to be favored by the observational constraints is Starobinsky inflation or R^2-inflation [200–202]. This is a special case of power-law $f(R)$-gravity, truncated at second order in R. It is given by the action[2]

$$S[g] = \frac{1}{16\pi G}\int \mathrm{d}^4x\sqrt{g}\left(2\Lambda - R + BR^2\right) . \tag{3.7}$$

At early cosmological times, the R^2-term gives rise to inflation through the classical equations of motion. If this modification of gravity drives inflation, the value of the

[2]Throughout this chapter, we will work with Euclidean signature for the metric. The Lorentzian action corresponding to Starobinsky inflation differs from (3.7) by a minus sign. We assume that the RG flows obtained from the Euclidean action contain the same information as their Lorentzian counterpart. For first studies into the construction of a functional RG flow on Lorentzian spacetimes see [55, 86].

Energy scale (eV)	Constraint
$k_{\text{infl}} = 10^{22}$	$B = -1.7 \times 10^{-46}\ \text{eV}^{-2}$
$k_{\text{lab}} = 10^{-5}$	$G = 6.7 \times 10^{-57}\ \text{eV}^{-2}$
$k_{\text{Hub}} = 10^{-33}$	$\Lambda = 4 \times 10^{-66}\ \text{eV}^{2}$

Table 3.1: *Observational constraints on the parameters of the action (3.7). For each parameter we indicate the energy scale at which the experiment is performed; these are the inflationary scale k_{infl}, laboratory scale k_{lab}, and the Hubble scale k_{Hub}.*

R^2-coupling B should be

$$B = -1.7 \times 10^{-46}\,\text{eV}^{-2} \tag{3.8}$$

at the time of inflation.

3.1.4 Scale dependence

We will now consider the $f(R)$-model in the context of the asymptotic safety scenario. In the light of the previous chapter, this suggests that the couplings Λ, G and B acquire a dependence on the energy scale k. Each coupling is then measured at a different distance scale, as explained in detail in the next section and summarized in Table 3.1.

In order to make contact with the Asymptotic Safety scenario, these constraints should be valid initial data for an asymptotically safe RG trajectory. This means that there should be an RG trajectory that satisfies the observational constraints, and furthermore is controlled by a UV fixed point at large energy scales. Within this setting, the RG trajectory should satisfy the constraints summarized in Table 3.2. The construction of a trajectory that meets all these requirements is a highly nontrivial task and constitutes the main result of this chapter.

3.2 Observational constraints on gravity

In this section we will discuss the observational constraints on the gravitational parameters in more detail.

At this point the following remark is in order. From Table 3.2, one may conclude that at each energy scale only one parameter is constrained. In the derivation, we assume that the other parameters take "reasonable" values, which we will check a posteriori. In particular, we assume that Newton's coupling G_k does not run between the scale of inflation and the laboratory scale where G is measured.

Energy scale (eV)	RG constraint
$k \gg M_{\rm P} = 2.4 \times 10^{27}$	NGFP
$k \simeq k_{\rm infl} = 10^{22}$	$B_k \simeq B_{\rm infl} = -1.7 \times 10^{-46}\ \text{eV}^{-2}$
$k \simeq k_{\rm lab} = 10^{-5}$	$G_k \simeq G = 6.7 \times 10^{-57}\ \text{eV}^{-2}$
$k \simeq k_{\rm Hub} = 10^{-33}$	$\Lambda_k \simeq \Lambda = 4 \times 10^{-66}\ \text{eV}^2$

Table 3.2: *Constraints on the action (3.7) in the RG framework. The conditions on the parameters are imposed at various scales and are the same as in Table 3.1. Moreover, we impose the condition that the RG trajectory approaches a NGFP at trans-Planckian scales $k \gg M_P$.*

3.2.1 Early-time cosmology

Assuming that the inflationary behavior of the universe originates from the R^2 term (Starobinsky inflation), we can derive a constraint on the parameter B in the action (3.7) from early-time cosmology. In the context of inflationary cosmology, it is generally assumed that the energy density of matter and the cosmological constant are negligible, in the sense that these do not alter the background dynamics significantly. We take as a working assumption that the RG flow of Λ_k does not spoil this assumption, and that the contribution from $\Lambda_{k_{\rm infl}}$ is indeed subdominant to the dynamics of the early universe.

Neglecting the cosmological constant term, the action (3.7) reduces to the Starobinsky action [200–202]. Constraints on this model can be obtained from observations of the CMB, as done by the Planck collaboration [197]. As these constraints rely on the inferred properties of the primordial perturbations when they left the Hubble horizon, we take the Hubble parameter at that time as the relevant energy scale:

$$k_{\rm infl} = H_{\rm infl} \simeq 10^{22}\ \text{eV}\,. \tag{3.9}$$

Constraints on inflationary models are usually parameterized in terms of an inflaton-field potential [197, 199]. At the classical level, an $f(R)$ action can be mapped into an action for gravity coupled to an inflaton field φ with potential $V(\varphi)$. The function f can then be related to the potential V. Following the derivation of Appendix B, the action (3.7) leads to the following potential:

$$V(\varphi) = \frac{M_{\rm P}^2}{8B}\left(1 - \mathrm{e}^{-\sqrt{2/3}\varphi/M_{\rm P}}\right)^2\,. \tag{3.10}$$

This characterizes the Higgs inflation model [203, 204]. Observations of the scalar spectral tilt n_s and the tensor-to-scalar ratio r put the following constraint on the value of

B [202, 205, 206]:

$$M \simeq 3.3 \times 10^{-3} M_{\rm P}\,, \tag{3.11}$$

where $M^4 = -\frac{M_{\rm P}^2}{8B}$. Written in terms of B_k, this implies the constraint

$$M_{\rm P}^2 B_k \simeq -1 \times 10^9\,, \tag{3.12}$$

with k taken at horizon crossing, $k = k_{\rm infl}$.

3.2.2 Late-time cosmology

Late-time cosmology is sensitive only to the value of the cosmological constant at very low energy scales, corresponding roughly to the current value of the Hubble parameter. Thus, we take

$$k_{\rm Hub} = 10^{-33}\ {\rm eV}\,. \tag{3.13}$$

While for early-time dynamics we assumed that action is dominated by the R^2-term, we take as working hypothesis here that the late-time dynamics of the universe is described by the Einstein-Hilbert action, compatible with the ΛCDM model discussed in subsection 3.1.1. As at this stage the curvature R is assumed to be small, we neglect the R^2-term as long as the RG flow does not drive B to extremely large values.

Current observations are in full agreement with a universe dominated at late times by a $2\Lambda - R$ action [207]. Specifically, the cosmological constant density parameter takes the value

$$\Omega_\Lambda \simeq 0.7\,. \tag{3.14}$$

Together with the current value of the Hubble parameter [208],

$$H_0 \simeq 70\ {\rm km\ s^{-1} Mpc^{-1}}\,, \tag{3.15}$$

we arrive at the following estimate:

$$\begin{aligned} \Omega_\Lambda \equiv \frac{\rho_{\rm vac}}{\rho_c} &= \frac{\Lambda}{8\pi G}\frac{8\pi G}{3H_0^2} \\ \Rightarrow \Lambda = \Omega_\Lambda \cdot 3H_0^2 &\simeq 4 \times 10^{-66}\ {\rm eV}^2\,. \end{aligned} \tag{3.16}$$

3.2.3 Measurements of Newton's constant

Current measurements of Newton's constant are based on laboratory experiments, made on a scale of about $10^{-2} - 10^{0}$ m [208]. This corresponds to an energy scale of $10^{-4} - 10^{-6}$ eV. Thus, we take

$$k_{\rm lab} \simeq 10^{-5}\ {\rm eV}\,. \tag{3.17}$$

At this length scale, Newton's coupling is measured to be [208]

$$G = 6.7 \times 10^{-57}\ \mathrm{eV}^{-2}\,. \tag{3.18}$$

As this measurement is obtained from a local experiment that is governed by Newtonian gravity, the cosmological constant and the R^2-coupling do not influence this result.

3.3 An RG approach to gravity

In this section, we will present the RG flow equations that govern the running of the coupling constants. We will discuss the construction of the flow equation for $f(R)$-gravity, as studied in e.g. [63, 64, 85]. As a first investigation, we will consider the case where $f(R)$ reduces to the Einstein-Hilbert action, i.e. we maintain only the cosmological constant and Newton's coupling. After that, we consider the case where the R^2-coupling comes into play. This analysis extends the earlier work [101].

We now put into practice the methods developed in chapter 2. In order to calculate the RG flow of gravity, we employ the background field method using the linear split (2.29). Following (2.32), we then start with the truncation of the effective average action

$$\Gamma_k[g, c, \bar{c}; \bar{g}] \simeq \Gamma_k^{\mathrm{grav}}[g] + \Gamma_k^{\mathrm{gf}}[g; \bar{g}] + S^{\mathrm{gh}}[g, c, \bar{c}; \bar{g}]\,, \tag{3.19}$$

where we use (2.33) and (2.35) for the gauge-fixing action and ghost action, respectively. To simplify the computations, we will set the gauge-fixing parameters α and β to

$$\alpha = 1\,, \qquad \beta = \frac{d}{2} - 1\,, \tag{3.20}$$

implementing harmonic gauge.

The operators of physical interest are contained in $\Gamma_k^{\mathrm{grav}}[g]$. For this, we will use the $f(R)$-action

$$\Gamma_k^{\mathrm{grav}}[g] = \frac{1}{16\pi G_k} \int \mathrm{d}^d x \sqrt{g}\, \bar{f}_k(R)\,, \tag{3.21}$$

where R denotes the Ricci scalar.

Inserting the ansatz (3.19) into the FRGE (1.13), we can obtain the k-dependence of G_k and $\bar{f}_k$ by projecting on actions of $f(R)$-type. The result is a partial differential equation for $\bar{f}_k(R)$. The flow equations are conveniently parameterized in terms of the dimensionless quantities

$$r = k^{-2} R\,; \qquad f_k(r) = k^{-2} \bar{f}_k(R)\,, \tag{3.22}$$

as well as the dimensionless Newton's coupling $g_k = k^2 G_k$ that was introduced in (1.9). By now, several incarnations of these flow equations have been constructed, using different choices for the gauge-fixing and parameterization of the fluctuation field [53, 63, 64, 67, 70, 71, 85, 98, 99].

3.3.1 The Einstein-Hilbert projection

As a first study, we will consider the projection onto the Einstein-Hilbert action, setting $B = 0$ in the action (3.7). Following the steps in [102], we arrive at the β-functions for the dimensionless Newton coupling g_k and the cosmological constant $\lambda_k = k^{-2}\Lambda_k$:

$$\begin{aligned} \partial_t g_k &= (d - 2 + \eta_N)\, g_k \\ \partial_t \lambda_k &= g_k\,(L_1 + \eta_N L_2) - (2 - \eta_N)\,\lambda_k\,, \end{aligned} \tag{3.23}$$

where again we have encountered the anomalous dimension of Newton's coupling η_N, defined in (1.11). The anomalous dimension η_N is of the form

$$\eta_N = \frac{B_1}{1 - g_k B_2} g_k\,. \tag{3.24}$$

The coefficients L_i and B_j are given by

$$\begin{aligned} B_1 &= \frac{1}{3}(4\pi)^{1-d/2}\Big(d(d+1)\Phi^1_{d/2-1}(-2\lambda) - 4d\Phi^1_{d/2-1}(0) \\ &\qquad - 6d(d-1)\Phi^2_{d/2}(-2\lambda) - 24\Phi^2_{d/2}(0)\Big) \\ B_2 &= -\frac{1}{6}(4\pi)^{1-d/2}\left(d(d+1)\tilde{\Phi}^1_{d/2-1}(-2\lambda) - 6d\tilde{\Phi}^2_{d/2}(-2\lambda)\right) \\ L_1 &= (4\pi)^{1-d/2}\left(d(d+1)\Phi^1_{d/2}(-2\lambda) - 4d\Phi^1_{d/2}(0)\right) \\ L_2 &= -\frac{1}{2}(4\pi)^{1-d/2} d(d+1)\tilde{\Phi}^1_{d/2}(-2\lambda)\,. \end{aligned} \tag{3.25}$$

The threshold functions $\Phi^p_n(w)$ and $\tilde{\Phi}^p_n(w)$ defined as

$$\begin{aligned} \Phi^p_n(w) &\equiv \frac{1}{\Gamma(n)}\int_0^\infty \mathrm{d}z\, z^{n-1}\frac{r(z) - z r'(z)}{(z + r(z) + w)^p} \\ \tilde{\Phi}^p_n(w) &\equiv \frac{1}{\Gamma(n)}\int_0^\infty \mathrm{d}z\, z^{n-1}\frac{r(z)}{(z + r(z) + w)^p}\,. \end{aligned} \tag{3.26}$$

Using the Litim regulator [209], these integrals are particularly simple and can be evaluated to

$$\Phi^p_n(w)\big|_{\text{Litim}} = \frac{1}{\Gamma(n+1)}\frac{1}{(1+w)^p}\,; \qquad \tilde{\Phi}^p_n(w)\big|_{\text{Litim}} = \frac{1}{\Gamma(n+2)}\frac{1}{(1+w)^p}\,. \tag{3.27}$$

We now set $d = 4$ and evaluate the flow equations. The β-functions (3.23) define a flow through the parameter space spanned by g and λ. An overview of the phase diagram is given in Figure 3.2.

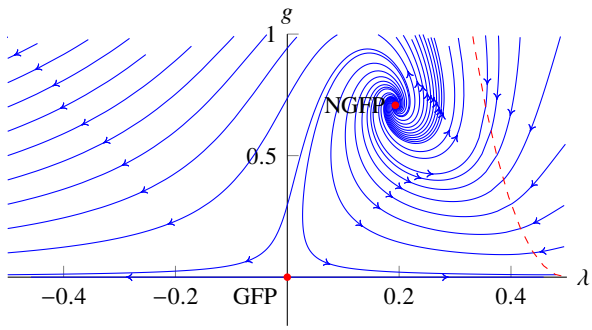

Figure 3.2: *Phase diagram of the Einstein-Hilbert projection. The fixed points are indicated by red dots, flow lines by blue arrows. The red line denotes the singularity in η_N. First obtained in [102].*

The RG flow is essentially controlled by two fixed points. First, we find a Gaussian fixed point, located at

$$g_* = \lambda_* = 0\,. \tag{3.28}$$

Second, we find a NGFP at the values

$$\lambda_* = 0.193\,; \qquad g_* = 0.707\,. \tag{3.29}$$

Linearizing the flow around the GFP, we find the canonical mass dimensions for the critical exponents:

$$\text{GFP:} \qquad \theta_1 = +2\,; \qquad \theta_2 = -2\,. \tag{3.30}$$

For the NGFP, we find the complex critical exponents

$$\text{NGFP:} \qquad \theta_{1,2} = 1.48 \pm 3.04i\,. \tag{3.31}$$

The positive real part shows that the NGFP is UV-attractive. The nonzero complex parts indicate a spiraling behavior around the fixed point. As the NGFP is UV-stable, it is a suitable candidate for the Asymptotic Safety scenario.

In addition, (3.23) shows that the locus $g = 0$ is a root of β_g. This implies that the RG flow cannot cross this line, as is visible in Figure 3.2. Since the measured value of Newton's constant is positive, RG trajectories in the region $g < 0$ do not correspond to the RG flow realized in nature. Furthermore, the anomalous dimension η_N has a singularity at $gB_2 = 1$. This is depicted as a dashed red line in Figure 3.2, where the flow changes direction.

We finish the discussion of the Einstein-Hilbert phase diagram by the following remark. The critical exponent θ_2 associated to the g-direction implies that the dimensionless Newton's coupling g_k runs proportional to k^2 in the vicinity of the GFP. Thus, we observe

that in this region the dimensionful Newton's coupling G_k freezes out. We identify this with a semi-classical regime.

3.3.2 RG flow of the R^2-system

We now turn to the system that includes higher powers of the curvature. A first study of the RG flow of higher-curvature truncations has been carried out in [84]. At the level of polynomial expansions, systematic searches have been done up to order R^6 [64, 85], R^8 [63], R^{35} [76, 77] and recently R^{70} [78].

We will use the flow equations for $f(R)$-gravity derived in [85], listed in Appendix C. We then project the flow equations onto the terms r^0, r^1 and r^2, in order to determine the scale-dependence of the action (3.7). Using the dimensionless couplings

$$\lambda_k\,, \qquad g_k\,, \qquad b_k = B_k k^2\,, \tag{3.32}$$

the β-functions

$$\partial_t \lambda_k = \beta_\lambda\left(\lambda_k, g_k, b_k\right)\,, \qquad \partial_t g_k = \beta_g\left(\lambda_k, g_k, b_k\right)\,, \qquad \partial_t b_k = \beta_b\left(\lambda_k, g_k, b_k\right) \tag{3.33}$$

can then be obtained from solving the system of linear equations listed in (C.9).

Fixed points, singularities and separation lines

As in the Einstein-Hilbert projection, we find a GFP located at

$$\text{GFP:} \qquad \lambda_* = g_* = b_* = 0\,. \tag{3.34}$$

In addition, the NGFP generalizes in the three-dimensional parameter space to

$$\text{NGFP:} \qquad \lambda_* = 0.133\,, \qquad g_* = 1.59\,, \qquad b_* = 0.119\,. \tag{3.35}$$

The dimensionless coupling multiplying the R^2-term takes the value

$$\frac{b_*}{16\pi g_*} = 1.5 \times 10^{-3}\,. \tag{3.36}$$

Linearizing the flow around the GFP, we find the canonical critical exponents

$$\text{GFP:} \qquad \theta_1 = +2\,, \qquad \theta_2 = -2\,, \qquad \theta_3 = -2\,. \tag{3.37}$$

Analyzing the eigendirections shows that the GFP is UV-attractive in the $g = 0$ plane and UV-repulsive in the other eigendirections. This confirms perturbative non-renormalizability, as discussed in subsection 1.2.2.

For the NGFP, the critical exponents read

$$\text{NGFP:} \qquad \theta_{1,2} = 1.26 \pm 2.45i\,, \qquad \theta_3 = 27.0\,, \tag{3.38}$$

indicating that the NGFP is UV-attractive in all directions. The large positive eigenvalue θ_3 is typical for the R^2 system (see e.g. [84]), and reduces significantly when higher-order curvature terms are included [64, 76, 85].

Apart from the fixed points, the RG flow is controlled by the singularity structure of the β-functions. The region containing the GFP and NGFP is constrained by two singular surfaces where the β-functions diverge. These two surfaces are pictured in Figure 3.3a, labeled "A" and "B". The surface A is parabola-shaped and runs approximately parallel to the b-axis. RG trajectories flowing towards positive values of λ for small k will terminate at A. The surface B extends approximately parallel to the λ-axis, and bounds trajectories flowing towards positive b. However, we find that RG trajectories typically do not terminate at B, since they are repelled once they come close to it.

Finally, we observe that also for the R^2-system the β-function β_g vanishes in the plane $g = 0$. Thus, the RG flow cannot cross this plane. As in subsection 3.3.1, we conclude that since the observed value of Newton's constant is positive, the quadrants where $g < 0$ can be classified as unphysical.

3.3.3 Construction of sample trajectories

We continue our study of the R^2-phase diagram by constructing explicit sample solutions. These are obtained by integrating the flow equations numerically. Our primary focus is on RG trajectories that emanate from the NGFP in the UV and undergo a crossover to the GFP as the RG time t is lowered. Typical examples of trajectories showing this behavior are depicted in Figure 3.3b. Following the discussion in [101, 104, 166], it is this type of solutions that gives rise to a classical regime resembling GR at low energy.

Following the classification in [104], we distinguish trajectories by the IR value of the cosmological constant. Similar to the Einstein-Hilbert case, one finds trajectories that flow towards negative cosmological constant (Type Ia, blue curves), positive Λ (Type IIIa, red curves) and towards vanishing Λ (Type IIa, orange curves). Typically, trajectories of Type IIIa terminate at the singular locus A as $k \to 0$.

In addition to the cosmological constant, one can also track the R^2-coupling b along the RG flow. We find that b tends to zero as $k \to 0$ for all trajectories. Let us first consider trajectories that flow towards $b \to 0$ from positive b. Starting in the IR and following the flow towards the UV, we find that such an RG trajectory first approaches the GFP, and then makes a sharp turn towards positive b. As it approaches the singularity B, it is eventually repelled in the direction of the NGFP. The fixed point then provides the UV completion as $t \to \infty$.

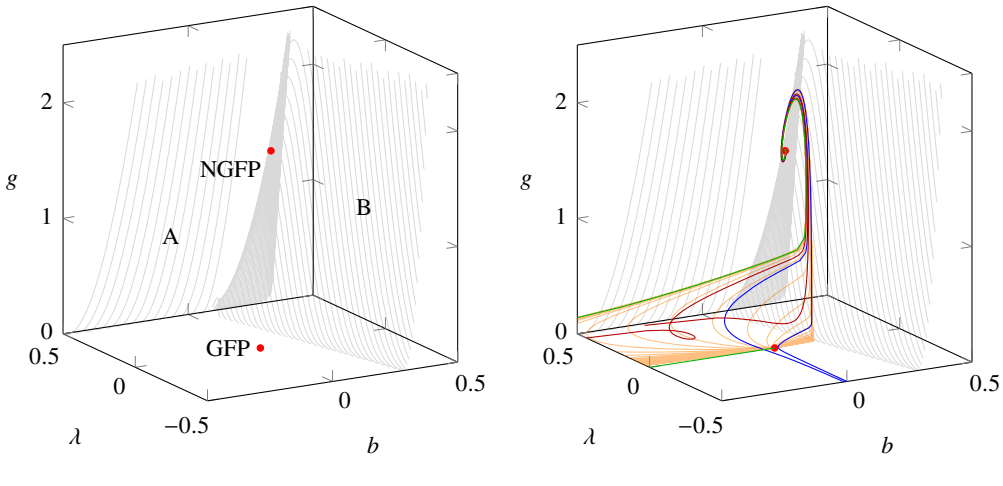

Figure 3.3: *Overview of the flow diagram obtained from the R^2-truncation.*
3.3a: *the GFP (3.34) and NGFP (3.35) are marked by the red dots. The singular planes stretch out in negative-b direction (A) and in negative-λ direction (B). Note that the singular planes do not disconnect the fixed points. This opens up the possibility for a crossover trajectory from the NGFP to the GFP, which is required for a viable semiclassical regime.*
3.3b: *selected RG trajectories. The red curves lead to a positive IR value of the cosmological constant and are denoted as Type IIIa-trajectories. These trajectories terminate in the singular plane A. The blue curves lead to a negative IR value of the cosmological constant and are denoted as Type Ia-trajectories. These avoid all singularities. The orange curves denote trajectories of Type IIa, defined as the separatrix of trajectories of Types Ia and IIIa. The IR limit of Type IIa trajectories is the GFP. Finally, the green curve marks the trajectory that meets the observational constraints given in Table 3.2.*

In contrast, a trajectory starting at $b \to 0$ from negative b that has passed the GFP makes a turn towards negative b. After obtaining a minimal value for b, it makes a sharp turn and flows back in the direction of the GFP before it crosses over to the NGFP regime. The flow of trajectories of this type may be bounded by the singular plane A. This ceiling may prevent solutions from reaching the basin of attraction of the NGFP so that they terminate at a finite value of t.

3.4 Trajectories consistent with observations

We are now in the position to look for an RG trajectory that satisfies all the conditions listed in Table 3.2. Since constraints listed in this table are imposed at different energy scales, the search of the corresponding RG trajectory is a rather complicated boundary value problem. In order to convert this setup into an initial value problem, we study the small-g expansion of the system in subsection 3.4.1 before constructing the RG trajectory numerically in subsection 3.4.2. The main result of this section is the trajectory displayed in Figure 3.5 which meets all cosmological requirements.

3.4.1 Initial values from the perturbative expansion

In this section, we construct initial data that serves as a starting point for the numerical integration of an RG trajectory compatible with cosmological observations. As a first study, we analyze the Einstein-Hilbert projection described in subsection 3.3.1. We then extend the calculation to include the R^2-coupling.

The Einstein-Hilbert case

Let us first consider the possibility of an RG trajectory that is consistent with the observed values for Newton's coupling and the cosmological constant. We observe that Newton's coupling has a value of the order 10^{-57} eV^{-2} at an energy scale $k_{\text{lab}} \simeq 10^{-5}$ eV. This indicates that the dimensionless parameter $g_k = k^2 G_k$ at k_{lab} has a very small value. Thus, an RG trajectory should reach a classical regime $g \ll 1$.

This motivates the expansion of the β-functions around $g = 0$. In order to obtain expanded flow equations that can be solved exactly, we write the β-functions in terms of the new couplings

$$g_k\,; \qquad \alpha_k = \lambda_k g_k\,. \tag{3.39}$$

Up to second order in g, the expanded β-function for g then reads

$$\partial_t g \simeq 2g - \frac{7}{3\pi} g^2\,. \tag{3.40}$$

The analytic solution then reads

$$g_k = \frac{g_{k_0} k^2}{k_0^2 + \frac{7}{6\pi} g_{k_0} \left(k^2 - k_0^2\right)}\,, \tag{3.41}$$

where g_{k_0} denotes an integration constant that specifies a particular RG trajectory. Restoring the dimensionful Newton's coupling, we obtain

$$G_k = \frac{1}{1 + \frac{7}{6\pi} G_{k_0} \left(k^2 - k_0^2\right)} G_{k_0}\,, \tag{3.42}$$

in accordance with [120]. Indeed, for $k^2 - k_0^2 \ll G_{k_0}$ Newton's coupling is approximately constant. Quantum corrections only occur as

$$k^2 \sim k_0^2 + \frac{6\pi}{7} G_{k_0}^{-1} \equiv k_G^2 \,. \tag{3.43}$$

At energies above the scale k_G, Newton's coupling is driven to zero quadratically.

For the cosmological constant, we expand the β-function for α_k up to second order in g:

$$\partial_t \alpha \simeq -\frac{14}{3\pi}\alpha g - \frac{11}{3\pi} g^2 \,. \tag{3.44}$$

Also this flow equation can be solved analytically:

$$\alpha_k = \frac{\alpha_{k_0} + \frac{11}{12\pi} g_{k_0}^2 \left(1 - k^4/k_0^4\right)}{\left(1 + \frac{7}{6\pi} g_{k_0} \left(k^2/k_0^2 - 1\right)\right)^2} \,. \tag{3.45}$$

This gives the following running for Λ_k [120]:

$$\Lambda_k = \alpha_k / G_k = \frac{\Lambda_{k_0} - \frac{11}{12\pi} G_{k_0} \left(k^4 - k_0^4\right)}{1 + \frac{7}{6\pi} G_{k_0} \left(k^2 - k_0^2\right)} \,. \tag{3.46}$$

For sufficiently small values of Λ_{k_0} this equation entails three scaling regimes of the cosmological constant. First of all, we observe that the denominator changes the running of Λ_k similar to G_k, starting at k_G. For $k \gg k_G$, the scale-dependence of Λ_k is governed by the NGFP and the cosmological constant grows quadratically. Secondly, the numerator introduces a new scale

$$k^4 \sim k_0^4 + \frac{12\pi}{11} \frac{\Lambda_{k_0}}{G_{k_0}} \equiv k_\Lambda^4 \,. \tag{3.47}$$

For $k \ll k_\Lambda$, Λ_k enters a classical regime where it freezes out. Between k_Λ and k_G, the running of Λ is proportional to k^4.

If $k \simeq k_0$, the dimensionful Newton's coupling is constant up to corrections of the order $k^2 - k_0^2$. Thus, the identification $k_0 = k_{\text{lab}}$ is convenient since this corresponds to the scale where G_k is measured. Evaluating (3.43) with this initial condition gives a value of k_G of the order of the Planck scale.

Inserting the measured value of the dimensionful Newton's constant into the dimensionless relation gives

$$g_{k_0} = 6.71 \times 10^{-67} \,. \tag{3.48}$$

Similarly, inserting $k \simeq k_{\text{Hub}}$ into the solution (3.45) allows us to calculate the value of α at laboratory scale:

$$\alpha_{k_0} = 2.68 \times 10^{-122} \,. \tag{3.49}$$

The initial values (3.48) and (3.49) serve as a starting point for a trajectory in the Einstein-Hilbert projection.

The R^2-case

We now extend the analysis from the previous subsection to include the R^2-coupling. We again set $k_0 = k_{\text{lab}}$ and write the flow in terms of the couplings g_k and α_k, as well as the additional dimensionless coupling

$$\beta_k = \frac{b_k}{16\pi g_k} \,. \tag{3.50}$$

In this way, we are able to solve the flow equations expanded in g.

Expanding the flow equations (3.33) up to second order in g gives the expressions[3]

$$\partial_t g \simeq 2g - \frac{23}{24\pi} g^2 \,, \qquad \partial_t \alpha \simeq -\frac{23}{12\pi}\alpha g - \frac{5}{12\pi} g^2 \,. \tag{3.51}$$

This leads to the solutions

$$g_k = \frac{k^2 g_{k_0}}{k_0^2 + \frac{23}{48\pi} g_{k_0}\left(k^2 - k_0^2\right)} \,, \qquad \alpha_k = \frac{\alpha_{k_0} + \frac{5}{48\pi} g_{k_0}^2 \left(1 - k^4/k_0^4\right)}{\left(1 + \frac{23}{48\pi} g_{k_0}^2 \left(k^2/k_0^2 - 1\right)\right)^2} \,. \tag{3.52}$$

Expanding the RG equation for β up to first order in g gives[4]

$$\partial_t \beta = \frac{109}{2160\pi^2} + \mathcal{O}(g) \,. \tag{3.53}$$

The solution of this equation is

$$\beta_k = \frac{109}{2160\pi^2} \log\left(\frac{k}{k_0}\right) + \beta_{k_0} \,. \tag{3.54}$$

This is the typical logarithmic running of a marginal coupling at one-loop level. Inserting the measured values at k_{infl} gives the initial value

$$\beta_{k_0} = -5.0 \times 10^8 \,. \tag{3.55}$$

Combining the results (3.48), (3.49) and (3.55), one readily arrives at the initial values for g_k, λ_k and b_k:

$$g_{k_0} = 6.71 \times 10^{-67} \,, \qquad \lambda_{k_0} = 3.99 \times 10^{-56} \,, \qquad b_{k_0} = -1.7 \times 10^{-56} \,. \tag{3.56}$$

This completes the starting point for numerical integration of the flow equation in the R^2-system.

[3] Compared to subsection 3.3.1, we have used a slightly different gauge-fixing and regulator. This yields slightly different numerical prefactors in (3.52); other qualitative and quantitative features remain the same up to high numerical precision.

[4] Expanding the flow equation up to second order in g gives a differential equation that cannot be solved analytically.

3.4.2 Constructing the RG trajectory realized by nature

Using the initial conditions derived in the previous section, we can now integrate the full β-functions. We use the numerical NDSolve routine in Mathematica. In order to keep track of the propagation of the small values of the initial conditions, we increase the working precision to 124 digits. As soon as the RG flow has reached a regime where the couplings take larger values, we reduce the precision to 25 digits to increase the speed of the computation. This allows tracking the RG flow from the classical regime up to the NGFP.

We first consider the Einstein-Hilbert case. The running of the dimensionful couplings Λ_k and G_k is depicted in Figure 3.4. The energy scales at which the observational constraints are imposed are marked by gray bars, and the typical scales k_G and k_Λ by a gray dashed bar.

We observe several remarkable features in Figure 3.4. First of all, we note that the trajectory indeed matches all observational constraints. Therefore, the expansion in small g is valid, and quantum effects only play a role at energy scales beyond inflation. We note that Newton's coupling starts to run at 10^{27} eV, which is in the same ballpark as the dynamically generated scale $k_G \simeq 10^{28}$ eV. For energy scales $k \gtrsim k_G$, Newton's coupling reaches a very small value.[5] For energies above k_G, Newton's coupling enters the fixed point regime, where G_k is driven to zero quadratically in k.

Secondly the cosmological constant Λ_k starts to run at $k_\Lambda \simeq 10^{-2}$ eV, corresponding to the length scale of 10^{-4} m. For $k < k_\Lambda$, Λ_k is constant and equal to the value quoted in Table 3.2. This is in agreement with the current measurements, that take place over cosmological scales. At intermediate energies $k_\Lambda \lesssim k \lesssim k_G$, the cosmological constant scales as $\Lambda_k \propto k^4$. Above the scale k_G, the cosmological constant is in the fixed point regime where it increases quadratically in k.

We now consider the R^2-system. Integrating the flow numerically from the initial conditions (3.56), we obtain an RG trajectory ranging from the Hubble scale $k_{\rm Hub}$ up to the NGFP. This solution is depicted as the green curve in Figure 3.3b. The running of the dimensionful couplings Λ_k, G_k and B_k is summarized in Figure 3.5. The values of the couplings at the relevant energy scales are presented in Table 3.3. The existence of this RG trajectory constitutes the main result of this chapter.

Qualitatively, the running of Λ_k and G_k follows the same pattern as in the Einstein-Hilbert truncation. Newton's coupling starts to run at an energy scale above the upper bound of the inflation scale of 10^{22} eV, which validates the assumption that quantum effects start to play a role beyond $k_{\rm infl}$. Compared to the flow of the Einstein-Hilbert truncation, we observe that the scale at which the running of G_k starts is shifted a few orders of magnitude towards the infrared, due to corrections stemming from the

[5] Cosmological consequences of a Planck-scale-vanishing Newton's coupling were discussed from a different perspective in [210, 211].

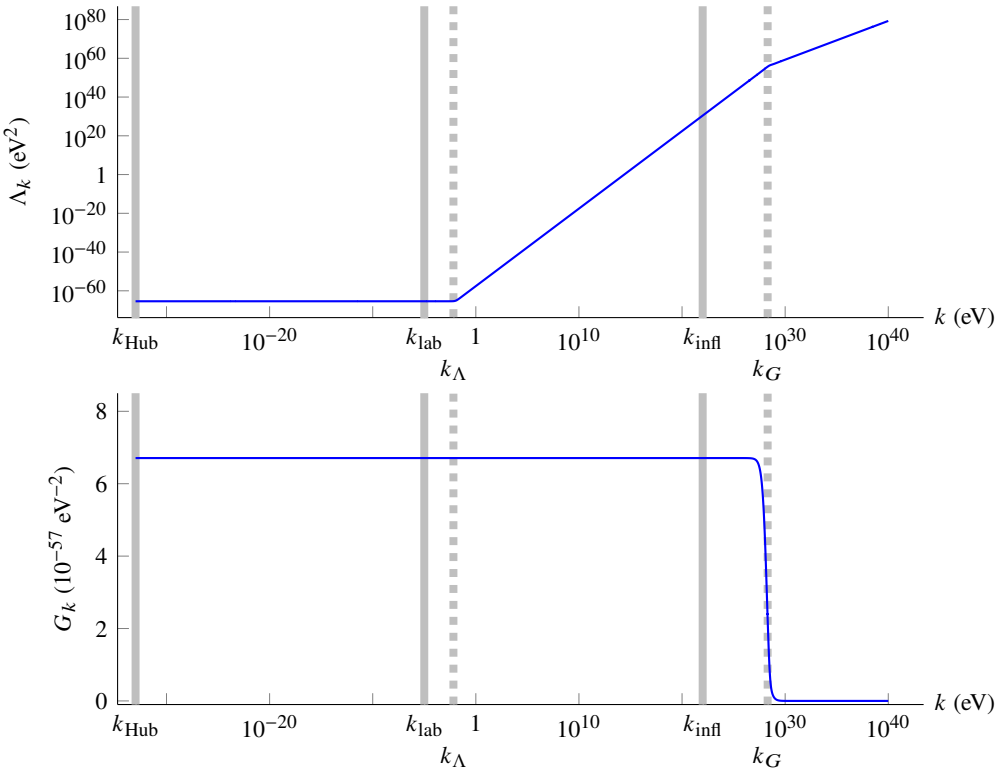

Figure 3.4: *RG trajectory satisfying cosmological constraints in the Einstein-Hilbert truncation. Top panel: cosmological constant Λ_k. Bottom panel: Newton's coupling G_k. The solid gray bars indicate the energy scales at which constraints are imposed; the dashed gray bars denote the energy scales k_G and k_Λ that are generated by the RG flow.*

R^2-coupling. However, this shift does not affect the analysis at the inflationary scale.

The R^2-coupling B_k itself remains constant and negative up to the same energy scale, after which it starts to increase. Crossing over to positive values at $k \simeq 10^{30}$ eV, it decreases quadratically as it enters the fixed point regime. Note that the positive sign of the fixed point value of b leads to so-called "stable inflation". Along the RG trajectory, we find a cross-over from positive to negative b, which then realizes the "unstable inflation"-scenario analyzed in [206].

We close this section by verifying the working assumptions in section 3.2 that the couplings take reasonable values. At the inflation scale, the assumption is that the cosmological constant does not affect the inflationary dynamics. This amounts to checking that the condition $\Lambda_k/\left(B_k R^2\right) \ll 1$ is valid when evaluated at $k = k_{\rm infl}$. Using the fact

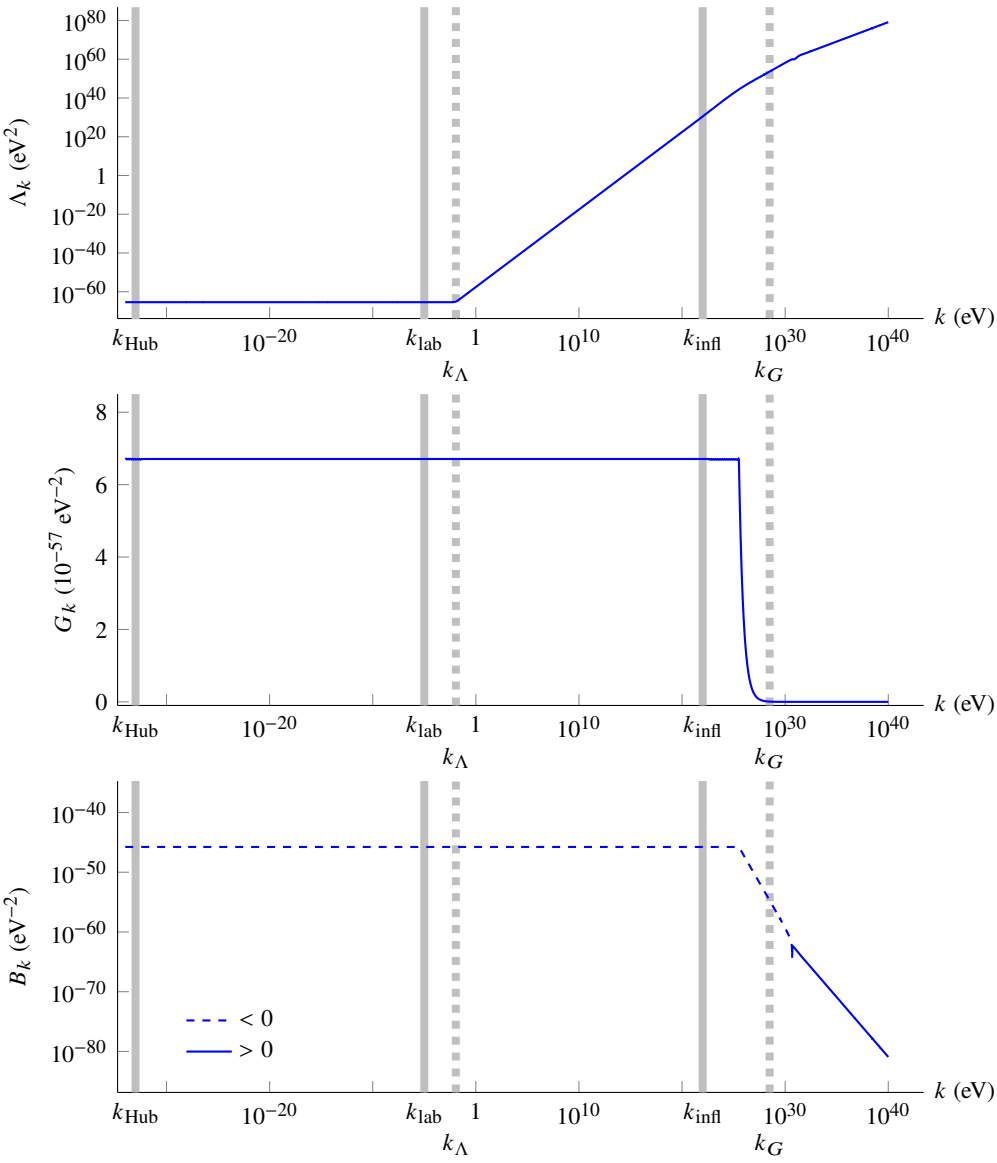

Figure 3.5: *RG trajectory passing through all points identified in Table 3.2. Top panel: cosmological constant Λ_k . Middle panel: Newton's coupling G_k . Bottom panel: R^2-coupling B_k . The gray bars indicate the energy scales at which constraints are imposed.*

Energy scale (eV)	Λ (eV^2)	G (10^{-57} eV^{-2})	B (10^{-46} eV^{-2})
$k_{\rm Hub} \simeq 10^{-33}$	$\mathbf{4 \times 10^{-66}}$	6.71	-1.7
$k_{\rm lab} \simeq 10^{-5}$	4×10^{-66}	**6.71**	-1.7
$k_{\rm infl} \simeq 10^{22}$	4×10^{30}	6.71	$\mathbf{-1.7}$

Table 3.3: *Selected values of the RG flow satisfying cosmological constraints. The parameters are constant, within numerical accuracy. The exception to this is the cosmological constant Λ. The bold values are constrained by observations, while the other values are predictions from the RG trajectory.*

that in approximately de Sitter background the scalar curvature is related to the Hubble parameter as $R = 12H^2$ and $H = k_{\rm infl}$, we find

$$\left.\frac{\Lambda_k}{B_k R^2}\right|_{k=k_{\rm infl}} \simeq 4 \times 10^{-15} \ll 1 \,. \tag{3.57}$$

Thus, our working assumptions at the inflation scale are indeed valid.

For the late-time cosmological dynamics, we have to check that the R^2-term does not affect the background universe evolution at $k_{\rm Hub}$. Again making use of the approximation that at late times we are in a quasi-de Sitter space, we find

$$B_k R^2 \simeq 10^{-161}\ \text{eV}^2 \,, \qquad \Lambda_k \simeq 10^{-66}\ \text{eV}^2 \,, \qquad R \simeq 10^{-65}\ \text{eV}^2 \,. \tag{3.58}$$

This establishes that the R^2-term can be neglected compared to the Einstein-Hilbert action. This validates the working assumptions made at the beginning of this chapter.

3.5 Conclusion

In this chapter, we have undertaken a first study in the application of the Asymptotic Safety scenario to cosmology. Starting with a review of the Einstein-Hilbert truncation, we have seen how to construct the RG flow of Newton's coupling and the cosmological constant. This exemplifies the ideas of chapter 1. For the Einstein-Hilbert truncation, we have shown the existence of a UV-attractive fixed point, providing a suitable completion of the QFT at high energies.

The existence of a NGFP persists if one includes a coupling tracking the flow of $\int \sqrt{g} R^2$. The fixed point is shown to have three relevant directions, giving rise to a three-dimensional UV-critical hypersurface. We have studied the phase diagram of this

system, and have investigated the possibility of an RG trajectory crossing over from the NGFP regime to a classical regime where Newton's coupling has frozen out.

We then turned to the construction of an RG trajectory that is compatible with cosmological observations. Starting from the seminal works [119, 120], cosmological scenarios based on modified gravitational dynamics have been studied extensively in various settings, as the result of scale-dependent couplings [114, 115, 118, 122, 165, 212–214], dilaton gravity [169, 215], Higgs inflation-inspired models [167, 216], non-Gaussian fixed point driven inflation [113, 116, 117], and anisotropic models [217]. All these investigations use a so-called RG -improvement which relates the RG scale k to a physical quantity like the Hubble scale or the Ricci scalar R in order to capture the "leading quantum gravity effects" of the system. These studies have raised the expectation that the early universe undergoes a period of power-law inflation and exhibits an almost-flat scalar power spectrum [121].

In contrast, the analysis described in this chapter matches RG data to cosmological constraints, without invoking the RG improvement procedure making a scale identification that feeds into the effective equations of motion. By solving the RG equations, we obtain the explicit running of the coupling constants Λ_k, G_k and B_k. The running of these couplings was then tested against the cosmological observations described in Table 3.2.

Studying the space of trajectories compatible with Asymptotic Safety provides two striking insights. Firstly, there are RG trajectories that are compatible with the measured values of Newton's coupling and the cosmological constant obtained at laboratory and Hubble scales, respectively. Moreover, an R^2-term can be included in the analysis that gives rise to a phase of early-time inflation, without spoiling the late-time cosmological evolution. The initial conditions for this cosmological model below the Planck scale are determined by the NGFP governing the gravitational dynamics above the Planck scale; we have explicitly constructed a trajectory emanating from the NGFP that gives rise both to the correct low-energy physics, as well as a realization of an inflationary phase that is in agreement with observations. Thus, Asymptotic Safety may give rise to Starobinsky inflation without introducing an ad hoc inflaton field. In this sense, the construction is minimal in attributing observed phenomena in early and late time dynamics of the universe to quantum gravity effects.[6]

Secondly, the constructed trajectories show how the RG flow may introduce new scales dynamically. As is illustrated in Figure 3.4 and Figure 3.5, the RG flow undergoes a crossover to a classical regime where the dimensionful couplings become constant. This crossover sets a scale which we identify as (of the order of) the Planck scale $M_{\rm P}$. This scale is generated dynamically when the RG flow leaves the scale-invariant regime associated to the NGFP. Similar to $\Lambda_{\rm QCD}$, it must be determined by experimental observation. Solutions to the flow equations also show that the Asymptotic Safety scenario is compatible with

[6]For a similar discussion at the level of effective field theory see [218, 219].

the small value of the cosmological constant. The observed value $\Lambda_{\rm obs}$ may be taken as an experimental input, fixing one of the initial conditions of the RG flow around the fixed point. While this viewpoint does not gives an explanation for the small value of the cosmological constant, it does ensure that one obtains a consistent theory ranging from cosmic to ultraviolet scales.

We close this chapter with an outline for future work. Investigations into higher orders in powers of the curvature have shown that classical power counting still provides a good guiding principle for determining the relevance of an interaction [75–78, 112], lending support to the general arguments [52] that the set of relevant interactions will be finite. As irrelevant interactions are constrained by Asymptotic Safety, the inclusion of these interactions will provide conditions on the space of couplings that may lead to testable predictions.

Furthermore, it is clear that the addition of matter fields will give contributions to the β-functions [60, 107, 130]. Naturally, this will give rise to different properties of a non-Gaussian fixed point, such as position and stability coefficients. At least for the class of gravity-dominated fixed points, these properties are qualitatively similar to the properties described in this chapter. Therefore, it is expected that the scenario developed here carries over to these cases as well. Naturally, it would be interesting to study the scale dependence of the cosmological parameters taking into account contributions from phase transitions in the matter sector, such as electroweak symmetry breaking (see [192–194] for discussions on this topic). However, since investigations into this direction have shown that these analyses grow in complexity rather quickly (see [136, 220, 221] for studies including Higgs phase transitions), this is left for follow-up investigations.

CHAPTER 4

AVOIDING OSTROGRADSKI INSTABILITIES WITHIN ASYMPTOTIC SAFETY

The following chapter is based on:

> D. Becker, C. Ripken, and F. Saueressig. *On avoiding Ostrogradski instabilities within Asymptotic Safety*. *J. High Energy Phys.* **12** (2017) 121. [arXiv:1709.09098].

Additional computational details are relegated to the accompanying Appendix D.

4.1 Introduction

In the previous chapters, we have seen how functional methods can be used to study the Asymptotic Safety scenario of quantum gravity. We have studied the RG flow of an $f(R)$-truncation and identified a non-Gaussian fixed point suitable for asymptotic safety. Furthermore, the RG flow allows for a trajectory that provides an effective action that is compatible with cosmological observations.

4.1.1 Gravity-matter systems

While the prospects of obtaining a quantum description of the gravitational force at all length scales is already intriguing, it is also clear that a realistic description of our world also requires the inclusion of matter degrees of freedom. While there has already been significant effort geared towards the understanding the role of the Asymptotic Safety

mechanism for gravity-matter systems, the picture is still far from complete.[1] In order to discuss potential UV-completions of gravity-matter systems it is useful to distinguish between the two cases where the matter sector of the underlying fixed point is Gaussian or non-Gaussian in the sense that matter self-interactions are either absent or turned on. On general grounds, one may expect though that non-trivial interactions in the gravitational sector also induce non-trivial matter self-couplings, see [134] for a detailed discussion. Depending on the details of the approximation used to investigate the fixed point structure of the gravity-matter system, it is conceivable that a matter fixed point which is actually non-Gaussian may be projected onto a Gaussian one if the approximation used to probe it does not include self-interactions. Conversely, a fixed point identified as Gaussian may split into a Gaussian and a non-Gaussian one once additional couplings are probed.

In order to get an idea which matter sectors could actually be compatible with Asymptotic Safety, refs. [128–130, 155] studied gravity-matter systems where the matter sector contains an arbitrary number of minimally coupled scalars N_s, vectors N_V, and Dirac fermions N_D. Complementary results for the case where spacetime carries a foliation structure have been reported in [108]. While there is substantial evidence for the statement that the matter content of the standard model of particle physics leads to a fixed point structure suitable for realizing the Asymptotic Safety mechanism, the precise values for N_S, N_V, and N_D supporting a NGFP are different. Restricting to the cases where the matter sector contains scalar fields only, [128–130, 155] report an upper bound $N_S \lesssim 16-20$, while in [108] no such bound is present in agreement with the initial works [161, 162]. This difference can be traced back to different definitions of Newton's coupling employed in the two sets of work: the former define Newton's coupling based on the flat space graviton propagator while the latter work with a background Newton's coupling. As argued in [155] matter degrees of freedom contribute differently in these settings. The two pictures are in qualitative agreement if N_s is small ("gravity rules") but start to deviate once the matter contribution becomes significant ("matter matters").

In a complementary approach, the fixed point structure arising within scalar-tensor theory has been studied in [150–152, 156, 157, 163, 222, 223].[2] This setup includes two arbitrary functions of the scalar field ϕ, a scale-dependent scalar potential $V_k(\phi)$ and a function $F_k(\phi)$ describing the coupling of the scalar to the Ricci scalar. In $d = 3$ this setting gives rise to a Wilson-Fisher type RG fixed point which can be understood as a gravitationally dressed version of the Wilson-Fisher fixed point known in a non-dynamical flat background. In $d = 4$ the analogous analysis identifies a fixed point with a Gaussian matter sector. In particular the scalar mass and ϕ^4-coupling vanish at this fixed point. Ref. [151] supplements this setting by a third scale-dependent function $K_k(\phi)$ dressing

[1] For early works on this topic see [161, 162].

[2] For related studies of RG flows of scalar field theories in a fixed (curved) background spacetime see [56, 224–226].

the scalar kinetic term. In this generalization also a non-Gaussian matter fixed point structure has been identified.

The influence of gravity on the flow of gauge-couplings has been discussed extensively in both perturbative [227–230] and non-perturbative [123, 125, 145, 146, 149] settings. Fundamental aspects related to the inclusion of fermions have been discussed in [131, 147] and the compatibility of light chiral fermions with asymptotic safety has been argued in [135, 142, 154]. Starting from the prediction of the Higgs mass based on Asymptotic Safety [168], mass hierarchies in the standard model and its extensions have been studied in [137, 144, 221] while the influence of gravitational interactions on the flow of Yukawa-couplings has been studied in [124, 140, 148, 159, 173, 231].[3]

Based on these works there have been several key insights related to asymptotically safe gravity-matter systems. Firstly, non-Gaussian fixed points in the matter sector may come with a higher predictive power than their Gaussian counterparts. In ref. [149] this property has been used to predict the value of the fine-structure constants based on the Asymptotic Safety mechanism. Secondly, a non-vanishing fixed point value for the U(1) hypercharge may provide a solution to the triviality problem of the standard model [123]. Thirdly, the ratio of the Higgs and top mass can be predicted correctly based on the Asymptotic Safety mechanism above the Planck scale [168].

These salient features are, however, accompanied by the lurking danger that the non-vanishing gravitational interactions may induce potentially dangerous terms in the effective action. Typical candidates are higher-derivative terms contributing to propagators of matter fields, associated to Ostrogradski instabilities (see section 1.4). In this chapter, we initiate the study of this class of interaction terms for gravity-matter flows. For transparency we focus on the simplest possible model comprising the Einstein-Hilbert action supplemented by minimally coupled scalar fields including a higher-derivative term in the scalar propagator. We show that, as expected, the higher-derivative term is generated along the RG flow. Quite remarkably, the higher-derivative coupling vanishes at the NGFPs providing candidate UV-completions of the flow. Thus the computation bypasses the instabilities typically associated with the presence of higher-derivative terms in the propagator in a highly non-trivial way. These findings constitute a highly non-trivial consistency test concerning the structure of asymptotically safe gravity-matter systems.

[3]For a controlled realization of the Asymptotic Safety mechanism in gauged Yukawa-systems and their phenomenological applications see [232–235].

4.1.2 The Ostrogradski instability and potential cures

As discussed already in section 1.4, a prototypical example of a higher-derivative theory that violates unitarity is given by a scalar field with a fourth-order kinetic term. The action

$$S = \frac{Z}{2}\int \frac{\mathrm{d}^d p}{(2\pi)^d}\phi\left[p^2 + Y p^4\right]\phi \tag{4.1}$$

gives rise to the scalar propagator

$$G\left(p^2\right) = \frac{1}{Z}\left(\frac{1}{p^2} - \frac{1}{p^2 + \frac{1}{Y}}\right). \tag{4.2}$$

From this propagator, we infer that the theory contains a massless state with positive density, and a negative-norm state of mass

$$\mu^2 = Y^{-1}. \tag{4.3}$$

This state is called the Ostrogradski ghost (or recently a Merlin state [236, 237]), yielding either an unstable theory, or states propagating backwards in time.

Although higher derivatives generically introduce severe fundamental flaws in a theory, there are a number of ways to bypass this problem. This can be done at both the classical and the quantum level.

One way for curing the Ostrogradski instability at the classical level is to lift the condition of non-degeneracy. In this case the higher-order time derivatives are removed by either combining them into total derivatives or using a gauge symmetry. In the former case, the total derivatives in the Lagrangian do not contribute to the dynamics. Provided that this procedure removes all higher-derivative terms, this results in a healthy theory. In the latter case, gauge symmetry can be used to impose an extra condition on the equations of motion. If these constraints remove the higher derivatives, the instability is cured as well.

A second option consists of generalizing the propagator to be a function of the momentum. Such theories are similar to what one finds in string theory [238]. This strategy results in a non-local theory which contains time-derivatives of infinite order. In this case the propagator does not admit a partial fraction decomposition. If additional poles in the physical spectrum are absent, the theory will nevertheless still be stable. However, the question of whether the resulting non-local theory is well-posed is subtle. An exposition of the treatment of this class of theories is given in [239, 240]. For a more detailed discussion of infinite-order theories in the context of gravity we refer to [241–245]. In chapter 5, we will study the RG properties of the generalized propagator. The question which functions of the momentum are compatible with unitarity is discussed further in a more mathematical context in chapter 6.

When assessing the stability of a higher-derivative theory at the quantum level, the situation becomes even more involved. In this case the dressed propagator of the theory can be obtained from the effective action Γ and one expects that for a stable theory this propagator does not give rise to Ostrogradski ghosts. Following the discussion of the classical case above, this may be realized in two ways:

1. pushing the mass of the Ostrogradski ghost to infinity.

2. completing the dressed propagator into an entire function.

The first case can be illustrated by considering the propagator (4.2). At the quantum level the coupling Y will depend on the renormalization group scale k, which we indicate by Y_k. The requirement that the higher-order derivative term does not contribute to the dressed propagator corresponds to demanding that $\lim_{k\to 0} Y_k \to 0$. This means that the ghost mass goes to infinity. The ghost then decouples from the spectrum of the theory and does not entail an instability.[4] This scenario may be realized in two ways. Firstly, the system may exhibit a fixed point located at $Y_* = 0$. The theory at the fixed point is scale-invariant and ghost-free. Secondly, an RG trajectory may be attracted to the $Y_k = 0$ hyperplane as $k \to 0$. The ghost will drop out of the effective propagator rendering the renormalized theory effectively ghost-free.

When investigating case 1, gravity plays an essential role. In its absence, the action (4.1) describes a one-parameter family of non-interacting theories parameterized by Y. The only ghost-free theory in this set is $Y = 0$. This picture changes once a minimal coupling to the gravitational field is included. In this case the gravitational interactions induce a non-trivial flow of Y_k, opening the door to the nontrivial scenarios described above.

At this stage the following remarks are in order. Firstly, we stress that the condition that the theory should be ghost-free applies to the dressed propagator (obtained at $k = 0$) only. At finite values of k it is expected that the process of integrating out quantum fluctuations mode-by-mode will generate higher-order derivative terms in the intermediate description. *This does not signal the sickness of the theory, as its degrees of freedom should be read off from the dressed propagator.* Secondly, investigating the case b) will require generalizing the simple ansatz (4.1) to a scale-dependent function of the momentum. In [246] it has been shown that this class of models suffices to obtain the Polyakov effective action from a renormalization group computation. This generalization is beyond the present work though.

[4] For a similar discussion in the context of higher-derivative gravity see [54].

4.2 RG flows including higher-derivative propagators

Following up on the general discussion of section 4.1, we now perform a RG computation determining the scale-dependence of the higher-derivative coupling Y in a gravity-matter setting. The key results of this section are the β-functions that govern the RG flow of our projection. These are given in (4.13), (4.14), (4.17) and (4.19).

4.2.1 The functional renormalization group equation and its projection

We use the functional tools introduced in chapter 2. We start with the FRGE (1.13), governing the scale-dependence of the EAA Γ_k. We approximate the solution to the FRGE by making a suitable truncation that retains the operators of interest. In the present setting, we study the following ansatz:

$$\Gamma_k[g,\phi,\bar{c},c;\bar{g}] \approx \Gamma_k^{\rm grav}[g] + \Gamma_k^{\rm scalar}[\phi,g] + \Gamma_k^{\rm gf}[g;\bar{g}] + S^{\rm gh}[g,\bar{c},c;\bar{g}]\,. \tag{4.4}$$

The gravitational part of this ansatz is taken to be of Einstein-Hilbert form

$$\Gamma_k^{\rm grav}[g] = \frac{1}{16\pi G_k}\int {\rm d}^4x\sqrt{g}\,\left[-R+2\Lambda_k\right]\,, \tag{4.5}$$

which includes a scale-dependent Newton's coupling G_k and a cosmological constant Λ_k. The gravitational sector is supplemented by a gauge-fixing action $\Gamma_k^{\rm gf}$ and a ghost term $S^{\rm gh}[g,\bar{c},c;\bar{g}]$ that we take to be the same as in (2.33) and (2.35) for $d=4$ spacetime dimensions. In order to facilitate the comparison with the results reported in [130], we implement the Feynman-harmonic gauge[5] $\alpha=1,\beta=1$. The gravitational part of Γ_k is supplemented by N_s scalar fields,

$$\Gamma_k^{\rm scalar}[\phi,g] = \frac{1}{2}Z_k\sum_{i=1}^{N_s}\int {\rm d}^4x\sqrt{g}\,\phi^i\,\left[\Delta + Y_k\,\Delta^2\right]\,\phi^i\,, \tag{4.6}$$

where $\Delta \equiv -g^{\mu\nu}\nabla_\mu\nabla_\nu$ is the Laplacian constructed from the full metric. Besides a wave-function renormalization Z_k, this ansatz contains a scale-dependent coupling Y_k associated with a higher-derivative contribution to the scalar propagator.

The right-hand side of the FRGE is then projected onto the β-functions as follows. The flow of G_k and Λ_k can be read off from the terms proportional to $\int {\rm d}^4x\sqrt{\bar{g}}\,\bar{R}$ and $\int {\rm d}^4x\sqrt{\bar{g}}$, respectively. These contributions are conveniently found by selecting $\bar{g}_{\mu\nu}$ as the metric on a 4-sphere and taking the value of the scalar field $\phi=0$. The resulting operator traces can then be evaluated using standard heat-kernel techniques [28, 63, 102].

[5] Compared to [130], we do not include an anomalous dimension for the ghost fields. Thus our results correspond to $\eta_c = 0$.

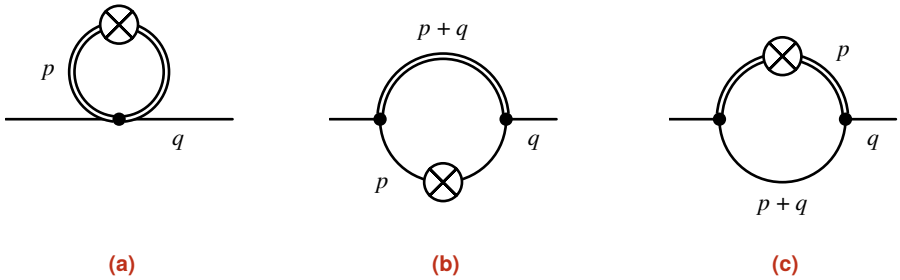

Figure 4.1: *Feynman diagrams encoding the scalar contributions to the β-functions. The solid and double line denote the scalar and graviton propagator, respectively. The crossed circle denotes the insertion of the cutoff operator* $\partial_t \mathcal{R}_k$.

The flow in the scalar sector is efficiently computed on an Euclidean background geometry $\bar{g}_{\mu\nu} = \delta_{\mu\nu}$ and by expanding the background scalar field $\phi(x)$ in terms of Fourier modes. Setting the graviton fluctuation fields to zero, the scalar sector appearing on the left-hand side of the flow equation is

$$\Gamma_k^{\text{scalar}}\big|_{h=0} = \frac{1}{2} Z_k \int \frac{\mathrm{d}^4 q}{(2\pi)^4} \phi\left(-q^2\right)\left(q^2 + Y_k q^4\right)\phi\left(q^2\right) . \tag{4.7}$$

Thus the scale-dependence of Z_k and Y_k is encoded in terms coming with two powers of the background scalar field and two and four powers of the momentum q, respectively. The Feynman diagrams generating these structures are depicted in Figure 4.1. They consist of a pure graviton tadpole (Figure 4.1a), and two diagrams with scalar-graviton loop formed by connecting two three-point vertices (Figure 4.1b and Figure 4.1c). The projection of the flow equation then requires extracting the contributions proportional to q^2 and q^4 from these diagrams.

4.2.2 Evaluating the flow equation

Starting from the ansatz (4.4), the goal is to find the β-functions determining the scale-dependence of G_k, Λ_k and Y_k as well as the scalar anomalous dimensions

$$\eta_N = G_k \partial_t G_k , \qquad \eta_s = -\partial_t \log Z_k . \tag{4.8}$$

The β-functions are conveniently expressed in terms of the dimensionless couplings

$$g_k \equiv k^{-2} G_k , \qquad \lambda_k \equiv k^2 \Lambda_k , \qquad y_k \equiv Y_k k^2 , \tag{4.9}$$

This information is obtained by substituting the ansatz into the FRGE and extracting the relevant interaction terms from the trace appearing on the right-hand side. The

explicit evaluation of this operator trace requires specifying the regulator function $\mathcal{R}_k$. Throughout this chapter, we will resort to a Litim-type regulator

$$\mathcal{R}_k = \mathcal{Z}_k\, k^2\, r\left(\Box/k^2\right), \qquad r(z) = (1-z)\Theta(1-z)\,. \tag{4.10}$$

The matrix-valued wave function renormalization $\mathcal{Z}_k$ is obtained from the substitution rule $\Box \mapsto P_k \equiv \Box + k^2 r\left(\Box/k^2\right)$. Following the nomenclature introduced in [63], the coarse-graining operator $\Box$ is chosen either as

$$\begin{aligned} &\text{Type I:} && \Box = \Delta\,, \\ &\text{Type II:} && \Box = \Delta + q\bar{R}\,, \end{aligned} \tag{4.11}$$

where the endomorphism $E \equiv q\bar{R}$ is chosen such that all curvature terms appearing in $\Gamma_k^{(2)}$ become part of the coarse-graining operator.

Due to the non-smooth character of the Litim profile (4.10), the extraction of external momenta from the traces is non-trivial. Contributions arising at the boundary of the momentum integrals have to be taken into account carefully. Our strategy for incorporating such terms is explained in detail in Appendix D.

The scale-dependence of the dimensionless couplings (4.9) is encoded in the β-functions which we define according to

$$\partial_t g_k = \beta_g(g,\lambda,y)\,, \qquad \partial_t \lambda_k = \beta_\lambda(g,\lambda,y)\,, \qquad \partial_t y_k = \beta_y(g,\lambda,y)\,. \tag{4.12}$$

For the dimensionless variables, the system of differential equations is autonomous in the sense that the β-functions are independent of k.

The explicit expressions for the β-functions in the gravitational sector are

$$\begin{aligned} \beta_g &= (2+\eta_N)\, g\,, \\ \beta_\lambda &= (\eta_N - 2)\lambda \\ &\quad + \frac{g}{48\pi}\left(\frac{120}{1-2\lambda} - \frac{20\eta_N}{1-2\lambda} - 96 + 2N_s(6-\eta_s) + \frac{3\beta_y + y(6-\eta_s)}{1+y}\right). \end{aligned} \tag{4.13}$$

The anomalous dimension of Newton's coupling is y- and N_s- dependent. Inspired by [102], it can be cast into the following form:

$$\eta_N(g,\lambda,y) = \frac{g\,(B_1(\lambda) + N_s\, B_3(\lambda,y))}{1 - g B_2(\lambda)}\,. \tag{4.14}$$

The functions B_1 and B_2 encode the contribution of the gravitational sector. For a Type I regulator, these functions have been determined in the seminal paper [102] and are listed in (3.25). For the Type II regulator, cf. (4.11), these functions become

$$B_1^{\text{Type II}} = -\frac{1}{3\pi}\left(\frac{13}{1-2\lambda} + 10\right), \qquad B_2^{\text{Type II}} = \frac{1}{12\pi}\frac{13}{1-2\lambda}\,. \tag{4.15}$$

Besides the gravitational self-interaction, there is a contribution of the scalar sector to the running of λ and g. For the latter, the additional scalar part is captured by

$$B_3 = \frac{1}{72\pi}\left(12 - 3\eta_s + \frac{4\beta_y + (4-\eta_s)\,y}{1+y}\right). \tag{4.16}$$

Note that the choice of regulator, (4.11), enters into B_1 and B_2 only.

Next, we turn to the β-functions of the scalar sector. The anomalous dimension for the scalar field can be expressed as

$$\eta_s = \frac{g}{1-gS_4}\left(S_1 + \eta_N\, S_2 + \beta_y\, S_3\right), \tag{4.17}$$

where the λ and y-dependent coefficients are given by

$$\begin{aligned}
S_1 &= \frac{1}{105\pi}\frac{1}{1-2\lambda}\left(\frac{2}{(1+y)^2} + \frac{1}{1+y} - 73 - 72y\right) \\
&\quad - \frac{1}{15\pi}\frac{1}{(1-2\lambda)^2}\left(\frac{1}{1+y} + 9 - 4y\right), \\
S_2 &= \frac{1}{60\pi}\frac{1}{(1-2\lambda)^2}\left(\frac{1}{1+y} + 4 - 3y\right), \\
S_3 &= -\frac{1}{7\pi}\frac{1}{1-2\lambda}\left(\frac{1}{6(1+y)^2} + \frac{11}{30(1+y)} + \frac{2}{5}\right), \\
S_4 &= -\frac{1}{35\pi}\frac{1}{1-2\lambda}\left(\frac{1}{4(1+y)^2} - \frac{1}{6(1+y)} - 3 - 2y\right).
\end{aligned} \tag{4.18}$$

The system is completed by the β-function for the higher-derivative coupling y. Its general structure follows a similar pattern as η_s:

$$\beta_y = \frac{1}{1-g\,S_8}\left((2+\eta_s)\,y + g\,(S_5 + \eta_N\, S_6 + \eta_s\, S_7)\right). \tag{4.19}$$

The functions S_5 to S_8 depend on λ and y and are found to be

$$\begin{aligned}
S_5 &= \frac{1}{15\pi}\frac{1}{1-2\lambda}\left(\frac{12}{(1+y)^2} - \frac{44}{1+y} + 32\right) - \frac{1}{30\pi}\frac{1}{(1-2\lambda)^2}\left(\frac{35}{1+y} + 25 + 85\,y\right), \\
S_6 &= \frac{1}{12\pi}\frac{1}{(1-2\lambda)^2}\left(\frac{3}{1+y} - 5 + 5\,y\right), \\
S_7 &= -\frac{1}{30\pi}\frac{1}{1-2\lambda}\left(\frac{3}{(1+y)^2} - \frac{11}{1+y} + 8\right), \\
S_8 &= -\frac{4}{15\pi}\frac{1}{1-2\lambda}\left(\frac{1}{(1+y)^2} - \frac{1}{1+y}\right).
\end{aligned} \tag{4.20}$$

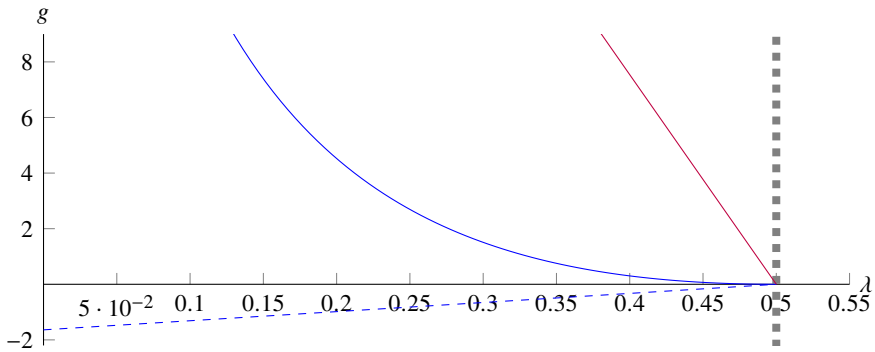

Figure 4.2: *Illustration of the singularity structure of the β-functions (4.13), (4.14), (4.17) and (4.19) projected onto the y = 0-plane. The thick dashed gray line indicates the fixed singularity at $\lambda^{sing} = 1/2$. At the blue and purple lines the anomalous dimensions η_N and η_s diverge respectively. The solid blue and purple lines apply to the Type I regulator while the dashed blue and purple lines are obtained from the Type II regularization procedure.*

The equations (4.13), (4.14), (4.17) and (4.19) form an implicit system which can be solved for the β-functions β_λ, β_y and anomalous dimensions η_N and η_s. In absence of the higher-derivative terms in the scalar propagator, which can be switched off by setting $y = 0$ and $\beta_y = 0$, the β-functions agree with the ones reported in [130] in the limit $\eta_c = 0$. This provides a non-trivial cross-check of our derivation.

4.2.3 Structural properties of the β-functions

The system of β-functions (4.13), (4.14), (4.17) and (4.19) possesses several interesting properties. Firstly, η_s and β_y depend on the number of scalar fields N_s only implicitly. This feature is readily deduced from the Feynman diagrams in Figure 4.1. These do not contain closed scalar loops that could give rise to terms proportional to N_s. The number of scalars then enters the flow in the scalar sector only indirectly through the value of the cosmological constant and the anomalous dimension of Newton's coupling. This suggests that the fixed point structure and flow pattern obtained from the β-functions will be rather stable under a change of the number of scalar fields.

Moreover, the β-functions possess several singular loci where either a β-function or an anomalous dimension diverges. The projection of these singular lines onto the $y = 0$-plane is shown in Figure 4.2.

Inspecting β_λ and β_y one encounters two singular lines

$$\lambda^{\text{sing}} = \frac{1}{2} \qquad \text{and} \qquad y^{\text{sing}} = -1\,, \tag{4.21}$$

where the denominators in the β-functions vanish. In addition one obtains singular lines when the anomalous dimensions η_N or η_s diverge. For η_N this locus is independent of y and N_s and implicitly parameterized by the relation

$$\eta_N^{\text{sing}}: \qquad gB_2(\lambda) = 1\,. \tag{4.22}$$

Since $B_2(\lambda)$ depends on the choice of coarse-graining operator, the Type I and Type II coarse-graining operators yield two different singularity structures. As illustrated in Figure 4.2, the Type I choice leads to a singular locus which screens the line $\lambda^{\text{sing}} = \frac{1}{2}$ for positive Newton's coupling while the Type II coarse-graining screens $\lambda^{\text{sing}} = \frac{1}{2}$ for $g < 0$. This observation may actually become important when "quenching the cosmological constant" along the lines proposed in [171] which presupposes that an RG trajectory emanating from the classical regime can actually reach the singular locus $\lambda^{\text{sing}} = \frac{1}{2}$.

The hypersurface on which the scalar anomalous dimension η_s diverges is given by a quadratic polynomial in g with λ- and y-dependent coefficients

$$\eta_s^{\text{sing}}: \qquad 1 - S_3 y - g\,(S_4 + S_3\,S_7 + S_8) + g^2 S_4 S_8 = 0\,. \tag{4.23}$$

For $y = 0$ the resulting line is depicted as the purple line in Figure 4.2. The hypersurface also screens the line $\lambda^{\text{sing}} = 1/2$ for $g > 0$. In the Type I coarse-graining procedure η_s^{sing} is sandwiched between η_N^{sing} and $\lambda^{\text{sing}} = 1/2$, while for the Type II procedure, it actually provides the screening of the $\lambda^{\text{sing}} = 1/2$-line. Thus the inclusion of scalar matter actually alters the singularity structure of the β-functions. At the same time, we expect that the system is rather insensitive to the inclusion of matter fields. The latter point will be confirmed in more detail by the analysis of the next section.

4.3 Properties of the renormalization group flow

We now discuss the properties of the RG flow entailed by the system (4.13), (4.14), (4.17) and (4.19). In subsection 4.3.1 we study the flow of the subsystem where the effects of the higher-derivative terms are switched off. The results provide the basis for analyzing the effects related to the presence of higher-derivative terms in the scalar propagator in subsection 4.3.2 and 4.3.3. Throughout the section we focus on the flow generated by the Type I coarse-graining operator.

4.3.1 Minimally coupled scalar fields

The system (4.12) constitutes a set of autonomous first-order differential equations capturing the scale-dependence of the couplings $\{g_k, \lambda_k, y_k\}$. The anomalous dimensions η_N and η_s can be obtained by evaluating (4.14) and (4.17) along a solution of this system.

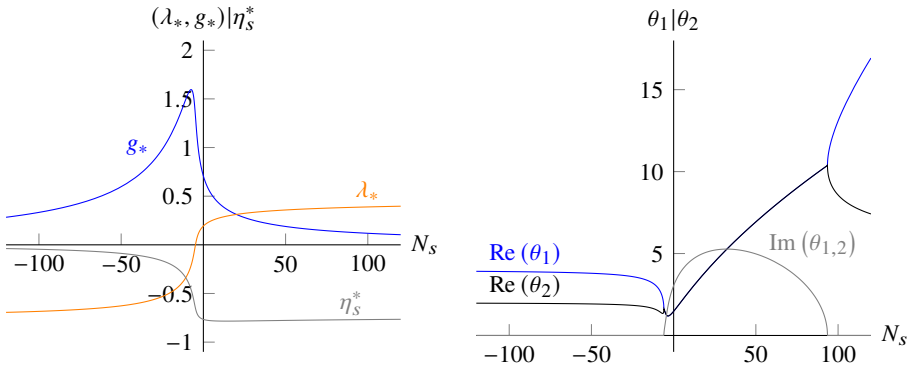

Figure 4.3: *Characteristics of the NGFP in the minimally coupled gravity-scalar system as a function of N_s. Its position in the (λ, g)-plane and the resulting scalar anomalous dimension η_s^* are shown in the left panel while the stability coefficients are displayed in the right panel. In order to mimic the behavior of fermionic matter, we also show the domain $N_s < 0$.*

In order to study the dynamics of this system, we investigate its fixed points. Recall from chapter 1 that these are given by the points $\{u_j^*\}$, satisfying

$$\beta_{u_i}\left(\{u_{j,*}\}\right) = 0\,. \tag{4.24}$$

Linearizing the flow at such a point provides us with the stability matrix $\mathbf{M}_{ij} = \frac{\partial \beta_i}{\partial u_j}\Big|_{u=u^*}$, whose eigenvectors and associated critical exponents signify relevant and irrelevant directions. Before delving into the analysis of the full system, it is useful to first analyze the subsystem obtained from setting $y_k = 0$, $\beta_y = 0$. In this approximation the contributions of the higher-derivative terms in the scalar sector are switched off and the projection of the flow equation is given by the Einstein-Hilbert action supplemented by an arbitrary number N_s of minimally coupled scalar fields. The RG flow resulting from similar projections has been studied in [108, 128, 130, 155, 162]. The analysis of this subsection then facilitates the comparison with these works.

Fixed point structure

The reduced system possesses two fixed points, a Gaussian and a non-Gaussian one. Like the GFP discussed in subsection 3.3.1, the GFP is situated at the origin and its stability coefficients are determined by the mass-dimension of the coupling constants,

$$(\lambda_*, g_*) = (0, 0)\,, \qquad \theta_1 = 2\,, \quad \theta_2 = -2\,. \tag{4.25}$$

N_s	g_*	λ_*	$g_*\lambda_*$	η_s^*	θ_1	θ_2
$-\infty$	0	$-3/4$	0	0	4	2
-100	0.333	-0.684	-0.228	-0.046	3.897	1.962
-6	1.530	-0.111	-0.170	-0.556	1.768	1.515
0	0.707	0.193	0.137	-0.766	$1.475 \pm 3.043i$	
1	0.655	0.208	0.136	-0.771	$1.603 \pm 3.281i$	
10	0.419	0.278	0.117	-0.784	$2.818 \pm 4.502i$	
100	0.119	0.389	0.046	-0.768	15.37	7.406
$+\infty$	0	1/2	0	-0.709	∞	4.76

Table 4.1: *Characteristic quantities for the NGFP appearing at selected values of N_s. The case $N_s = 0$ corresponds to the Einstein-Hilbert truncation. Several quantities seem to converge when taking the limit $N_s \to \pm\infty$.*

The anomalous dimensions vanish at this fixed point. The stability coefficients indicate that the GFP is a saddle point in the (λ, g)–plane exhibiting one UV-attractive and one UV-repulsive eigendirection, see also the left diagram of Figure 4.4. The GFP exists for all values N_s.

In addition the system possesses a one-parameter family of NGFPs parameterized by the number of scalar fields N_s. The position and stability of this family is shown in the left and right diagram of Figure 4.3, respectively. By virtue of (4.13) all NGFPs come with $\eta_N^* = -2$. Explicit values of the position (λ_*, g_*), the universal product $\Lambda_* G_* = \lambda_* g_*$, the scalar anomalous dimension evaluated at the fixed point η_s^*, and the stability coefficients for selected values of N_s are provided in Table 4.1.

Notably, there is a NGFP for both positive and negative values of N_s. In the study of gravity-matter systems where fermionic matter is included, the contributions from the fermionic sector to the β-functions come with an opposite sign relative to the bosonic sector. In the present case, we can mimic this behavior by studying negative values of N_s.

The one-parameter family of NGFP solutions exhibits a maximal value of $g_* = 1.60$ at $N_s = -7.47$. The cosmological constant λ_* has an inflection point at $(N_s, \lambda_*) = (-5.23, -0.0519)$ and has a zero at $N_s = -4.81$. The anomalous dimension has a minimum at $(N_s, \eta_s^*) = (14.3, -0.784)$; it has inflection points at $(N_s, \eta_s^*) = (-5.45, -0.600)$ and $(N_s, \eta_s^*) = (35.5, -0.780)$. The analysis of the stability coefficients displayed in the right diagram of Figure 4.3 shows that all NGFPs are UV-attractive in the (λ, g)-plane. The critical exponents θ_i have a non-zero imaginary part for $N_s \in [-6, 83]$ only. For other values of N_s the critical exponents turn out to be real.

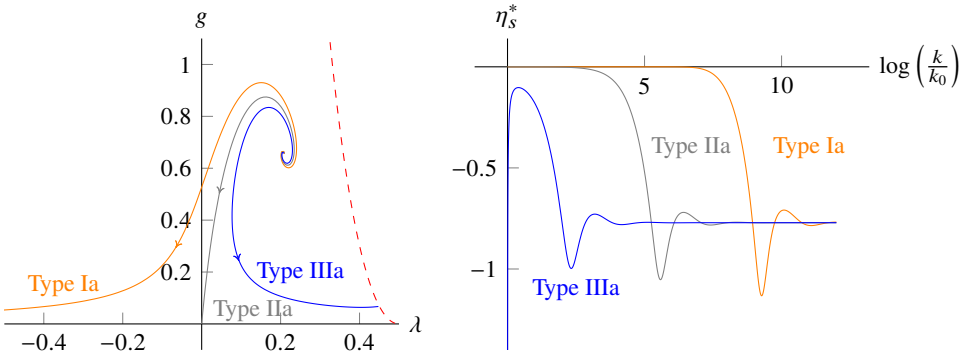

Figure 4.4: *Three prototypical RG trajectories obtained from numerically integrating the reduced system of β-functions for $N_s = 1$ (left). The flow is governed by the interplay of the NGFP and GFP. The scalar anomalous dimension η_s along the trajectories is shown in the right diagram. The anomalous dimension η_s is negative semi-definite along the entire RG flow. In the UV ($k \to \infty$) the anomalous dimension η_s approaches its fixed point value $\eta_s^* = -0.771$ independently of the specific initial conditions. In the IR η_s remains negative and vanishes asymptotically for the solutions of Type Ia and Type IIa. Trajectories of Type IIIa terminate in the singular line η_N^{sing} (red dashed line) triggering the divergence of η_s at a finite value of k.*

In the interval $N_s \in [-4, 16]$ the NGFP discussed above is the only non-trivial fixed point solution. Outside this window the simplified system possesses additional NGFPs. These are, however, separated from the GFP by the singular lines depicted in Figure 4.2. They are disconnected from the region where classical physics is expected to reside. Therefore, these fixed points will not be discussed in detail.

Flows away from the NGFP

Beyond the vicinity of the NGFP, where the linearized approximation of the flow is valid, the RG trajectories can be constructed by integrating the β-functions of the reduced system numerically. In the case where the critical exponents of the NGFP are complex ($N_s \in [-6, 83]$) the resulting phase diagram follows the same classification as in the case of pure gravity [104] that was discussed in subsection 3.3.3. For the case $N_s = 1$ three prototypical RG trajectories are shown in the left diagram of Figure 4.4. The trajectories undergo a crossover from the NGFP, controlling the high-energy regime, to the GFP, controlling the classical regime of the theory.

The scalar anomalous dimension obtained along these sample RG trajectories is shown

in the right panel of Figure 4.4. Notably $\eta_s(k) \leq 0$ along the entire flow: at the NGFP one has $\eta_s^* = -0.771$ and the scalar anomalous dimension approaches zero when the flow enters the classical regime governed by the GFP. Thus the anomalous dimension induced by the gravitational quantum corrections suppresses the propagation of scalar modes on all scales. The rapid increase of $|\eta_s|$ for the Type IIIa trajectory close to its termination point is a clear indication that the present approximation is insufficient in this regime and should thus not be given too much significance.

4.3.2 Fixed point structure including higher-derivative terms

We now focus on the fixed point structure of the full system (4.12) including the higher-derivative coupling y_k. Following the structure of the last subsection, we first discuss the fixed point structure of the system.

Inspecting the β-functions, one finds that the GFP (4.25) has the following extension

$$(\lambda_*, g_*, y_*) = (0, 0, 0)\,, \qquad \theta_1 = 2\,, \quad \theta_2 = -2\,, \quad \theta_3 = -2\,. \tag{4.26}$$

Again there is a GFP for all values of N_s and the anomalous dimensions vanish at this fixed point. The stability coefficients indicate that the GFP is a saddle point in the (λ, g, y)-plane exhibiting one UV-attractive and two UV-repulsive eigendirections. In particular, it may serve as an IR attractor for RG flows starting at $g_k > 0$ which subsequently leave the GFP regime along the unstable direction.

The analysis of possible NGFPs starts with the following, intriguing observation: when restricted to $y = 0$, the β-function β_y, given in (4.19), simplifies to

$$\beta_y\big|_{y=0} = \frac{g}{6\pi}\frac{2+\eta_N}{(1-2\lambda)^2}\,. \tag{4.27}$$

Thus β_y supports a fixed point at $y_* = 0$ if $\eta_N^* = -2$. From β_g one finds that the later condition is precisely the anomalous dimension of Newton's coupling at any NGFP. This shows that there is an extension of the NGFP discussed in the previous section to the full system, i.e., for all values of N_s we obtain a NGFP with $y_* = 0$. This family of NGFPs will be called NGFP_0 in the sequel. Remarkably, the balancing between the anomalous dimension η_N^* and the other contributions to β_y works for $d = 4$ only. In any other spacetime dimension the fixed point is shifted away from the $y = 0$-plane.

A numerical investigation of the fixed point structure for $N_s \in [-100, 100]$ reveals the existence of three families of NGFPs, parameterized by N_s, and located in the physically interesting region. The three families are conveniently labeled by the sign of the fixed point value y_* which is either negative (NGFP_- branch), zero (NGFP_0 branch), or positive (NGFP_+ branch). The positions and stability coefficients of these fixed points are shown in Figure 4.5. In addition the characteristics for the NGFPs found for $N_s = 1$ are collected in Table 4.2. The detailed properties of the fixed point solutions are the following.

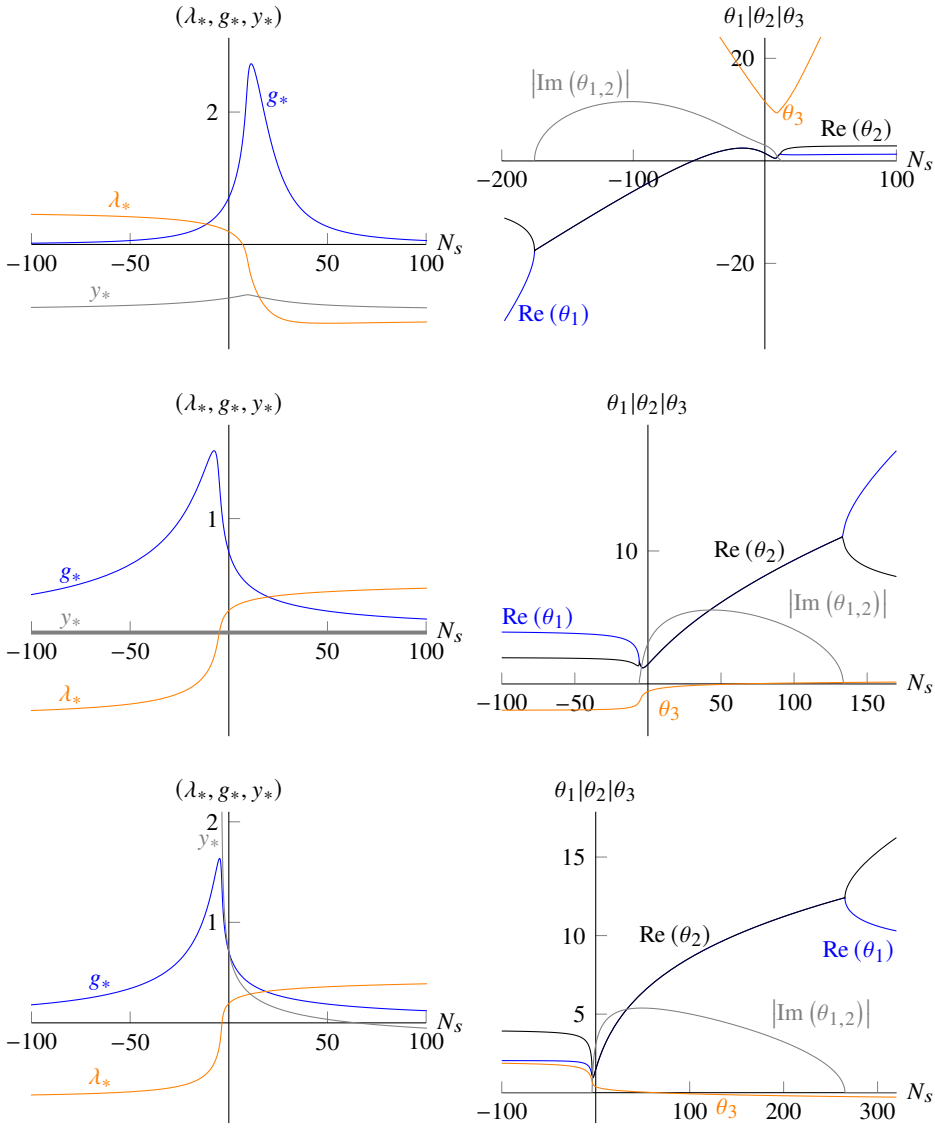

Figure 4.5: *Illustration of the fixed point structure resulting from the full system of β-functions (4.12) as a function of N_s. The characteristics of the NGFP$_-$, NGFP$_0$, and NGFP$_+$ are shown in the first, second, and third row, respectively.*

	g_*	λ_*	y_*	$g_*\lambda_*$	η_s^*	θ_1	θ_2	θ_3
GFP	0	0	0	0	0	+2	−2	−2
NGFP$_-$	0.776	0.176	−0.804	0.137	−0.721	$1.26 \pm 2.92i$		11.4
NGFP$_0$	0.655	0.208	0	0.136	−0.771	$1.60 \pm 3.28i$		−0.527
NGFP$_+$	0.646	0.211	0.621	0.136	−0.775	$1.63 \pm 3.34i$		0.358

Table 4.2: *Characteristic features of the four fixed points arising from the full set of β-functions (4.12) for $N_s = 1$.*

NGFP$_-$

The characteristic properties of this family of fixed points is shown in the first line of Figure 4.5. Their defining criterion is that they are located at $y_* < 0$ for all values of N_s. The position y_* is found to be in the interval $-1 < y_* \lesssim -0.76$ and approaches the singularity $y^{\text{sing}} = -1$ in the scalar propagator if $|N_s|$ becomes large. The profile for g_* is peaked at $N_s \approx 11.3$ where $g_* \approx 2.73$. The cosmological constant λ_* undergoes a crossover from $\lambda_* < 0$ for $N_s \gtrsim 7$ to $\lambda_* > 0$ for negative values N_s. For large negative values N_s the fixed points are pushed into the corner of singular lines $\lambda^{\text{sing}} = 1/2$, $y^{\text{sing}} = -1$.

The stability coefficients are displayed in the upper right diagram of Figure 4.5. In the interval $N_s \in [-100, 100]$ all three stability coefficients come with a positive real part indicating that all three couplings are UV-relevant. Within the interval $-30 \lesssim N_s \lesssim 11$ the two critical exponents θ_1 and θ_2 form a complex pair, indicating a spiraling behavior of the RG flow towards NGFP$_-$ in their respective eigendirections. Outside this window all θ_j are real-valued. The scalar anomalous dimension η_s^* is shown in Figure 4.6. For $N_s \lesssim 20$ one has $\eta_s^* < 0$, indicating a suppression of the scalar propagator at high energies. At $N_s \approx 20$ there is a transition to very small and positive values $\eta_s^* \lesssim 0.1$. Notably this is the only fixed point configuration where η_s^* is actually positive.

NGFP$_0$

The characteristic features of this class of fixed points are displayed in the middle line of Figure 4.5. All fixed points in this family are located at $y_* = 0$. Therefore this family constitutes the natural extension of the NGFP seen in the last subsection. The profiles specifying the position of these fixed points in the (λ, g)-plane resemble the one of NGFP$_-$ discussed above, with the difference that their values are scaled and mirrored around $N_s \approx 0$. This implies that the fixed point is pushed towards the singularity at $\lambda = 1/2$ for large *positive* N_s. The transition to $\lambda_* < 0$ happens at negative $N_s \approx -4.81$ and the maximum value of $g_* \approx 1.60$ is obtained at $N_s \approx -7.47$.

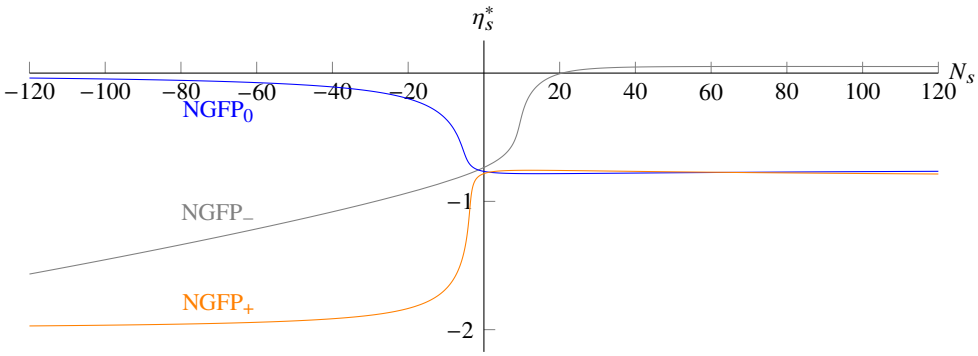

Figure 4.6: *Fixed point value of the scalar anomalous dimension η_s^* evaluated for the three classes of fixed points NGFP$_-$, NGFP$_0$, and NGFP$_+$ as a function of N_s.*

The stability properties of the class NGFP$_0$ can again be read off from the stability coefficients displayed in Figure 4.5. Two of their stability coefficients always come with a positive real part (indicating that the directions are UV-attractive). On the interval $N_s \in (-6, 82]$ they form a complex conjugate pair while outside this range both of them are real-valued. The third coefficient θ_3 changes sign at $N_s = 67$. For smaller values $\theta_3 < 0$, indicating that the corresponding NGFP$_0$ is actually a saddle point in the (λ, g, y)-plane. For $N_s > 67$ all three stability coefficients have positive real parts so that the fixed points are UV-attractors in this case. The scalar anomalous dimension η_s^* remains negative throughout and is bounded by $|\eta_s^*| < 0.77$.

NGFP$_+$

This class of fixed points is characterized in the bottom line of Figure 4.5. This class comes with a positive y_* which grows very rapidly for negative values of N_s. The positions of the fixed points in the (λ, g)-plane are qualitatively the same as the ones found for NGFP$_0$. For large positive values $N_s \gtrsim 64$ the location y_* changes sign. At this point it becomes problematic to track the family of solutions further. Since y_* is no longer positive at this point we adopt this as an upper bound on N_s in this case.

All stability coefficients appearing in this family possess a positive real part so that the NGFP$_+$ are UV-attractors in the (λ, g, y)-plane. Similar to the other fixed points, the stability coefficients θ_1 and θ_2 are real for $N_s \lesssim -3.5$ while for $N_s \gtrsim -3.5$ they form a complex pair. The scalar anomalous dimension η_s^* is negative throughout and takes values between $-2 \lesssim \eta_s^* \lesssim -0.77$.

At this point the following remark is in order. Combining (4.2) and (4.9), the mass of

the Ostrogradski ghost is

$$\mu^2 = \frac{k^2}{y_*} \,. \tag{4.28}$$

Thus μ^2 will become infinite for any RG trajectory approaching a NGFP as $k \to \infty$. This is just a consequence of the fact that a fixed point cannot support a dimensionful scale. The relation (4.28) also reveals that the fixed points NGFP_0 are special. Owed to their position at $y_* = 0$ the mass of the Ostrogradski ghost *is infinite for all values* k. In this way, the NGFP_0 realize the first class of loopholes discussed in subsection 4.1.2. Thus the extra degree of freedom is not present and one expects that the resulting theory *does not suffer from an Ostrogradski instability* although it lives in a theory space which a priori permits the presence of higher-derivative terms in the propagator.

4.3.3 Phase diagram including higher-derivative terms

We now extend the local analysis of the RG flow to a global picture. For concreteness, we focus on the case $N_s = 1$. The details of the fixed point structure arising in this setting are summarized in Table 4.2. Since the essential features of the flow are set by its fixed point structure, it is clear that the analysis applies to an entire window $-6 \lesssim N_s \lesssim 11$ where the fixed point structure and stability coefficients exhibit the same qualitative behavior.

The global structure of the RG flow is obtained by integrating the β-functions (4.12) numerically. A characteristic set of trajectories obtained this way is shown in Figure 4.7. Figure 4.7a shows the RG trajectories connecting the three NGFPs (gray lines) and the NGFPs with the GFP (orange lines). Since both $\text{NGFP}_\pm$ act as UV-attractors in the (λ, y, g)-plane and the NGFP_0 possesses one IR-attractive eigendirection there is a single RG trajectory emanating from either $\text{NGFP}_\pm$ for $k \to \infty$ and ending at the NGFP_0 as $k \to 0$. The GFP possesses two IR-attractive eigendirections. As a result, one finds a unique trajectory that starts from NGFP_0 and connects to the GFP $k \to 0$ (green line). This trajectory is the intersection of the two-dimensional UV-critical hypersurface of NGFP_0 with the two-dimensional IR-critical hypersurface of the GFP. In addition there are two families of solutions which originate from $\text{NGFP}_\pm$ and end at the GFP, again coming from the intersection of the three-dimensional UV-critical hypersurfaces of the NGFPs with the IR-critical hypersurface of the GFP. These flows are exemplified by the orange lines. All together this set constitutes the generalization of the Type IIa trajectory displayed in Figure 4.4.

Figure 4.7b then illustrates the generalization of the trajectories of Type Ia and Type IIIa to the (λ, y, g)–plane. These trajectories may emanate from all three NGFPs and subsequently cross over to the GFP. From the vicinity of the GFP they either flow to large negative values λ_k (Type Ia) or positive λ_k (Type IIIa) such that their projection to the (λ, g)-plane resembles the left diagram of Figure 4.4. The latter class again terminates in the hypersurface η_N^{sing} at a finite value k. Notably, for all physically interesting

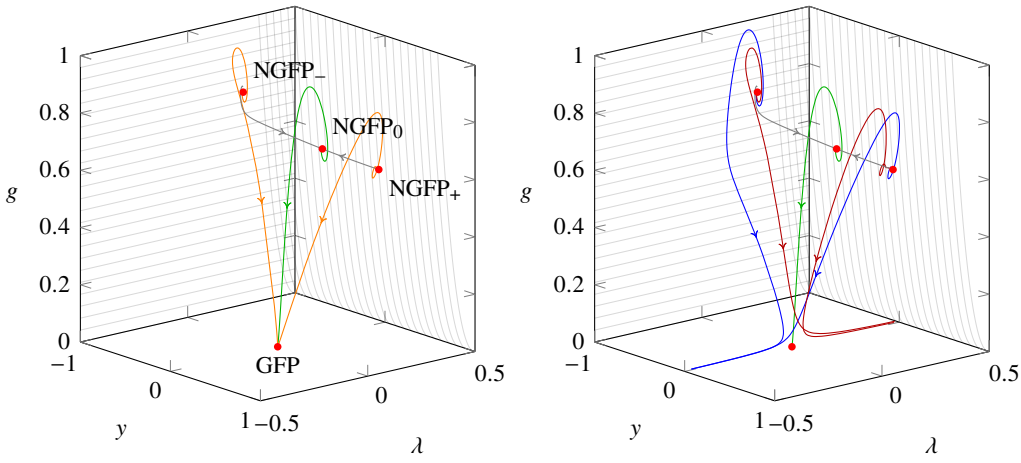

Figure 4.7: *Illustration of the phase diagram resulting from the β-functions (4.12) for $N_s = 1$. The GFP and the three NGFPs are marked with red points while the singular loci $y^{sing} = -1$ and η_N^{sing} are shaded in gray. All arrows point from UV to IR.*

4.7a: *The three NGFPs, $NGFP_-$, $NGFP_0$ and $NGFP_+$, together with the GFP are denoted by red dots. Dark gray lines denote the RG trajectories connecting $NGFP_\pm$ and $NGFP_0$. The green curve depicts the RG trajectory connecting $NGFP_0$ and the GFP. Typical examples from the set of trajectories between $NGFP_\pm$ and the GFP are drawn in orange. Together the trajectories span a 2-dimensional surface.*

4.7b: *Typical RG trajectories undergoing a crossover from the NGFP to the classical regime controlled by the GFP. Depending on whether the classical value of the cosmological constant found along the flow is positive (red curves) or negative (blue curves) the trajectories are termed Type IIIa and Type Ia, respectively. The red solutions terminate at η_N^{sing}.*

trajectories which exhibit a crossover to the GFP, y_k flows to zero in the IR, provided that the underlying trajectories do not terminate at a finite value k. When evaluating the scalar anomalous dimension η_s along the RG trajectories shown in Figure 4.7 one again obtains the qualitative behavior shown in the right diagram of Figure 4.4: for large k, the value of η_s is determined by its fixed point value η_s^*. Once the RG trajectory enters the vicinity of the GFP quantum effects become small, $\eta_s \ll 1$ asymptotically.

4.3.4 Ghost-free RG flows in the infrared

In order to determine the stability of the theory in the presence of higher-derivative terms one has to study the renormalized scalar propagator obtained from the effective average action Γ_k in the limit $k \to 0$. Defining $Y_0 \equiv \lim_{k\to 0} Y_k$ the (squared) renormalized mass of the Ostrogradski ghost is

$$\mu_0^2 = \frac{1}{Y_0} \tag{4.29}$$

Hence the extra modes will disappear from the spectrum if $Y_0 = 0$. Thus the focus of the investigation is on the IR behavior of y_k. Figure 4.7 demonstrates that all physically interesting RG trajectories have the property that the dimensionless coupling y_k goes to zero in the IR. This leaves three potential scenarios for the dimensionful coupling $Y_k = y_k k^{-2}$:

1. The dimensionless coupling y_k approaches zero slower than quadratically. The canonical scaling of Y_k will dominate the flow and Y_0 diverges. In this case the ghost becomes massless and eats up the scalar degree of freedom, see (4.2).

2. The dimensionless coupling falls off faster than k^2. The anomalous scaling dominates the flow, and $Y_k \to 0$. The Ostrogradski ghost decouples and the theory is stable.

3. The dimensionless coupling converges exactly quadratically. The dimensionful coupling Y_k approaches a constant, which can be zero or nonzero. The theory is stable only if this constant is zero.

We will now discuss the IR behavior of the several classes of trajectories. Most of the physically interesting trajectories fall into the classes Type Ia, Type IIa, or Type IIIa introduced in Figure 4.4. The only trajectories which are not captured by this classification are the trajectories connecting the NGFPs which will be discussed separately. Our investigation reveals that the phase diagrams shown in Figure 4.7 contains RG trajectories realizing all of the three cases described above.

Trajectories ending at the GFP (Type IIa)

We start our analysis by considering Type IIa trajectories for which the cosmological constant Λ_k flows to zero for $k \to 0$. In this case the IR completion of the trajectory is provided by the GFP (4.26). The IR-attractive hypersurface of the GFP is spanned by the two eigenvectors associated with the negative stability coefficients $\theta_2 = \theta_3 = -2$. The explicit expressions for these eigenvectors are $e_1 = \hat{y}$ and $e_2 = \frac{2+N_s}{16\pi}\hat{\lambda} + \hat{g}$, where $\hat{y}$, $\hat{\lambda}$ and

$\hat{g}$ are the unit vectors along the y, λ and g-axis, respectively. By linearizing the flow at the GFP one finds that along these scaling directions

$$y_k = y_{k_0}\left(\frac{k^2}{k_0^2}\right) \quad \Leftrightarrow \quad Y_k = Y_{k_0}\,. \tag{4.30}$$

Hence, there is a single RG trajectory, specified by $Y_{k_0} = 0$, for which $Y_0 = 0$ and the mass of the Ostrogradski ghost becomes infinite. This is the trajectory that has no initial component in the $\hat{y}$-direction, i.e. the one that approaches the GFP along e_2. Integrating the β-functions numerically one finds that this trajectory belongs to the UV-critical hypersurface of NGFP$_-$.

Trajectories of Type Ia and IIIa

Figure 4.4 illustrates the existence of RG trajectories where λ_k flows towards negative (Type Ia) or positive infinity (Type IIIa) as $k \to 0$. In order to determine the IR behavior of these trajectories, we numerically integrate the β-functions. Trajectories of Type IIIa terminate at η_N^{sing} at a finite value of k and cannot be completed to $k = 0$ in the present approximation. Therefore, we limit our analysis to trajectories of Type Ia which extend to $k = 0$. The IR values $Y_0 \equiv \lim_{k\to 0} Y_k$ arising within this class of solutions are conveniently illustrated by studying the behavior of RG trajectories piercing the (y, g)-plane located at $\lambda = -0.1$ since the flow is essentially perpendicular to this plane. The resulting structure is illustrated in Figure 4.8.

The plot shows that Type Ia trajectories can emanate from all three NGFPs: trajectories coming from NGFP$_0$ pass the plane at the blue line while trajectories above (below) this line lie in the UV-critical surface of NGFP$_+$ (NGFP$_-$). Trajectories where $Y_0 = 0$ span the black line in this diagram. Thus there is a one-dimensional surface of solutions where the renormalized squared mass of the Ostrogradski ghost, (4.29), is infinite. In this case the additional degree of freedom does not propagate. Imposing the physical requirement that the renormalized scalar propagator does not give rise to an Ostrogradski ghost may then be used to fix one of the free parameters of the theory from stability considerations.

Trajectories flowing to NGFP$_0$

The final option for taking an IR limit consists in approaching NGFP$_0$ along its IR-attractive eigendirection. From Figure 4.7 one sees that there are two trajectories emanating from either NGFP$_\pm$ which end at NGFP$_0$ as $k \to 0$. Linearizing the RG flow at the NGFP$_0$ and using the stability coefficient along the IR attractive eigendirection listed in Table 4.2 yields the RG evolution of y_k for these trajectories:

$$\lim_{k\to 0} y_k = \left(\frac{k}{k_0}\right)^{0.527} y_{k_0} \quad \Longrightarrow \quad Y_k = \left(\frac{k_0}{k}\right)^{1.473} Y_{k_0}\,. \tag{4.31}$$

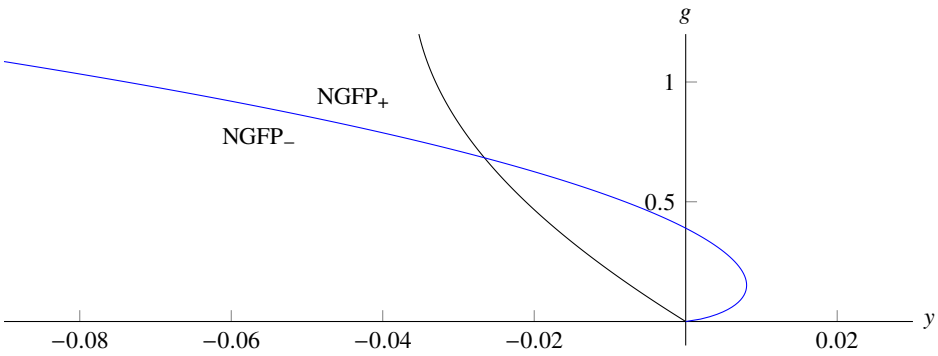

Figure 4.8: *Behavior of the RG trajectories passing through (y, g)-plane situated at $\lambda = -0.1$. Trajectories passing the plane above (below) the blue line emanate from $NGFP_+$ ($NGFP_-$) while the high-energy behavior of trajectories building up the blue line is governed by the $NGFP_0$. Trajectories for which $\lim_{k\to 0} Y_k = 0$ are indicated by the black line.*

Since the scaling of the dimensionless y is significantly smaller than k^2, the dimensionful Y diverges as $k \to 0$ for all initial values $y \neq 0$. As a consequence the IR value of the ghost mass vanishes and the two terms describing the propagation of the scalar field in (4.2) mutually cancel. Loosely speaking, the physical degree of freedom is eaten by the ghost so that the scalar does not propagate anymore. This cancellation mechanism, however, is only robust if no further powers of the momentum are generated in the scalar propagator. In chapter 5, we will study the RG system where arbitrary powers of the momentum are present. This will provide a verification of the cancellation of the degrees of freedom in the present context.

4.4 Conclusions and outlook

In this chapter, we have used the effective average action Γ_k to study the RG flow of gravity coupled to scalar matter. Our ansatz for Γ_k is given by the Einstein-Hilbert action coupled to an arbitrary number of scalar fields. The novel feature of the setup is the inclusion of a higher-derivative term in the scalar propagator. At the classical level, these actions suffer from the Ostrogradski instability: the appearance of degrees of freedom with a wrong-sign kinetic term, so-called Ostrogradski ghosts. This renders the theory either unstable or non-unitary. At the same time it is clear that a generic RG flow may generate such potentially dangerous higher-derivative terms dynamically, through the coupling to gravity. We have initiated the systematic study of these terms in the RG framework with the goal of assessing their hazard potential for asymptotically safe theories.

The quantity that actually encodes the relevant information on the spectrum of the theory is the *renormalized propagator*. Exploiting that the effective average action obeys $\lim_{k\to 0}\Gamma_k = \Gamma$ with Γ being the standard effective action, this quantity can be accessed in the IR-limit of the flow. Within the present approximation the stability properties of the theory are captured by the IR-value of the (squared) Ostrogradski ghost mass $\mu_0^2 = Y_0^{-1}$. The ghost decouples from the spectrum if $Y_0 = 0$, so that the setting may give rise to stable (or equivalently unitary) theories even though the generic actions include higher-derivative kinetic terms.

The detailed study of the RG flow then established the following picture. In absence of the higher-derivative term the setting studied in this work gives rise to a unique non-Gaussian fixed point (NGFP) suitable for rendering the gravity-matter system asymptotically safe. Upon including the scale-dependent Ostrogradski ghost mass, this NGFP splits up into three NGFPs which are labeled by the sign of Y_*. Notably there is one fixed point solution NGFP_0 for which $Y_* = 0$ for all values of k.

When projected to the (λ, y, g)-plane (see Figure 4.7) the system of NGFPs essentially possesses a UV-critical hypersurface with three relevant directions. Within this space we have identified a two-dimensional subspace of RG trajectories that have a ghost-free IR limit. Phrased differently, the Ostrogradski ghost mass corresponds to a relevant direction of the NGFPs, introducing a new free parameter. The freedom coming with this free parameter can be fixed by the physical requirement that the theory should contain only physical degrees of freedom in the IR. In this way the construction elegantly circumvents the potential danger of Ostrogradski instabilities by introducing a new free parameter and a mechanism to fix its value simultaneously. In this way the analysis in section 4.3 shows that the set of complete, unitary RG trajectories obtained from the full (λ, g, y)-system (4.12) is in one-to-one correspondence with the one found in the reduced system excluding the higher-derivative coupling.

As a byproduct, our analysis also provided new insights into potential bounds on the number of scalar fields compatible with the asymptotic safety mechanism. Throughout the calculation, we used a coarse-graining operator of Type I (see [63] for an extended discussion), and extracted the running of η_N from the background Newton's coupling. The resulting analysis indicates that there are NGFPs suitable for realizing asymptotic safety for all values N_s. The characteristic fixed point properties shown in Figure 4.3 are strikingly similar to the ones found for foliated gravity-matter systems [108]. Notably, our results also agree with the ones reported in [130], where an upper bound $N_s \lesssim 17$ has been obtained. The crucial difference between the two settings lies in the choice of coarse-graining operator in the gravitational sector: our analysis uses a Type I coarse-graining operator while [130] resorts to a coarse-graining operator of Type II. If the analysis of subsection 4.3.1 is repeated for a coarse-graining operator of Type II, which effectively replaces (3.25) by (4.15), the reduced system (4.12) gives rise to the same upper bound on the number of scalar fields $N_s \lesssim 17$. From Figure 4.2 one then expects that the singular

line η_N^{sing} plays a decisive role in stabilizing the NGFP for large values N_s.

The results reported in [128, 155] study a similar gravity-matter system. However, these computations are based on a different definition of Newton's coupling which makes the direct comparison between the approaches rather intricate. In chapter 5, we develop the correspondence between these calculations.

Our analysis demonstrates that the existence of unitary RG trajectories is a non-trivial feature. A priori, a kinetic function of polynomial type is bound to have multiple roots, yielding ghosts in the particle spectrum. This suggests that the present computation should be extended by studying polynomial truncations of higher order.

A more radical approach would be to construct the RG flow of the scalar propagator retaining non-polynomial momentum dependence. This entails a generalization of (4.6) to

$$\Gamma_k^{\text{scalar}}[\phi, g] = \int \mathrm{d}^d x \sqrt{g} \phi f_k(\Delta) \phi \,. \tag{4.32}$$

In chapter 5 we calculate the RG flow of this system. The so-called *form factor* $f_k(\Delta)$ opens up the possibility to have analytic kinetic functions without multiple roots. This gives a ghost-free spectrum. An example is a propagator of the type $\mathrm{e}^{-\Delta}\left(\Delta + m^2\right)^{-1}$ studied e.g. in the context of non-local gravity models [241–245, 247].

It is not straightforward to see whether the propagator contains a ghost state, if it is a general function of the momentum. In chapter 6, we study the conditions on a Euclidean field theory that give rise to unitarity in a more mathematical setting. We then prove a theorem that states the necessary and sufficient conditions for a large class of propagators arising from (4.32) to be ghost-free.

CHAPTER 5

FORM FACTORS IN ASYMPTOTIC SAFETY

The following chapter is based on:

> B. Knorr, C. Ripken, and F. Saueressig. *Form Factors in Asymptotic Safety: conceptual ideas and computational toolbox. Class. Quant. Grav.* (2019) [arXiv:1907.02903].

Additional computational details are relegated to Appendix E and Appendix F. Numerical algorithms are implemented in the Mathematica files `fpsolver.nb` and `flowequations.wls`.[1]

5.1 Introduction

In the previous chapters, we have shown how to use the effective average action as a solution to the FRGE to construct an approximate non-perturbative RG flow for gravity and matter. Central in this procedure was a truncation to certain operators of interest, see section 2.2. The type of truncation determines the character of the resulting RG equation, whether it is an ordinary differential equation, partial differential equation or integro-differential equation. In chapter 4, we encountered a truncation which retained a finite number of couplings. The resulting RG equations were ODEs. Chapter 3 gave an example of a truncation with an infinite number of couplings, a truncation of the form $\int \sqrt{g} f(R)$. As is demonstrated in Appendix C, the resulting flow equations are PDEs, that reduced to ODEs when we restrict f to second order in R. In this chapter, we will study a scheme that gives rise to an integro-differential flow equation.

[1] These files may be downloaded from `https://arxiv.org/src/1907.02903v1/anc`.

The choice of operators that are retained in the truncated EAA is physically motivated. In chapter 3, we studied monomials that are relevant for cosmological observations. In chapter 4, we discussed higher-order derivative operators acting on a scalar field coupled to gravity, which had important consequences for the Ostrogradski instability.

These expansions are not systematic, in the sense that they have no straightforward generalization that incorporates *all* allowed monomials in the EAA. One such expansion scheme is the vertex expansion (2.40)

$$\Gamma_k\left[h;\bar{g}\right] = \sum_m \frac{1}{m!}\int \mathrm{d}^d x\sqrt{\bar{g}}\left[\Gamma_k^{(m)}\left[\bar{g}\right]\right]^{\mu_1\nu_1\cdots\mu_m\nu_m} h_{\mu_1\nu_1}\cdots h_{\mu_m\nu_m}\,. \tag{5.1}$$

Here the vertices $\Gamma_k^{(m)}\left[\bar{g}\right]$ are operators that depend both on background curvatures and on the momenta of the fluctuation fields in terms of covariant background derivatives. As discussed in subsection 2.3.1, the downside to this expansion is that it does not obey split symmetry (2.37), which signals a breaking of background independence.

Opposite to this approach we can expand the EAA in monomials that are manifestly split-symmetric, which is exemplified by the $f(R)$-truncation. The idea of this chapter is to set up a systematic expansion that parameterizes all possible split-symmetric operators for gravity and gravity-matter systems. Gravity-matter systems have been studied extensively, as in e.g. [60, 73, 74, 89, 108, 111, 112, 117, 123–128, 130–146, 149–152, 154–156, 160–163, 170–173, 248].

We will set up an expansion by constructing manifestly split-symmetric invariants. A natural ordering principle in the case of gravity-matter systems is the number of matter systems and curvature tensors. For the case of pure gravity, the expansion of the EAA is then of the form

$$\Gamma_k[g] = \sum_n \frac{1}{n!}\int \mathrm{d}^d x\sqrt{g}\,\mathcal{F}_n\left[g\right]\mathcal{R}_1\cdots\mathcal{R}_n\,. \tag{5.2}$$

This depends only on the metric g rather than that relying on a background metric $\bar{g}$ and fluctuation h. The operators $\mathcal{F}_n\left(\Delta_1,\cdots,\Delta_n\right)$ are called *form factors*. Generically, these are functions of the Laplacian operators Δ_i constructed from the metric g acting on the curvature tensors $\mathcal{R}_i$, respectively. To simplify the notation, we have suppressed any tensorial indices in (5.2). For gravity-matter systems, a similar expansion can be written down.

At this point, we note that the expansion (5.2) is contained in the expansion (5.1), since each term $\mathcal{F}_n\mathcal{R}_1\cdots\mathcal{R}_n$ can be expanded in a (possibly infinite) series of background operators acting on fluctuation fields. Since the form factors are manifestly split-symmetric, this imposes nontrivial relations *between the fluctuation vertices* that parameterize a split-symmetric vertex expansion.

In section 5.2, we will give a detailed discussion of form factors in gravity-matter system, including a list of the lowest-order terms for various gravity-matter systems and

pure gravity. We then proceed with the construction of the map from the background form factors of a scalar-tensor system to the associated interacting vertices. In section 5.3, we compute the RG flow of the propagator of the scalar-tensor system, keeping full momentum dependence. We conclude with a summary of the results and a discussion of implications for other work in this thesis in section 5.4. Details on several computations in this chapter have been relegated to Appendix E and Appendix F.

5.2 Form factors in gravity and gravity-matter systems

We start our investigation with describing the momentum-dependent form factors for gravity and gravity-matter systems. We assume that we can freely integrate by parts, without generating boundary terms. For details regarding notation and conventions, see Appendix A.

5.2.1 Form factors for split-symmetry invariant actions

In this section, we list the form factors for different types of matter coupled to gravity. We will consider scalar matter, Abelian gauge fields, and fermions. We conclude this section with form factors constructed for pure gravity.

Scalars

For scalar fields ϕ, there is one form factor associated with the kinetic term

$$\Gamma_k^{s,\mathrm{kin}}[\phi, g] = \frac{1}{2}\int \mathrm{d}^d x \sqrt{g}\phi f_k^{(\phi\phi)}(\Delta)\phi\,. \tag{5.3}$$

In analogy to computations in flat Minkowski space, we define the wave-function renormalization of the scalar field according to [130]:

$$Z_k^s \equiv \frac{\partial}{\partial p^2} f_k^{(\phi\phi)}\left(p^2\right)\Big|_{p^2=0}\,. \tag{5.4}$$

Correspondingly, we have an anomalous dimension given by

$$\eta_s(k) \equiv -\partial_t \log Z_k^s\,. \tag{5.5}$$

One may also extract the zero-momentum behavior of the form factor. In this way, we define the gap parameter

$$\mu_k^2 \equiv \left(Z_k^2\right)^{-1} f_k^{(\phi\phi)}\left(p^2\right)\Big|_{p^2=0}\,. \tag{5.6}$$

If $f^{(\phi\phi)}\left(p^2\right)$ is a linear function of p^2 and ϕ is in the symmetric phase, then μ_k has the interpretation of the mass of the scalar field, since it corresponds to the pole of the (Wick-rotated) Lorentzian propagator. For a general form factor, this interpretation does not hold; one has to analyze the pole structure of the (Wick-rotated) form factor in order to gain insight into the masses of the propagating fields.

To linear order in the spacetime curvature, the scalar sector gives rise to two additional form factors,

$$\begin{aligned}\Gamma_k^{(\mathrm{R}\phi\phi)}[\phi,g] &= \int \mathrm{d}^d x\sqrt{g}\, f_k^{(\mathrm{R}\phi\phi)}\left(\Delta_1,\Delta_2,\Delta_3\right) R\phi\phi\,,\\ \Gamma_k^{(\mathrm{Ric}\phi\phi)}[\phi,g] &= \int \mathrm{d}^d x\sqrt{g}\, f_k^{(\mathrm{Ric}\phi\phi)}\left(\Delta_1,\Delta_2,\Delta_3\right) R^{\mu\nu}\left(\nabla_\mu\nabla_\nu\phi\right)\phi\,.\end{aligned} \tag{5.7}$$

Here Δ_i is the Laplacian acting on the i-th field, i.e. $\Delta_1\left(R\phi\phi\right) = \left(\Delta_1 R\right)\phi\phi$. An investigation of correlations of this type without form factors in a bi-metric setup has been carried out in [73], and in a Brans-Dicke motivated context in [150, 151, 163, 225]. The monomials listed in (5.7) constitute a complete set of form factors at first order in the spacetime curvature. The invariant

$$\int \mathrm{d}^d x\sqrt{g} f_k\left(\Delta_1,\Delta_2,\Delta_3\right) R^{\mu\nu}\left(\nabla_\mu\phi\right)\left(\nabla_\nu\phi\right) \tag{5.8}$$

can be mapped to this basis set through integration by parts and the use of the second Bianchi identity. Moreover, any pair of contracted covariant derivatives acting on different fields may be eliminated by means of the identity

$$\begin{aligned}&\int \mathrm{d}^d x\sqrt{g} H_1 H_2\left(\Delta H_3\right)\\ &\qquad = \int \mathrm{d}^d x\sqrt{g}\left[\left(\Delta H_1\right)H_2 + H_1\left(\Delta H_2\right) + 2\left(\nabla_\mu H_1\right)\left(\nabla^\mu H_2\right)\right]H_3\,,\end{aligned} \tag{5.9}$$

where the H_i represent arbitrary tensor fields. These manipulations typically also produce additional curvature tensors by the commutation of covariant derivatives. Since these are of higher order in R, they will not be considered at this stage.

Vectors

The kinetic term of an Abelian gauge field A_μ with field strength $F_{\mu\nu} = \nabla_\mu A_\nu - \nabla_\nu A_\mu$ reads

$$\Gamma_k^{\mathrm{v}}\left[A_\mu, g\right] = \frac{1}{4}\int \mathrm{d}^d x\sqrt{g} F_{\mu\nu}F^{\mu\nu}\,, \tag{5.10}$$

where all indices are raised and lowered with respect to the spacetime metric $g_{\mu\nu}$. This term can be generalized to include the form factor $f_k^{\mathrm{v}}(\Delta)$:

$$\Gamma_k^{\mathrm{v,kin}}\left[A_\mu, g\right] = \frac{1}{4}\int \mathrm{d}^d x \sqrt{g} F_{\mu\nu} f_k^{\mathrm{v}}(\Delta) F^{\mu\nu}\,. \tag{5.11}$$

Similar to the scalar case, $f_k^{\mathrm{v}}(x)\big|_{x=0}$ encodes the wave-function renormalization for the vector fields. In the case of non-Abelian gauge fields, the connection D_μ is given by ∇_μ supplemented by an additional connection piece built from A_μ.

In $d = 4$ spacetime dimensions there is a second interaction monomial constructed from two powers of the field strength tensor contracted with a totally antisymmetric ϵ-tensor. Like for the kinetic term (5.10), one could also generalize this term by including a form factor. By partial integration, one can bring this invariant to the form $\int \epsilon^{\mu\nu\rho\sigma} A_\mu \nabla_\nu f(\Delta) \nabla_\rho A_\sigma$. We will now assume that f can be expanded in a Taylor series in Δ. For the non-constant terms, commuting ∇_ν with the Laplacian gives an additional field strength tensor. For the constant term, the commutator is zero. However, contraction of ∇_ν and ∇_ρ with the ϵ-tensor gives a field strength tensor. As a consequence the interaction monomial contains either three powers of the field strength, or an additional spacetime curvature and will thus not be considered here.

Fermions

Our construction of the form factors for fermionic fields builds on the spin-base formalism developed in [147, 249, 250]. We start by introducing (spacetime-dependent) Dirac matrices γ_μ satisfying the Clifford algebra

$$\{\gamma_\mu, \gamma_\nu\} = 2 g_{\mu\nu} \mathbb{1}\,, \qquad \gamma_\mu \in \mathrm{Mat}(d_\gamma \times d_\gamma, \mathbb{C})\,, \quad d_\gamma = 2^{\lfloor d/2 \rfloor}\,, \tag{5.12}$$

where $\mathbb{1}$ denotes the unit matrix in Dirac space. Dirac fermions are then represented by a Grassmann-valued d_γ-component vector ψ. Fermion bilinears are formed with the metric $\mathfrak{h}$ on Dirac space, where $\mathfrak{h} \in \mathrm{Mat}\left(d_\gamma \times d_\gamma, \mathbb{C}\right)$ is antihermitian, $\mathfrak{h}^\dagger = -\mathfrak{h}$, and has unit determinant. The conjugate of a Dirac spinor is then defined as $\bar{\psi} \equiv \psi^\dagger \mathfrak{h}$. This ensures that $\left(\bar{\psi}\psi\right)^\dagger = \bar{\psi}\psi$ is real.

Since the properties of the Clifford algebra depend on the dimension of spacetime, the discussion will focus on four-dimensional (Euclidean-signature) spacetimes admitting a spin-structure. In this case the γ_μ can be chosen to satisfy the reality property $(\gamma_\mu)^\dagger = \mathfrak{h}\gamma_\mu\mathfrak{h}^{-1}$. Moreover, the Clifford algebra admits an additional operator $\gamma_* = \frac{1}{24}\sqrt{g}\,\epsilon_{\mu\nu\rho\sigma}\gamma^\mu\gamma^\nu\gamma^\rho\gamma^\sigma$, where ϵ is the standard Levi-Civita symbol. It satisfies $\mathrm{tr}\,\gamma_* = 0$, $(\gamma_*)^\dagger = \mathfrak{h}\gamma_*\mathfrak{h}^{-1}$, and $(\gamma_*)^2 = \mathbb{1}$. This allows to distinguish the left- and right-handed components of the Dirac spinor by the projection operators $\Gamma_\pm = \frac{1}{2}\left(\mathbb{1} + \gamma_*\right)$. Given a set of Dirac matrices, satisfying (5.12) and the reality properties for the γ_μ

uniquely determines $\mathfrak{h}$. In order to construct a kinetic term for the fermions, we introduce a covariant derivative ∇_μ containing the spin-base connection Γ_μ,[2]

$$\nabla_\mu \psi = \partial_\mu \psi + \Gamma_\mu \psi \,, \qquad \nabla_\mu \bar{\psi} = \partial_\mu \bar{\psi} - \bar{\psi} \Gamma_\mu \,. \tag{5.13}$$

The spin-base connection Γ_μ is completely determined in terms of the Dirac matrices and the Levi-Civita connection,

$$\Gamma_\mu = \sum_{n=1}^{4} m_{\mu\rho_1\cdots\rho_n} \gamma^{\rho_1\cdots\rho_n} \,, \qquad m_{\mu\rho_1\cdots\rho_n} \equiv \frac{(-1)^{\frac{n(n+1)}{2}} \operatorname{tr}\left(\gamma_{\rho_1\cdots\rho_n}\left[(D_\mu \gamma^\nu), \gamma_\nu\right]\right)}{8\, n!\, (4\,(1-(-1)^n) - 2n)} \,, \tag{5.14}$$

where $D_\mu \gamma^\nu = \partial_\mu \gamma^\nu + \Gamma^\nu{}_{\mu\rho}\gamma^\rho$ and $\gamma^{\rho_1\cdots\rho_n} = 1/n!(\gamma^{\rho_1}\cdots\gamma^{\rho_n} + \ldots)$ is the completely antisymmetrized product of n Dirac matrices. The connection ensures that $\nabla_\mu \psi$ transforms as a covector under general coordinate transformations and as a vector under SL $(d_\gamma, \mathbb{C})$ spin-base transformations. As an important property, $\not{\nabla} \equiv \gamma^\mu \nabla_\mu$ satisfies the Lichnerowicz relation

$$\Delta_{\mathrm{D}} \equiv (i\not{\nabla})^2 = \left(-g^{\mu\nu}\nabla_\mu \nabla_\nu + \frac{1}{4}R\right) \mathbb{1} \,. \tag{5.15}$$

Based on these prerequisites, it is now straightforward to introduce the three independent form factors appearing at the level of fermion bilinears,

$$\begin{aligned}
\Gamma_k^{\mathrm{D},1}[\bar{\psi}, \psi, g] &= \int \mathrm{d}^4x \sqrt{g}\, \bar{\psi}\, f_k^{\mathrm{D},1}(\Delta_{\mathrm{D}})\ (\mathbf{i}\not{\nabla})\, \psi \,, \\
\Gamma_k^{\mathrm{D},2}[\bar{\psi}, \psi, g] &= \int \mathrm{d}^4x \sqrt{g}\, \bar{\psi}\, f_k^{\mathrm{D},2}(\Delta_{\mathrm{D}})\ \gamma_*\, \not{\nabla}\, \psi \,, \\
\Gamma_k^{\mathrm{D},3}[\bar{\psi}, \psi, g] &= \int \mathrm{d}^4x \sqrt{g}\, \bar{\psi}\, f_k^{\mathrm{D},3}(\Delta_{\mathrm{D}})\ \psi \,, \\
\Gamma_k^{\mathrm{D},4}[\bar{\psi}, \psi, g] &= \int \mathrm{d}^4x \sqrt{g}\, \bar{\psi}\, f_k^{\mathrm{D},4}(\Delta_{\mathrm{D}})\ \gamma_*\, \psi \,.
\end{aligned} \tag{5.16}$$

The form factors $f_k^{\mathrm{D},1}(\Delta_{\mathrm{D}})$ and $f_k^{\mathrm{D},2}(\Delta_{\mathrm{D}})$ generalize the kinetic term. In particular, linear combinations of $f_k^{\mathrm{D},1}(0)$ and $f_k^{\mathrm{D},2}(0)$ define the wave-function renormalizations for the two chiral components of the Dirac field. The form factors $f_k^{\mathrm{D},3}(\Delta_{\mathrm{D}})$ and $f_k^{\mathrm{D},4}(\Delta_{\mathrm{D}})$ generalize the mass terms to momentum-dependent functions. Again the k-dependent mass of the fermion is associated with the roots of the (Lorentzian-signature) Dirac equation. In a flat background the relevant equation is

$$\left[f_k^{\mathrm{D},1}(\Box)(i\not{\partial}) + f_k^{\mathrm{D},2}(\Box)\,\gamma_*\,\not{\partial} - \left(f_k^{\mathrm{D},3}(\Box) + f_k^{\mathrm{D},4}(\Box)\,\gamma_*\right)\right]\psi = 0 \,, \tag{5.17}$$

[2]The connection piece of ∇_μ can be generalized to also contain a spin-torsion part $\Delta\Gamma_\mu$. This case will not be considered here.

so that the construction accommodates scale-dependent mass terms for the right- and left-handed components of the Dirac fermion. Owed to the presence of the scalar curvature term in (5.15) the form factors $f_k^{\mathrm{D},i}(\Delta_{\mathrm{D}})$ have a non-trivial overlap with scale-dependent functions $f_k(R)$ built from the Ricci scalar. A natural way to disentangle these two sets of functions is to take the flat-space limit where the latter are trivial.

Gravity

The first set of non-trivial form factors in the gravitational sector appears at second order in the spacetime curvature. In this case the basis for the split symmetry invariant form factors can be chosen as

$$\begin{aligned}\Gamma_k^{\mathrm{C}}[g] &= \frac{1}{16\pi G_k}\int \mathrm{d}^d x\sqrt{g}\, C_{\mu\nu\rho\sigma}\, W_k^{\mathrm{C}}(\Delta)\, C^{\mu\nu\rho\sigma}\,,\\ \Gamma_k^{\mathrm{R}}[g] &= \frac{1}{16\pi G_k}\int \mathrm{d}^d x\sqrt{g}\, R\, W_k^{\mathrm{R}}(\Delta)\, R\,.\end{aligned} \tag{5.18}$$

The choice of these basis terms is distinguished in the sense that the form factors $W_k^{\mathrm{C}}(\Delta)$ and $W_k^{\mathrm{R}}(\Delta)$ lead to a non-trivial momentum dependence of the transverse-traceless and scalar propagator, respectively, when the background in (2.29) is chosen as flat Euclidean space. The third potential invariant $\int \mathrm{d}^d x\sqrt{g}\, R_{\mu\nu}\, R^{\mu\nu}$ does not give rise to an additional form factor. Any term of the form $\int \mathrm{d}^d x\sqrt{g}\, R_{\mu\nu}\, \Delta^n\, R^{\mu\nu}$, where $n \geq 1$ can be mapped to the basis elements and higher-order curvature terms by means of the second Bianchi identity (A.4). To demonstrate this, we first note that

$$\begin{aligned}\nabla^\alpha\nabla_\alpha R_{\rho\sigma\mu\nu} &= -\nabla^\alpha\left[\nabla_\rho R_{\sigma\alpha\mu\nu} + \nabla_\sigma R_{\alpha\rho\mu\nu}\right]\\ &= 2\nabla_\rho\nabla_{[\mu}R_{\nu]\sigma} - 2\nabla_\sigma\nabla_{[\mu}R_{\nu]\rho} + \mathcal{O}\left(R^2\right)\,,\end{aligned} \tag{5.19}$$

where we commuted two covariant derivatives and made use of the contracted Bianchi identity (A.5) in the second step. Contracting with a Riemann tensor, this implies

$$R^{\rho\sigma\mu\nu}\nabla^2 R_{\rho\sigma\mu\nu} = 4R^{\rho\sigma\mu\nu}\nabla_\rho\nabla_\mu R_{\nu\sigma} + \mathcal{O}\left(R^2\right)\,. \tag{5.20}$$

Integrating this equation over spacetime then allows to integrate by parts, so that the covariant derivatives appearing on the right-hand side can again be arranged to act on the Riemann tensor. Again making use of the contracted Bianchi identity establishes that

$$\int \mathrm{d}^d x\sqrt{g}\left[R^{\rho\sigma\mu\nu}\Delta R_{\rho\sigma\mu\nu} - 4R^{\mu\nu}\Delta R_{\mu\nu} + R\Delta R\right] = \mathcal{O}\left(R^3\right)\,. \tag{5.21}$$

This relation readily extends to higher powers of the Laplacian. This case involves additional commutators when reordering the covariant derivatives before performing the

integration by parts. These additional commutators only provide further terms of order $\mathcal{O}\left(R^3\right)$, so that (5.21) is correct for all positive powers Δ^n. Using (A.3) in order to eliminate the Riemann tensor in favor of the Weyl tensor leads to a similar relation, albeit with different numerical coefficients,

$$\int \mathrm{d}^d x\sqrt{g}\left[C^{\rho\sigma\mu\nu}\Delta C_{\rho\sigma\mu\nu} - 4\frac{d-3}{d-2}R^{\mu\nu}\Delta R_{\mu\nu} + \frac{d(d-3)}{(d-1)(d-2)}R\Delta R\right] = \mathcal{O}\left(R^3\right) . \tag{5.22}$$

This establishes that the monomials (5.18) are indeed the only form factors that appear at second order in the curvature, see also [251] for related discussions.[3] However, in dimensions higher than four, the Ricci-squared term without form factor has to be included, since it cannot be eliminated by the Euler characteristic.

At this stage the following remark is in order. The two monomials $\int \mathrm{d}^d x\ \sqrt{g}$ and $\int \mathrm{d}^d x\sqrt{g}R$ spanning the Einstein-Hilbert action do not lend themselves to a generalization by introducing a non-trivial form factor. Adding a function $f_k(\Delta)$ acting on the Ricci scalar in $\mathcal{O}_{\mathrm{R}}$ leads to integrands which are total derivatives and thus merely contribute surface terms to the action. This case will not be considered any further at this stage.

5.2.2 Form factors in the vertex expansion of a scalar-tensor theory

Having discussed the form factors of a scalar-tensor theory obeying split symmetry in section 5.2.1, we now investigate the role of form factors in the framework of a vertex expansion. In this case, we consider fluctuations of the gravitational field $h_{\mu\nu}$ in a flat Euclidean background $\bar{g}_{\mu\nu} = \delta_{\mu\nu}$. This setting allows to introduce momentum-dependent form factors in the interaction vertices. The flat background allows to use derivatives $\partial_{i\mu}$ with $\Box_i \equiv -\partial_i^2$ and momenta $p_{i\mu}$ interchangeably. Again, we adopt the convention that the index i denotes the field on which the derivative acts. For notational brevity, we drop the subscript k and it is understood implicitly that all form factors also depend on the scale k. Where necessary, we use a subscript to enumerate the tensor structures that a given form factor is associated to.

Classification of interaction vertices in powers of h

We start by generalizing the nomenclature introduced in (2.40) to the scalar-tensor case. In the presence of two fields, we have

$$\Gamma_k\left[h,\phi;\bar{g}\right] = \sum_{m,n}\frac{1}{n!m!}\int \mathrm{d}^d x\sqrt{\bar{g}}\left[\Gamma_k^{(m,n)}\left[\bar{g}\right]\right]^{\mu_1\nu_1\cdots\mu_m\nu_m} h_{\mu_1\nu_1}\cdots h_{\mu_m\nu_m}\phi^n . \tag{5.23}$$

[3] This statement assumes that the form factors possess a well-defined (inverse) Laplace transform (E.10), which we tacitly assume throughout the entire work.

In this expression, we have denoted the vertex encoding the interaction of m h-fields and n ϕ-fields by $\Gamma_k^{(m,n)}[\bar{g}]$. Notably, the symmetry properties in the vertices in terms of their momentum-dependence and tensor structure appear automatically, once they are extracted from (5.23) using the variational principle.

Order $\mathcal{O}(h^0)$ The lowest-order vertex describes the propagation of a scalar field in a flat background and does not contain the graviton fluctuation field,

$$\Gamma_k|_{\phi\phi} = \frac{1}{2}\int \mathrm{d}^d x\, f^{(\phi\phi)}(\Box)\phi\,. \tag{5.24}$$

Here we use a vertical line followed by a string of fields to denote the projection of (5.23) onto the corresponding string of fields. Going to momentum space and taking two functional derivatives with respect to ϕ then yields the (symmetrized) two-point vertex

$$\Gamma_k^{(0,2)}\left(p^2\right) = f^{(\phi\phi)}\left(p^2\right)\,. \tag{5.25}$$

Order $\mathcal{O}(h^1)$ For nonzero orders in h, the vertices $\Gamma_k^{(m,n)}[\bar{g}]^{\mu_1\nu_1\cdots\mu_n\nu_n}$, with $m \geq 1$ contain a nontrivial tensor structure. For $m = 1$ and $n = 2$, there are four form factors $f_{\mathcal{T}}^{(h\phi\phi)}$, associated to the independent tensor structures

$$\Gamma_k|_{h\phi\phi} = \int \mathrm{d}^d x \left[f_{(\bar{g})}^{(h\phi\phi)}\delta^{\mu\nu} + f_{(11)}^{(h\phi\phi)}\partial_1^\mu\partial_1^\nu + f_{(22)}^{(h\phi\phi)}\partial_2^\mu\partial_2^\nu + f_{(12)}^{(h\phi\phi)}\partial_1^\mu\partial_2^\nu \right] h_{\mu\nu}\phi\phi\,. \tag{5.26}$$

Note that in order to obtain a complete basis, the fourth structure is necessary. While partial integration allows us to write

$$\int \mathrm{d}^d x\, \partial_1^\mu\partial_2^\nu h_{\mu\nu}\phi\phi = -\frac{1}{2}\int \mathrm{d}^d x\, \left(\partial_1^\mu\partial_1^\nu h_{\mu\nu}\right)\phi^2\,, \tag{5.27}$$

identities of this form no longer hold if there is a form factor which contains Laplacians acting on the two ϕ-fields with different powers.

The momentum dependence of the form factors is conveniently parameterized by the squares of the momenta associated with the three fields,

$$f_{\mathcal{T}}^{(h\phi\phi)} = f_{\mathcal{T}}^{(h\phi\phi)}\left(p_1^2, p_2^2, p_3^2\right)\,. \tag{5.28}$$

Combinations of the form $y_{ij} = p_{i\mu}p_j^\mu$, $i,j = 1,2,3$, $i \neq j$ can be easily eliminated as independent arguments, using momentum conservation at the vertex. For any three-point vertex, this gives

$$p_1^\mu + p_2^\mu + p_3^\mu = 0\,, \tag{5.29}$$

which entails

$$p_3^2 = (p_{1\mu} + p_{2\mu})\,(p_1^\mu + p_2^\mu) = p_1^2 + p_2^2 + 2y_{12}\,. \tag{5.30}$$

Solving this relation for y_{12} allows us to express y_{12} in terms of the p_i^2. Identities for the other y_{ij} can be obtained along the same lines, yielding

$$y_{12} = \frac{p_3^2 - p_1^2 - p_2^2}{2}\,, \qquad y_{13} = \frac{p_2^2 - p_1^2 - p_3^2}{2}\,, \qquad y_{23} = \frac{p_1^2 - p_2^2 - p_3^2}{2}\,. \tag{5.31}$$

These relations allow to eliminate any dependence of $f_{\mathcal{T}}^{(h\phi\phi)}$ on y_{ij} in favor of the p_i^2.

We close the discussion of the vertex expansion with the following remarks. The classification of the form factors related to higher-order vertices follows the same pattern as the one for the three-point vertices. Firstly, one determines the independent arguments of $f_{\mathcal{T}}^{(h^m\phi^n)}$ using momentum conservation at the vertex. Secondly, one determines the independent tensor structures providing a suitable basis for the expansion (5.23). Notably, the number of tensor structures proliferates rather quickly. The vertex with $m = n = 2$ is discussed in detail in Appendix F. In this case there are 35 independent tensor structures that all come with their own form factor,

$$f_{\mathcal{T}}^{(hh\phi\phi)} = f_{\mathcal{T}}^{(hh\phi\phi)}\left(p_1^2, p_2^2, p_3^2, y_{12}, y_{13}, y_{23}\right)\,. \tag{5.32}$$

Momentum conservation at the vertex implies that any form factor appearing in a four-point vertex can depend on six different combinations of the incoming momenta. Systematically eliminating p_4^μ by imposing momentum conservation at the vertex, $p_4^\mu = -\left(p_1^\mu + p_2^\mu + p_3^\mu\right)$, leads to the arguments appearing in (5.32).

The vertex expansion can readily be generalized to an arbitrary background $\bar{g}_{\mu\nu}$. In this case, there is the additional complication that operator structures acting on the same field no longer commute. For example, the Laplacian $\bar{\Delta}_1$ no longer commutes with $\bar{\nabla}_{1\mu}\bar{\nabla}_i^\mu$, where $i \neq 1$. This raises the need to impose some convention on how the operators are ordered. This is particularly relevant for the vertex functions of higher order, such as the four-point vertex discussed in Appendix F where the form factors depend on a subset of both $\bar{\Delta}_i$ and $\bar{\nabla}_{i\mu}\bar{\nabla}_j^\mu$. In this case one may impose that all $\bar{\nabla}_{i\mu}\bar{\nabla}_j^\mu$ are to the left of all $\bar{\Delta}_i$ and $\bar{\Delta}_j$. Different choices for the operator orderings are equivalent up to terms of order $\mathcal{R}$.

5.2.3 Mapping between interaction vertices and split-symmetric interactions

At this stage it is natural to ask about the relation between the split symmetry invariant form factors introduced in section 5.2.1 and the vertex expansion in the previous section. In order to address this question we expand the split symmetry invariant action (5.3) in

terms of graviton fluctuations in a flat background $\bar{g}_{\mu\nu} = \delta_{\mu\nu}$. We can then give the result in terms of projected components appearing in the expansion (5.23). At zeroth order in the h-fields, this yields

$$\Gamma_k^{s,\mathrm{kin}}\Big|_{\phi\phi} = \frac{1}{2}\int \mathrm{d}^d x\, \phi f^{(\phi\phi)}(\Box)\phi\,. \tag{5.33}$$

The terms linear in h originate from expanding $\sqrt{g}$ and the form factor respectively. The former follow from

$$\sqrt{g} \simeq 1 + \frac{1}{2}h + \frac{1}{8}h^2 - \frac{1}{4}h^{\mu\nu}h_{\mu\nu} + \mathcal{O}\left(h^3\right)\,. \tag{5.34}$$

The latter arise from expanding the Laplacian acting on scalar fields in powers of h:

$$\Delta\phi \simeq \left[\Box + \mathbb{d}_1 + \mathbb{d}_2 + \cdots\right]\phi\,, \tag{5.35}$$

where $\mathbb{d}_i$ denotes the operator containing i h-fields. Explicit computation of the first two orders gives

$$\begin{aligned}
\mathbb{d}_1 &= h_{\mu\nu}\partial^\mu\partial^\nu + \left(\partial^\mu h_{\mu\nu}\right)\partial^\nu - \frac{1}{2}\left(\partial_\alpha h\right)\partial^\alpha\,,\\
\mathbb{d}_2 &= -h^\alpha_\mu h_{\alpha\nu}\partial^\mu\partial^\nu - h^{\alpha\beta}\left(\partial_\beta h_{\alpha\mu}\right)\partial^\mu - h^\beta_\mu\left(\partial^\gamma h_{\beta\gamma}\right)\partial^\mu\\
&\quad + \frac{1}{2}h^{\alpha\beta}\left(\partial_\mu h_{\alpha\beta}\right)\partial^\mu + \frac{1}{2}h^{\mu\nu}\left(\partial_\mu h\right)\partial_\nu\,.
\end{aligned} \tag{5.36}$$

Combining these basic expansions with the computational techniques introduced in Appendix E allows to calculate the variation of functions of the Laplacian. This results in the following expansion coefficient:

$$\begin{aligned}
\Gamma_k^{s,\mathrm{kin}}\Big|_{h\phi\phi} = \frac{1}{2}\int \mathrm{d}^d x \Bigg[&\frac{1}{2}f^{(\phi\phi)}\left(\Box_2\right)h\phi\phi\\
&+ \int_0^\infty \mathrm{d}s\, \tilde{f}^{(\phi\phi)}(s)\sum_{j=0}^{\infty}\frac{(-s)^{j+1}}{(j+1)!}\sum_{l=0}^{j}\binom{j}{l}(-1)^l\left(\Box^{j-l}\phi\right)\mathbb{d}_1\Box^l\mathrm{e}^{-s\Box}\phi\Bigg]\,.
\end{aligned} \tag{5.37}$$

Here $\tilde{f}^{(\phi\phi)}(s)$ denotes the inverse Laplace transform of the form factor $f^{(\phi\phi)}(\Box)$. Remarkably, all sums and the Laplace transform can be performed explicitly. Labeling the Laplacians acting on h, the first and second scalar field by $\Box_1$, $\Box_2$ and $\Box_3$ respectively, we

find

$$\begin{aligned}
&\int_0^\infty \mathrm{d}s\, \tilde{f}^{(\phi\phi)}(s) \sum_{j=0}^{\infty} \frac{(-s)^{j+1}}{(j+1)!} \sum_{l=0}^{j} \binom{j}{l} (-1)^l \Box_2^{j-l}\, \Box_3^l\, \mathrm{e}^{-s\Box_3} h\phi\phi \\
&= \int_0^\infty \mathrm{d}s\, \tilde{f}^{(\phi\phi)}(s) \sum_{j=0}^{\infty} \frac{(-s)^{j+1}}{(j+1)!} (\Box_2 - \Box_3)^j\, \mathrm{e}^{-s\Box_3} h\phi\phi \\
&= (\Box_2 - \Box_3)^{-1} \int_0^\infty \mathrm{d}s\, \tilde{f}^{(\phi\phi)}(s) \left(\mathrm{e}^{-s(\Box_2-\Box_3)} - 1\right) \mathrm{e}^{-s\Box_3} h\phi\phi \\
&= (\Box_2 - \Box_3)^{-1} \left(f^{(\phi\phi)}(\Box_2) - f^{(\phi\phi)}(\Box_3)\right) h\phi\phi\,.
\end{aligned} \tag{5.38}$$

A series expansion of the second line shows that the coefficient is finite also on the locus $\Box_2 - \Box_3 = 0$. Substituting this result into (5.37) yields the final form of the coefficient $\Gamma_k^{s,\mathrm{kin}}\Big|_{h\phi\phi}$:

$$\begin{aligned}
\Gamma_k^{s,\mathrm{kin}}\Big|_{h\phi\phi} = \frac{1}{2} \int \mathrm{d}^d x \Bigg[&\frac{1}{2} \delta^{\mu\nu} f^{(\phi\phi)}(\Box_2) \\
&+ \frac{f^{(\phi\phi)}(\Box_2) - f^{(\phi\phi)}(\Box_3)}{\Box_2 - \Box_3} \left(\partial_3^\mu \partial_3^\nu + \partial_1^\mu \partial_3^\nu - \frac{1}{2} \delta^{\mu\nu} \partial_{1\alpha} \partial_3^\alpha\right) \Bigg] h_{\mu\nu} \phi\phi\,.
\end{aligned} \tag{5.39}$$

The expansion of the monomials (5.7) around a flat background starts at order h; therefore they do not contribute to $\Gamma_k|_{\phi\phi}$. The terms $\Gamma_k^{(\mathrm{R}\phi\phi)}\Big|_{h\phi\phi}$ and $\Gamma_k^{(\mathrm{Ric}\phi\phi)}\Big|_{h\phi\phi}$ are found by replacing the curvature tensors by their leading coefficients in h. They read

$$\Gamma_k^{\mathrm{R}\phi\phi}|_{h\phi\phi} = \int \mathrm{d}^d x\, f^{(\mathrm{R}\phi\phi)}(\Box_1, \Box_2, \Box_3) \left[\Box_1 \delta^{\mu\nu} + \partial_1^\mu \partial_1^\nu\right] h_{\mu\nu} \phi\phi\,, \tag{5.40}$$

and

$$\begin{aligned}
\Gamma_k^{\mathrm{Ric}\phi\phi}\Big|_{h\phi\phi} = \frac{1}{2} \int \mathrm{d}^d x\, f^{(\mathrm{Ric}\phi\phi)}(\Box_1, \Box_2, \Box_3) \Big[&(\Box_1 + \Box_2 - \Box_3)\, \partial_1^\mu\, \partial_2^\nu \\
&- \frac{1}{4} (\Box_1 + \Box_2 - \Box_3)^2\, \delta^{\mu\nu} + \Box_1\, \partial_2^\mu\, \partial_2^\nu \Big] h_{\mu\nu} \phi\phi\,.
\end{aligned} \tag{5.41}$$

The structure of the four-point vertex can be analyzed along the same lines. Since the intermediate steps and results are rather lengthy, this calculation has been relegated to Appendix F. At this stage, it is sufficient to remark that split-symmetric actions containing more than one curvature tensor do not contribute to the $(h\phi\phi)$-vertex when expanded around a flat background. Thus, (5.39), (5.40) and (5.41) capture all contributions originating from a split-symmetric action.

We are now in a position to discuss the relation between the split symmetry invariant interaction monomials and the vertex expansion discussed in section 5.2.1 and section 5.2.2, respectively. In general, any split-symmetric action will give rise to an infinite tower of interaction vertices $\Gamma_k^{(m,n)}$ when one expands in graviton fluctuations around a background $\bar{g}$. This tower then implies that there is a relation between the form factors appearing in the split-symmetric action and the vertex expansion.[4] We illustrate this general property for the form factor appearing in the scalar kinetic term (5.3). Combining (5.33) and (5.39) gives the expansion of the split-symmetric scalar kinetic term $\Gamma_k^{s,\mathrm{kin}}[\phi, g]$. In a flat background spacetime, up to terms of second order in h we have:

$$\Gamma_k^{s,\mathrm{kin}} = \frac{1}{2}\int \mathrm{d}^d x \left\{ \phi f^{(\phi\phi)}(\Box)\phi + \left[\delta^{\mu\nu} f^{(\phi\phi)}(\Box_2) \right.\right.$$
$$\left.\left. + \frac{f^{(\phi\phi)}(\Box_2) - f^{(\phi\phi)}(\Box_3)}{\Box_2 - \Box_3} \left(\partial_2^\mu \partial_2^\nu + \partial_1^\mu \partial_2^\nu - \frac{1}{2}\delta^{\mu\nu}\partial_{1\alpha}\partial_2^\alpha \right) \right] h_{\mu\nu}\phi\phi + \mathcal{O}\left(h^2\right) \right\}. \tag{5.42}$$

Here we used the symmetry in the two ϕ-fields to exchange the indices 2 and 3. By comparing (5.42) to (5.24) and (5.26), we see that split symmetry entails a specific relation between the form factors appearing in the vertex expansion. The $(\phi\phi)$-vertex receives contributions from the scalar kinetic term only, and anticipating this we deliberately chose the same name for the two functions.

At the level of the $(h\phi\phi)$-vertices, the split-symmetric expansions (5.39), (5.40) and (5.41) induce the following form factors associated with the tensor structures (5.26):

$$\begin{aligned}
f_{(\bar{g})}^{(h\phi\phi)} &= \frac{1}{8}\left[f^{(\phi\phi)}\left(p_2^2\right) + f^{(\phi\phi)}\left(p_3^2\right) - p_1^2 \frac{f^{(\phi\phi)}\left(p_2^2\right) - f^{(\phi\phi)}\left(p_3^2\right)}{p_2^2 - p_3^2} \right] \\
&\qquad + p_1^2 f^{(\mathrm{R}\phi\phi)} - \frac{1}{8}\left(p_1^2 + p_2^2 - p_3^2\right)^2 f^{(\mathrm{Ric}\phi\phi)}, \\
f_{(11)}^{(h\phi\phi)} &= f^{(\mathrm{R}\phi\phi)}, \\
f_{(22)}^{(h\phi\phi)} &= \frac{1}{2}\frac{f^{(\phi\phi)}\left(p_2^2\right) - f^{(\phi\phi)}\left(p_3^2\right)}{p_2^2 - p_3^2} + \frac{1}{2}p_1^2 f^{(\mathrm{Ric}\phi\phi)}, \\
f_{(12)}^{(h\phi\phi)} &= \frac{1}{2}\frac{f^{(\phi\phi)}\left(p_2^2\right) - f^{(\phi\phi)}\left(p_3^2\right)}{p_2^2 - p_3^2} + \frac{1}{2}\left(p_1^2 + p_2^2 - p_3^2\right) f^{(\mathrm{Ric}\phi\phi)},
\end{aligned} \tag{5.43}$$

In order to ease the notation we have suppressed the arguments of all functions that depend on all three squared momenta. This establishes that split symmetry enforces

[4] A similar relation also holds once terms breaking split symmetry are added, such as the regulator and the gauge-fixing term. These are controlled by the Nielsen identity (2.38). The modifications induced by these terms will not be discussed here.

relations between the four independent form factors appearing in the vertex expansion. In other words, extracting the parts of the $(h\phi\phi)$-vertices that can be completed into split-symmetric actions requires contributions from all four tensor structures. Furthermore, the corresponding momentum-dependent form factors are fixed in terms of the two free functions $f^{(\mathrm{R}\phi\phi)}$ and $f^{(\mathrm{Ric}\phi\phi)}$ by the relations (5.43). This also establishes that there are two combinations of tensor structures that cannot be completed into split-symmetric monomials. At a practical level, this suggests that the amount of split symmetry breaking induced by the regulator and gauge-fixing terms can be quantified by these equations. This provides a much more straightforward way to check how strongly full diffeomorphism symmetry is broken than the evaluation of the nontrivial Nielsen identity (2.38).

For the form factors associated to vertices of higher order, $f_{\mathcal{T}}^{(h^m\phi^2)}$ where $m \geq 2$, relations can be obtained along the same lines. Their explicit construction requires classifying all split-symmetric invariants containing up to m powers of the curvature tensor. Subsequently, this set of actions is expanded in the fluctuation field up to m-th order. The result is then compared to the classification of tensor structures involving m h-fields and two scalars. Given that $f_{\mathcal{T}}^{(hh\phi\phi)}$ already gives rise to 35 tensor structures, it is clear that already the next order of relations will be very involved. We relegate partial results to Appendix F.

We close the section with a conceptual remark. In general, the EAA does not reduce to a functional of only one metric in the limit $k \to 0$. The reason is that the Nielsen identity is still nontrivial even in this limit, in particular because the gauge-fixing term is still present. Our discussion of form factors then might serve as an approximate solution to the Nielsen identity. This approximation does not include the breaking induced by gauge-fixing. Demanding split symmetry restoration may fix an infinite number of couplings. In the specific example of the $(h\phi\phi)$-vertices, split symmetry restoration (up to the nontrivial part of the Nielsen identity) at $k = 0$ corresponds to imposing the boundary conditions (5.43). This fixes two linear combinations of the form factors introduced in (5.26).

5.3 Momentum-dependent propagators in the scalar-tensor model

After our survey of the conceptual properties of momentum-dependent form factors, we now turn to computational techniques that allow to determine the form factors as solutions of the FRGE. For clarity, we focus on the simplest case and consider the form factor associated to the kinetic term (5.3). This generalizes the second-order kinetic term studied in chapter 4 to a full function of the Laplacian. This section is organized as follows. In subsection 5.3.1 we present the setup, whereas in subsection 5.3.2 we give the explicit flow equations. The results are presented in subsection 5.3.3.

5.3.1 Setup

We study the flow of the form factor of a scalar field coupled to gravity. As explained in the previous section, we approximate the flow of the three- and four-point vertex based on a diffeomorphism-invariant ansatz for the EAA:

$$\Gamma_k\,[g,\phi,\bar{c},c;\bar{g}] \approx \Gamma_k^{\rm grav}[g] + \Gamma_k^{\rm scalar}[\phi,g] + \Gamma_k^{\rm gf}[g;\bar{g}] + S^{\rm gh}[g,\bar{c},c;\bar{g}]. \tag{5.44}$$

The gravitational part is taken to be the Einstein-Hilbert action, discussed in subsection 3.3.1:

$$\Gamma_k^{\rm grav}[g] = \frac{1}{16\pi G_k}\int {\rm d}^d x\sqrt{g}\;\left[2\Lambda_k - R\right]\,. \tag{5.45}$$

This includes a scale-dependent Newton's coupling G_k and the cosmological constant Λ_k. The gauge-fixing action $\Gamma_k^{\rm gf}$ and resulting ghost action are given in (2.33) and (2.35) respectively. For the moment, we keep the gauge-fixing parameters α and β arbitrary.

Finally, the form factor of the real scalar field is given by

$$\Gamma_k^{\rm scalar}[\phi,g] = \frac{1}{2}Z_k^s\int {\rm d}^d x\sqrt{g}\,\phi\,\bar{f}_k(\Delta)\phi\,, \tag{5.46}$$

where $\Delta = -g^{\mu\nu}\nabla_\mu\nabla_\nu$ is the Laplacian constructed from the full metric g. The couplings are parameterized with a scale-dependent wave-function renormalization Z_k; the strength of the gravitational interaction is encoded in the function $\bar{f}_k$, which is subject to the constraint

$$\bar{f}'(0) = 1\,. \tag{5.47}$$

Following chapter 4, the gravity-matter system is expected to possess a NGFP suitable for asymptotic safety, see also [130, 155, 161, 4] for additional evidence. This fixed point is already visibly in the simplest projection, where $\Gamma_k^{\rm scalar}[\phi,g]$ is approximated by the classical action of a minimally coupled scalar field, setting

$$Z_k = 1, \qquad \bar{f}_k(\Delta) = \Delta\,. \tag{5.48}$$

For $d = 4$ it is situated at positive values of Newton's coupling and cosmological constant and exhibits a complex pair of critical exponents with a positive real part. Hence, the fixed point acts as a UV-attractor for the RG flow in the (G,Λ)-plane. It is connected to the one found for pure gravity through an analytic continuation in the number of scalar fields.

5.3.2 Flow equations

We now present the β-functions of the scalar-tensor system derived from the ansatz (5.44). These are expressed in dimensionless variables; for the gravitational sector, we have the

dimensionless Newton's coupling $g = k^2 G_k$ and cosmological constant $\lambda_k = k^{-2}\Lambda_k$. In the scalar sector, we have the dimensionless form factor defined via

$$\bar{f}(z) = k^{-2} f\left(k^2 z\right) . \tag{5.49}$$

In addition, we introduce the gravitational and scalar anomalous dimensions, respectively:

$$\eta_N = (G_k)^{-1}\,\partial_t G_k\,, \qquad \eta_s = -\,(Z_k)^{-1}\,\partial_t Z_k\,. \tag{5.50}$$

For simplicity, we present the flow equations in Feynman-harmonic gauge, corresponding to setting the gauge-fixing parameters $\alpha = 1$, $\beta = \frac{d}{2} - 1$. Finally, we introduce the dimensionless regulator shape function r as

$$R_k(z) = k^2 r\left(\frac{z}{k^2}\right) , \tag{5.51}$$

where R_k denotes the scalar part of the regulator $\mathcal{R}_k$.

Gravitational β-functions

The gravitational β-functions are explicitly given by

$$\partial_t g = (d - 2 + \eta_N)\, g\,. \qquad \partial_t \lambda = g\,(L_1(\lambda) + L_3[f] + \eta_N L_2(\lambda)) - (2 - \eta_N)\,\lambda\,. \tag{5.52}$$

The anomalous dimension takes the form

$$\eta_N = \frac{g\,(B_1(\lambda) + B_3[f])}{1 - g B_2(\lambda)}\,. \tag{5.53}$$

The functions $B_1(\lambda)$, $B_2(\lambda)$, $L_1(\lambda)$ and $L_2(\lambda)$ only depend on the gravitational couplings, and were first derived in [102]. They are given explicitly in (3.25).

The functionals B_3 and L_3 arise from the inclusion of the form factor f, and read

$$\begin{aligned} B_3[f] &= \frac{2}{3}(4\pi)^{1-d/2}\left(\Phi^1_{d/2-1}[f] - \frac{1}{2}\eta_s \tilde{\Phi}^1_{d/2-1}[f]\right) \\ L_3[f] &= (4\pi)^{1-d/2}\left(\Phi^1_{d/2}[f] - \frac{1}{2}\eta_s \tilde{\Phi}^1_{d/2}[f]\right) . \end{aligned} \tag{5.54}$$

In these expressions, we have conveniently used the generalized threshold functionals

$$\begin{aligned} \Phi^p_n[f] &= \frac{1}{\Gamma(n)}\int_0^\infty \mathrm{d}z z^{n-1}\frac{r(z) - z r'(z)}{(f(z) + r(z))^p} \\ \tilde{\Phi}^p_n[f] &= \frac{1}{\Gamma(n)}\int_0^\infty \mathrm{d}z z^{n-1}\frac{r(z)}{(f(z) + r(z))^p} . \end{aligned} \tag{5.55}$$

If $f(z) = z + w$ is linear in z, these functionals reduce to the threshold functionals as defined in (3.26):

$$\Phi^p_n(w) = \Phi^p_n\left[z + w\right] \qquad \tilde{\Phi}^p_n(w) = \tilde{\Phi}^p_n\left[z + w\right] . \tag{5.56}$$

Propagator β-function

The flow equation for f is given by

$$\left(1-\frac{1}{2}\eta_s\right) f\left(q^2\right)+\frac{1}{2}\partial_t f\left(q^2\right)-q^2 f'\left(q^2\right)=\mathcal{K}_1+\mathcal{K}_2+\mathcal{K}_3\,, \tag{5.57}$$

where the $\mathcal{K}_i$ correspond to the three Feynman diagrams in Figure 5.1. Structurally, the diagrams consist of a momentum and angular integral over a number of graviton and scalar propagators, and an insertion of the derivative of the regulator, connected by their vertex functions. The structural part of the diagrams reads

$$\begin{aligned}
\mathcal{K}_1 &= -32\pi g \int \mathrm{d}\mu\,[\eta_N]\,\mathcal{V}_1(p,q,x)\left(G_0^{\mathrm{grav}}(p^2)\right)^2\,,\\
\mathcal{K}_2 &= 32\pi g \int \mathrm{d}\mu\,[\eta_s]\,\mathcal{V}_2(p,q,x) G_0^{\mathrm{grav}}(\mathfrak{s})\left(G_0^{\mathrm{scalar}}(p^2)\right)^2\,,\\
\mathcal{K}_3 &= 32\pi g \int \mathrm{d}\mu\,[\eta_N]\,\mathcal{V}_3(p,q,x) G_0^{\mathrm{scalar}}(\mathfrak{s})\left(G_0^{\mathrm{grav}}(p^2)\right)^2\,.
\end{aligned} \tag{5.58}$$

Here we have introduced the Mandelstam variable $\mathfrak{s}=p^2+q^2+2pqx$. We define the regularized integrals

$$\int \mathrm{d}\mu[\eta] \equiv \frac{S_{d-2}}{(2\pi)^d}\int_0^\infty \mathrm{d}p\, p^{d-1}\int_{-1}^1 \mathrm{d}x\left(1-x^2\right)^{\frac{d-3}{2}}\times \left[r\left(p^2\right)-\frac{1}{2}\eta r\left(p^2\right)-p^2 r'\left(p^2\right)\right]\,, \tag{5.59}$$

where $\eta\in\{\eta_s,\eta_N\}$. In this expression, S_n denotes the area of the n-sphere, given by

$$S_n=\frac{(n+1)\pi^{\frac{n+1}{2}}}{\Gamma\left(\frac{n+1}{2}+1\right)}\,. \tag{5.60}$$

The regularized dimensionless graviton and matter propagators are

$$G_0^{\mathrm{grav}}(z)=(z+r(z)-2\lambda)^{-1}\,, \tag{5.61a}$$

$$G_0^{\mathrm{scalar}}(z)=(f(z)+r(z))^{-1}\,. \tag{5.61b}$$

The vertex functions $\mathcal{V}_i$ are given by

$$\begin{aligned}
\mathcal{V}_1 = &-\frac{1}{8}d(d+1)f\left(q^2\right)+\frac{1}{2}f'\left(q^2\right)q^2\left(d-\frac{\mathfrak{s}-p^2+\frac{d-4}{d-2}q^2}{\mathfrak{s}-q^2}\right)\\
&+\frac{1}{2}\frac{f(\mathfrak{s})-f\left(q^2\right)}{\mathfrak{s}-q^2}q^2\left(1+\frac{\mathfrak{s}-p^2+\frac{d-4}{d-2}q^2}{\mathfrak{s}-q^2}\right)\,,
\end{aligned} \tag{5.62a}$$

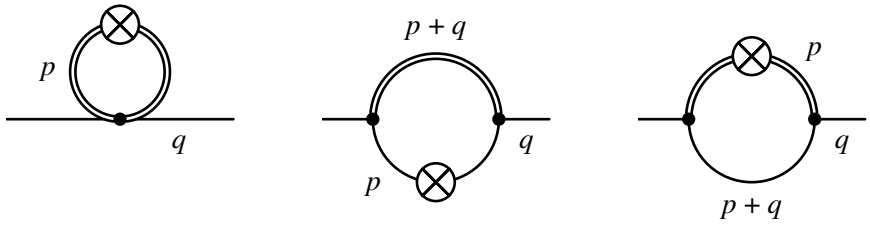

Figure 5.1: *Feynman diagrams contributing to the flow of the scalar form factor. The solid and double lines denote the scalar and graviton propagators, respectively. The crossed circle denotes the insertion of the cutoff operator $\partial_t \mathcal{R}_k$. 5.1a: tadpole diagram $\mathcal{K}_1$. 5.1b and 5.1c: self energy diagrams $\mathcal{K}_2$ and $\mathcal{K}_3$.*

$$\mathcal{V}_2 = -\frac{d}{2}\frac{1}{d-2}\left(f\left(p^2\right)\right)^2 + \frac{1}{2}\left(\mathfrak{s} + \frac{d+2}{d-2}p^2 - q^2\right) f\left(p^2\right)\frac{f\left(p^2\right) - f\left(q^2\right)}{p^2 - q^2} \tag{5.62b}$$
$$- \left(\frac{\mathfrak{s}}{2} + \frac{1}{d-2}p^2 - q^2\right)\left(\frac{f\left(p^2\right) - f\left(q^2\right)}{p^2 - q^2}\right)^2 p^2\,,$$

$$\mathcal{V}_3 = -\frac{d}{2}\frac{1}{d-2}\left(f\left(\mathfrak{s}^2\right)\right)^2 + \frac{1}{2}\left(p^2 + \frac{d+2}{d-2}\mathfrak{s} - q^2\right) f\left(\mathfrak{s}\right)\frac{f\left(\mathfrak{s}\right) - f\left(q^2\right)}{\mathfrak{s} - q^2} \tag{5.62c}$$
$$- \left(\frac{p^2}{2} + \frac{1}{d-2}\mathfrak{s} - q^2\right)\left(\frac{f\left(\mathfrak{s}\right) - f\left(q^2\right)}{\mathfrak{s} - q^2}\right)^2 \mathfrak{s}\,.$$

Note that the vertices $\mathcal{V}_2$ and $\mathcal{V}_3$ are related by the exchange $\mathfrak{s} \leftrightarrow p^2$, consistent with the observation that the corresponding self-energy diagrams $\mathcal{K}_2$ and $\mathcal{K}_3$ differ only in the insertion of the regulator $\partial_t \mathcal{R}_k$ and a relabeling of momenta.

We remark that the left-hand side of the β-function is a function of q^2, while on the right-hand side also odd powers of q are present. The right-hand side can be properly symmetrized by the observation that odd powers of the angular variable x integrate to zero.

From the flow equation for f, we derive a separate equation for η_s. This is done by taking two derivatives with respect to q and setting $q = 0$. Using the requirement $f'(0) = 1$ gives an implicit equation for η_s:

$$\eta_s = -\frac{\mathrm{d}^2}{\mathrm{d}q^2}\left(\mathcal{K}_1 + \mathcal{K}_2 + \mathcal{K}_3\right)\Big|_{q=0, f'(0)=1}\,. \tag{5.63}$$

The explicit expression for η_s is rather lengthy, so we refer to the supplementary notebook `fpsolver.nb` in [1] for further details.

5.3.3 Fixed point properties

In the following section we will discuss the solution of the set of flow equations presented in (5.52) and (5.57). We will focus on the fixed point, where all couplings are independent of the renormalization group scale k.

We will concentrate on the Landau-harmonic gauge. This is obtained by the following choice for α and β:

$$\text{Landau-harmonic gauge:} \qquad \alpha = 0\,, \quad \beta = \frac{d}{2} - 1\,. \tag{5.64}$$

Behavior at $q = 0$ As a start, we consider the behavior of f at zero momentum. Evaluating at $q = 0$, the flow equation reduces to the form

$$\frac{1}{2}\partial_t f(0) = \left[\mathcal{L}_0\left(g, \lambda, \eta_s, f; \alpha, \beta\right) - \left(1 - \frac{1}{2}\eta_s\right)\right] f(0)\,. \tag{5.65}$$

We conclude that at the fixed point, this equation is satisfied if either $f(0) = 0$, or if $\mathcal{L}_0 = 1 - \frac{1}{2}\eta_s$. We find that if $f(0) = 0$ at some point of an RG trajectory, then $f(0)$ vanishes along the entire trajectory. Furthermore, given a numerical solution, this gives a non-trivial check whether one or both of these conditions hold.

Asymptotic behavior Next, we study the asymptotic properties of the fixed point solution. To this end, we make the ansatz that for large momentum q^2, the function f behaves as $f\left(q^2\right) \sim f_\infty q^{2n}$, where $f_\infty, n > 0$. Inserting this into the fixed point equation gives a consistent equation for $n < 2$. Within this range, the diagram $\mathcal{K}_2$ is always sub-leading.

Next, we study the asymptotic behavior around the Landau-harmonic gauge, (5.64). To this end, we first write the gauge parameter β as $\beta = \left(\frac{d}{2} - 1\right) + \Delta\beta$ and then make an expansion around $\alpha = 0$, $\Delta\beta = 0$. Expanding then around large q gives the asymptotic relation

$$\begin{aligned} -\frac{1}{2}\eta_s - (n-1) = 32\pi g \frac{(d-2n)(d-2(n-1))}{d} \int \mathrm{d}\mu\,[\eta_N] \times \\ \left(\frac{d-1}{d-2}\left[\frac{d-4}{8} - \frac{4}{d(d+2)}\Delta\beta\right] G_0^{\mathrm{grav}}\left(p^2\right)^2 + \frac{1}{4}\frac{\alpha}{p^2 + r\left(p^2\right)}\right) + \mathcal{O}(\alpha^2, \Delta\beta^2)\,. \end{aligned} \tag{5.66}$$

For the exact Landau limit and harmonic gauge, $\alpha = 0, \Delta\beta = 0$, we find that the right-hand side of this equation vanishes exactly in $d = 4$ dimensions. This means that the canonical relation $n = 1 - \frac{1}{2}\eta_s$ holds exactly; thus, the asymptotic behavior of f receives no direct quantum corrections due to gravity.

Truncating the expansion to first order in α and $\Delta\beta$, we find a quadratic equation for n. This equation can be solved in terms of η_s, g and λ. Expanding to first order in g, we find that n is of the form

$$n = 1 - \frac{1}{2}\eta_s + \mathcal{O}(g)\,. \tag{5.67}$$

This confirms the expectation that the fall-off behavior of the propagator is determined to leading order by the anomalous dimension and receives additional quantum corrections at higher orders. By definition, the anomalous dimension is determined at $q = 0$, and is therefore governed by the small-momentum properties of f.

The anomalous dimension Similar to the asymptotic exponent n, we can study the anomalous dimension η_s close to Landau-harmonic gauge. Expanding (5.63) around $\alpha, \Delta\beta = 0$ gives

$$-\eta_s = 32\pi g\left(\frac{(d-4)(d-1)}{4}\int \mathrm{d}\mu\,[\eta_N]\, G_0^{\mathrm{grav}}\left(p^2\right)^2 + \alpha\mathcal{W}\right) + \mathcal{O}\left(\alpha^2, \Delta\beta^2\right)\,, \tag{5.68}$$

where $\mathcal{W}$ is given by

$$\begin{aligned}\mathcal{W}[\lambda, \eta_N, \eta_s, f] = &\int \mathrm{d}\mu\,[\eta_N]\,\frac{(d-2)p^2 + 2f\left(p^2\right)\left(f\left(p^2\right)G_0^{\mathrm{scalar}}\left(p^2\right) - 1\right)}{2p^2\left(p^2 + r\left(p^2\right)\right)^2} \\ &+ \int \mathrm{d}\mu\,[\eta_s]\,\frac{f\left(p^2\right)^2}{p^2\left(p^2 + r\left(p^2\right)\right)}G_0^{\mathrm{scalar}}\left(p^2\right)^2\,.\end{aligned} \tag{5.69}$$

Remarkably, the anomalous dimension is independent of $\Delta\beta$ to first order in $\Delta\beta$. Taking the Landau limit $\alpha = 0$, we see that the anomalous dimension vanishes exactly in $d = 4$.

The exact solution in Landau limit As we have seen, in $d = 4$, the Landau-harmonic gauge (5.64) gives an anomalous dimension $\eta_s = 0$; furthermore, we have found that the asymptotic exponent n must be exactly 1. In fact, if we evaluate the full fixed point equation in this gauge, we find that the function

$$f_*(z) = f_{\mathrm{lin}}(z) = z \tag{5.70}$$

is an exact solution. In other words, no non-trivial two-point function will be generated by this solution. This constitutes the most important result of this section.

It is important to note that this statement holds independently of the choice of regulator. Thus, a different choice of α and β cannot be reabsorbed into a different choice of regulator. Therefore, variations in the fixed point solution for a different gauge choice probe the gauge dependence of the RG flow.

The exact solution $f_*(z) = z$ implies that the dimensionless mass parameter (5.6) vanishes at the fixed point,

$$\mu_* = 0. \tag{5.71}$$

In combination with the observation that f is positive, this entails that the scalar propagator corresponds to a single massless scalar degree of freedom.

In order to study the stability of the fixed point, one should construct the stability matrix associated to the form factor. At this stage, the following conceptual remark is in order. The relation (5.61b) (with the regulator $r(z)$ set to zero) shows that the form factor f is closely related to the propagator the scalar field,

$$\left(G^{\text{scalar}}\right)^{-1} \propto f(p^2) \propto \mathcal{Z}^s(p^2)\left(p^2 + \mu^2\right). \tag{5.72}$$

In general, we assume that the prefactor $\mathcal{Z}^s(p^2)$ is positive, and may be absorbed in a field redefinition without affecting the pole structure of the propagator. This suggests to generalize (5.5) to a momentum-dependent anomalous dimension $\eta_s^*(p^2) \equiv -\partial_t \log \mathcal{Z}_*^s(p^2)$. It is then natural that there are no stability coefficient associated with deformations of $\mathcal{Z}_*^s(p^2)$.[5] In the case at hand, we have the exact solution $\eta_s^*(p^2) = 0$.

Owing to this observation, the stability of the form factor is limited to the stability of the gap parameter μ [59]. We note that, since the fixed point is trivial, the critical exponent associated to μ^2 is just the canonical one,

$$\theta_{\mu^2} = +2\,, \tag{5.73}$$

given by the classical mass dimension.

Solutions in Feynman gauge The fact that the linear solution solves the fixed point equations in Landau-harmonic gauge is a highly nontrivial result. For Feynman-harmonic gauge, the function f_{lin} is not a solution. Since the equation (5.57) is a highly nonlinear integro-differential equation (IDE), we have to resort to numerical methods to find a solution. In `fpsolver.nb`, we have implemented a numerical algorithm that searches for a numerical solution. At the time of writing, we have not been able to find a fixed point solution in this gauge.

However, we can insert f_{lin} on the right-hand side of (5.57) to obtain a one-loop approximation. However, solving the resulting linear differential equation gives either a singularity at $q = 0$, or a root at positive momentum. Both features are undesirable, and show the necessity of using non-perturbative approximations.

[5] In this analysis we have tacitly assumed that the function f_* has a single root. If f_* has multiple roots, as was the case in chapter 4, each root has an associated gap parameter $\mu_1, \mu_2, \ldots$ and corresponding stability coefficient.

5.4 Conclusion and discussion

In this chapter we have provided a detailed account of momentum-dependent form factors in quantum field theory and their role in the Asymptotic Safety program. Conceptually, the role of the form factors may be understood as follows. The object carrying the relevant information on the QFT is the quantum effective action $\Gamma \equiv \Gamma_{k=0}$. This functional serves as a generating function for all 1PI correlation functions. It is obtained as the endpoint of an RG trajectory where all quantum fluctuations are integrated out. Asymptotic Safety then entails that all couplings $\bar{u}_i(k = 0)$ in Γ are determined by the fundamental parameters identifying the RG flow infinitesimally close to the NGFP. The map between the fundamental parameters and the $\bar{u}_i(k = 0)$ is obtained by solving the flow equation and constructing the complete RG trajectory. This picture has some profound consequences.

Firstly, the momentum dependence of the couplings $\bar{u}_i(k = 0)$ originates from momentum-dependent form factors *evaluated at* $k = 0$. A priori, this is conceptually different from the dependence of the couplings $\bar{u}_i(k)$ on the coarse-graining scale k, which originates from integrating out quantum fluctuations shell-by-shell in momentum space. In simple cases, the k-dependence of the couplings may be identified with their dependence on an external momentum p. However, form factors capturing the momentum dependence of the interaction vertices go far beyond this approximation. In particular they also cover "anisotropic" situations where external momenta differ from each other.

Secondly, as discussed in section 5.2.1, the cosmological constant and Newton's coupling cannot be promoted to momentum-dependent form factors, since the inclusion of the differential operators leads to surface terms in Γ_k. Thus $G_{k=0}$ and $\Lambda_{k=0}$ are numbers which are independent of the external momenta in a scattering process. In this way the RG picture is reconciled with the statement that the (renormalized) cosmological constant and Newton's coupling "do not run" [252].

Thirdly, form factors are essential when expanding the EAA in split-symmetric monomials, as explained in detail in section 5.1. In setting up the FRGE, the necessity of introducing a gauge-fixing and regulator breaks diffeomorphism symmetry with a background metric $\bar{g}_{\mu\nu}$. Using form factors, one can self-consistently close the RG equation by means of monomials that depend on g only, keeping the breaking of diffeomorphism symmetry to a minimum.

The actual computation of the form factors featuring in Asymptotic Safety is still in its infancy. Our goal was to give a detailed survey of the computational techniques which allow to explore this new research area. We illustrated these techniques based on the simplest example by computing the gravitational corrections to the form factor governing the propagation of a scalar field minimally coupled to the Einstein-Hilbert action. Structurally, the β-functions governing the flow of the scalar propagator, (5.57), already exhibit all the features also expected in the gravitational sector or more complex gravity-matter systems: the scale-dependence is encoded in a non-linear IDE. Solving

reference	η_*^{s}	Δ
[130]	−0.361	—
[155]	0	—
polynomial expansion[6]	−0.771	—
form factors	0	1

Table 5.1: *Comparison of the scalar anomalous dimension η_*^{s} reported in the literature. As an important novel feature, the form factor $f_*^{(\phi\phi)}(p^2)$ allows to analyze the asymptotic behavior of the scalar two-point function (propagator) at large momenta.*

this type of equations is highly nontrivial, and can only be done in very special cases.

The main result of this analysis is discussed in subsection 5.3.3. Here it is established that the scalar kinetic term of the gravity-scalar fixed point previously studied in [107, 108, 111, 130, 155, 161] extends to a complete form factor which is well-defined for all momenta. Remarkably, for harmonic gauge ($\beta = \frac{d}{2} - 1$) and Landau limit ($\alpha \to 0$), the propagator $f(z) = z$ is an exact solution to the flow equation.

A particular feature of this solution is a vanishing gap parameter μ_*. This supports the conjecture [73] that the scalar sector of the gravity-matter system is shift-symmetric, i.e. it is invariant under the transformation $\phi \to \phi + c$, where c is a constant.

The analysis of perturbations around this solution shows that, as expected, the gap parameter of the scalar is a relevant parameter. Since the fixed point solution is trivial, the anomalous dimension vanishes. Table 5.1 compares this value to results reported in the literature. The results are in remarkable agreement with [155], despite a different closure of the split-symmetry. Since the underlying computations of [130] use a different choice for the field decomposition and the implementation of the regulator function, one should not expect a matching of the results beyond the qualitative agreement here.

The scaling of the scalar propagator in the large-momentum regime follows from the scaling analysis in subsection 5.3.3 and is given by

$$\lim_{p^2\to\infty} G_*^{\mathrm{s}}(p^2) \propto \frac{1}{p^{2\alpha}}\,, \qquad \alpha = 1\,. \tag{5.74}$$

By performing a Fourier transform to position space, this asymptotic behavior then governs the short-distance asymptotics of the scalar two-point correlator. Explicitly,

$$\langle\phi(x)\phi(y)\rangle \simeq \frac{1}{|x-y|^{2\Delta}}\,, \qquad \Delta = \frac{1}{2}(d-2\alpha) = 1\,. \tag{5.75}$$

[6] See chapter 4.

Notably, this fall-off is compatible with the unitarity bounds on the scaling behavior of scalar correlators stating that $\Delta \geq \Delta_{\text{min}} = 1$ [253, 254].

An important point, which so far has not been addressed in the literature, is the relation between the form factors at the fixed point $f_*(\{p_i\})$ and in the quantum effective action $f_{k=0}(\{p_i\})$. Establishing this connection requires solving the k-dependent IDE with suitable boundary conditions. In the scalar case discussed in this chapter this computation would proceed as follows. The first step constructs the eigenperturbations associated with the three relevant directions explicitly. Adding perturbations into the relevant directions then gives different initial conditions for the projected flow equation imposed at asymptotically large values of k. The latter is then mapped to the couplings appearing in the quantum effective action $\Gamma_{k=0}$ by solving the IDE (5.57). While this analysis is crucial for understanding whether the non-Gaussian fixed point is connected to the observed "low-energy world", this computation is beyond the scope of the present work.

An important cross-check along these lines may be provided by the effective field theory treatment of gravity [255], recently reviewed in [256–259]. Suppose that instead of tracing the renormalization group flow to the deep infrared, $k = 0$, the solution of the IDE is constructed up to a finite scale $k^2 = \Lambda^2 \lesssim M_{\text{Pl}}^2$. Provided that the structure of the effective average action at this scale resembles the Einstein-Hilbert action, the resulting quantum effective action should resemble the one found in the effective field theory treatment, at least at the perturbative level.

Clearly, understanding the momentum-dependent form factors associated with the non-Gaussian fixed points appearing in gravity and gravity-matter systems and the resulting quantum effective actions constitute formidable computational tasks. However, already from the pioneering works [59, 109], it is clear that the form factors related to the two-point functions of the fluctuation fields (non-perturbative propagators) may hold the key to understanding the structure of spacetime at short distances. Also the fate of spacetime singularities, omnipresent in GR, is closely linked to understanding the structure of the graviton propagator at trans-Planckian momenta. Thus, form factors may be the key towards unlocking some of the most fundamental questions in quantum gravity. Therefore, research addressing these challenges may very well be worth the effort.

CHAPTER 6

REFLECTION POSITIVITY IN HIGHER-DERIVATIVE SCALAR THEORIES

The following chapter is based on:

> F. Arici, D. Becker, C. Ripken, F. Saueressig, and W. D. van Suijlekom. *Reflection positivity in higher derivative scalar theories*. *J. Math. Phys.* **59**.8 (2018) 082302. [arXiv:1712.04308].

The following chapter studies under which conditions higher-derivative theories violate or satisfy unitarity. We will restrict ourselves to a flat background and to Euclidean signature. We will study the Euclidean equivalent of unitarity, called reflection positivity.

6.1 Unitarity and reflection positivity

Apart from consistency conditions on a QFT such as renormalizability, which is necessary for avoiding unwanted divergencies, we may also impose additional physical constraints on a QFT. A prominent property is unitarity, as discussed in chapter 1. Unitarity ensures positivity of transition amplitudes in scattering processes, yielding a consistent probabilistic interpretation of the quantum theory.

Unitarity of a QFT on flat Minkowski space has been made precise in the form of the Wightman axioms [260], as conditions on the correlation functions. Osterwalder and Schrader [261, 262] showed that one can construct a Lorentzian QFT from a probabilistic theory on a Euclidean manifold $\mathcal{M}$, provided that the latter satisfies the Osterwalder–Schrader axioms. The Euclidean theory can then be mapped to a Lorentzian QFT by

means of a Wick rotation. This is the content of the Osterwalder–Schrader reconstruction theorem.

In this thesis, we have encountered Euclidean QFTs as the natural framework for the FRG. Furthermore, in Euclidean theories the inner product on $\mathcal{M}$ is positive definite and the Laplace operator Δ is elliptic, yielding a mathematical toolbox stocked with a functional calculus that is under better control than in the Lorentzian case.

The Osterwalder–Schrader axioms (see the standard work [263] for a detailed exposé) can be phrased as a set of conditions on the partition function $Z[J]$, which can be written formally as the path integral $\int \mathcal{D}\varphi\, \mathrm{e}^{-S[\varphi]+J\cdot\varphi}$ (see section 2.1). The Osterwalder-Schrader axioms are then:

1. Analyticity
2. Regularity
3. Euclidean invariance
4. Reflection positivity
5. Ergodicity

We will now explain these axioms in detail. The first two axioms ensure that the partition function is sufficiently "nice" such that e.g. correlators can be calculated by taking functional derivatives. The third axiom, Euclidean invariance, translates to Lorentz invariance in the corresponding Lorentzian QFT. Ergodicity corresponds to the requirement that the vacuum state is unique.

Reflection positivity stands out in the sense that it is the only axiom that explicitly refers to a Euclidean time direction. It singles out a specific direction in Euclidean space, which eventually will translate to the Lorentzian causal structure. In general, reflection positivity of a partition function $Z[J]$ is given by the following requirement. Let $\{J_i\,(t,\vec{x})\}$ be a finite sequence of test functions on d-dimensional Euclidean space $\mathbb{R}^d$ such that $J_i\,(t,\vec{x})$ is zero for $t < 0$. Reflection positivity then states that for any such sequence, the matrix

$$\mathbf{B}_{ij} = Z\left[J_i - \Theta\, J_j\right] \tag{6.1}$$

is positive. Note that the condition on the support of the J_i already isolates the t-direction as a special direction in $\mathbb{R}^d$. Together with the time reflection operator Θ, which will be defined in full rigor in section 6.2, this selects the Euclidean time direction.

Reflection positivity has been proven for only a few theories, including the Klein-Gordon theory or the Dirac operator (see for instance [261, 264]). We consider free scalar theories with a covariance operator or propagator of the form $C(\Delta)$ on flat, non-dynamical

Euclidean spacetime. In this case, the partition function can be written as

$$\log Z[J] = -\frac{1}{2}\langle J, C(\Delta)J\rangle \ . \tag{6.2}$$

In particular, this case includes the Klein-Gordon propagator $\left(\Delta + m^2\right)^{-1}$, which has been proven to be reflection positive. However, propagators of the form $C^{-1} = p_n(\Delta)$, where p_n denotes a polynomial of degree $n \geq 2$, are commonly expected to be reflection positivity violating, based on the classical theorem by Ostrogradski [176].

The main result of this chapter is Theorem 6.2, which gives for a large class of functions C a necessary and sufficient condition such that reflection positivity is satisfied. For example, the theorem proves violation of reflection positivity for a propagator of the form $C\left(p^2\right) = \left(p^2 + m^2\right)^{-1} - \left(p^2 + M^2\right)^{-1}$, as was also shown in [265].

The rest of this chapter is organized as follows. In section 6.2, we introduce a rigorous definition of reflection positivity of a propagator $C(\Delta)$, and state the theorem Theorem 6.2. We then prove the theorem in section 6.2 and section 6.3. We illustrate the theorem by selected cases where reflection positivity is confirmed or violated in section 6.4. We close the chapter with an outlook on possible extensions of the theorem and applications in theoretical physics in section 6.5.

6.2 Setup and sufficient conditions

We start by setting up the functional spaces for which the theorem will hold. The key ingredient for reflection positivity is the time-reflection operator $\theta\colon \mathbb{R}^d \to \mathbb{R}^d$, given by $(t, \vec{x}) \mapsto (-t, \vec{x})$ on flat Euclidean spacetime. The time reflection operator gives rise to the operator Θ on the space of square-integrable functions $\mathrm{L}^2(\mathbb{R}^d)$ by pullback of θ. That is, for $f \in \mathrm{L}^2(\mathbb{R}^d)$, we define

$$\Theta f := f \circ \theta \, . \tag{6.3}$$

Following the conventions of [264], we define $\mathcal{S}\left(\mathbb{R}_+\right)$ to be the space of Schwartz functions $f \in \mathcal{S}(\mathbb{R})$ such that $\operatorname{supp} f \subseteq \mathbb{R}_+ := [0, \infty)$. By $\mathcal{S}\left(\mathbb{R}^d_+\right)$ we denote the completed topological tensor product $\mathcal{S}\left(\mathbb{R}_+\right) \hat{\otimes} \mathcal{S}\left(\mathbb{R}^{d-1}\right)$, that is, the space of functions f such that $f \in \mathcal{S}\left(\mathbb{R}^d\right)$ and $\operatorname{supp} f \subseteq \{x \in \mathbb{R}^d, t \geq 0\}$.

For the free theory, reflection positivity can be phrased as the following condition on the covariance operator C:

Definition 6.1 (Reflection positivity). *Let C be a covariance operator that commutes with the time reflection operator Θ. Then C is said to satisfy reflection positivity if for all $J \in \mathcal{S}\left(\mathbb{R}^d_+\right)$, we have the inequality*

$$\langle J, C\,\Theta J\rangle \geq 0 \, . \tag{6.4}$$

Based on this definition, we derive the necessary and sufficient conditions for a large class of free propagators to satisfy reflection positivity.

Theorem 6.2. *Let C be a real rational function which has no poles on $\mathbb{R}_+$. A necessary and sufficient condition for the operator $C(\Delta)$ to satisfy reflection positivity is that the poles of C all lie on $\mathbb{R}_-$, are simple and have non-negative residue.*

An essential ingredient in the proof of this theorem is establishing a relation between reflection positivity of $C(\Delta)$ and its pole structure. We find that the inner product $I[J] \equiv \langle J, C\,\Theta\,J\rangle$ is a sum over the residues at the poles, deformed by some J and the pole-dependent prefactor. Thus, the properties of the poles—their degree, and their position—determine whether $I[J]$ is non-negative for all J.

Essential for the theorem is that a real rational function C admits a unique representation in terms of its partial fraction decomposition [266, Corollary 5.5.4]:

$$C(x) = \sum_{j=1}^{N} \left(\sum_{n=1}^{k_j} a_{jn} \left(x - z_j\right)^{-n} \right) + p(x)\,. \tag{6.5}$$

where p is a real polynomial. The number $z_j \in \mathbb{C}$ is a pole of order k_j for C, writing $\operatorname{ord}\left(C, z_j\right) = k_j$. The set of poles of C is denoted by $\mathcal{P}_C$. We assume that C has no poles on the positive real line, i.e. $\mathcal{P}_C \cap \mathbb{R}_+ = \emptyset$. In the physics setting, a pole on the positive real line corresponds to a *negative* squared mass. The existence of such a particle would allow for obtaining an infinite amount of energy by creating particles from the vacuum, which we exclude on physical grounds.

Using Fourier transforms and the pseudo-differential calculus on $\mathbb{R}^d$ (see [267, 268]), together with the property that C has no poles on $\mathbb{R}_+$, we can write the operator $C(\Delta)$ as a sum of powers of resolvents plus a local operator $p(\Delta)$,

$$C(\Delta) = \sum_{j=1}^{N} \left(\sum_{n=1}^{k_j} a_{jn} \left(\Delta - z_j\right)^{-n} \right) + p(\Delta)\,, \tag{6.6}$$

acting on Schwartz space $\mathcal{S}\left(\mathbb{R}^d_+\right)$.

The coefficients a_{jn} appearing in the expansion (6.5) are the residues, given by the expression

$$a_{jn} = \operatorname*{res}_{z \to z_j} \left(\left(z - z_j\right)^{n-1} C(z) \right)\,. \tag{6.7}$$

It is easy to check that for the complex conjugate $\overline{C(z)}$ the reality condition $\overline{C(z)} = C(\bar{z})$ implies that if z_j is a complex pole of order k_j, then $\bar{z}_j$ is also a pole of order k_j.

Let us remark that the operator $C(\Delta)$ can be decomposed into the sum of simpler operators, coming from separate poles,

$$\begin{aligned} C_\lambda(\Delta) &= \sum_{n=1}^{k} \left(a_n (\Delta - \lambda)^{-n} + \bar{a}_n \left(\Delta - \bar{\lambda}\right)^{-n} \right) , \quad \lambda \in \mathbb{C}\backslash\mathbb{R} , \operatorname{ord}(C, \lambda) = k \\ C_\mu(\Delta) &= \sum_{n=1}^{k} a_n (\Delta - \mu)^{-n} , \qquad\qquad \mu \in \mathbb{R}_- , \operatorname{ord}(C, \mu) = k . \end{aligned} \tag{6.8}$$

For later reference, we use the following notation for the Klein-Gordon propagator with (possibly complex) mass $w \in \mathbb{C}\backslash\mathbb{R}_+$:

$$I_w[J] = \left\langle J, \Theta \left(\Delta - w\right)^{-1} J \right\rangle . \tag{6.9}$$

Proposition 6.3. *Let C be a real rational function with partial fraction decomposition (6.5). The $I[J]$ for the covariance operator $C(\Delta)$ can be written as*

$$I[J] = \sum_{j=1}^{N} \sum_{n=1}^{k_j} a_{jn} \frac{1}{(n-1)!} \frac{\mathrm{d}^{n-1}}{\mathrm{d}z_j^{n-1}} I_{z_j}[J] . \tag{6.10}$$

Proof. Substituting the expression for $C(\Delta)$ into $I[J]$, we obtain

$$I[J] = \langle J, p(\Delta)\, \Theta J \rangle + \sum_{j=1}^{N} \sum_{n=1}^{k_j} a_{jn} \frac{1}{(n-1)!} \frac{\mathrm{d}^{n-1}}{\mathrm{d}z_j^{n-1}} \left\langle J, \Theta \left(\Delta - z_j\right)^{-1} J \right\rangle . \tag{6.11}$$

Since p is a polynomial, $p(\Delta)$ is a local operator; therefore, the inner product $\langle J, \Theta\, p(\Delta) J \rangle$ vanishes since for $J \in \mathcal{S}\left(\mathbb{R}^d_+\right)$, $\operatorname{supp} J \cap \operatorname{supp} \Theta J = \{0\}$. □

From this proposition, we conclude that reflection positivity is directly linked to the pole structure of the propagator. We are now in a position to prove the *if* part of the main theorem.

Proposition 6.4. *A sufficient condition for $C(\Delta)$ to satisfy reflection positivity is that the poles of C all lie on $\mathbb{R}_-$, are simple and possess a non-negative residue.*

Proof. In [264, 269–271], it is shown that for all $J \in \mathcal{S}\left(\mathbb{R}^d_+\right)$, the integral $I_\mu[J] \geq 0$, $\mu \in \mathbb{R}$, is non-negative. If all poles are simple and in $\mathbb{R}_-$, we can write

$$I[J] = \sum_{j=1}^{N} a_j I_{\mu_j}[J] , \tag{6.12}$$

with $a_j = \operatorname{res}_{z \to \mu_j} C(z)$. The claim then follows from the assumption that all residues are non-negative. □

In the next section, we will prove the proposition that the condition in Proposition 6.4 is actually a necessary condition for reflection positivity. We will show that reflection positivity is violated whenever there are complex poles, real poles of higher order, or real poles with negative residue.

6.3 Necessary conditions for reflection positivity

6.3.1 Properties of the Klein-Gordon quadratic form

We have seen in the previous section that the Klein-Gordon propagator and its integral $I_w[J]$ play a key role in the discussion of reflection positivity. In this subsection, we will prove three lemmata that will allow us to construct functions $J \in \mathcal{S}\left(\mathbb{R}^d_+\right)$ such that $I_w[J]$ and its derivatives explicitly violate the inequality (6.4).

Lemma 6.5. *Let $w \in \mathbb{C}\backslash\mathbb{R}_+$, $J \in \mathcal{S}\left(\mathbb{R}^d_+\right)$, and $I_w[J]$ be defined as in (6.9). The following identity holds true:*

$$I_w[J] = -\pi i \int \frac{\mathrm{d}^{d-1}p}{\sqrt{w-\vec{p}^2}} \tilde{J}^*\left(-\overline{\sqrt{w-\vec{p}^2}}, \vec{p}\right) \tilde{J}\left(\sqrt{w-\vec{p}}, \vec{p}\right). \tag{6.13}$$

Proof. The proof consists of computing a contour integral in p^0. Factorizing the measure, we obtain after Fourier transforming that

$$I_w[J] = \int \mathrm{d}^{d-1}\vec{p} \int_{-\infty}^{\infty} \mathrm{d}p^0 \frac{\tilde{J}^*\left(-p^0, \vec{p}\right) \tilde{J}\left(p^0, \vec{p}\right)}{\left(p^0\right)^2 + \vec{p}^2 - w}. \tag{6.14}$$

The integral over p^0 can be calculated by closing the contour in the lower half-plane. This gives

$$I_w[J] = \lim_{R\to\infty} \int \mathrm{d}^{d-1}\vec{p} \int_{\Gamma_R} \mathrm{d}s \frac{\tilde{J}^*\left(-s, \vec{p}\right) \tilde{J}\left(s, \vec{p}\right)}{s^2 - \left(w - \vec{p}\right)^2}, \tag{6.15}$$

where Γ_R is a large semicircle of radius R such that $\Gamma_R \subset \{z \in \mathbb{C} \mid \mathrm{Im}(z) \leq 0\}$. The integrand is meromorphic in the interior of the contour, since $\tilde{J}\left(s, \vec{p}\right)$ is analytic in the lower half-plane by the Paley-Wiener theorem (cf. [268, Theorem 7.2.4]). Furthermore, since the integral over p^0 is over the reals, we can extend $\tilde{J}\left(p^0, \vec{p}\right)$ to an analytic function by considering $\tilde{J}^*\left(\bar{s}, \vec{p}\right)$. Finally, the contribution of the semicircular arc of Γ_R to the integral vanishes in the limit $R \to \infty$, since the same Paley-Wiener theorem ensures that $\tilde{J}$ is falling off sufficiently fast.

The contour integral is now calculated by the residue theorem; the integrand has poles at $\pm\sqrt{w-\vec{p}^2}$, with the convention that $\sqrt{w-\vec{p}^2}$ lies in the lower half-plane (see

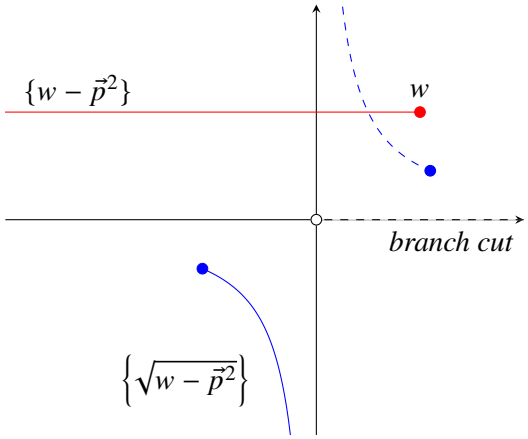

Figure 6.1: *The two square roots (in blue) of $w - \vec{p}^2$ as $\vec{p}$ varies over $\mathbb{R}^{d-1}$ (in red). We adopt the convention that $\sqrt{w - \vec{p}^2}$ lies in the lower half-plane (solid blue line). The branch cut will never be crossed because of our assumption that $w \notin \mathbb{R}_+$.*

Figure 6.1). The integral is then given by

$$\begin{aligned} I_w[J] &= -2\pi i \int \mathrm{d}^{d-1}\vec{p} \operatorname*{res}_{s \to \sqrt{w-\vec{p}^2}} \frac{\tilde{J}^*(-\bar{s}, \vec{p})\, \tilde{J}(s, \vec{p})}{s^2 - w - \vec{p}^2} \\ &= -\pi i \int \frac{\mathrm{d}^{d-1}p}{\sqrt{w - \vec{p}^2}} \tilde{J}^*\left(-\overline{\sqrt{w - \vec{p}^2}}, \vec{p}\right) \tilde{J}\left(\sqrt{w - \vec{p}}, \vec{p}\right) . \end{aligned} \tag{6.16}$$

In this expression, we have calculated the integral by factorizing the denominator $s^2 - w - \vec{p}^2 = \left(s - \sqrt{w - \vec{p}^2}\right)\left(s + \sqrt{w - \vec{p}^2}\right)$ into first-order roots. Since $\tilde{J}(s, \vec{p})$ and $\tilde{J}^*(-\bar{s}, \vec{p})$ are analytic, the second line then follows from a straightforward application of the residue theorem.

□

The second lemma is a homogeneity property of $I_w[J]$, which follows from the previous lemma.

Lemma 6.6. *Let $J \in \mathcal{S}\left(\mathbb{R}^d_+\right)$, and let q be a polynomial. Then $q(\Delta)J \in \mathcal{S}\left(\mathbb{R}^d_+\right)$, and*

$$I_w\left[q(\Delta)J\right] = \overline{q(\bar{w})} q(w) I_w[J] , \tag{6.17}$$

for all $w \in \mathbb{C} \backslash \mathbb{R}_+$.

Proof. Since q is a polynomial, the operator $q(\Delta)$ is local. Thus, the support of $q(\Delta)J$ is contained in the support of J, which is contained in $\mathbb{R}^d_+$. Furthermore, since J is smooth, $q(\Delta)J$ is smooth as well.

We then apply Lemma 6.5 to calculate $I_w[q(\Delta)J]$,

$$I_w\left[q(\Delta)J\right] = -\pi i \int \frac{\mathrm{d}^{d-1}\vec{p}}{\sqrt{w-\vec{p}^2}} \widetilde{(q(\Delta)J)}^* \left(-\sqrt{w-\vec{p}^2}, \vec{p}\right) \widetilde{(q(\Delta)J)}\left(\sqrt{w-\vec{p}^2}, \vec{p}\right), \tag{6.18}$$

where $\widetilde{(q(\Delta)J)}$ denotes the Fourier transform of the function $q(\Delta)J$. Since we have $\widetilde{(q(\Delta)J)}(p) = q(p^2)\tilde{J}(p)$ and $\widetilde{(q(\Delta)J)}^*(p) = \overline{q(p^2)}\tilde{J}^*(p)$, this can be rewritten as

$$I_w\left[q(\Delta)J\right] = -\pi i \overline{q(\bar{w})} q(w) \int \frac{\mathrm{d}^{d-1}\vec{p}}{\sqrt{w-\vec{p}^2}} \tilde{J}^*\left(-\sqrt{w-\vec{p}^2}, \vec{p}\right) \tilde{J}\left(\sqrt{w-\vec{p}^2}, \vec{p}\right), \tag{6.19}$$

which we recognize as $\overline{q(\bar{w})}q(w)I_w[J]$. This completes the proof. □

Reflection positivity is satisfied trivially if $I[J]$ is zero for all $J \in \mathcal{S}\left(\mathbb{R}^d_+\right)$. In order to exclude this case, we show that one can always construct a J such that $I_w[J]$ is nontrivial. This is shown in the following lemma.

Lemma 6.7. *Let $I_w[J]$ be defined as in (6.9). Then there exists a $J \in \mathcal{S}\left(\mathbb{R}^d_+\right)$ for which*

$$I_w[J] \neq 0. \tag{6.20}$$

Proof. First note that $I_w[J]$ extends to a continuous quadratic form on $\mathrm{L}^2(\mathbb{R}^d_+)$, so that by a density argument it suffices to show that there exists a $J \in \mathrm{L}^2(\mathbb{R}^d_+)$ for which $I_w[J] \neq 0$. We consider the following explicit candidate:

$$J(\tau, \vec{x}) = \chi_{[a,b]}(\tau) \cdot (c_1 \cdots c_{d-1})^{1/4} \, \mathrm{e}^{-\pi\left(c_1 x_1^2 + \cdots + c_{d-1}x_{d-1}^2\right)}, \tag{6.21}$$

where $\chi_{[a,b]}$ is the indicator function on the interval $[a,b] \subset \mathbb{R}_+$ and $c_1, \ldots, c_{d-1} > 0$. One readily checks that for z in the lower half-plane we have

$$\tilde{J}(z, \vec{p}) = \frac{1}{2\pi i z}\left(\mathrm{e}^{-2\pi i a z} - \mathrm{e}^{-2\pi i b z}\right) \frac{\mathrm{e}^{-\pi\left(p_1^2/c_1 + \cdots + p_{d-1}^2/c_{d-1}\right)}}{(c_1 \cdots c_{d-1})^{1/4}}. \tag{6.22}$$

We may now invoke Lemma 6.5 to show that for this J, we have

$$I_w[J] = -\frac{1}{4\pi i} \int \frac{\mathrm{d}^{d-1}\vec{p}}{\left(w-\vec{p}^2\right)^{3/2}} \left(\mathrm{e}^{-2\pi i a\sqrt{w-\vec{p}^2}} - \mathrm{e}^{-2\pi i b\sqrt{w-\vec{p}^2}}\right)^2 \times \frac{\mathrm{e}^{-\pi\left(p_1^2/c_1 + \cdots + p_{d-1}^2/c_{d-1}\right)}}{(c_1 \cdots c_{d-1})^{1/4}}. \tag{6.23}$$

Now observe that as we let $c_1,\ldots,c_{d-1} \to 0$ the Gaussian integrals converge to the Dirac delta distribution $\delta(\vec{p})$ (note, however, that this only applies to the combined expression for $\tilde{J}^*(-\bar{z},\vec{p})\,\tilde{J}(z,\vec{p})$ appearing in integral expression (6.23) for $I_w[J]$; it is not the case that the function $\tilde{J}(z,\vec{p})$ itself converges to a Dirac delta distribution). Moreover, it is sufficient to consider this limiting case, since if the above integral is non-zero in this limit, there must exist finite values of $c_1,\ldots,c_{d-1}$ for which the $I_w[J]$ is also non-zero. It is now straightforward to compute that in this limit we have

$$I_w[J]|_{c_1,\ldots,c_{d-1}\to 0} = -\frac{1}{2^{(d+3)/2}\pi i} w^{-3/2}\left(\mathrm{e}^{-2\pi i a\sqrt{w}} - \mathrm{e}^{-2\pi i b\sqrt{w}}\right)^2 , \tag{6.24}$$

which is indeed non-zero for generic values of a and b. □

6.3.2 Reduction to separate poles

Before we proceed to consider the various cases, we will show that, whenever we have a term in the sum (6.5) which on its own violates reflection positivity, we can always tune J in such a way that $I[J]$ only depends on this term. This follows from Lemma 6.7, combined with the homogeneity property of Lemma 6.6.

Lemma 6.8. *For any pole $\lambda \in \mathcal{P}_C$, there exists a $J \in \mathcal{S}(\mathbb{R}^d_+)$ such that*

$$I[J] = \langle J, C_\lambda(\Delta)\,\Theta\,J\rangle . \tag{6.25}$$

Proof. Let $J \in \mathcal{S}(\mathbb{R}^d_+)$ be such that $I_\lambda[J] \neq 0$, by Lemma 6.7. We consider the polynomial

$$q(z) = \prod_{z_j \in \mathcal{P}_C \setminus \{\lambda,\bar{\lambda}\}} (z - z_j)^{k_j} . \tag{6.26}$$

By definition,

$$I[q(\Delta)J] = \sum_j \sum_{n=1}^{k_j} a_{jn} \frac{1}{(n-1)!} \frac{\mathrm{d}^{n-1}}{\mathrm{d}z^{n-1}} I_z[q(\Delta)J]\Big|_{z=z_j} , \tag{6.27}$$

with the first sum running over the set of poles $\mathcal{P}_C$. If we set $q_j(z) = q(z)/(z-z_j)^{k_j}$, it is easy to see that the sums

$$\sum_{n=1}^{k_j} a_{jn} \frac{1}{(n-1)!} \frac{\mathrm{d}^{n-1}}{\mathrm{d}z^{n-1}} I_z[q(\Delta)J]$$
$$= \sum_{n=1}^{k_j} a_{jn} \frac{1}{(n-1)!} \frac{\mathrm{d}^{n-1}}{\mathrm{d}z^{n-1}} (z-z_j)^{k_j} (z-\bar{z}_j)^{k_j} I_z\left[q_j(\Delta)J\right] \tag{6.28}$$

vanish upon evaluation at $z_j \neq \lambda, \bar{\lambda}$.

Therefore, the only terms that are left in the sum (6.27) are the ones corresponding to $\lambda, \bar{\lambda}$, giving

$$I[q(\Delta)J] = \langle q(\Delta)J, C_\lambda(\Delta)\,\Theta\, q(\Delta)J\rangle \ , \tag{6.29}$$

which proves the claim. □

6.3.3 Violation of reflection positivity

We are now ready to prove that the condition in Proposition 6.4 is also necessary. This is achieved by constructing functions in $\mathcal{S}\left(\mathbb{R}^d_+\right)$ that violate reflection positivity in all the cases that are not covered by the conditions in Proposition 6.4. In Proposition 6.9, we consider complex poles, while poles of higher order are excluded in Proposition 6.10.

Proposition 6.9. *Let us assume that C has a pole in the upper half-plane. Then there exists a $J \in \mathcal{S}\left(\mathbb{R}^d_+\right)$ such that*

$$I[J] < 0\,. \tag{6.30}$$

Proof. In view of Lemma 6.8, we may assume, without loss of generality, that C has exactly two complex conjugate poles, λ and $\bar{\lambda}$, of order k, with $\mathrm{Im}(\lambda) > 0$.

Let $J \in \mathcal{S}\left(\mathbb{R}^d_+\right)$ be such that $I_\lambda[J] \neq 0$, which is always possible in view of Lemma 6.7. Let us choose a polynomial ansatz for q defined as follows:

$$q(z) = (z-\lambda)^{k-1}h(z)\,, \quad h(z) = \frac{1-\bar{\alpha}}{2i\,\mathrm{Im}(\lambda)}(z-\lambda)+1\,. \tag{6.31}$$

Note that the polynomial h is chosen in such a way that $h(\lambda) = 1$ and $\overline{h(\bar{\lambda})} = \alpha$.

We now compute

$$\begin{aligned} I[q(\Delta)J] =& 2\,\mathrm{Re}\sum_{n=1}^{k} a_n \frac{1}{(n-1)!}\,\frac{\mathrm{d}^{n-1}}{\mathrm{d}z^{n-1}} I_z[q(\Delta)J]\Big|_{z=\lambda} \\ =& 2\,\mathrm{Re}\sum_{n=1}^{k} a_n \frac{1}{(n-1)!}\,\frac{\mathrm{d}^{n-1}}{\mathrm{d}z^{n-1}} (z-\lambda)^{k-1}\left(z-\bar{\lambda}\right)^{k-1} h(z)\overline{h(\bar{z})} I_z[J]\Big|_{z=\lambda} \\ =& 2\,\mathrm{Re}\left(\alpha\cdot a_k\,(2i\,\mathrm{Im}(\lambda))^{k-1}\,I_\lambda[J]\right)\,. \end{aligned} \tag{6.32}$$

In the first step, we have applied Lemma 6.6. In the last step, we have used that $(z-\lambda)^{k-1}$ vanishes at λ, with all of its derivatives, except for the $(k-1)$-th. Note that $\mathrm{Im}(\lambda) \neq 0$, and $I_\lambda[J] \neq 0$ by construction, hence we can choose α to make the above expression negative. This completes the proof. □

The case of real poles of order greater than one can be treated in a similar way.

Proposition 6.10. *Suppose that $C(z)$ has a pole in the upper half-plane. Then there exists a $J \in \mathcal{S}\left(\mathbb{R}^d_+\right)$ such that*

$$I[J] < 0\,. \tag{6.33}$$

Proof. By Lemma 6.8, it is not restrictive to assume that C has exactly one pole μ of order $k > 1$.

Let $J \in \mathcal{S}\left(\mathbb{R}^d_+\right)$ be such that $I_\mu[J] \neq 0$, which again is always possible in view of Lemma 6.7.

We proceed similarly to the proof of Proposition 6.9 and choose for q a polynomial of the form

$$q(z) = \alpha(z-\mu)^{k-1} + 1\,. \tag{6.34}$$

Computing $I[q(\Delta)J]$, we obtain

$$\begin{aligned} I[q(\Delta)J] &= \sum_{n=1}^{k} a_n \frac{1}{(n-1)!} \frac{\mathrm{d}^{n-1}}{\mathrm{d}z^{n-1}} I_z[q(\Delta)J]\Big|_{z=\mu} \\ &= \sum_{n=1}^{k} a_n \frac{1}{(n-1)!} \frac{\mathrm{d}^{n-1}}{\mathrm{d}z^{n-1}} \left(1 + 2\alpha(z-\mu)^{k-1} + \alpha^2(z-\mu)^{2(k-1)}\right) I_z[J]\Big|_{z=\mu} \\ &= I[J] + 2\alpha \cdot a_k I_\mu[J]\,, \end{aligned} \tag{6.35}$$

where we have used Lemma 6.6 in the first step. In the second step, we observed that all derivatives of $(z-\mu)^k$ evaluated at μ vanish, except for the $(k-1)$-st. Note that a_k is non-zero by assumption and $I_\mu[J]$ is non-zero by construction; thus, we can choose α such that $I[q(\Delta)J] < 0$, which proves the claim. □

Finally, whenever C has a real single pole with negative residue, we can use Lemma 6.8 to construct a J such that $I[J]$ only depends on that pole. The sign of the residue will automatically imply that reflection positivity is violated.

Combined with the proof that simple real poles with non-negative residue satisfy reflection positivity, we have completed the proof of our main result.

Theorem 6.2. *Let C be a real rational function which has no poles on $\mathbb{R}_+$. A necessary and sufficient condition for the operator $C(\Delta)$ to satisfy reflection positivity is that the poles of C all lie on $\mathbb{R}_-$, are simple and have non-negative residue.*

6.4 Selected cases

In order to put the theorem into context, we will give some physical examples of higher-derivative theories which may or may not violate reflection positivity. We will consider

the Klein–Gordon case (subsection 6.4.1), a propagator with negative residue (subsection 6.4.2), complex poles (subsection 6.4.3), and poles of order higher than one (subsection 6.4.4). Finally, we will study a propagator which does not fall into the class covered by Theorem 6.2, and show which proof strategies fail in this case (subsection 6.4.5).

6.4.1 The Klein–Gordon operator

The first case we consider is the Klein–Gordon operator, given by $C\left(p^2\right) = (p^2 + m^2)^{-1}$, where $m^2 > 0$. This case is extensively studied [264, 269–271] and will turn out to be reflection positive. Indeed, using Lemma 6.5, we find

$$I_{-m^2}[J] = \pi \int \frac{\mathrm{d}^{d-1}\vec{p}}{\sqrt{m^2 + \vec{p}^2}} \left| \tilde{J}\left(-i\sqrt{m^2 + \vec{p}^2}, \vec{p}\right)\right|^2 , \tag{6.36}$$

where we have used that $\sqrt{-1} = -i$, in accordance with the sign convention of the square root in Lemma 6.5. It is clear that this is a positive number, and therefore the Klein–Gordon operator is reflection positive.

6.4.2 Negative residues

We now study the canonical example of an Ostrogradski ghost [265]. Consider the propagator

$$C\left(p^2\right) = \frac{M^2 - m^2}{(p^2 + m^2)(p^2 + M^2)} = \frac{1}{p^2 + m^2} - \frac{1}{p^2 + M^2} . \tag{6.37}$$

We now define the polynomial $q(s) = \left(s + m^2\right)$; using Lemma 6.8 and 6.6, we find

$$I\left[q(\Delta)J\right] = -(m^2 - M^2)^2 I_{-M^2}[J]. \tag{6.38}$$

Since $I_{-M^2}[J] \geq 0$, this indeed violates reflection positivity.

6.4.3 Complex poles

Thirdly, we consider a propagator with a complex pole, given by

$$C\left(p^2\right) = \left(p^2 + m^2 + i\Gamma\right)^{-1} + \left(p^2 + m^2 - i\Gamma\right)^{-1} , \tag{6.39}$$

where $m^2, \Gamma > 0$. From a physical perspective, the parameter Γ signals a decay width, and therefore an unstable fundamental degree of freedom. We will now show that this propagator is not reflection positive. First, we consider an arbitrary $J \in \mathcal{S}(\mathbb{R}^d_+)$. By Lemma 6.7, we can assume that $I[J] \neq 0$. If $I[J] < 0$, we have shown violation of reflection positivity, and there is nothing to prove.

Assume therefore that $I[J] > 0$. In light of Proposition 6.9, we choose

$$q(s) = \frac{2}{2i\Gamma}\left(s + m^2 - i\Gamma\right) + 1\,. \tag{6.40}$$

Then, using Lemma 6.6, we compute

$$I\left[q(\Delta)J\right] = 2\,\mathrm{Re}\; I_{-m^2+i\Gamma}\left[q(\Delta)J\right] = -I[J], \tag{6.41}$$

which is clearly negative. Thus, $q(\Delta)J$ violates reflection positivity.

6.4.4 Higher order poles

We now consider the propagator $C\left(p^2\right) = \left(p^2 + m^2\right)^{-2}$. According to Proposition 6.10, this should violate reflection positivity. With the same reasoning as in the previous section, assume for $J \in \mathcal{S}\left(\mathbb{R}^d_+\right)$ that $I_{-m^2}[J] > 0$. Then set $q(s) = \alpha\left(s + m^2\right) + 1$. Computing $I\left[q(\Delta)J\right]$, we obtain

$$I\left[q(\Delta)J\right] = I[J] + 2\alpha I_{-m^2}[J]. \tag{6.42}$$

Choosing $\alpha < -\frac{I[J]}{2I_{-m^2}[J]}$, $I\left[q(\Delta)J\right]$ becomes negative, and reflection positivity is violated.

6.4.5 Non-rational propagators

Finally, we explore the limits of Theorem 6.2, by considering a propagator which is non-rational. Let $C\left(p^2\right) = \left(p^2 + m^2\right)^{-1} \exp\left(-p^2\right)$. Propagators of this type are inspired by e.g. non-local gravity models [244].

The function C is a bounded function on $\mathbb{R}_+$, and therefore defines a bounded operator $C(\Delta)$. However, analytically continuing to a complex function $C(z)$ gives a function that diverges exponentially as $\mathrm{Im}(z) \to \pm\infty$.

This poses a problem when closing the contour in Lemma 6.5; in order to calculate the p^0-integral, the contribution from the arc in the negative half-plane has to vanish. For rational functions, this is satisfied since the Schwartz functions $\mathcal{S}\left(\mathbb{R}^d_+\right)$ decay faster than any rational function at infinity. For the exponential function C, this is not satisfied and therefore the contribution to the contour integral cannot be neglected.

A possibility for restoring the requirements for Lemma 6.5 is imposing a stricter condition on the class of admissible J's. In order to calculate the contour integral for $C(z)$, one should restrict the class of Schwartz functions to functions that decay faster than any exponential.

6.5 Conclusion

The main result of this chapter is Theorem 6.2, where we give necessary and sufficient conditions for reflection positivity in a large class of scalar field theories on flat Euclidean spacetime. We have studied scalar theories with a propagator of the form $C(\Delta)$, where C is a real rational function without poles on $\mathbb{R}_+$. Our theorem states that the only functions C that yield a reflection positive theory have simple poles on $\mathbb{R}_-$ and non-negative residue.

We have illustrated the theorem by some physical examples in section 6.4. First, we have shown that the Klein-Gordon propagator $\left(\Delta + m^2\right)^{-1}$ is indeed reflection positive. Secondly, we have explicitly demonstrated violation of reflection positivity in subsection 6.4.2, subsection 6.4.3 and subsection 6.4.4. These examples emphasize the caution that has to be taken with theories containing a polynomial kinetic function, such as $f(\Delta) = Z\left(\Delta + Y\Delta^2\right)$ that was studied in chapter 4. Our theorem demonstrates the importance of imposing additional constraints on the effective action $\Gamma_{k=0}$, in order to obtain a theory that is reflection positive.

There are several cases that are not covered by the theorem. Notably, the case where $C(\Delta) = \left(\Delta + m^2\right)^{-1} f(\Delta)$, where $f(\Delta)$ is an entire, analytic function with suitable falloff conditions is covered only partially by the theorem. Propagators of this form underlie the program of non-local theories of gravity (see [244] for a review) and arise naturally in the context of noncommutative geometry [272–274] and asymptotic safety [28, 103, 158, 4], as we have seen in chapter 5.

The theorem is also bypassed by constructions along the lines of a $\mathcal{PT}$-symmetric quantum mechanics, as advocated in [275, 276]. This setup builds on a nontrivial modification of the inner product (6.4).

One may extend the theorem along different lines. First of all, we may relax our assumptions on the analytic properties of C to cover the entire class of non-local propagators. Secondly, one may consider non-scalar and interacting fields. The generalization to non-scalar fields may go along the same lines as in [264]. Interacting fields may prove to be more problematic, since the condition for reflection positivity does not reduce to a simple positivity condition of an inner product. On the classical level, the conditions for obtaining an Ostrogradski ghost-free theory have been studied in [174]. Finally, one may generalize Theorem 6.2 to non-flat spacetimes. As a first step, one might consider reflection positivity on a curved manifold equipped with a foliation structure. For the case of the Klein-Gordon operator, the corresponding generalization for the Osterwalder-Schrader axioms have been studied in [264, 270, 271].

CHAPTER 7

CONCLUSION

In the introduction of this thesis, we encountered general relativity and the Standard Model of particle physics as the basis for our current understanding of the fundamental forces and particles in our universe. While conceptually very different, they are extremely successful in their domains of applicability. The Standard Model, formulated as a quantum theory, has been tested with high precision at small length scales. On the other hand, general relativity provides an excellent description of the universe at large scales. However, coming up with a unified description of a quantum theory of gravity has proven to be rather difficult. The application of perturbative quantization techniques to GR results in a non-renormalizable theory, either leading to UV-divergences, or to a loss of predictivity due to an infinite number of counterterms in the action.

On closer inspection, this phenomenon hinges on a perturbative analysis. Weinberg's conjecture that the renormalization group flow of gravity possesses a non-perturbative fixed point [34] may be an elegant way to reconcile the laws of QFT with general relativity. Such a NGFP leads to the Asymptotic Safety scenario. Due to the fixed point, UV divergences are avoided. In addition, predictive power is restored if the NGFP has a finite-dimensional UV-critical hypersurface. This can be described by a finite number of free parameters, whilst giving relations for an infinite number of irrelevant parameters.

The development of functional methods [38, 102] has paved the way for a systematic study of this conjecture. Combined with the background field method and truncations, we can study approximations to solutions of the functional renormalization group equation for gravity in terms of the effective average action Γ_k [28, 29].

While Asymptotic Safety is a promising candidate for a theory of quantum gravity, it should pass several tests. First and foremost, a theory should provide predictions that can be tested by experiment. Asymptotic Safety predicts relations between UV-irrelevant and -relevant couplings, which are fixed by the finite-dimensional UV-critical hypersurface. Secondly, a theory should be self-consistent. An open problem in the self-consistency

of Asymptotic Safety is the question of unitarity. Since Γ_k may contain operators of arbitrarily high order, this is an complicated question.

Within this context, we focused in this thesis on the following observational and structural aspects of asymptotically safe quantum gravity:

1. We tested compatibility of Asymptotic Safety with cosmological observations.
2. We demonstrated that Ostrogradski ghosts can be avoided by the renormalization group.
3. We classified form factors and calculated the full momentum dependence of a higher-derivative scalar propagator.
4. We provided necessary and sufficient conditions for reflection positivity in higher-derivative scalar theories.

Astrophysical observations, in particular those of the CMB by the Planck satellite, highly constrain theoretical models. One of these models, so-called Starobinsky inflation supplemented with a cosmological constant, is in excellent agreement with the observations. This model is described by an $f(R)$-action truncated to second order in R. It contains three couplings: the cosmological constant Λ, Newton's constant G and the R^2-coupling B that drives early-time inflation. Measurements of the scalar spectral tilt n_s and the tensor-to-scalar ratio r of fluctuations in the CMB determine the value of B. Measurements on the large-scale structure give a constraint on Λ. Finally, Newton's constant can be observed in laboratory experiments. Each of these parameters is measured at a characteristic energy scale.

In chapter 3 we have studied whether Asymptotic Safety is compatible with this model. To this end, we have investigated the RG flow of the aforementioned R^2-action. In this analysis, we reproduced the NGFP of gravity, demonstrating the asymptotically safe UV limit of the theory. Next, we studied the flow away from the fixed point. Each trajectory emanating from the NGFP gives a specific dependence of the couplings on the RG scale k. Identifying the RG scale with the scale at which the couplings are measured, we obtain three experimental constraints for the three couplings in the Starobinsky model. Each of these constraints is imposed at a different scale k.

We have constructed the RG trajectory, shown in Figure 3.5, that emanates from the NGFP and in addition satisfies all three experimental constraints. This provides evidence that the Asymptotic Safety scenario is consistent with observations from cosmology.

Apart from renormalizability, unitarity is an important consistency condition on a quantum theory. For instance, theories with a p^4-kinetic term suffer from the Ostrogradski instability. The higher-order term leads to an Ostrogradski ghost in the Kallén-Lehmann spectrum, whose negative norm leads to a violation of unitarity. In the context of the FRG, such actions are dangerous as they may be generated automatically along the

RG flow through gravitational interactions. However, the Ostrogradski instability can be lifted by pushing the ghost mass to infinity when flowing towards $k \to 0$. This decouples the ghost from the particle spectrum. In chapter 4, we have studied the RG flow of a higher-derivative scalar field coupled to gravity. We established that the system contains three NGFPs, suitable for asymptotic safety. Furthermore, within its UV critical hypersurfaces lie specific trajectories for which the ghost decouples in the IR, as is shown in subsection 4.3.4. This evidence that the RG allows for gravity-matter systems which are both asymptotically safe and ghost-free constitutes the main result of this chapter.

In chapter 5, we introduced form factors as generalized expansion coefficients in the EAA. They are functions of the Laplacian acting on monomials constructed from the fundamental fields of the theory. The expansion of such actions in a given background is manifestly split-symmetric, providing an important constraint en route to background independence. We classified the lowest-order form factors for gravity-matter systems and pure gravity. In addition, we obtained a mapping between the form factor expansion and the vertex expansion.

After that, we studied the form factor associated to a scalar kinetic term. This generalizes the p^4-kinetic term from chapter 4 to a full function of the momentum. We calculated the RG equations of the form factor coupled to gravity, and looked for fixed points. Remarkably, in Landau-harmonic gauge the kinetic term of a minimally coupled scalar field turned out to be an exact solution to the RG equation. An important feature of this form factor is that the form factor is manifestly positive. Its only root is at zero momentum, corresponding to a single scalar degree of freedom of zero mass. The construction of this form factor is the most important result of this chapter.

Finally, we studied the mathematical foundations of unitarity in chapter 6. Unitarity on Euclidean flat spacetime can be defined through the Osterwalder-Schrader axioms. Central in these axioms is the requirement of reflection positivity, a positivity condition on the propagator in combination with a reflection in Euclidean time. The main result of this chapter is Theorem 6.2. This result gives for a large class of higher-derivative theories a set of necessary and sufficient conditions for reflection positivity. In particular, we prove that the p^4-propagator from chapter 4 is not reflection positive, and therefore violates unitarity. This stresses the importance of studying the properties of the effective action $\Gamma_{k=0}$, and the extra constraints that should be imposed on RG trajectories describing a realistic quantum theory.

The results presented in this thesis provide a starting point for several directions of follow-up research. On the observable side, the study of the UV-critical hypersurface can give valuable predictions that could be tested experimentally. Within the $f(R)$-truncation, irrelevant operators are of the form $\int \sqrt{g} R^m$, where $m > 2$. The value of the corresponding couplings in the IR are therefore determined by a trajectory in the UV-critical hypersurface. An interesting follow-up investigation along the lines of chapter 3 would be to reconstruct this hypersurface, for instance when including the R^3-operator.

The associated couplings are then fixed in terms of the couplings (Λ, G, B) and can therefore be predicted. This prediction can be tested against the latest cosmological observations.

The results presented in chapter 4 and chapter 5 show that the study of Ostrogradski ghosts and form factors are closely related. On the one hand, the computation of the form factor in chapter 5 shows that a polynomial truncation of the momentum dependence in the propagator may lead to spurious poles. On the other hand, if a pole associated to an Ostrogradski ghost is present at some scale k in the RG flow, it may turn out to be harmless, by the mechanisms shown in chapter 4. Therefore, the flow of form factors away from the fixed point is an important topic that should be addressed.

The computation of form factors is still at an early stage. However, they may play a key role in the understanding of the structure of spacetime at small distances through the gravitational two-point function (see the pioneering works [59, 109] for results in an RG context), or in cosmology (for a study of the effects of form factors on inflation, see [277]). Form factors are also expected to contribute in an essential way to higher-order vertices, revealing new insights into the nature of interactions. Thus, understanding the behavior of form factors will provide an intriguing line of inquiry in the coming years.

Unitarity of more complicated, interacting systems such as gravity remains an unsolved problem, however. Also here form factors may provide vital information, such as the pole structure of the propagator. In chapter 5, we demonstrated that the scalar propagator remains positive definite when gravitational corrections are taken into account. Whether such properties are also present in pure gravity and other gravity-matter systems, and how this is related to unitarity, are important questions to be answered in follow-up investigations.

In this thesis, we have discussed both structural and observational facets of quantum theory and quantum gravity in particular. Both aspects are essential in a satisfactory theory describing nature. On the one hand, a theory should be structurally consistent, while on the other hand a theory should be testable by experiment. This thesis has made contributions in both directions, linking the renormalization group flow of gravity to cosmological observations, and by studying the properties of unitarity in higher-derivative theories. Form factors open up an exciting new window in both areas, and are therefore expected to shape interesting future research.

APPENDIX A

NOTATION AND CONVENTIONS

In this chapter, we will introduce some notation that we have used throughout this thesis.

A.1 Spacetime manifold

We will denote by $\mathcal{M}$ a d-dimensional Riemannian manifold. The manifold $\mathcal{M}$ is equipped with a (positive-definite) metric g. In general, indices of the tangent bundle will be denoted by Greek indices. Symmetrization and anti-symmetrization are denoted by round and square brackets, and normalized to unit strength,

$$H_{\alpha\beta} = H_{(\alpha\beta)} + H_{[\alpha\beta]}\,. \tag{A.1}$$

The metric g induces the Levi-Civita connection, whose covariant derivative is denoted by ∇. The covariant Laplacian is given by $\Delta = -g^{\mu\nu}\nabla_\mu\nabla_\nu$.

The Riemann curvature tensor is defined by the commutator of two covariant derivatives. For a covariant vector field X_μ, we denote

$$\left[\nabla_\alpha, \nabla_\beta\right] X_\mu = R_{\alpha\beta\mu}{}^{\nu} X_\nu\,. \tag{A.2}$$

The Ricci tensor and scalar are formed from the contraction of the Riemann tensor, i.e. $R_{\alpha\mu} = R_{\alpha\nu\mu}{}^{\nu}$, $R = g^{\mu\nu}R_{\mu\nu}$. The Weyl tensor is the traceless part of the Riemann tensor,

$$C_{\mu\nu\rho\sigma} = R_{\mu\nu\rho\sigma} - \frac{2}{d-2}\left(g_{\mu[\rho}R_{\sigma]\nu} - g_{\nu[\rho}R_{\sigma]\mu}\right) + \frac{2}{(d-1)(d-2)}Rg_{\mu[\rho}g_{\sigma]\nu}\,. \tag{A.3}$$

The Riemann tensor satisfies the first and second Bianchi identity,

$$R_{\mu[\nu\rho\sigma]} = 0\,, \qquad \nabla_{[\alpha}R_{\mu\nu]\rho\sigma} = 0\,. \tag{A.4}$$

From the latter identity it follows that

$$\nabla^{\alpha} R_{\alpha\beta\mu\nu} = 2\nabla_{[\mu} R_{\nu]\beta} \,, \qquad \nabla^{\nu} R_{\mu\nu} = \frac{1}{2}\nabla_{\mu} R \,. \tag{A.5}$$

An often-employed technique is the background-field method. This consists of an expansion of the full metric g in terms of a background metric. This background metric will be denoted by $\bar{g}$. Covariant objects formed from this metric will be denoted by a bar, e.g. $\bar{\nabla}$ and $\bar{\Delta}$. The full metric g can then be expressed in terms of the background metric and a fluctuation field. In this thesis, we will only use the linear parameterization, which expands g as

$$g_{\mu\nu} = \bar{g}_{\mu\nu} + h_{\mu\nu} \,. \tag{A.6}$$

We reserve the symbol $\Box$ for the Laplacian in flat space $\bar{g}_{\mu\nu} = \delta_{\mu\nu}$, i.e.

$$\Box = -\delta^{\mu\nu}\partial_{\mu}\partial_{\nu} \,. \tag{A.7}$$

Action functionals contain strings of fields built out of the fundamental fields themselves or in the form of curvature tensors. The projection of an action to a string of fields is denoted by the action monomial followed by a vertical line carrying the string of fields onto which the action is projected as a subscript. For instance, the projection of the volume term to the string given by one power of the metric fluctuation is denoted by

$$\int \mathrm{d}^d x \sqrt{g} \Big|_h = \frac{1}{2} \int \mathrm{d}^d x \sqrt{\bar{g}}\, h \,. \tag{A.8}$$

Derivatives acting on the i-th field in the string carry the number of the field as a subscript, i.e.,

$$\int \mathrm{d}^d x \sqrt{g}\ (\Delta_1\Delta_2\Delta_3)\,(R_1R_2R_3) = \int \mathrm{d}^d x \sqrt{g}\ (\Delta R_1)\,(\Delta R_2)\,(\Delta R_3) \ . \tag{A.9}$$

Notably, differential operators with different subscripts commute since they are acting on different fields.

A.2 Fourier space

In many cases the computation can be simplified by adopting flat Euclidean space as background. In this case it is convenient to switch to momentum space and work with the Fourier-transformed fields,

$$\phi(p) = \int \mathrm{d}^d x\, \phi(x)\, \mathrm{e}^{-ipx} \,, \tag{A.10}$$

where we use the same symbol for the fields in position and momentum space. In this case the form factors depend on the field's momenta. We adopt the convention that all momenta are incoming, so that momentum conservation at an n-point vertex implies

$$\sum_{i=1}^{n} p_i = 0\,. \tag{A.11}$$

Starting from an action functional, the resulting interaction vertices are obtained by taking suitable variations with respect to the (fluctuation) fields. This automatically leads to a symmetrization in the tensor and momentum structures, e.g.

$$\begin{aligned}
&\frac{\delta}{\delta\phi(p_4)}\frac{\delta}{\delta\phi(p_3)}\frac{\delta}{\delta h_{\rho\sigma}(p_2)}\frac{\delta}{\delta h_{\mu\nu}(p_1)} h_{\alpha\beta}(q_1) h_{\gamma\delta}(q_2)\phi(q_3)\phi(q_4) \\
&\quad = \Big[\mathbb{1}_{\alpha\beta}{}^{\mu\nu}\mathbb{1}_{\gamma\delta}{}^{\rho\sigma}\delta(q_1-p_1)\delta(q_2-p_2) + \mathbb{1}_{\alpha\beta}{}^{\rho\sigma}\mathbb{1}_{\gamma\delta}{}^{\mu\nu}\delta(q_1-p_2)\delta(q_2-p_1)\Big]\times \\
&\qquad\qquad \Big[\delta(q_3-p_3)\delta(q_4-p_4) + \delta(q_3-p_4)\delta(q_4-p_3)\Big]\,,
\end{aligned} \tag{A.12}$$

for the $(hh\phi\phi)$-vertex. Here, the identity on the space of symmetric $d\times d$ matrices is

$$\mathbb{1}_{\alpha\beta}{}^{\mu\nu} \equiv \frac{1}{2}\left(\delta^{\mu}_{\alpha}\delta^{\nu}_{\beta} + \delta^{\nu}_{\alpha}\delta^{\mu}_{\beta}\right) \tag{A.13}$$

and $\delta(x)$ is the usual Dirac delta in d dimensions.

APPENDIX B

F(R)-GRAVITY IN THE JORDAN AND EINSTEIN FRAME

In this appendix, we study the map of a $f(R)$-theory for gravity to a tensor-scalar system. In this case, we will refer to the $f(R)$-action as being in the Jordan frame. Using a suitable redefinition of degrees of freedom, we can recast this action using the classical equations of motion as an action consisting of the Einstein-Hilbert action plus an additional scalar [218, 219]. This frame is called the Einstein frame. In this appendix we give a derivation of the map between the two frames, following [278].

We start from a (Lorentzian) $f(R)$-theory accompanied by a generic action for matter fields:

$$S = \frac{M_{\mathrm{P}}^2}{2} \int \mathrm{d}^4x \sqrt{-g} f(R) + S_{\mathrm{m}} \left(g_{\mu\nu}\right) \ . \tag{B.1}$$

Note that for completeness we include a matter action, even though this will not be relevant in a cosmological context. Subsequently, we introduce an auxiliary scalar field ϕ in the form of

$$S = \frac{M_{\mathrm{P}}^2}{2} \int \mathrm{d}^4x \sqrt{-g} \left[f(\phi) + f'(\phi) \left(R - \phi\right)\right] + S_{\mathrm{m}} \left(g_{\mu\nu}\right) \ , \tag{B.2}$$

where the prime denotes a derivative with respect to its argument. Under the assumption that $f''(\phi) \neq 0$, the equations of motion include the condition $\phi = R$, indicating the use of ϕ as Lagrange multiplier. Thus, the two theories (B.1) and (B.2) are equivalent on-shell. Under the assumption that $f'(\phi) > 0$, we now perform the conformal rescaling $f'(\phi) g_{\mu\nu} \equiv \tilde{g}_{\mu\nu}$. This brings the gravitational part of the action into Einstein-Hilbert

form:

$$S = \frac{M_P^2}{2}\int \mathrm{d}^4x\sqrt{-\tilde{g}}\Big[\tilde{R} - \frac{3}{2f'(\phi)^2}\tilde{g}^{\mu\nu}\tilde{\nabla}_\mu f'(\phi)\tilde{\nabla}_\nu f'(\phi) - \frac{1}{f'(\phi)^2}\left(\phi f'(\phi) - f(\phi)\right)\Big] + S_\mathrm{m}\left(\tilde{g}_{\mu\nu}/f'(\phi)\right) . \tag{B.3}$$

In order to obtain a canonical kinetic term for the scalar field, we introduce the new field φ according to

$$f'(\phi) = \mathrm{e}^{\sqrt{2/3}\varphi/M_P} . \tag{B.4}$$

If $f'(\phi)$ is monotonic, this relation implicitly defines a map $\phi(\varphi)$. This yields the action

$$S = \int \mathrm{d}^4x\sqrt{\tilde{g}}\left[\frac{M_P^2}{2}\tilde{R} - \frac{1}{2}(\nabla\varphi)^2 - V(\varphi)\right] + S_\mathrm{m}\left(\tilde{g}_{\mu\nu}/F'\right) , \tag{B.5}$$

where $F' = \mathrm{e}^{\sqrt{2/3}\varphi/M_P}$. The scalar potential is given by the implicit expression

$$V(\varphi) = \frac{M_P^2}{2f'\left(\phi(\varphi)\right)^2}\left(\phi(\varphi)f'\left(\phi(\varphi)\right) - f\left(\phi(\varphi)\right)\right) . \tag{B.6}$$

For the $f(R)$ type action (B.1), the transformation can be carried out explicitly. In particular, for the cosmology-inspired truncation[1]

$$f(R) = -2\Lambda + R - BR^2 . \tag{B.7}$$

For $B = 0$ the action (B.1) is already in the Einstein frame. For $B \neq 0$, we evaluate the relation (B.4) to obtain

$$1 - 2B\phi = \mathrm{e}^{\sqrt{2/3}\varphi/M_P} \Rightarrow \quad \phi = \frac{1 - \mathrm{e}^{\sqrt{2/3}\varphi/M_P}}{2B} . \tag{B.8}$$

Inserting this into the potential (B.6) gives

$$V(\varphi) = \frac{M_P}{2}\left[-\frac{1}{4B} + \frac{1}{2B}\mathrm{e}^{-\sqrt{2/3}\varphi/M_P} + \left(-\frac{1}{4B} + 2\Lambda\right)\mathrm{e}^{-2\sqrt{2/3}\varphi/M_P}\right] . \tag{B.9}$$

This potential gives the starting point for the analysis of the cosmological dynamics in chapter 3.

[1]Note that we are working with an action that differs from (3.7) by an overall minus sign. We correct for this by writing the potential (3.10) with opposite sign from the one obtained here.

APPENDIX C

FLOW EQUATIONS OF F(R)-GRAVITY

In this appendix, we present the flow equations for the $f(R)$-gravitational theory that was discussed in chapter 3. Flow equations of this type of truncation have been derived in [53, 64, 76, 85, 99], and their properties have been analyzed in detail by various groups (see [53, 65–67, 70, 71, 98] for selected works and further references). For now, we review the flow equations derived in [85]; in order for this thesis to be a self-contained manuscript, we review the main results. See also [279] for further details regarding the construction of flow trajectories.

We take the ansatz for the EAA to be

$$\Gamma_k[g;\bar{g}] = \Gamma_k^{\mathrm{f}}[g] + S_{\mathrm{gf}}[g-\bar{g};\bar{g}] + S_{\mathrm{gh}} + S_{\mathrm{aux}}\,, \tag{C.1}$$

with

$$\Gamma_k^{\mathrm{f}}[g] = \frac{1}{16\pi G_k}\int d^4x\sqrt{g}\,f_k(R)\,. \tag{C.2}$$

This term is supplemented by a scale-independent gauge-fixing term implementing geometrical gauge in the Landau limit. The ansatz for Γ_k is then completed by the corresponding ghost action and auxiliary fields exponentiating Jacobians arising from field redefinitions. Details on these terms can be found in the original article [85].

The flow of f is then found by inserting (C.1) into the FRGE and projecting the resulting flow on functions of the scalar curvature. This results in a partial differential equation governing the scale dependence of $f_k(R)$. We express the equation in terms of the dimensionless quantities

$$r \equiv k^{-2}R\,; \qquad \mathcal{F}_k(r) \equiv \frac{1}{16\pi G_k}k^{-4}f_k\left(k^2 r\right)\,. \tag{C.3}$$

The partial differential equation satisfied by $\mathcal{F}_k$ then reads [85]

$$384\pi^2\left(\partial_t\mathcal{F}_k + 4\mathcal{F}_k - 2r\mathcal{F}_k'\right) = \sum_{i=1}^{6} c_i\,, \tag{C.4}$$

with the c_i given by

$$\begin{aligned}
c_1 &= \left[5r^2\theta\left(1-\tfrac{r}{3}\right) - (12+4r-\tfrac{61}{90})r^2\right]\left[1-\tfrac{r}{3}\right]^{-1},\\
c_2 &= 10r^2\theta\left(1-\tfrac{r}{3}\right),\\
c_3 &= \left[10r^2\theta\left(1-\tfrac{r}{4}\right) - r^2\theta\left(1+\tfrac{r}{4}\right) - (36+6r-\tfrac{67}{60}r^2)\right]\left[1-\tfrac{r}{4}\right]^{-1},\\
c_4 &= \left[\eta_f\left(10-5r-\tfrac{271}{36}r^2+\tfrac{7249}{4536}r^3\right) + (60-20r-\tfrac{271}{18}r^2)\right]\left[1+\tfrac{\mathcal{F}_k}{\mathcal{F}_k'}-\tfrac{r}{3}\right]^{-1},\\
c_5 &= \tfrac{5r^2}{2}\Big[\eta_f\left(\left(1+\tfrac{r}{3}\right)\theta\left(1+\tfrac{r}{3}\right) + \left(2+\tfrac{r}{3}\right)\theta\left(1+\tfrac{r}{6}\right)\right)\\
&\qquad + 2\theta\left(1+\tfrac{r}{3}\right) + 4\theta\left(1+\tfrac{r}{6}\right)\Big]\left[1+\tfrac{\mathcal{F}_k}{\mathcal{F}_k'}-\tfrac{r}{3}\right]^{-1},\\
c_6 &= \Big[\mathcal{F}_k'\,\eta_f\left(6+3r+\tfrac{29}{60}r^2+\tfrac{37}{1512}r^3\right)\\
&\qquad + (\partial_t\mathcal{F}_k'' - 2r\mathcal{F}_k''')\left(27-\tfrac{91}{20}r^2-\tfrac{29}{30}r^3-\tfrac{181}{3360}r^4\right)\\
&\qquad + \mathcal{F}_k''\left(216-\tfrac{91}{5}r^2-\tfrac{29}{15}r^3\right) + \mathcal{F}_k'\left(36+12r+\tfrac{29}{30}r^2\right)\Big]\\
&\qquad\qquad \times\left[2\mathcal{F}_k + 3\mathcal{F}_k'\left(1-\tfrac{2}{3}r\right) + 9\mathcal{F}_k''\left(1-\tfrac{r}{3}\right)^2\right]^{-1}.
\end{aligned} \tag{C.5}$$

Here, a prime denotes a derivative with respect to the dimensionless curvature scalar r and η_f is the anomalous dimension of $f_k'(R)$,

$$\eta_f = \frac{1}{\mathcal{F}_k'}\left(\partial_t\mathcal{F}_k' + 2\mathcal{F}_k' - 2r\mathcal{F}_k''\right). \tag{C.6}$$

Using the dimensionless variables introduced in (3.32), the dimensionless object $\mathcal{F}_k(r)$ corresponding to the action (3.7) is

$$\mathcal{F}_k(r) = \frac{1}{16\pi g_k}\left(2\lambda_k - r + b_k r^2\right). \tag{C.7}$$

Substituting this expression into (C.4) and subsequently expanding the result in a power series around $r = 0$ the β-functions for the couplings λ_k, g_k and b_k can be read off from the three lowest-order terms in this expansion. Concretely,

$$\partial_t g_k = \beta_g(g,\lambda,b)\,, \qquad \partial_t\lambda_k = \beta_\lambda(g,\lambda,b)\,, \qquad \partial_t b_k = \beta_b(g,\lambda,b)\,, \tag{C.8}$$

where the β_i are obtained as the solution of the following linear system of equations

$$
\begin{aligned}
&-\frac{6\left(9g_k\beta_b-9b_k\beta_g+72b_kg_k+\beta_g-8g_k\right)}{g_k(18b_k+4\lambda_k-3)}-\frac{80-\frac{10\beta_g}{g_k}}{1-2\lambda_k}\\
&\qquad+\frac{48\left(-\pi\lambda_k\beta_g+\pi g_k\beta_\lambda+4\pi g_k\lambda_k\right)}{g_k^2}+48=0\,, \qquad \text{(C.9a)}\\
&-\frac{-20\beta_b+40b_k+\frac{5\beta_g}{g_k}-30}{1-2\lambda_k}-\frac{3\left(4g_k\beta_b-4b_k\beta_g+24b_kg_k+\beta_g-6g_k\right)}{g_k(18b_k+4\lambda_k-3)}\\
&-\frac{36b_k\left(9g_k\beta_b-9b_k\beta_g+72b_kg_k+\beta_g-8g_k\right)}{g_k(18b_k+4\lambda_k-3)^2}-\frac{2(6b_k\lambda_k-1)\left(80-\frac{10\beta_g}{g_k}\right)}{3(2\lambda_k-1)^2}\\
&\qquad-\frac{24\pi\left(2g_k-\beta_g\right)}{g_k^2}+23=0\,, \qquad \text{(C.9b)}\\
&-\frac{216b_k^2\left(9g_k\beta_b-9b_k\beta_g+72b_kg_k+\beta_g-8g_k\right)}{g_k(18b_k+4\lambda_k-3)^3}\\
&\qquad-\frac{18b_k\left(4g_k\beta_b-4b_k\beta_g+24b_kg_k+\beta_g-6g_k\right)}{g_k(18b_k+4\lambda_k-3)^2}\\
&\qquad-\frac{2(6b_k\lambda_k-1)\left(-20\beta_b+40b_k+\frac{5\beta_g}{g_k}-30\right)}{3(2\lambda_k-1)^2}\\
&\qquad-\frac{-186g_k\beta_b+186b_k\beta_g-744b_kg_k+29\beta_g-116g_k}{60g_k(18b_k+4\lambda_k-3)}\\
&\qquad-\frac{-40b_k\beta_b+10\beta_b+80b_k^2-20b_k+\frac{271\beta_g}{36g_k}-\frac{271}{9}}{1-2\lambda_k}+\frac{24\pi\left(g_k\beta_b-b_k\beta_g\right)}{g_k^2}\\
&\qquad-\frac{\left(-72b_k^2\lambda_k+30b_k\lambda_k+9b_k-4\right)\left(80-\frac{10\beta_g}{g_k}\right)}{9(2\lambda_k-1)^3}+\frac{15\left(4g_k-\beta_g\right)}{2g_k(2\lambda_k-1)}-\frac{872}{45}=0\,. \qquad \text{(C.9c)}
\end{aligned}
$$

The β-functions (C.9) are the main result of this appendix and underlie the analysis of the gravitational RG flow performed in chapter 3.

We remark that in [99] a similar flow equation was derived based on a physical gauge-fixing condition. While the resulting equation gives rise to a qualitatively similar structure in terms of fixed points, it also possesses a singular hypersurface of codimension 1 that separates the NGFP from the classical region, see [65] for further analysis. Thus the corresponding solutions do not exhibit a crossover from the NGFP to a classical regime which is crucial for connecting the construction to a viable low-energy dynamics.

APPENDIX D

EXPANDING TRACE ARGUMENTS INCLUDING STEP FUNCTIONS

This appendix is edited from [4].

In this appendix, we collect technical details underlying the evaluations of momentum-space integrals that are regulated by the Litim cutoff. These are encountered in the derivation of the β-functions in chapter 4. The Litim cutoff is often used because it allows us to evaluate many momentum-space integrals analytically. When used in higher-order momentum expansions, however, special care has to be taken with regard to its non-smooth nature.

D.1 Explicit form of vertex functions and propagators

We start by deriving the relevant propagators and interaction vertices from the ansatz for the higher-derivative scalar field coupled to gravity given in (4.4).

In the remainder of this appendix, we employ the Feynman-harmonic gauge fixing condition $\alpha = 1, \beta = \frac{d}{2} - 1$, cf. (2.33). By expanding the gauge-fixed Einstein-Hilbert action up to second order in $h_{\mu\nu}$ one finds that the inverse gravitational propagator is given by

$$\left[\Gamma_k^{(hh)}\right]^{\mu\nu\alpha\beta} = \frac{1}{32\pi G_k}\left(p^2 - 2\Lambda_k\right)\left[(\mathbb{1} - P_h) - \frac{d-2}{2}P_h\right]^{\mu\nu\alpha\beta}, \tag{D.1}$$

where $\mathbb{1}_{\mu\nu}{}^{\alpha\beta}$ is the unit on the space of symmetric tensors, defined in (A.13) and

$[P_h]_{\mu\nu}{}^{\alpha\beta} \equiv d^{-1}\delta_{\mu\nu}\delta^{\alpha\beta}$ the projector on the trace mode. The inverse scalar propagator is obtained from (4.6) and reads

$$\Gamma_k^{(\phi\phi)} = Z_k \left(p^2 + Y_k\, p^4\right) . \tag{D.2}$$

To simplify the notation, we have suppressed the unit operator acting on the N_s scalar fields. This inverse propagator contains the scale-dependent wave-function renormalization Z_k and the inverse ghost mass Y_k.

For later convenience, we introduce the following short-hand notations for the scale-dependent coefficients α_n^w multiplying the p^{2n}-terms in the (scalar part) of (D.1) and (D.2),

$$\begin{aligned} \alpha_0^{hh} &= -\tfrac{\Lambda_k}{16\pi G_k}\,, & \alpha_1^{hh} &= \tfrac{1}{32\pi G_k}\,, & \alpha_2^{hh} &= 0\,, \\ \alpha_0^{\phi\phi} &= 0\,, & \alpha_1^{\phi\phi} &= Z_k\,, & \alpha_2^{\phi\phi} &= Z_k Y_k\,, \end{aligned} \tag{D.3}$$

and all coefficients α_n^w with $n \geq 3$ vanishing.

Applying the implicit regulator prescription $p^2 \mapsto P_k = p^2 + R_k\left(p^2\right)$ to the propagators (D.1) and (D.2) gives

$$\left[\mathcal{R}_k^{hh}\right]^{\mu\nu,\alpha\beta} = \frac{1}{32\pi G_k}\, R_k \left[(\mathbb{1} - P_h) - \tfrac{d-2}{2} P_h\right]^{\mu\nu,\alpha\beta} \tag{D.4a}$$

$$\mathcal{R}_k^{\phi\phi} = Z_k \left(1 + Y_k \left(2\, p^2 + R_k\right)\right) R_k\,. \tag{D.4b}$$

In addition to the propagators, one also needs the (momentum-dependent) three- and four-point vertices containing one and two derivatives with respect to the background scalar field. We denote the momenta associated with the graviton fluctuations, scalar fluctuations, and background scalar field by $\tilde{p}$, p, and q. Note that this is in contrast to the convention in section 5.2.2 where we used partial integration to remove all partial derivatives from the graviton fluctuation. The 3-point vertex obtained from (4.6) is then given by

$$\left[\Gamma^{(h\phi\phi)}(\tilde{p}, p, q)\right]^{\mu\nu} = \frac{1}{2} Z_k \left(p^\mu q^\nu + p^\nu q^\mu - \frac{1}{2}\delta^{\mu\nu}(p\cdot q)\right) . \tag{D.5}$$

Note that this can be obtained from (5.43) by setting $f^{(\phi\phi)}\left(p^2\right) = Z_k p^2$ and the other form factors to zero.

Finally, the 4-point vertex is

$$\begin{aligned} \left[\Gamma^{(hh\phi\phi)}\right]^{\mu\nu\rho\sigma} = -\frac{1}{2} Z_k \Bigg[&\left(\frac{1}{4}\delta^{\mu\nu}\delta^{\rho\sigma} - \frac{1}{2}\delta^{\mu\rho}\delta^{\nu\sigma}\right)(q_1\cdot q_2) \\ &- \bar{g}^{\mu\nu} q_1^\rho q_2^\sigma + 2\bar{g}^{\mu\rho} q_1^\sigma q_2^\nu \Bigg] . \end{aligned} \tag{D.6}$$

All vertices are understood to contain the appropriate symmetrizations in the external indices and are subject to momentum conservation. Moreover, we set $Y_k = 0$ in order to keep the expressions for the vertices at a readable length. The contributions proportional to Y_k are easily generated by a computer algebra program. Their precise form is irrelevant for the discussion of the general structures below.

For the Litim-type cutoff [209, 280] the dimensionful profile function R_k is given by

$$R_k(p^2) = (k^2 - p^2)\Theta(k^2 - p^2)\,. \tag{D.7}$$

The key advantage of this regulator is that it allows for an analytic evaluation of the loop integrals shown in Figure 4.1. However, the distributional character of the regulator renders the expansion in the external momenta q non-trivial. The next subsection discusses how this expansion can be implemented consistently, also taking into account the non-trivial boundary terms arising in the expansion procedure.

D.1.1 Loop-integrations with a distributional regulator

The loop integrals encountered in chapter 4 contain a trace over spacetime indices and an integration over loop momenta. We adopt the conventions that the absolute values of the loop momentum and external momentum are denoted by p and q and $p \cdot q = pq\cos(\vartheta)$ defines their relative angle ϑ. Moreover, the loop momentum is shifted such that the external momentum does not appear in the argument of the regulator insertion $\partial_t R_k$. The spacetime indices are taken into account by stringing together the propagators and vertices contracting the corresponding index structures.

One then encounters q-dependent scalar loop-integrals of the form

$$I^{w_1 w_2}_{(m,n)} \equiv \int \frac{\mathrm{d}^d p}{(2\pi)^d} \frac{F_k(q,p,\cos(\vartheta))\,\partial_t \mathcal{R}_k^{w_2}(p^2)}{\left(\sum_{l=0}^2 \alpha_l^{w_1}(\vec{p}+\vec{q})^{2l} + \mathcal{R}_k^{w_1}((\vec{p}+\vec{q})^2)\right)^m \left(\sum_{l=0}^2 \alpha_l^{w_2} p^{2l} + \mathcal{R}_k^{w_2}(p^2)\right)^n}\,. \tag{D.8}$$

Here $w_1, w_2 \in \{h, \phi\}$ denotes the type of regulator insertion. In a slight abuse of notation, the symbol $\mathcal{R}_k^{hh}(p^2)$ is used to refer to the scalar part of (D.4a). The function $F_k(q,p,\cos(\vartheta))$ captures the momentum dependence of the vertices. The n-point functions (D.5) and (D.6) illustrate that F is polynomial in q and p. In particular it has a well-defined series expansion around $q = 0$. Noting that the vertices (D.5) and (D.6) come with one and two powers of the external momentum, respectively, it is easy to verify that this expansion starts at order q^2.

The goal of this section is to study the q-dependence of (D.8). In chapter 4, we are interested in the running of the anomalous dimension η_s and the higher-derivative

coupling Y_k. These can be extracted from the Taylor coefficient of q^2 and q^4, respectively. Thus, the evaluation of the Taylor expansion will suffice.

For a general profile function R_k the integrals (D.8) cannot be computed analytically. Moreover, the presence of the external momentum q and the scale-dependent couplings make their numerical evaluation computationally very expensive. The profile function (D.7) allows to bypass this problem by restricting the p-integration to a compact domain and giving rise to cancellations in the propagators. The former property can be verified by noting that the logarithmic k-derivative of (D.4), evaluated for a Litim profile, has the form

$$\partial_t \mathcal{R}_k^w(p^2) = \bar{b}_k^w(p^2)\,\Theta(k^2 - p^2)\,, \tag{D.9}$$

where

$$\begin{aligned} \bar{b}_k^{hh}(p^2) &= \frac{1}{32\pi G_k}\left(2k^2 - \eta_N\left(k^2 - p^2\right)\right)\,, \\ \bar{b}_k^{\phi\phi}(p^2) &= Z_k\left(2k^2 - \eta_s(k^2 - p^2) + (\partial_t Y_k - \eta_s Y_k)(k^4 - p^4) + 4\,Y_k\,k^4\right)\,. \end{aligned} \tag{D.10}$$

Inspecting (D.8) for the case $m = 0$ reveals that the step functions appearing in the numerator and denominator have the same support. As a result the integrals for the case $m = 0$ simplify significantly:

$$I_{(0,n)}^{w_1 w_2} \equiv \int \mathrm{d}\Omega_{d-2} \int_{-1}^{1} \mathrm{d}x \int_0^k \frac{\mathrm{d}p}{(2\pi)^d}\, p^{d-1}\, \frac{F_k(q,p,x)\,\bar{b}_k^w(p^2)}{\left(\sum_{l=0}^2 \alpha_l^w\, k^{2l}\right)^n}\,. \tag{D.11}$$

Here $\int \mathrm{d}\Omega_{d-2} = \frac{(n-1)\,\pi^{\frac{n-1}{2}}}{\Gamma\left(\frac{n-1}{2}+1\right)}$ is the surface area of the $(d-2)$-sphere and the spacetime indices on F_k and $\bar{b}_k^w(p^2)$ are suppressed for readability. Furthermore, we have made a substitution of variables $x \equiv \cos(\vartheta)$. Owed to the simple structure of the denominator, which is independent of p and ϑ the evaluation of these integrals is rather straightforward.

The case where $m \neq 0$ is non-trivial. Because of the step-function in the numerator, the full integration domain is reduced to a d-dimensional ball of radius k, i.e., $p \in [0, k]$ and $x \in [-1, 1]$. In this domain the set of propagators exponentiated by n again undergoes the simplification (D.11). In the propagators containing $(p+q)^2$, the regulator leads to terms proportional to $\Theta\left(k^2 - (\vec{p} + \vec{q})^2\right)$. As illustrated in Figure D.1, the value of the step function has a non-trivial dependence on the absolute value of q and the angle ϑ.

Thus, unless $q = 0$, there is always a part of the integration domain on which the denominator retains its dependence on the integration variables x, p. As a result performing the integral becomes very involved. In order to complete the evaluation of the flow equation we then expand the integrands around $q = 0$, *taking the distributional character of the integrand into account*. This allows us to obtain analytic expressions for the resulting integrals. This is achieved as follows. The first step uses the Heaviside function

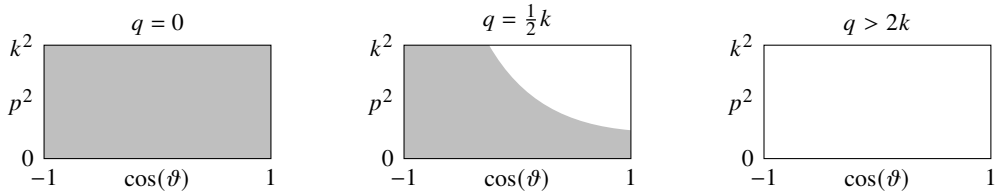

Figure D.1: *The value of* $\Theta\left(k^2-(\vec{p}+\vec{q})^2\right)$ *for three different values of* q*. In the gray regions the step function evaluates to* 1 *while it vanishes in the white regions.*

in the numerator of (D.8) to restrict the integration domain to $p \in [0,k]$. Following the derivation of (D.11) the factor $\left(\sum_{l=0}^{2}\alpha_l^{w_2}p^{2l}+\mathcal{R}_k^{w_2}(p^2)\right)^n$ becomes independent of p and q. Together with the angular integration $\int \mathrm{d}\Omega$ it can then be absorbed into a prefactor

$$N_k^n(w) \equiv \left(\sum_{l=0}^{2}\alpha_l^w\, k^{2l}\right)^{-n} \int \mathrm{d}\Omega_{d-2}\,, \tag{D.12}$$

so that (D.8) reduces to

$$I^{w_1w_2}_{(m,n)} = N_k^n(w_2)\int_{-1}^{1}\mathrm{d}x\int_0^k \frac{\mathrm{d}p}{(2\pi)^d}\,\frac{p^{d-1}\,F_k(q,p,x)\,\bar{b}_k^{w_2}(p^2)}{\left(\sum_{\ell=0}^{\infty}\alpha_\ell^{w_1}(\vec{p}+\vec{q})^{2\ell}+\mathcal{R}_k^{w_1}((\vec{p}+\vec{q})^2)\right)^m}\,. \tag{D.13}$$

In the next step we eliminate the step function from the denominator. To this purpose we insert the following partition of unity

$$1 = \Theta\left((\vec{p}+\vec{q})^2-k^2\right)+\Theta\left(k^2-(\vec{p}+\vec{q})^2\right)\,, \tag{D.14}$$

defined in the weak sense.[1] Furthermore we set $\Theta(0)=\frac{1}{2}$, so that this point is distributed evenly among the two terms. Inserting (D.14) into (D.13) then gives

$$I^{w_1w_2}_{(m,n)} = N_k^n(w_2)\int_{-1}^{1}\mathrm{d}x\int_0^k \frac{\mathrm{d}p}{(2\pi)^d}p^{d-1}F_k(q,p,x)\,\bar{b}_k^{w_2}(p^2)\times \left\{\frac{\Theta\left((\vec{p}+\vec{q})^2-k^2\right)}{\left(\sum_{\ell=0}^{2}\alpha_\ell^{w_1}(\vec{p}+\vec{q})^{2\ell}\right)^m}+\frac{\Theta\left(k^2-(\vec{p}+\vec{q})^2\right)}{\left(\sum_{\ell=0}^{2}\alpha_\ell^{w_1}k^{2\ell}\right)^m}\right\}\,. \tag{D.15}$$

[1] Regarding Θ as a distribution over the real numbers, this partition makes sense everywhere except at zero. However, this is a measure-zero set and does not affect the behavior of the distribution.

We will now consider the expansion of (D.15) around $q = 0$. The integral kernel itself is a distribution and thus its formal expansion yields distributional coefficients. In a weak sense, which is sufficient in the present context, the formal expansion coefficients can be constructed by using the integral representation of the Heaviside distribution

$$\Theta(s) \equiv \lim_{\epsilon \to 0^+} \frac{1}{2\pi i} \int_{-\infty}^{\infty} \mathrm{d}t \ (t - i\epsilon)^{-1} \, \mathrm{e}^{its} \,. \tag{D.16}$$

Substituting $s = (\pm(k^2 - (\vec{p} + \vec{q})^2))$ and expanding the kernel in powers of q, we obtain, after taking the proper limit,

$$\begin{aligned} \Theta\left(\pm\left(k^2 - (\vec{p} + \vec{q})^2\right)\right) \simeq \Theta\left(\pm\left(k^2 - p^2\right)\right) \mp 2px\delta\left(\pm\left(k^2 - p^2\right)\right) q \\ + \left[2p^2 x\delta'\left(\pm\left(k^2 - p^2\right)\right) \mp \delta\left(\pm\left(k^2 - p^2\right)\right)\right] q^2 + \mathcal{O}(q^3) \,. \end{aligned} \tag{D.17}$$

Since the expansion of $F_k(q, p, \cos(\vartheta))$ starts at order q^2 it then suffices to terminate this expansion at order q^2. When inserting this representation into (D.15) we encounter terms in which the delta-distribution has to be evaluated on the boundary of the integral domain. Using $\Theta(0) \equiv \frac{1}{2}$, these can be evaluated by noting that

$$\int_{[0,a]} \mathrm{d}z \, G(z)\delta(a - z) \equiv \tfrac{1}{2} G(a) \,, \tag{D.18}$$

which follows from

$$\begin{aligned} G(a) &= G(0) + \int_{[0,a]} \mathrm{d}z \, \partial_z G(z) \, \Theta(a - z) \\ &= \tfrac{1}{2} G(a) + \int_{[0,a]} \mathrm{d}z \, G(z)\delta(a - z) \,. \end{aligned} \tag{D.19}$$

Finally, terms containing the n-th derivative of the delta-function are evaluated using

$$\int_{[0,1]} \mathrm{d}z \, G(z) \, \partial_s^n \delta(s)\big|_{s=\pm(1-z)} = \tfrac{1}{2}(\pm 1)^n G^{(n)}(1) \,. \tag{D.20}$$

The weak identities (D.18) and (D.20) are sufficient to derive the relevant trace contributions for the scalar β-functions.

D.1.2 Master integrals

We close the discussion by deriving a set of master integrals, which form the basis of our loop computations

$$\tilde{I}_{w,m}(q,\cos(\vartheta)) \equiv \int_0^k \frac{\mathrm{d}p}{(2\pi)^d}\, f(p) \left\{ \frac{\Theta\left((\vec{p}+\vec{q})^2 - k^2\right)}{\left(\sum_{\ell=0}^2 \alpha_\ell^w (\vec{p}+\vec{q})^{2\ell}\right)^m} + \frac{\Theta\left(k^2 - (\vec{p}+\vec{q})^2\right)}{\left(\sum_{\ell=0}^2 \alpha_\ell^w k^{2\ell}\right)^m} \right\} . \tag{D.21}$$

Based on the relation (D.17), these integrals admit a series expansion in q,

$$\tilde{I}_{w,m}(q,\cos(\vartheta)) \simeq \tilde{I}^{(0)}_{w,m} + \tilde{I}^{(1)}_{w,m}\, q + \frac{1}{2}\tilde{I}^{(2)}_{w,m}\, q^2 + \mathcal{O}(q^3) . \tag{D.22}$$

The series coefficients $\tilde{I}^{(n)}_{w,m}$ depend on $\cos(\vartheta)$. The first three coefficients in this expansion are found by substituting (D.17) into (D.21) and evaluating the resulting integrals using the identities (D.18) and (D.20),

$$\begin{aligned}
\tilde{I}^{(0)}_{w,m} &= \left(\sum_{\ell=0}^2 \alpha_\ell^w k^{2\ell}\right)^{-m} \int_0^k \frac{\mathrm{d}p}{(2\pi)^d}\, f(p) , \\
\tilde{I}^{(1)}_{w,m} &= 0 , \\
\tilde{I}^{(2)}_{w,m} &= -mk^3 \cos^2(\vartheta) \left(\alpha_1^w + 2\alpha_2^w k^2\right) \left(\sum_{l=0}^2 \alpha_l^w k^{2l}\right)^{-(m+1)} \frac{f(k)}{(2\pi)^d} .
\end{aligned} \tag{D.23}$$

This result completes the discussion on carrying out the momentum integrals encountered in chapter 4. Note that the surface terms do not enter into the computation of the scalar anomalous dimension. They contribute to higher-order kinetic terms in the propagator only.

APPENDIX E

VARYING FUNCTIONS OF LAPLACIANS

This appendix is dedicated to setting up the machinery for expanding functions $f(\Delta)$ of the Laplacian to a given order in the fluctuation field $h_{\mu\nu}$. The objective is to retain all covariant derivatives, which is central for computing the momentum-dependence of the form factors discussed in chapter 5. This appendix is edited from [1]. We start by introducing the concept of multicommutators and their properties in section E.1 before discussing the expansion of $f(\Delta)$ in section E.2.

E.1 Multicommutators and combinatorial identities

Let Q, X, Y, Z denote some (differential) operators. The multicommutator is then defined recursively as

$$[X,Y]_l \equiv [X,[X,Y]_{l-1}]\,, \qquad [X,Y]_0 \equiv Y\,, \qquad l \in \mathbb{N}\,. \tag{E.1}$$

For $l = 1$, this reduces to the standard commutator

$$[X,Y]_1 = [X,Y] = XY - YX\,. \tag{E.2}$$

The multicommutator is additive in its second argument,

$$[X,Y+Z]_l = [X,Y]_l + [X,Z]_l\,, \tag{E.3}$$

and, for a constant parameter $s \in \mathbb{R}$, obeys the homogeneity property

$$[sX,Y]_l = s^l [X,Y]_l\,, \qquad [X,sY]_l = s[X,Y]_l. \tag{E.4}$$

This implies that the multicommutator is linear in its second argument. A multicommutator containing a product of operators in the second argument can be expressed as a finite sum:

$$[X, YZ]_m = \sum_{l=0}^{m} \binom{m}{l} [X, Y]_l [X, Z]_{m-l} \,. \tag{E.5}$$

For $X = Z = \Delta$, this entails the useful identity

$$[\Delta, Y\Delta]_l = [\Delta, Y]_l \Delta \,. \tag{E.6}$$

Using the multicommutator, we can give exact expressions for commuting differential operators. In particular, one can prove by induction that

$$Q^m Y = \sum_{l=0}^{m} \binom{m}{l} [Q, Y]_l Q^{m-l} \,, \tag{E.7}$$

and

$$YQ^m = \sum_{l=0}^{m} \binom{m}{l} (-1)^l Q^{m-l} [Q, Y]_l \,. \tag{E.8}$$

Finally, we note that when integrated over spacetime, multicommutators may be resolved by employing the identity

$$\int \mathrm{d}^d x \sqrt{g}\, Y [\Delta, Z]_m X = \int \mathrm{d}^d x \sqrt{g} \sum_{l=0}^{m} (-1)^l \left(\Delta^{m-l} Y\right) Z \left(\Delta^l X\right) \,, \tag{E.9}$$

which is again proven by induction.

E.2 Expanding functions of the Laplacian in terms of fluctuation fields

We are now in a position to evaluate the expansion of $f(\Delta)$ in terms of fluctuations $h_{\mu\nu}$ around a fixed background metric $\bar{g}_{\mu\nu}$. In the first step we express $f(\Delta)$ in terms of the inverse Laplace transform $\tilde{f}(s)$,

$$f(\Delta) = \int_0^\infty \mathrm{d}s\, \tilde{f}(s)\, \mathrm{e}^{-s\Delta} \,, \tag{E.10}$$

which we always assume to exist. This covers in particular logarithms of the Laplacian which can be represented as [281],

$$\log(\Delta) = \int_0^\infty \mathrm{d}s\, \frac{\mathrm{e}^{-s} - \mathrm{e}^{-s\Delta}}{s} \,. \tag{E.11}$$

At this stage, the problem of carrying out the h-expansion simplifies to expanding the exponential function and subsequently undoing the Laplace transform.

We then note that the Laplacian $\Delta = -g^{\mu\nu}\nabla_\mu\nabla_\nu$ admits an expansion

$$\Delta = \bar{\Delta} + \mathbb{d}_1 + \mathbb{d}_2 + \dots , \tag{E.12}$$

where $\bar{\Delta}$ is the Laplacian constructed from the background metric and the expansion coefficients $\mathbb{d}_m$ contain m powers of the metric fluctuation $h_{\mu\nu}$. The $\mathbb{d}_m$ depend on the tensor structure on which the Laplacian acts. For example, for a scalar ϕ, we have

$$\begin{aligned}
\mathbb{d}_1^\phi &= h_{\mu\nu}\bar{\nabla}^\mu\bar{\nabla}^\nu + \left(\bar{\nabla}^\mu h_{\mu\nu}\right)\bar{\nabla}^\nu - \frac{1}{2}\left(\bar{\nabla}_\alpha h\right)\bar{\nabla}^\alpha , \\
\mathbb{d}_2^\phi &= -h_\mu{}^\alpha h_{\alpha\nu}\bar{\nabla}^\mu\bar{\nabla}^\nu - h^{\alpha\beta}\left(\bar{\nabla}_\beta h_{\alpha\mu}\right)\bar{\nabla}^\mu - h_\mu{}^\beta\left(\bar{\nabla}^\gamma h_{\beta\gamma}\right)\bar{\nabla}^\mu \\
&\quad + \frac{1}{2}h^{\alpha\beta}\left(\bar{\nabla}_\mu h_{\alpha\beta}\right)\bar{\nabla}^\mu + \frac{1}{2}h^{\mu\nu}\left(\bar{\nabla}_\mu h\right)\bar{\nabla}_\nu .
\end{aligned} \tag{E.13}$$

The next step substitutes the expansion (E.12) into the exponential and subsequently expands in the fluctuation field. At this stage we first note the auxiliary identity

$$\frac{\mathrm{d}}{\mathrm{d}\epsilon}\mathrm{e}^{X+\epsilon Y} = V(\epsilon;X,Y)\,\mathrm{e}^{X+\epsilon Y} = \mathrm{e}^{X+\epsilon Y}\,\tilde{V}(\epsilon;X,Y) , \tag{E.14}$$

where

$$\begin{aligned}
V(\epsilon;X,Y) &= \sum_{j=0}^{\infty}\frac{1}{(j+1)!}[X+\epsilon Y,Y]_j , \\
\tilde{V}(\epsilon;X,Y) &= \sum_{j=0}^{\infty}\frac{(-1)^j}{(j+1)!}[X+\epsilon Y,Y]_j .
\end{aligned} \tag{E.15}$$

The expressions for $V(\epsilon;X,Y)$ and $\tilde{V}(\epsilon;X,Y)$ thereby follow from expanding the exponential in its Taylor series, taking the derivative with respect to ϵ and a subsequent reordering of terms employing the identities (E.7) and (E.8). This result can then be used to construct the expansion of $\mathrm{e}^{X+\epsilon Y}$ in ϵ either bringing the exponential factor to the left

$$\mathrm{e}^{X+\epsilon Y} = \mathrm{e}^X\left[1+\epsilon\tilde{V}(0;X,Y) + \frac{\epsilon^2}{2}\left(\tilde{V}(0;X,Y)^2 + \tilde{V}_\epsilon(0;X,Y)\right) + \mathcal{O}\left(\epsilon^3\right)\right] , \tag{E.16}$$

or to the right

$$\mathrm{e}^{X+\epsilon Y} = \left[1+\epsilon V(0;X,Y) + \frac{\epsilon^2}{2}\left(V(0;X,Y)^2 + V_\epsilon(0;X,Y)\right) + \mathcal{O}\left(\epsilon^3\right)\right]\mathrm{e}^X . \tag{E.17}$$

In these expressions, the subscript ϵ indicates a derivative with respect to ϵ before setting ϵ to zero. A straightforward calculation shows that

$$V_\epsilon(0;X,Y) = \sum_{j=0}^{\infty}\sum_{k=1}^{\infty}\frac{1}{(k+j+2)!}\left[X,[Y,[X,Y]_k]\right]_j , \tag{E.18}$$

and

$$\tilde{V}_\epsilon(0;X,Y) = \sum_{j=0}^{\infty}\sum_{k=1}^{\infty} \frac{(-1)^{k+j+1}}{(k+j+2)!}[X,[Y,[X,Y]_k]]_j \,. \tag{E.19}$$

Replacing the operators X and Y by the background Laplacian $\bar{\Delta}$ and the expansion coefficients $\mathbb{d}_m$ then allows to extract the required powers of the fluctuation field from the exponential $\mathrm{e}^{-s\Delta}$. We stress that this expansion is exact in the sense that there is no approximation on the momentum structure, i.e., all derivatives acting on fields are retained.

We conclude our derivation with a summary of the algorithm described above:

1. rewrite the function as a Laplace transform,
2. calculate the coefficients $\mathbb{d}_i$ defined in (E.12) up to the required order,
3. rescale the metric fluctuation $h_{\mu\nu}$ by a control parameter ϵ,
4. choose whether to order the exponential of the background Laplacian to the left or the right of the expansion,
5. use the corresponding expansion formula and set ϵ to 1 after truncating the series at the desired order,
6. undo the Laplace transform.

Depending on the concrete situation, once the expansion is done one can do the sums over the multi-commutators using the scaling properties (E.4) together with identities of the type (E.9) and perform the Laplace transform. If this is not possible, one can nevertheless handle all the expressions as they are, and perform the sums and the transform at the very end, after the functional trace has been calculated.

APPENDIX F

THE SCALAR-TENSOR 4-POINT VERTEX

In this appendix we discuss the general structure of the $(hh\phi\phi)$-vertex. This appendix is edited from [1]. Most of the discussion extends straightforwardly to general four-point vertices. We first note that any four-point form factor has six independent variables, which we take as the squares of three momenta and the scalar products between them,

$$f_{\mathcal{T}}^{(hh\phi\phi)} = f_{\mathcal{T}}^{(hh\phi\phi)}\left(p_1^2, p_2^2, p_3^2, y_{12}, y_{13}, y_{23}\right) . \tag{F.1}$$

In this,

$$p_{i\mu}p_j^{\mu} = y_{ij} \tag{F.2}$$

denotes the scalar product between two different momenta. All other combinations can be related to these variables by momentum conservation:

$$\begin{aligned} p_4^2 &= p_1^2 + p_2^2 + p_3^2 + 2y_{12} + 2y_{13} + 2y_{23} , \\ y_{14} &= -p_1^2 - y_{12} - y_{13} , \\ y_{24} &= -p_2^2 - y_{12} - y_{23} , \\ y_{34} &= -p_3^2 - y_{13} - y_{23} . \end{aligned} \tag{F.3}$$

If one wants to resolve any four-point function numerically, it is useful to parameterize the (cosine of the) angles instead of the full scalar product to get a fixed domain in all variables.

Note that starting from the four-point function, the covariantization to curved space is non-trivial. For the three-point function, no ordering ambiguity exists since the different Laplacians commute as they act on different objects. Here this is no longer the case since Δ_1 and $\nabla_{1\mu}\nabla_2^{\mu}$, etc., no longer commute.

Now we have to find an operator basis. There are five different types of tensor structures, depending on the number of derivatives contracted with the graviton fluctuations. To write down a basis, we introduce a shorthand notation on the basis of lexicographic ordering of indices. In general, a tensor structure looks like

$$\mathcal{T}^{\alpha\beta\gamma\delta} h_{\alpha\beta}(p_1) h_{\gamma\delta}(p_2) \phi(p_3) \phi(p_4) \,, \tag{F.4}$$

where $\mathcal{T}$ can consist of either the background metric or derivatives acting on either field. We will choose the convention that all derivatives acting on $\phi(p_4)$ will be integrated by parts. Then, there are the following 59 tensor structures, where we have taken into account the symmetry of the individual index pairs $(\alpha\beta)$ and $(\gamma\delta)$. First, there are those where $\mathcal{T}$ only contains the metric:

$$\begin{aligned} \mathcal{T}^{\alpha\beta\gamma\delta} &= \frac{1}{2}\left(\bar{g}^{\alpha\gamma}\bar{g}^{\beta\delta} + \bar{g}^{\alpha\delta}\bar{g}^{\beta\gamma}\right) \;\leftrightarrow\; f^{(hh\phi\phi)}_{(\mathbb{1})} \,, \\ \mathcal{T}^{\alpha\beta\gamma\delta} &= \frac{1}{d}\bar{g}^{\alpha\beta}\bar{g}^{\gamma\delta} \;\leftrightarrow\; f^{(hh\phi\phi)}_{(\bar{g}\bar{g})} \,. \end{aligned} \tag{F.5}$$

There are three different types of structures with one metric and two derivatives in $\mathcal{T}$. Using lexicographic ordering, we denote the six functions of type 1 by

$$\mathcal{T}^{\alpha\beta\gamma\delta} = \bar{g}^{\alpha\beta}\partial_i^{\gamma}\partial_j^{\delta} \;\leftrightarrow\; f^{(hh\phi\phi)}_{(\bar{g}\,ij)} \,, \tag{F.6}$$

where $i \in \{1,2,3\}$ and $j \in \{1,2,3\}$, $j \geq i$, indicate which field the derivatives act upon. For example, the expression $(\bar{g}13)$ denotes the term

$$f^{(hh\phi\phi)}_{(\bar{g}13)}\left(p_1^2, p_2^2, p_3^2, y_{12}, y_{13}, y_{23}\right)\left(\partial^{\gamma} h(p_1)\right) h_{\gamma\delta}(p_2)\left(\partial^{\delta}\phi(p_3)\right)\phi\,(p_4) \,. \tag{F.7}$$

Dual to these are the six terms

$$\mathcal{T}^{\alpha\beta\gamma\delta} = \bar{g}^{\gamma\delta}\partial_i^{\alpha}\partial_j^{\beta} \;\leftrightarrow\; f^{(hh\phi\phi)}_{(ij\,\bar{g})} \,, \tag{F.8}$$

with the same set of possibilities for i and j as above. The third type is

$$\mathcal{T}^{\alpha\beta\gamma\delta} = \bar{g}^{\beta\delta}\partial_i^{\alpha}\partial_j^{\gamma} \;\leftrightarrow\; f^{(hh\phi\phi)}_{(i\,\bar{g}\,j)} \,, \tag{F.9}$$

where both i and j are in $\{1,2,3\}$, giving rise to nine combinations. Finally, there are 36 terms without metrics,

$$\mathcal{T}^{\alpha\beta\gamma\delta} = \partial_i^{\alpha}\partial_j^{\beta}\partial_k^{\gamma}\partial_l^{\delta} \;\leftrightarrow\; f^{(hh\phi\phi)}_{(ijkl)} \,, \tag{F.10}$$

where again due to symmetry reasons, $i \leq j$ and $k \leq l$. Not all of these 59 structures are independent though, because we still have the symmetry of exchanging the two h-fields

while also swapping the two corresponding momenta. Going through all tensor structures, we find that the following are actually *dependent*:

$$\begin{aligned}(11\bar{g}),(12\bar{g}),(13\bar{g}),(22\bar{g}),(23\bar{g}),(33\bar{g}),(2\bar{g}2),(3\bar{g}1),(3\bar{g}2),\\ (2212),(1213),(2213),(1222),(2222),(2322),(1123),(1223),\\ (2223),(2323),(1133),(1233),(1333),(2233),(2333)\,.\end{aligned} \tag{F.11}$$

As an example, a form factor corresponding to $(11\bar{g})$ maps to $(\bar{g}22)$ in the following way:

$$\begin{aligned}&f^{hh\phi\phi}_{(11\bar{g})}\left(p_1^2,p_2^2,p_3^2,y_{12},y_{13},y_{23}\right)\left(\partial^\mu\partial^\nu h_{\mu\nu}(p_1)\right)h(p_2)\phi(p_3)\phi(p_4)\\ &\quad\to f^{hh\phi\phi}_{(11\bar{g})}\left(p_2^2,p_1^2,p_3^2,y_{12},y_{23},y_{13}\right)h(p_1)\left(\partial^\mu\partial^\nu h_{\mu\nu}(p_2)\right)\phi(p_3)\phi(p_4)\,.\end{aligned} \tag{F.12}$$

For convenience, we will retain the redundant structures in the discussion below, bearing in mind these relations.

Performing a Fourier transform and using (A.12), we have

$$\begin{aligned}&\Gamma^{(hh\phi\phi)\mu\nu\rho\sigma}(p_1,p_2,p_3,p_4)\\ &\quad=\int_{q_1\cdots q_4}\sum_{\mathcal{T}}\mathcal{T}^{\alpha\beta\gamma\delta}f^{(hh\phi\phi)}_{\mathcal{T}}\left(q_1^2,q_2^2,q_3^2,q_{1\mu}q_2^\mu,q_{1\mu}q_3^\mu,q_{2\mu}q_3^\mu\right)\times\\ &\qquad\left[\delta(q_3-p_3)\delta(q_4-p_4)+\delta(q_3-p_4)\delta(q_4-p_3)\right]\times\\ &\left[\mathbb{1}_{\alpha\beta}{}^{\mu\nu}\mathbb{1}_{\gamma\delta}{}^{\rho\sigma}\delta(q_1-p_1)\delta(q_2-p_2)+\mathbb{1}_{\alpha\beta}{}^{\rho\sigma}\mathbb{1}_{\gamma\delta}{}^{\mu\nu}\delta(q_1-p_2)\delta(q_2-p_1)\right].\end{aligned} \tag{F.13}$$

It is understood that all occurrences of p_4 are replaced by $-p_1-p_2-p_3$. The last line reinforces why the tensor structures in (F.11) are dependent.

For the derivation of the flow equation for the kinetic term of the scalar field, we need to derive the form factors corresponding to all tensor structures above from our single-metric ansatz. To lighten the notation, we will in the following suppress the superscript $(\phi\phi)$ on f. The expansion of our ansatz in metric fluctuations reads

$$\begin{aligned}\frac{1}{2}\int \mathrm{d}^dx\sqrt{g}\,\phi f(\Delta)\phi&=\frac{1}{2}\int\mathrm{d}^dx\int_0^\infty\mathrm{d}s\,\tilde{f}(s)\,\sqrt{g}\,\phi\mathrm{e}^{-s\Delta}\phi\\ &\simeq\frac{1}{2}\int\mathrm{d}^dx\int_0^\infty\mathrm{d}s\,\tilde{f}(s)\,\sqrt{\bar{g}}\left[1+\frac{1}{2}h+\frac{1}{8}h^2-\frac{1}{4}h_{\mu\nu}h^{\mu\nu}\right]\times\\ &\qquad\phi\Bigg[1+V\left(0;-s\bar{\Delta},-s\mathbb{d}_1-s\mathbb{d}_2\right)\\ &\qquad+\frac{1}{2}\left(V\left(0;-s\bar{\Delta},-s\mathbb{d}_1\right)^2+V_\epsilon\left(0;-s\bar{\Delta},-s\mathbb{d}_1\right)\right)\Bigg]\mathrm{e}^{-s\bar{\Delta}}\phi\,.\end{aligned} \tag{F.14}$$

We split the contributions to the four-point function into pieces:

- $$\frac{1}{8}\int \mathrm{d}^d x\sqrt{\bar{g}}\left[\frac{1}{2}h^2 - h_{\mu\nu}h^{\mu\nu}\right]\phi f\left(\bar{\Delta}\right)\phi\,, \tag{F.15a}$$
- $$\frac{1}{4}\int \mathrm{d}^d x\sqrt{\bar{g}}\int_0^\infty \mathrm{d}s\,\tilde{f}(s)\,h\,\phi\sum_{j\geq 0}\frac{1}{(j+1)!}\left[-s\bar{\Delta},-s\mathbb{d}_1\right]_j \mathrm{e}^{-s\bar{\Delta}}\phi\,, \tag{F.15b}$$
- $$\frac{1}{2}\int \mathrm{d}^d x\sqrt{\bar{g}}\int_0^\infty \mathrm{d}s\,\tilde{f}(s)\,\phi\sum_{j\geq 0}\frac{1}{(j+1)!}\left[-s\bar{\Delta},-s\mathbb{d}_2\right]_j \mathrm{e}^{-s\bar{\Delta}}\phi\,, \tag{F.15c}$$
- $$\frac{1}{4}\int \mathrm{d}^d x\sqrt{\bar{g}}\int_0^\infty \mathrm{d}s\,\tilde{f}(s)\,\phi\sum_{j\geq 0}\frac{1}{(j+1)!}\left[-s\bar{\Delta},-s\mathbb{d}_1\right]_j \times \sum_{l\geq 0}\frac{1}{(l+1)!}\left[-s\bar{\Delta},-s\mathbb{d}_1\right]_l \mathrm{e}^{-s\bar{\Delta}}\phi\,, \tag{F.15d}$$
- $$\frac{1}{4}\int \mathrm{d}^d x\sqrt{\bar{g}}\int_0^\infty \mathrm{d}s\,\tilde{f}(s)\,\phi\times\sum_{j\geq 0}\sum_{k\geq 1}\frac{1}{(j+k+2)!}\left[-s\bar{\Delta},\left[-s\mathbb{d}_1,\left[-s\bar{\Delta},-s\mathbb{d}_1\right]_k\right]\right]_j \mathrm{e}^{-s\bar{\Delta}}\phi\,. \tag{F.15e}$$

The $\mathbb{d}_i$ are the ones obtained from the scalar Laplacian. We calculate the general vertex functions in the basis as above. The first term gives contributions

$$\begin{aligned}\frac{1}{16}f\left(p_3^2\right) &\overset{+}{\longmapsto} f^{(hh\phi\phi)}_{(\bar{g}\bar{g})}\,,\\ -\frac{1}{8}f\left(p_3^2\right) &\overset{+}{\longmapsto} f^{(hh\phi\phi)}_{(\mathbb{1})}\,.\end{aligned} \tag{F.16}$$

Here and in the following, the sign $\overset{+}{\longmapsto}$ signals that the term on the left contributes to the form factor(s) on the right. For the second term we calculate

$$\begin{aligned}&\frac{1}{4}\int \mathrm{d}^d x\sqrt{\bar{g}}\int_0^\infty \mathrm{d}s\,\tilde{f}(s)\,h\,\phi\sum_{j\geq 0}\frac{(-s)^{j+1}}{(j+1)!}\left[\bar{\Delta},\mathbb{d}_1\right]_j \mathrm{e}^{-s\bar{\Delta}}\phi\\ &= \frac{1}{4}\int \mathrm{d}^d x\sqrt{\bar{g}}\int_0^\infty \mathrm{d}s\,\tilde{f}(s)\,h\,\phi\sum_{j\geq 0}\frac{(-s)^{j+1}}{(j+1)!}\left(p_1^2+2y_{13}\right)^j \mathbb{d}_1\mathrm{e}^{-sp_3^2}\phi\\ &= \frac{1}{4}\int \mathrm{d}^d x\sqrt{\bar{g}}\int_0^\infty \mathrm{d}s\,\tilde{f}(s)\sum_{j\geq 0}\frac{(-s)^{j+1}}{(j+1)!}\left(p_1^2+2y_{13}\right)^j \mathrm{e}^{-sp_3^2}\times\\ &\qquad\left[\partial_3^\alpha\partial_3^\beta+\partial_1^\alpha\partial_3^\beta+\frac{1}{2}\bar{g}^{\alpha\beta}y_{13}\right]h_{\alpha\beta}h\phi\phi\,.\end{aligned} \tag{F.17}$$

Here we chose the momentum of the h in the $\mathbb{d}_1$ as p_1 and that of the ϕ to the right as p_3. Such a choice is not a problem since the variation of the vertex gives the correct

symmetrization automatically. For non-exceptional momenta (which is the case for our tadpole diagram), we can further do the sum, thus the contribution of this term is

$$\begin{aligned}\frac{1}{4}\frac{f\left(p_1^2+2y_{13}+p_3^2\right)-f\left(p_3^2\right)}{p_1^2+2y_{13}} &\overset{+}{\longmapsto} f^{(hh\phi\phi)}_{(33\bar{g})}, f^{(hh\phi\phi)}_{(13\bar{g})};\\ \frac{1}{8}y_{13}\frac{f\left(p_1^2+2y_{13}+p_3^2\right)-f\left(p_3^2\right)}{p_1^2+2y_{13}} &\overset{+}{\longmapsto} f^{(hh\phi\phi)}_{(\bar{g}\bar{g})}.\end{aligned} \tag{F.18}$$

For the exceptional momentum configuration $p_1^2 + 2y_{13} = 0$, the finite difference goes over to a derivative,

$$\lim_{p_1^2+2y_{13}\to 0}\frac{f\left(p_1^2+2y_{13}+p_3^2\right)-f\left(p_3^2\right)}{p_1^2+2y_{13}} = f'\left(p_3^2\right), \tag{F.19}$$

which can also be verified directly from the sum representation above, where all terms with $j > 0$ vanish, and the Laplace transform can be carried out trivially. As a general strategy we propose to insert the sum representation, which involves the inverse Laplace transform of f, as above into any given diagram, and only do the sum and back-transform afterwards. This correctly accounts for potentially exceptional momentum configurations.

We continue with the next term,

$$\begin{aligned}\frac{1}{2}\int \mathrm{d}^d x\sqrt{\bar{g}}\int_0^\infty \mathrm{d}s\,\tilde{f}(s)\,\phi\sum_{j\geq 0}\frac{(-s)^{j+1}}{(j+1)!}\left[\bar{\Delta},\mathbb{d}_2\right]_j \mathrm{e}^{-s\bar{\Delta}}\phi\\ = \frac{1}{2}\int \mathrm{d}^d x\sqrt{\bar{g}}\int_0^\infty \mathrm{d}s\,\tilde{f}(s)\,\phi\sum_{j\geq 0}\frac{(-s)^{j+1}}{(j+1)!}\times\\ \left(p_1^2+p_2^2+2y_{12}+2y_{13}+2y_{23}\right)^j\mathbb{d}_2\mathrm{e}^{-sp_3^2}\phi.\end{aligned} \tag{F.20}$$

For this we need

$$\begin{aligned}\phi\,\mathbb{d}_2\phi = \Big[&-\bar{g}^{\beta\delta}\partial_3^\alpha\partial_3^\gamma-\bar{g}^{\beta\delta}\partial_3^\alpha\partial_1^\gamma-\bar{g}^{\beta\delta}\partial_1^\alpha\partial_3^\gamma\\ &-\frac{1}{2}y_{13}\bar{g}^{\alpha\gamma}\bar{g}^{\beta\delta}+\frac{1}{2}\bar{g}^{\gamma\delta}\partial_2^\alpha\partial_3^\beta\Big]h_{\alpha\beta}h_{\gamma\delta}\phi\phi.\end{aligned} \tag{F.21}$$

In the tadpole diagram this contribution enters with exceptional momenta, we thus follow the strategy advertised above. Denoting

$$\mathfrak{Z} = \frac{1}{2}\int_0^\infty \mathrm{d}s\,\tilde{f}(s)\sum_{j\geq 0}\frac{(-s)^{j+1}}{(j+1)!}\left(p_1^2+p_2^2+2y_{12}+2y_{13}+2y_{23}\right)^j\mathrm{e}^{-sp_3^2}, \tag{F.22}$$

the contributions are

$$\begin{aligned} -3 &\overset{+}{\longmapsto} f^{(hh\phi\phi)}_{(3\bar{g}3)}, f^{(hh\phi\phi)}_{(3\bar{g}1)}, f^{(hh\phi\phi)}_{(1\bar{g}3)}, \\ -\frac{1}{2}y_{13}3 &\overset{+}{\longmapsto} f^{(hh\phi\phi)}_{(\mathbb{1})}, \\ \frac{1}{2}3 &\overset{+}{\longmapsto} f^{(hh\phi\phi)}_{(23\bar{g})}. \end{aligned} \tag{F.23}$$

For the fourth term,

$$\begin{aligned} &\frac{1}{4}\int \mathrm{d}^d x\sqrt{\bar{g}}\int_0^\infty \mathrm{d}s\,\tilde{f}(s)\,\phi\sum_{j\geq 0}\frac{1}{(j+1)!}\left[-s\bar{\Delta},-s\mathbb{d}_1\right]_j\times \\ &\qquad\sum_{l\geq 0}\frac{1}{(l+1)!}\left[-s\bar{\Delta},-s\mathbb{d}_1\right]_l \mathrm{e}^{-s\bar{\Delta}}\phi \\ &= \frac{1}{4}\int \mathrm{d}^d x\sqrt{\bar{g}}\int_0^\infty \mathrm{d}s\,\tilde{f}(s)\,\phi\sum_{j\geq 0}\sum_{l\geq 0}\frac{(-s)^{j+l+2}}{(j+1)!(l+1)!}\times \\ &\qquad\left(p_2^2+2y_{12}+2y_{23}\right)^j\left(p_1^2+2y_{13}\right)^l \mathrm{e}^{-sp_3^2}\,\mathbb{d}_1^2\phi\,, \end{aligned} \tag{F.24}$$

and the last term,

$$\begin{aligned} &\frac{1}{4}\int \mathrm{d}^d x\sqrt{\bar{g}}\int_0^\infty \mathrm{d}s\,\tilde{f}(s)\,\phi\sum_{j\geq 0}\sum_{k\geq 1}\frac{1}{(j+k+2)!}\times \\ &\qquad\left[-s\bar{\Delta},\left[-s\mathbb{d}_1,\left[-s\bar{\Delta},-s\mathbb{d}_1\right]_k\right]\right]_j \mathrm{e}^{-s\bar{\Delta}}\phi \\ &= \frac{1}{4}\int \mathrm{d}^d x\sqrt{\bar{g}}\int_0^\infty \mathrm{d}s\,\tilde{f}(s)\,\phi\sum_{j\geq 0}\sum_{k\geq 1}\frac{(-s)^{j+k+2}}{(j+k+2)!}\mathrm{e}^{-sp_3^2}\times \\ &\qquad\left(p_1^2+p_2^2+2y_{12}+2y_{13}+2y_{23}\right)^j\left(\mathbb{d}_1\left[\bar{\Delta},\mathbb{d}_1\right]_k-\left[\bar{\Delta},\mathbb{d}_1\right]_k\mathbb{d}_1\right)\phi \\ &= \frac{1}{4}\int \mathrm{d}^d x\sqrt{\bar{g}}\int_0^\infty \mathrm{d}s\,\tilde{f}(s)\,\phi\sum_{j\geq 0}\sum_{k\geq 1}\frac{(-s)^{j+k+2}}{(j+k+2)!}\mathrm{e}^{-sp_3^2}\times \\ &\qquad\left(p_1^2+p_2^2+2y_{12}+2y_{13}+2y_{23}\right)^j\left(\left(p_1^2+2y_{13}\right)^k-\left(p_1^2+2y_{12}+2y_{13}\right)^k\right)\mathbb{d}_1^2\phi\,. \end{aligned} \tag{F.25}$$

In both cases we thus need

$$\phi\,\mathbb{d}_1^2\phi = \phi\,\mathbb{d}_1\left[\partial_3^\alpha\partial_3^\beta+\partial_1^\alpha\partial_3^\beta+\frac{1}{2}\bar{g}^{\alpha\beta}y_{13}\right]h_{\alpha\beta}\phi \tag{F.26a}$$

$$= \left[(\partial_1^\gamma + \partial_3^\gamma)(\partial_1^\delta + \partial_3^\delta) + \partial_2^\gamma(\partial_1^\delta + \partial_3^\delta) + \frac{1}{2}\bar{g}^{\gamma\delta}(y_{12} + y_{23})\right] \times \tag{F.26b}$$
$$\left[\partial_3^\alpha \partial_3^\beta + \partial_1^\alpha \partial_3^\beta + \frac{1}{2}\bar{g}^{\alpha\beta} y_{13}\right] h_{\alpha\beta} h_{\gamma\delta} \phi\phi$$
$$= \Bigg[(3311) + (1311) + \frac{1}{2}y_{13}(\bar{g}11) + 2(3313) + 2(1313) + y_{13}(\bar{g}13) \tag{F.26c}$$
$$+ (3333) + (1333) + \frac{1}{2}y_{13}(\bar{g}33) + (3312) + (1312) + \frac{1}{2}y_{13}(\bar{g}12)$$
$$+ (3323) + (1323) + \frac{1}{2}y_{13}(\bar{g}23) + \frac{1}{2}(y_{12} + y_{23})(33\bar{g})$$
$$+ \frac{1}{2}(y_{12} + y_{23})(13\bar{g}) + \frac{1}{4}y_{13}(y_{12} + y_{23})(\bar{g}\bar{g})\Bigg] h_{\alpha\beta} h_{\gamma\delta} \phi\phi \,.$$

With the shorthand

$$\mathfrak{X} = \frac{1}{4}\int_0^\infty \mathrm{d}s\, \tilde{f}(s) \sum_{j\geq 0}\sum_{l\geq 0} \frac{(-s)^{j+l+2}}{(j+1)!(l+1)!} \left(p_2^2 + 2y_{12} + 2y_{23}\right)^j \left(p_1^2 + 2y_{13}\right)^l \mathrm{e}^{-sp_3^2}$$
$$+ \frac{1}{4}\int_0^\infty \mathrm{d}s\, \tilde{f}(s) \sum_{j\geq 0}\sum_{k\geq 1} \frac{(-s)^{j+k+2}}{(j+k+2)!} \left(p_1^2 + p_2^2 + 2y_{12} + 2y_{13} + 2y_{23}\right)^j \mathrm{e}^{-sp_3^2} \times$$
$$\left(\left(p_1^2 + 2y_{13}\right)^k - \left(p_1^2 + 2y_{12} + 2y_{13}\right)^k\right), \tag{F.27}$$

we have the final contributions

$$\begin{aligned}
\mathfrak{X} &\overset{+}{\longmapsto} f^{(hh\phi\phi)}_{(3311)}, f^{(hh\phi\phi)}_{(1311)}, f^{(hh\phi\phi)}_{(3333)}, f^{(hh\phi\phi)}_{(1333)}, f^{(hh\phi\phi)}_{(3312)}, f^{(hh\phi\phi)}_{(1312)}, \\
&\qquad\qquad f^{(hh\phi\phi)}_{(3323)}, f^{(hh\phi\phi)}_{(1323)}, \\
2\mathfrak{X} &\overset{+}{\longmapsto} f^{(hh\phi\phi)}_{(3313)}, f^{(hh\phi\phi)}_{(1313)}, \\
\frac{1}{2}y_{13}\mathfrak{X} &\overset{+}{\longmapsto} f^{(hh\phi\phi)}_{(\bar{g}11)}, f^{(hh\phi\phi)}_{(\bar{g}33)}, f^{(hh\phi\phi)}_{(\bar{g}12)}, f^{(hh\phi\phi)}_{(\bar{g}23)}, \\
y_{13}\mathfrak{X} &\overset{+}{\longmapsto} f^{(hh\phi\phi)}_{(\bar{g}13)}, \\
\frac{1}{2}(y_{12} + y_{23})\mathfrak{X} &\overset{+}{\longmapsto} f^{(hh\phi\phi)}_{(33\bar{g})}, f^{(hh\phi\phi)}_{(13\bar{g})}, \\
\frac{1}{4}y_{13}(y_{12} + y_{23})\mathfrak{X} &\overset{+}{\longmapsto} f^{(hh\phi\phi)}_{(\bar{g}\bar{g})}.
\end{aligned} \tag{F.28}$$

We can now compile the full list of all form factors that do not vanish in our ansatz:

$$f^{(hh\phi\phi)}_{(\mathbb{1})} = -\frac{1}{8}f\left(p_3^2\right) - \frac{1}{2}y_{13}\mathfrak{Z}\,, \tag{F.29a}$$

$$f^{(hh\phi\phi)}_{(\bar{g}\bar{g})} = \frac{1}{16}f(p_3^2) + \frac{1}{8}y_{13}\frac{f\left(p_1^2 + 2y_{13} + p_3^2\right) - f\left(p_3^2\right)}{p_1^2 + 2y_{13}} + \frac{1}{4}y_{13}(y_{12} + y_{23})\mathfrak{X}\,, \tag{F.29b}$$

$$f^{(hh\phi\phi)}_{(\bar{g}11)} = f^{(hh\phi\phi)}_{(\bar{g}12)} = f^{(hh\phi\phi)}_{(\bar{g}23)} = f^{(hh\phi\phi)}_{(\bar{g}33)} = \frac{1}{2} y_{13} \mathfrak{X}\,, \tag{F.29c}$$

$$f^{(hh\phi\phi)}_{(\bar{g}13)} = y_{13} \mathfrak{X}\,, \tag{F.29d}$$

$$f^{(hh\phi\phi)}_{(13\bar{g})} = f^{(hh\phi\phi)}_{(33\bar{g})} = \frac{1}{4} \frac{f\left(p_1^2 + 2y_{13} + p_3^2\right) - f\left(p_3^2\right)}{p_1^2 + 2y_{13}} + \frac{1}{2}(y_{12} + y_{23}) \mathfrak{X}\,, \tag{F.29e}$$

$$f^{(hh\phi\phi)}_{(23\bar{g})} = \frac{1}{2} \mathfrak{Z}\,, \tag{F.29f}$$

$$f^{(hh\phi\phi)}_{(1\bar{g}3)} = f^{(hh\phi\phi)}_{(3\bar{g}1)} = f^{(hh\phi\phi)}_{(3\bar{g}3)} = -\mathfrak{Z}\,, \tag{F.29g}$$

$$f^{(hh\phi\phi)}_{(1311)} = f^{(hh\phi\phi)}_{(1312)} = f^{(hh\phi\phi)}_{(1323)} = f^{(hh\phi\phi)}_{(1333)} = f^{(hh\phi\phi)}_{(3311)} = f^{(hh\phi\phi)}_{(3312)} = f^{(hh\phi\phi)}_{(3323)} = f^{(hh\phi\phi)}_{(3333)} = \mathfrak{X}\,, \tag{F.29h}$$

$$f^{(hh\phi\phi)}_{(1313)} = f^{(hh\phi\phi)}_{(3313)} = 2\mathfrak{X}\,. \tag{F.29i}$$

PUBLICATIONS

[1] B. Knorr, C. Ripken, and F. Saueressig. *Form Factors in Asymptotic Safety: conceptual ideas and computational toolbox*. *Class. Quant. Grav.* (2019) [arXiv:1907.02903].

[2] G. Gubitosi, R. Ooijer, C. Ripken, and F. Saueressig. *Consistent early and late time cosmology from the RG flow of gravity*. *J. Cosmol. Astropart. Phys.* **1812**.12 (2018) 004. [arXiv:1806.10147].

[3] G. Gubitosi, F. Saueressig, and C. Ripken. *Scales and hierachies in asymptotically safe quantum gravity: a review*. *Found. Phys.* **49**.9 (2019) 972. [arXiv:1901.01731].

[4] D. Becker, C. Ripken, and F. Saueressig. *On avoiding Ostrogradski instabilities within Asymptotic Safety*. *J. High Energy Phys.* **12** (2017) 121. [arXiv:1709.09098].

[5] F. Arici, D. Becker, C. Ripken, F. Saueressig, and W. D. van Suijlekom. *Reflection positivity in higher derivative scalar theories*. *J. Math. Phys.* **59**.8 (2018) 082302. [arXiv:1712.04308].

BIBLIOGRAPHY

[6] I. Newton. *Philosophiæ Naturalis Principia Mathematica*. 1687.

[7] J. C. Maxwell. *A dynamical theory of the electromagnetic field*. *Philos. Trans. Roy. Soc. London* **155** (1865) 459.

[8] D. J. Griffiths. *Introduction to Elementary Particles*. Wiley, 1987.

[9] M. E. Peskin and D. V. Schroeder. *An Introduction to quantum field theory*. Reading: Addison-Wesley, 1995.

[10] S. Weinberg. *The Quantum theory of fields. Vol. 1: Foundations*. Cambridge University Press, 2005.

[11] S. Weinberg. *The quantum theory of fields. Vol. 2: Modern applications*. Cambridge University Press, 1996.

[12] ATLAS collaboration. *Observation of a new particle in the search for the Standard Model Higgs boson with the ATLAS detector at the LHC*. *Phys. Lett. B* **716** (2012) 1. [arXiv:1207.7214].

[13] CMS collaboration. *Observation of a new boson at a mass of 125 GeV with the CMS experiment at the LHC*. *Phys. Lett. B* **716** (2012) 30. [arXiv:1207.7235].

[14] B. Schutz. *A First Course in General Relativity*. Cambridge University Press, 2009.

[15] S. M. Carroll. *Spacetime and geometry: An introduction to general relativity*. San Francisco: Addison-Wesley, 2004.

[16] C. W. Misner, K. S. Thorne, and J. A. Wheeler. *Gravitation*. San Francisco: W. H. Freeman, 1973.

[17] R. M. Wald. *General Relativity*. Chicago: Chicago University Press, 1984.

[18] A. Zee. *Einstein Gravity in a Nutshell*. New Jersey: Princeton University Press, 2013.

[19] LIGO Scientific, Virgo collaboration. *Observation of Gravitational Waves from a Binary Black Hole Merger*. *Phys. Rev. Lett.* **116**.6 (2016) 061102. [arXiv:1602.03837].

[20] J. Mielczarek and T. Trzeniewski. *Towards the map of quantum gravity*. *Gen. Relativ. Gravitation* **50**.6 (2018) 68. [arXiv:1708.07445].

[21] J. Polchinski. *String theory. Vol. 1: An introduction to the bosonic string*. Cambridge Monographs on Mathematical Physics. Cambridge University Press, 2007.

[22] J. Polchinski. *String theory. Vol. 2: Superstring theory and beyond*. Cambridge Monographs on Mathematical Physics. Cambridge University Press, 2007.

[23] B. Zwiebach. *A first course in string theory*. Cambridge University Press, 2006.

[24] L. Smolin. *An Invitation to loop quantum gravity*. In: *Proceedings, 3rd International Symposium on Quantum theory and symmetries (QTS3): Cincinnati, USA, September 10-14, 2003*. [Rev. Mod. Phys.(2004)]. 2004, 655. [arXiv:hep-th/0408048].

[25] C. Rovelli and F. Vidotto. *Covariant Loop Quantum Gravity*. Cambridge Monographs on Mathematical Physics. Cambridge University Press, 2014.

[26] J. Ambjørn, A. Goerlich, J. Jurkiewicz, and R. Loll. *Nonperturbative Quantum Gravity*. *Phys. Rep.* **519** (2012) 127. [arXiv:1203.3591].

[27] R. Loll. *Quantum Gravity from Causal Dynamical Triangulations: A Review*. (2019) [arXiv:1905.08669].

[28] R. Percacci. *An Introduction to Covariant Quantum Gravity and Asymptotic Safety*. **3**. 100 Years of General Relativity. World Scientific, 2017.

[29] M. Reuter and F. Saueressig. *Quantum Gravity and the Functional Renormalization Group*. Cambridge University Press, 2019.

[30] D. J. Kapner, T. S. Cook, E. G. Adelberger, J. H. Gundlach, B. R. Heckel, C. D. Hoyle, and H. E. Swanson. *Tests of the gravitational inverse-square law below the dark-energy length scale*. *Phys. Rev. Lett.* **98** (2007) 021101. [arXiv:hep-ph/0611184].

[31] G. 't Hooft and M. J. G. Veltman. *One loop divergencies in the theory of gravitation*. *Ann. Inst. Henri Poincaré, phys. theor.* **A20** (1974) 69.

[32] M. H. Goroff and A. Sagnotti. *The Ultraviolet Behavior of Einstein Gravity*. *Nucl. Phys. B* **266** (1986) 709.

[33] S. Weinberg. *What is quantum field theory, and what did we think it is?* In: *Conceptual foundations of quantum field theory. Proceedings, Symposium and Workshop, Boston, USA, March 1-3, 1996*. 1996, 241. [arXiv:hep-th/9702027].

[34] S. Weinberg. *Ultraviolet Divergences in Quantum Theories of Gravitation*. In: *General Relativity: An Einstein Centenary Survey*. 1980, 790.

[35] S. Weinberg. *Living with Infinities*. 2009. [arXiv:0903.0568].

[36] S. Weinberg. *Effective Field Theory, Past and Future*. *PoS Proc. Sci.* **CD09** (2009) 001. [arXiv:0908.1964].

[37] K. G. Wilson and J. B. Kogut. *The Renormalization group and the epsilon expansion*. *Phys. Rep.* **12** (1974) 75.

[38] C. Wetterich. *Exact evolution equation for the effective potential*. *Phys. Lett. B* **301** (1993) 90. [arXiv:1710.05815].

[39] T. R. Morris. *The Exact renormalization group and approximate solutions*. *Int. J. Mod. Phys. A* **9** (1994) 2411. [arXiv:hep-ph/9308265].

[40] M. Reuter and C. Wetterich. *Effective average action for gauge theories and exact evolution equations*. *Nucl. Phys. B* **417** (1994) 181.

[41] J. Polchinski. *Renormalization and Effective Lagrangians*. *Nucl. Phys. B* **231** (1984) 269.

[42] K. S. Stelle. *Classical Gravity with Higher Derivatives*. *Gen. Relativ. Gravitation* **9** (1978) 353.

[43] H.-S. Tsao. *Conformal Anomalies in a General Background Metric*. *Phys. Lett.* **68** (1977) 79.

[44] L. S. Brown. *Stress Tensor Trace Anomaly in a Gravitational Metric: Scalar Fields*. *Phys. Rev. D* **15** (1977) 1469.

[45] D. M. Capper and M. J. Duff. *The one loop neutrino contribution to the graviton propagator*. *Nucl. Phys. B* **82** (1974) 147.

[46] D. M. Capper, M. J. Duff, and L. Halpern. *Photon corrections to the graviton propagator*. *Phys. Rev. D* **10** (1974) 461.

[47] T. Aida, Y. Kitazawa, H. Kawai, and M. Ninomiya. *Conformal invariance and renormalization group in quantum gravity near two-dimensions*. *Nucl. Phys. B* **427** (1994) 158. [arXiv:hep-th/9404171].

[48] H. Kawai, Y. Kitazawa, and M. Ninomiya. *Scaling exponents in quantum gravity near two-dimensions*. *Nucl. Phys. B,* **393** (1993) 280. [arXiv:hep-th/9206081].

[49] H. Kawai, Y. Kitazawa, and M. Ninomiya. *Ultraviolet stable fixed point and scaling relations in (2+epsilon)-dimensional quantum gravity*. *Nucl. Phys. B* **404** (1993) 684. [arXiv:hep-th/9303123].

[50] H. Kawai and M. Ninomiya. *Renormalization Group and Quantum Gravity*. *Nucl. Phys. B* **336** (1990) 115.

[51] D. Becker and M. Reuter. *En route to Background Independence: Broken split-symmetry, and how to restore it with bi-metric average actions*. *Ann. Phys.* **350** (2014) 225. [arXiv:1404.4537].

[52] D. Benedetti. *On the number of relevant operators in asymptotically safe gravity*. *Europhys. Lett.* **102**.2 (2013) 20007. [arXiv:1301.4422].

[53] D. Benedetti and F. Caravelli. *The Local potential approximation in quantum gravity*. *J. High Energy Phys.* **06** (2012) 017. Erratum: [282]. [arXiv:1204.3541].

[54] D. Benedetti, P. F. Machado, and F. Saueressig. *Asymptotic safety in higher-derivative gravity*. *Mod. Phys. Lett. A* **24** (2009) 2233. [arXiv:0901.2984].

[55] J. Biemans, A. Platania, and F. Saueressig. *Quantum gravity on foliated spacetimes: Asymptotically safe and sound*. *Phys. Rev. D* **95**.8 (2017) 086013. [arXiv:1609.04813].

[56] I. H. Bridle, J. A. Dietz, and T. R. Morris. *The local potential approximation in the background field formalism*. *J. High Energy Phys.* **1403** (2014) 093. [arXiv:1312.2846].

[57] N. Christiansen. *Four-Derivative Quantum Gravity Beyond Perturbation Theory*. (2016) [arXiv:1612.06223].

[58] N. Christiansen, B. Knorr, J. Meibohm, J. M. Pawlowski, and M. Reichert. *Local Quantum Gravity*. *Phys. Rev. D* **92**.12 (2015) 121501. [arXiv:1506.07016].

[59] N. Christiansen, B. Knorr, J. M. Pawlowski, and A. Rodigast. *Global Flows in Quantum Gravity*. *Phys. Rev. D* **93**.4 (2016) 044036. [arXiv:1403.1232].

[60] N. Christiansen, D. F. Litim, J. M. Pawlowski, and M. Reichert. *Asymptotic safety of gravity with matter*. *Phys. Rev. D* **97**.10 (2018) 106012. [arXiv:1710.04669].

[61] N. Christiansen, D. F. Litim, J. M. Pawlowski, and A. Rodigast. *Fixed points and infrared completion of quantum gravity*. *Phys. Lett. B* **728** (2014) 114. [arXiv:1209.4038].

[62] A. Codello, G. D'Odorico, and C. Pagani. *Consistent closure of renormalization group flow equations in quantum gravity*. *Phys. Rev. D* **89**.8 (2014) 081701. [arXiv:1304.4777].

[63] A. Codello, R. Percacci, and C. Rahmede. *Investigating the Ultraviolet Properties of Gravity with a Wilsonian Renormalization Group Equation*. *Ann. Phys.* **324** (2009) 414. [arXiv:0805.2909].

[64] A. Codello, R. Percacci, and C. Rahmede. *Ultraviolet properties of $f(R)$-gravity*. *Int. J. Mod. Phys. A* **23** (2008) 143. [arXiv:0705.1769].

[65] G. P. De Brito, N. Ohta, A. D. Pereira, A. A. Tomaz, and M. Yamada. *Asymptotic safety and field parametrization dependence in the $f(R)$ truncation*. *Phys. Rev. D* **98**.2 (2018) 026027. [arXiv:1805.09656].

[66] M. Demmel, F. Saueressig, and O. Zanusso. *RG flows of Quantum Einstein Gravity in the linear-geometric approximation*. *Ann. Phys.* **359** (2015) 141. [arXiv:1412.7207].

[67] M. Demmel, F. Saueressig, and O. Zanusso. *A proper fixed functional for four-dimensional Quantum Einstein Gravity*. *J. High Energy Phys.* **08** (2015) 113. [arXiv:1504.07656].

[68] T. Denz, J. M. Pawlowski, and M. Reichert. *Towards apparent convergence in asymptotically safe quantum gravity*. *Eur. Phys. J. C* **78**.4 (2018) 336. [arXiv:1612.07315].

[69] J. A. Dietz and T. R. Morris. *Background independent exact renormalization group for conformally reduced gravity*. *J. High Energy Phys.* **04** (2015) 118. [arXiv:1502.07396].

[70] J. A. Dietz and T. R. Morris. *Asymptotic safety in the $f(R)$ approximation*. *J. High Energy Phys.* **01** (2013) 108. [arXiv:1211.0955].

[71] J. A. Dietz and T. R. Morris. *Redundant operators in the exact renormalisation group and in the $f(R)$ approximation to asymptotic safety*. *J. High Energy Phys.* **07** (2013) 064. [arXiv:1306.1223].

[72] I. Donkin and J. M. Pawlowski. *The phase diagram of quantum gravity from diffeomorphism-invariant RG-flows*. (2012) [arXiv:1203.4207].

[73] A. Eichhorn, S. Lippoldt, and V. Skrinjar. *Nonminimal hints for asymptotic safety*. *Phys. Rev. D* **97**.2 (2018) 026002. [arXiv:1710.03005].

[74] A. Eichhorn and M. Schiffer. *$d = 4$ as the critical dimensionality of asymptotically safe interactions*. *Phys. Lett. B* **793** (2019) 383. [arXiv:1902.06479].

[75] K. Falls, C. R. King, D. F. Litim, K. Nikolakopoulos, and C. Rahmede. *Asymptotic safety of quantum gravity beyond Ricci scalars*. *Phys. Rev. D* **97**.8 (2018) 086006. [arXiv:1801.00162].

[76] K. Falls, D. F. Litim, K. Nikolakopoulos, and C. Rahmede. *Further evidence for asymptotic safety of quantum gravity*. *Phys. Rev. D* **93**.10 (2016) 104022. [arXiv:1410.4815].

[77] K. Falls, D. F. Litim, K. Nikolakopoulos, and C. Rahmede. *A bootstrap towards asymptotic safety*. (2013) [arXiv:1301.4191].

[78] K. G. Falls, D. F. Litim, and J. Schröder. *Aspects of asymptotic safety for quantum gravity*. *Phys. Rev. D* **99**.12 (2019) 126015. [arXiv:1810.08550].

[79] H. Gies, B. Knorr, and S. Lippoldt. *Generalized Parametrization Dependence in Quantum Gravity*. *Phys. Rev. D* **92**.8 (2015) 084020. [arXiv:1507.08859].

[80] W. B. Houthoff, A. Kurov, and F. Saueressig. *Impact of topology in foliated Quantum Einstein Gravity*. *Eur. Phys. J. C* **77** (2017) 491. [arXiv:1705.01848].

[81] B. Knorr. *Infinite order quantum-gravitational correlations*. *Class. Quant. Grav.* **35**.11 (2018) 115005. [arXiv:1710.07055].

[82] B. Knorr and S. Lippoldt. *Correlation functions on a curved background*. *Phys. Rev. D* **96**.6 (2017) 065020. [arXiv:1707.01397].

[83] P. Labus, T. R. Morris, and Z. H. Slade. *Background independence in a background dependent renormalization group*. *Phys. Rev. D* **94**.2 (2016) 024007. [arXiv:1603.04772].

[84] O. Lauscher and M. Reuter. *Flow equation of quantum Einstein gravity in a higher derivative truncation*. *Phys. Rev. D* **66** (2002) 025026. [arXiv:hep-th/0205062].

[85] P. F. Machado and F. Saueressig. *On the renormalization group flow of $f(R)$-gravity*. *Phys. Rev. D* **77** (2008) 124045. [arXiv:0712.0445].

[86] E. Manrique, S. Rechenberger, and F. Saueressig. *Asymptotically Safe Lorentzian Gravity*. *Phys. Rev. Lett.* **106** (2011) 251302. [arXiv:1102.5012].

[87] E. Manrique and M. Reuter. *Bimetric Truncations for Quantum Einstein Gravity and Asymptotic Safety*. *Ann. Phys.* **325** (2010) 785. [arXiv:0907.2617].

[88] E. Manrique, M. Reuter, and F. Saueressig. *Bimetric Renormalization Group Flows in Quantum Einstein Gravity*. *Ann. Phys.* **326** (2011) 463. [arXiv:1006.0099].

[89] E. Manrique, M. Reuter, and F. Saueressig. *Matter Induced Bimetric Actions for Gravity*. *Ann. Phys.* **326** (2011) 440. [arXiv:1003.5129].

[90] T. R. Morris. *Large curvature and background scale independence in single-metric approximations to asymptotic safety*. *J. High Energy Phys.* **11** (2016) 160. [arXiv:1610.03081].

[91] T. R. Morris and A. W. H. Preston. *Manifestly diffeomorphism invariant classical Exact Renormalization Group*. *J. High Energy Phys.* **06** (2016) 012. [arXiv:1602.08993].

[92] S. Nagy. *Lectures on renormalization and asymptotic safety*. *Ann. Phys.* **350** (2014) 310. [arXiv:1211.4151].

[93] C. M. Nieto, R. Percacci, and V. Skrinjar. *Split Weyl transformations in quantum gravity*. *Phys. Rev. D* **96**.10 (2017) 106019. [arXiv:1708.09760].

[94] A. Nink. *Field Parametrization Dependence in Asymptotically Safe Quantum Gravity*. *Phys. Rev. D* **91**.4 (2015) 044030. [arXiv:1410.7816].

[95] A. Nink and M. Reuter. *The unitary conformal field theory behind 2D Asymptotic Safety*. *J. High Energy Phys.* **02** (2016) 167. [arXiv:1512.06805].

[96] N. Ohta, R. Percacci, and A. D. Pereira. *Gauges and functional measures in quantum gravity II: Higher derivative gravity*. *Eur. Phys. J. C* **77**.9 (2017) 611. [arXiv:1610.07991].

[97] N. Ohta, R. Percacci, and A. D. Pereira. *Gauges and functional measures in quantum gravity I: Einstein theory*. *J. High Energy Phys.* **06** (2016) 115. [arXiv:1605.00454].

[98] N. Ohta, R. Percacci, and G. P. Vacca. *Renormalization Group Equation and scaling solutions for $f(R)$ gravity in exponential parametrization*. *Eur. Phys. J. C* **76**.2 (2016) 46. [arXiv:1511.09393].

[99] N. Ohta, R. Percacci, and G. P. Vacca. *Flow equation for $f(R)$ gravity and some of its exact solutions*. *Phys. Rev. D* **92**.6 (2015) 061501. [arXiv:1507.00968].

[100] R. Percacci and G. P. Vacca. *The background scale Ward identity in quantum gravity*. *Eur. Phys. J. C* **77**.1 (2017) 52. [arXiv:1611.07005].

[101] S. Rechenberger and F. Saueressig. *The R^2 phase-diagram of QEG and its spectral dimension*. *Phys. Rev. D* **86** (2012) 024018. [arXiv:1206.0657].

[102] M. Reuter. *Nonperturbative evolution equation for quantum gravity*. *Phys. Rev. D* **57** (1998) 971. [arXiv:hep-th/9605030].

[103] M. Reuter and F. Saueressig. *Quantum Einstein Gravity*. *New J. Phys.* **14** (2012) 055022. [arXiv:1202.2274].

[104] M. Reuter and F. Saueressig. *Renormalization group flow of quantum gravity in the Einstein-Hilbert truncation*. *Phys. Rev. D* **65** (2002) 065016. [arXiv:hep-th/0110054].

[105] M. Safari and G. P. Vacca. *Covariant and background independent functional RG flow for the effective average action*. *Journal of High Energy Physics* **11** (2016) 139. [arXiv:1607.07074].

[106] N. Alkofer. *Asymptotically safe $f(R)$-gravity coupled to matter II: Global solutions*. *Phys. Lett. B* **789** (2019) 480. [arXiv:1809.06162].

[107] N. Alkofer and F. Saueressig. *Asymptotically safe $f(R)$-gravity coupled to matter I: the polynomial case*. *Ann. Phys.* **396** (2018) 173. [arXiv:1802.00498].

[108] J. Biemans, A. Platania, and F. Saueressig. *Renormalization group fixed points of foliated gravity-matter systems*. *J. High Energy Phys.* **05** (2017) 093. [arXiv:1702.06539].

[109] L. Bosma, B. Knorr, and F. Saueressig. *Resolving Spacetime Singularities within Asymptotic Safety*. *Phys. Rev. Lett.* **123**.10 (2019) 101301. [arXiv:1904.04845].

[110] N. Christiansen, K. Falls, J. M. Pawlowski, and M. Reichert. *Curvature dependence of quantum gravity*. *Phys. Rev. D* **97**.4 (2018) 046007. [arXiv:1711.09259].

[111] A. Eichhorn, P. Labus, J. M. Pawlowski, and M. Reichert. *Effective universality in quantum gravity*. *SciPost Phys.* **5**.4 (2018) 031. [arXiv:1804.00012].

[112] A. Eichhorn, S. Lippoldt, J. M. Pawlowski, M. Reichert, and M. Schiffer. *How perturbative is quantum gravity? Phys. Lett. B* **792** (2019) 310. [arXiv:1810.02828].

[113] A. Bonanno. *An effective action for asymptotically safe gravity*. *Phys. Rev. D* **85** (2012) 081503. [arXiv:1203.1962].

[114] A. Bonanno, A. Contillo, and R. Percacci. *Inflationary solutions in asymptotically safe $f(R)$ theories*. *Class. Quant. Grav.* **28** (2011) 145026. [arXiv:1006.0192].

[115] A. Bonanno, G. Esposito, C. Rubano, and P. Scudellaro. *The Accelerated expansion of the Universe as a crossover phenomenon*. *Class. Quant. Grav.* **23** (2006) 3103. [arXiv:astro-ph/0507670].

[116] A. Bonanno and A. Platania. *Asymptotically safe inflation from quadratic gravity*. *Phys. Lett. B* **750** (2015) 638. [arXiv:1507.03375].

[117] A. Bonanno, A. Platania, and F. Saueressig. *Cosmological bounds on the field content of asymptotically safe gravitymatter models*. *Phys. Lett. B* **784** (2018) 229. [arXiv:1803.02355].

[118] A. Bonanno and M. Reuter. *Entropy signature of the running cosmological constant*. *J. Cosmol. Astropart. Phys.* **0708** (2007) 024. [arXiv:0706.0174].

[119] A. Bonanno and M. Reuter. *Cosmology with selfadjusting vacuum energy density from a renormalization group fixed point*. *Phys. Lett.* **B527** (2002) 9. [arXiv:astro-ph/0106468].

[120] A. Bonanno and M. Reuter. *Cosmology of the Planck era from a renormalization group for quantum gravity*. *Phys. Rev.* **65** (2002) 043508. [arXiv:hep-th/0106133].

[121] A. Bonanno and F. Saueressig. *Asymptotically safe cosmology A status report*. *C. R. Phys.* **18** (2017) 254. [arXiv:1702.04137].

[122] Y.-F. Cai and D. A. Easson. *Asymptotically safe gravity as a scalar-tensor theory and its cosmological implications*. *Phys. Rev. D* **84** (2011) 103502. [arXiv:1107.5815].

[123] N. Christiansen and A. Eichhorn. *An asymptotically safe solution to the U(1) triviality problem*. *Phys. Lett. B* **770** (2017) 154. [arXiv:1702.07724].

[124] N. Christiansen, A. Eichhorn, and A. Held. *Is scale-invariance in gauge-Yukawa systems compatible with the graviton?* *Phys. Rev. D* **96**.8 (2017) 084021. [arXiv:1705.01858].

[125] J.-E. Daum, U. Harst, and M. Reuter. *Running Gauge Coupling in Asymptotically Safe Quantum Gravity*. *J. High Energy Phys.* **01** (2010) 084. [arXiv:0910.4938].

[126] G. P. De Brito, Y. Hamada, A. D. Pereira, and M. Yamada. *On the impact of Majorana masses in gravity-matter systems*. *Journal of High Energy Physics* **08** (2019) 142. [arXiv:1905.11114].

[127] B. Dobrich and A. Eichhorn. *Can we see quantum gravity? Photons in the asymptotic-safety scenario*. *J. High Energy Phys.* **06** (2012) 156. [arXiv:1203.6366].

[128] P. Donà, A. Eichhorn, P. Labus, and R. Percacci. *Asymptotic safety in an interacting system of gravity and scalar matter*. *Phys. Rev. D* **93**.4 (2016) 044049. Erratum: [283]. [arXiv:1512.01589].

[129] P. Donà, A. Eichhorn, and R. Percacci. *Consistency of matter models with asymptotically safe quantum gravity*. *Can. J. Phys.* **93**.9 (2015) 988. [arXiv:1410.4411].

[130] P. Donà, A. Eichhorn, and R. Percacci. *Matter matters in asymptotically safe quantum gravity*. *Phys. Rev. D* **89**.8 (2014) 084035. [arXiv:1311.2898].

[131] P. Donà and R. Percacci. *Functional renormalization with fermions and tetrads*. *Phys. Rev. D* **87**.4 (2013) 045002. [arXiv:1209.3649].

[132] A. Eichhorn. *An asymptotically safe guide to quantum gravity and matter*. *Front. Astron. Space Sci.* **5** (2019) 47. [arXiv:1810.07615].

[133] A. Eichhorn. *Status of the asymptotic safety paradigm for quantum gravity and matter*. In: *Black Holes, Gravitational Waves and Spacetime Singularities Rome, Italy, May 9-12, 2017*. 2017. [arXiv:1709.03696].

[134] A. Eichhorn. *Quantum-gravity-induced matter self-interactions in the asymptotic-safety scenario*. *Phys. Rev. D* **86** (2012) 105021. [arXiv:1204.0965].

[135] A. Eichhorn and H. Gies. *Light fermions in quantum gravity*. *New J. Phys.* **13** (2011) 125012. [arXiv:1104.5366].

[136] A. Eichhorn, Y. Hamada, J. Lumma, and M. Yamada. *Quantum gravity fluctuations flatten the Planck-scale Higgs potential*. *Phys. Rev. D* **97**.8 (2018) 086004. [arXiv:1712.00319].

[137] A. Eichhorn and A. Held. *Top mass from asymptotic safety*. *Phys. Lett. B* **777** (2018) 217. [arXiv:1707.01107].

[138] A. Eichhorn and A. Held. *Mass difference for charged quarks from asymptotically safe quantum gravity*. *Phys. Rev. Lett.* **121**.15 (2018) 151302. [arXiv:1803.04027].

[139] A. Eichhorn and A. Held. *Viability of quantum-gravity induced ultraviolet completions for matter*. *Phys. Rev. D* **96**.8 (2017) 086025. [arXiv:1705.02342].

[140] A. Eichhorn, A. Held, and J. M. Pawlowski. *Quantum-gravity effects on a Higgs-Yukawa model*. *Phys. Rev. D* **94**.10 (2016) 104027. [arXiv:1604.02041].

[141] A. Eichhorn, A. Held, and C. Wetterich. *Quantum-gravity predictions for the fine-structure constant*. *Phys. Lett. B* **782** (2018) 198. [arXiv:1711.02949].

[142] A. Eichhorn and S. Lippoldt. *Quantum gravity and Standard-Model-like fermions*. *Phys. Lett. B* **767** (2017) 142. [arXiv:1611.05878].

[143] A. Eichhorn, S. Lippoldt, and M. Schiffer. *Zooming in on fermions and quantum gravity*. *Phys. Rev. D* **99** (2019) 086002. [arXiv:1812.08782].

[144] A. Eichhorn and M. M. Scherer. *Planck scale, Higgs mass, and scalar dark matter*. *Phys. Rev. D* **90**.2 (2014) 025023. [arXiv:1404.5962].

[145] A. Eichhorn and F. Versteegen. *Upper bound on the Abelian gauge coupling from asymptotic safety*. *J. High Energy Phys.* **01** (2018) 030. [arXiv:1709.07252].

[146] S. Folkerts, D. F. Litim, and J. M. Pawlowski. *Asymptotic freedom of Yang-Mills theory with gravity*. *Phys. Lett. B* **709** (2012) 234. [arXiv:1101.5552].

[147] H. Gies and S. Lippoldt. *Fermions in gravity with local spin-base invariance*. *Phys. Rev. D* **89**.6 (2014) 064040. [arXiv:1310.2509].

[148] Y. Hamada and M. Yamada. *Asymptotic safety of higher derivative quantum gravity non-minimally coupled with a matter system*. *J. High Energy Phys.* **08** (2017) 070. [arXiv:1703.09033].

[149] U. Harst and M. Reuter. *QED coupled to QEG*. *J. High Energy Phys.* **1105** (2011) 119. [arXiv:1101.6007].

[150] T. Henz, J. M. Pawlowski, A. Rodigast, and C. Wetterich. *Dilaton Quantum Gravity*. *Phys. Lett. B* **727** (2013) 298. [arXiv:1304.7743].

[151] T. Henz, J. M. Pawlowski, and C. Wetterich. *Scaling solutions for Dilaton Quantum Gravity*. *Phys. Lett. B* **769** (2017) 105. [arXiv:1605.01858].

[152] P. Labus, R. Percacci, and G. P. Vacca. *Asymptotic safety in $O(N)$ scalar models coupled to gravity*. *Phys. Lett. B* **753** (2016) 274. [arXiv:1505.05393].

[153] D. F. Litim. *Renormalisation group and the Planck scale*. *Philos. Trans. R. Soc. London, Ser. A* **369** (2011) 2759. [arXiv:1102.4624].

[154] J. Meibohm and J. M. Pawlowski. *Chiral fermions in asymptotically safe quantum gravity*. *Eur. Phys. J. C* **76**.5 (2016) 285. [arXiv:1601.04597].

[155] J. Meibohm, J. M. Pawlowski, and M. Reichert. *Asymptotic safety of gravity-matter systems*. *Phys. Rev. D* **93**.8 (2016) 084035. [arXiv:1510.07018].

[156] G. Narain and R. Percacci. *Renormalization Group Flow in Scalar-Tensor Theories. I. Class. Quant. Grav.* **27** (2010) 075001. [arXiv:0911.0386].

[157] G. Narain and C. Rahmede. *Renormalization Group Flow in Scalar-Tensor Theories. II. Class. Quant. Grav.* **27** (2010) 075002. [arXiv:0911.0394].

[158] M. Niedermaier and M. Reuter. *The Asymptotic Safety Scenario in Quantum Gravity*. *Living Rev. Relativ.* **9** (2006) 5.

[159] K.-y. Oda and M. Yamada. *Non-minimal coupling in HiggsYukawa model with asymptotically safe gravity*. *Class. Quant. Grav.* **33**.12 (2016) 125011. [arXiv:1510.03734].

[160] J. M. Pawlowski, M. Reichert, C. Wetterich, and M. Yamada. *Higgs scalar potential in asymptotically safe quantum gravity*. *Phys. Rev. D* **99**.8 (2019) 086010. [arXiv:1811.11706].

[161] R. Percacci and D. Perini. *Constraints on matter from asymptotic safety*. *Phys. Rev. D* **67** (2003) 081503. [arXiv:hep-th/0207033].

[162] R. Percacci and D. Perini. *Asymptotic safety of gravity coupled to matter*. *Phys. Rev. D* **68** (2003) 044018. [arXiv:hep-th/0304222].

[163] R. Percacci and G. P. Vacca. *Search of scaling solutions in scalar-tensor gravity*. *Eur. Phys. J. C* **75**.5 (2015) 188. [arXiv:1501.00888].

[164] M. Reuter and F. Saueressig. *Asymptotic Safety, Fractals, and Cosmology*. *Lect. Notes Phys.* **863** (2013) 185. [arXiv:1205.5431].

[165] M. Reuter and F. Saueressig. *From big bang to asymptotic de Sitter: Complete cosmologies in a quantum gravity framework*. *J. Cosmol. Astropart. Phys.* **0509** (2005) 012. [arXiv:hep-th/0507167].

[166] M. Reuter and H. Weyer. *Quantum gravity at astrophysical distances? J. Cosmol. Astropart. Phys.* **0412** (2004) 001. [arXiv:hep-th/0410119].

[167] I. D. Saltas. *Higgs inflation and quantum gravity: An exact renormalisation group approach*. *J. Cosmol. Astropart. Phys.* **1602** (2016) 048. [arXiv:1512.06134].

[168] M. Shaposhnikov and C. Wetterich. *Asymptotic safety of gravity and the Higgs boson mass*. *Phys. Lett. B* **683** (2010) 196. [arXiv:0912.0208].

[169] A. Tronconi. *Asymptotically Safe Non-Minimal Inflation*. *J. Cosmol. Astropart. Phys.* **1707**.07 (2017) 015. [arXiv:1704.05312].

[170] G. P. Vacca and O. Zanusso. *Asymptotic Safety in Einstein Gravity and Scalar-Fermion Matter*. *Phys. Rev. Lett.* **105** (2010) 231601. [arXiv:1009.1735].

[171] C. Wetterich. *Graviton fluctuations erase the cosmological constant*. *Phys. Lett. B* **773** (2017) 6. [arXiv:1704.08040].

[172] C. Wetterich and M. Yamada. *Variable Planck mass from gauge invariant flow equation*. (2019) [arXiv:1906.01721].

[173] O. Zanusso, L. Zambelli, G. P. Vacca, and R. Percacci. *Gravitational corrections to Yukawa systems*. *Phys. Lett. B* **689** (2010) 90. [arXiv:0904.0938].

[174] M. Crisostomi, R. Klein, and D. Roest. *Higher Derivative Field Theories: Degeneracy Conditions and Classes*. *J. High Energy Phys.* **06** (2017) 124. [arXiv:1703.01623].

[175] R. P. Woodard. *Ostrogradsky's theorem on Hamiltonian instability*. *Scholarpedia* **10**.8 (2015) 32243. [arXiv:1506.02210].

[176] M. Ostrogradski. *Mémoires sur les équations différentielles, relatives au problème des isopérimètres*. *Mem. Acad. St. Petersbourg* **6**.4 (1850) 385.

[177] U. Ellwanger. *Flow equations for N point functions and bound states*. *Z. Phys. C: Part. Fields* **62** (1994) 503. [,206(1993)]. [arXiv:hep-ph/9308260].

[178] J. M. Pawlowski. *Aspects of the functional renormalisation group*. *Ann. Phys.* **322** (2007) 2831. [arXiv:hep-th/0512261].

[179] B. Delamotte. *An Introduction to the nonperturbative renormalization group*. *Lect. Notes Phys.* **852** (2012) 49. [arXiv:cond-mat/0702365].

[180] T. Aida, Y. Kitazawa, J. Nishimura, and A. Tsuchiya. *Two loop renormalization in quantum gravity near two-dimensions*. *Nucl. Phys. B* **444** (1995) 353. [arXiv:hep-th/9501056].

[181] M. Demmel and A. Nink. *Connections and geodesics in the space of metrics*. *Phys. Rev. D* **92**.10 (2015) 104013. [arXiv:1506.03809].

[182] D. F. Litim and J. M. Pawlowski. *Renormalization group flows for gauge theories in axial gauges*. *Journal of High Energy Physics* **09** (2002) 049. [arXiv:hep-th/0203005].

[183] D. F. Litim and J. M. Pawlowski. *Wilsonian flows and background fields*. *Phys. Lett. B* **546** (2002) 279. [arXiv:hep-th/0208216].

[184] J. M. Pawlowski. *Geometrical effective action and Wilsonian flows*. (2003) [arXiv:hep-th/0310018].

[185] M. Safari. *Splitting Ward identity*. *Eur. Phys. J. C* **76**.4 (2016) 201. [arXiv:1508.06244].

[186] C. M. Will. *The Confrontation between General Relativity and Experiment*. *Living Rev. Relativ.* **17** (2014) 4. [arXiv:1403.7377].

[187] Particle Data Group collaboration. *Review of Particle Physics*. *Phys. Rev. D* **98**.3 (2018) 030001.

[188] Supernova Search Team collaboration. *Observational evidence from supernovae for an accelerating universe and a cosmological constant*. *Astron. J.* **116** (1998) 1009. [arXiv:astro-ph/9805201].

[189] Supernova Cosmology Project collaboration. *Measurements of* Ω *and* Λ *from 42 high redshift supernovae*. *Astrophys. J.* **517** (1999) 565. [arXiv:astro-ph/9812133].

[190] Planck collaboration. *Planck 2013 results. XXII. Constraints on inflation*. *Astron. Astrophys.* **571** (2014) A22. [arXiv:1303.5082].

[191] J. L. Cervantes-Cota and G. Smoot. *Cosmology today-A brief review*. *AIP Conf. Proc.* **1396**.1 (2011) 28. [arXiv:1107.1789].

[192] J. Martin. *Everything You Always Wanted To Know About The Cosmological Constant Problem (But Were Afraid To Ask)*. *C. R. Phys.* **13** (2012) 566. [arXiv:1205.3365].

[193] A. Padilla. *Lectures on the Cosmological Constant Problem*. (2015) [arXiv:1502.05296].

[194] J. Sola. *Cosmological constant and vacuum energy: old and new ideas*. *J. Phys. Conf. Ser.* **453** (2013) 012015. [arXiv:1306.1527].

[195] S. Weinberg. *The Cosmological Constant Problem*. *Rev. Mod. Phys.* **61** (1989) 1.

[196] G. 't Hooft. *Naturalness, Chiral Symmetry, and Spontaneous Chiral Symmetry Breaking*. In: *Recent Developments in Gauge Theories*. Ed. by G. 't Hooft, C. Itzykson, A. Jaffe, H. Lehmann, P. K. Mitter, I. M. Singer, and R. Stora. Boston, MA: Springer, 1980, 135.

[197] Planck collaboration. *Planck 2015 results. XX. Constraints on inflation*. *Astron. Astrophys.* **594** (2016) A20. [arXiv:1502.02114].

[198] A. H. Guth. *The Inflationary Universe: A Possible Solution to the Horizon and Flatness Problems*. *Phys. Rev. D* **23** (1981) 347. [Adv. Ser. Astrophys. Cosmol.3,139(1987)].

[199] J. Martin, C. Ringeval, and V. Vennin. *Encyclopædia Inflationaris*. *Phys. Dark Univ.* **5-6** (2014) 75. [arXiv:1303.3787].

[200] V. F. Mukhanov and G. V. Chibisov. *Quantum Fluctuations and a Nonsingular Universe*. *JETP Lett.* **33** (1981) 532. [Pisma Zh. Eksp. Teor. Fiz.33,549(1981)].

[201] A. A. Starobinsky. *A New Type of Isotropic Cosmological Models Without Singularity*. *Phys. Lett. B* **91** (1980) 99.

[202] A. A. Starobinsky. *The Perturbation Spectrum Evolving from a Nonsingular Initially De-Sitter Cosmology and the Microwave Background Anisotropy*. *Sov. Astron. Lett.* **9** (1983) 302.

[203] F. L. Bezrukov and M. Shaposhnikov. *The Standard Model Higgs boson as the inflaton*. *Phys. Lett. B* **659** (2008) 703. [arXiv:0710.3755].

[204] A. O. Barvinsky, A. Y. Kamenshchik, and A. A. Starobinsky. *Inflation scenario via the Standard Model Higgs boson and LHC*. *J. Cosmol. Astropart. Phys.* **0811** (2008) 021. [arXiv:0809.2104].

[205] L.-H. Liu, T. Prokopec, and A. A. Starobinsky. *Inflation in an effective gravitational model and asymptotic safety*. *Phys. Rev. D* **98**.4 (2018) 043505. [arXiv:1806.05407].

[206] T. d. P. Netto, A. M. Pelinson, I. L. Shapiro, and A. A. Starobinsky. *From stable to unstable anomaly-induced inflation*. *Eur. Phys. J. C* **76**.10 (2016) 544. [arXiv:1509.08882].

[207] Planck collaboration. *Planck 2015 results. XIII. Cosmological parameters*. *Astron. Astrophys.* **594** (2016) A13. [arXiv:1502.01589].

[208] Particle Data Group collaboration. *Review of Particle Physics*. *Chin. Phys. C* **40**.10 (2016) 100001.

[209] D. F. Litim. *Optimized renormalization group flows*. *Phys. Rev. D* **64** (2001) 105007. [arXiv:hep-th/0103195].

[210] G. Amelino-Camelia, M. Arzano, G. Gubitosi, and J. Magueijo. *Gravity as the breakdown of conformal invariance*. *Int. J. Mod. Phys. D* **24**.12 (2015) 1543002. [arXiv:1505.04649].

[211] F. Brighenti, G. Gubitosi, and J. Magueijo. *Primordial perturbations in a rainbow universe with running Newton constant*. *Phys. Rev. D* **95**.6 (2017) 063534. [arXiv:1612.06378].

[212] B. Guberina, R. Horvat, and H. Stefancic. *Renormalization group running of the cosmological constant and the fate of the universe*. *Phys. Rev. D* **67** (2003) 083001. [arXiv:hep-ph/0211184].

[213] A. Babic, B. Guberina, R. Horvat, and H. Stefancic. *Renormalization-group running cosmologies. A Scale-setting procedure*. *Phys. Rev. D* **71** (2005) 124041. [arXiv:astro-ph/0407572].

[214] S. Weinberg. *Asymptotically Safe Inflation*. *Phys. Rev. D* **81** (2010) 083535. [arXiv:0911.3165].

[215] M. Reuter and H. Weyer. *Renormalization group improved gravitational actions: A Brans-Dicke approach*. *Phys. Rev. D* **69** (2004) 104022. [arXiv:hep-th/0311196].

[216] Y.-F. Cai, Y.-C. Chang, P. Chen, D. A. Easson, and T. Qiu. *Planck constraints on Higgs modulated reheating of renormalization group improved inflation*. *Phys. Rev. D* **88** (2013) 083508. [arXiv:1304.6938].

[217] G. D'Odorico and F. Saueressig. *Quantum phase transitions in the Belinsky-Khalatnikov-Lifshitz universe*. *Phys. Rev. D* **92**.12 (2015) 124068. [arXiv:1511.00247].

[218] A. Codello and R. K. Jain. *On the covariant formalism of the effective field theory of gravity and its cosmological implications*. *Class. Quant. Grav.* **34**.3 (2017) 035015. [arXiv:1507.07829].

[219] A. Codello and R. K. Jain. *A Unified Universe*. *Eur. Phys. J. C* **78**.5 (2018) 357. [arXiv:1603.00028].

[220] H. Gies and R. Sondenheimer. *Higgs Mass Bounds from Renormalization Flow for a Higgs-top-bottom model*. *Eur. Phys. J. C* **75**.2 (2015) 68. [arXiv:1407.8124].

[221] A. Eichhorn, H. Gies, J. Jaeckel, T. Plehn, M. M. Scherer, and R. Sondenheimer. *The Higgs Mass and the Scale of New Physics*. *Journal of High Energy Physics* **04** (2015) 022. [arXiv:1501.02812].

[222] D. Benedetti and F. Guarnieri. *Brans-Dicke theory in the local potential approximation*. *New J. Phys.* **16** (2014) 053051. [arXiv:1311.1081].

[223] J. Borchardt and B. Knorr. *Solving functional flow equations with pseudo-spectral methods*. *Phys. Rev. D* **94** (2016) 025027. [arXiv:1603.06726].

[224] D. Benedetti. *Critical behavior in spherical and hyperbolic spaces*. *J. Stat. Mech: Theory Exp.* **1501** (2015) P01002. [arXiv:1403.6712].

[225] I. L. Shapiro, P. Morais Teixeira, and A. Wipf. *On the functional renormalization group for the scalar field on curved background with non-minimal interaction*. *Eur. Phys. J. C* **75** (2015) 262. [arXiv:1503.00874].

[226] M. Guilleux and J. Serreau. *Quantum scalar fields in de Sitter space from the nonperturbative renormalization group*. *Phys. Rev. D* **92**.8 (2015) 084010. [arXiv:1506.06183].

[227] S. P. Robinson and F. Wilczek. *Gravitational correction to running of gauge couplings*. *Phys. Rev. Lett.* **96** (2006) 231601. [arXiv:hep-th/0509050].

[228] A. R. Pietrykowski. *Gauge dependence of gravitational correction to running of gauge couplings*. *Phys. Rev. Lett.* **98** (2007) 061801. [arXiv:hep-th/0606208].

[229] D. Ebert, J. Plefka, and A. Rodigast. *Absence of gravitational contributions to the running Yang-Mills coupling*. *Phys. Lett. B* **660** (2008) 579. [arXiv:0710.1002].

[230] D. J. Toms. *Quantum gravity and charge renormalization*. *Phys. Rev. D* **76** (2007) 045015. [arXiv:0708.2990].

[231] H. Gies, R. Sondenheimer, and M. Warschinke. *Impact of generalized Yukawa interactions on the lower Higgs mass bound*. *Eur. Phys. J. C* **77**.11 (2017) 743. [arXiv:1707.04394].

[232] D. F. Litim and F. Sannino. *Asymptotic safety guaranteed*. *J. High Energy Phys.* **12** (2014) 178. [arXiv:1406.2337].

[233] J. K. Esbensen, T. A. Ryttov, and F. Sannino. *Quantum critical behavior of semisimple gauge theories*. *Phys. Rev. D* **93**.4 (2016) 045009. [arXiv:1512.04402].

[234] A. D. Bond and D. F. Litim. *Theorems for Asymptotic Safety of Gauge Theories*. *Eur. Phys. J. C* **77**.6 (2017) 429. Erratum: [284]. [arXiv:1608.00519].

[235] A. D. Bond, G. Hiller, K. Kowalska, and D. F. Litim. *Directions for model building from asymptotic safety*. *J. High Energy Phys.* **08** (2017) 004. [arXiv:1702.01727].

[236] J. F. Donoghue and G. Menezes. *The arrow of causality and quantum gravity*. (2019) [arXiv:1908.04170].

[237] J. F. Donoghue and G. Menezes. *Unitarity, stability and loops of unstable ghosts*. (2019) [arXiv:1908.02416].

[238] T. Biswas and S. Talaganis. *String-Inspired Infinite-Derivative Theories of Gravity: A Brief Overview*. *Mod. Phys. Lett.* **A30**.03n04 (2015) 1540009. [arXiv:1412.4256].

[239] N. Barnaby and N. Kamran. *Dynamics with infinitely many derivatives: The Initial value problem*. *J. High Energy Phys.* **02** (2008) 008. [arXiv:0709.3968].

[240] N. Barnaby and N. Kamran. *Dynamics with Infinitely Many Derivatives: Variable Coefficient Equations*. *J. High Energy Phys.* **12** (2008) 022. [arXiv:0809.4513].

[241] L. Modesto. *Super-renormalizable Quantum Gravity*. *Phys. Rev. D* **86** (2012) 044005. [arXiv:1107.2403].

[242] L. Modesto and L. Rachwal. *Super-renormalizable and finite gravitational theories*. *Nucl. Phys. B* **889** (2014) 228. [arXiv:1407.8036].

[243] S. Giaccari, L. Modesto, L. Rachwa, and Y. Zhu. *Finite Entanglement Entropy of Black Holes*. *Eur. Phys. J. C* **78**.6 (2018) 459. [arXiv:1512.06206].

[244] L. Modesto and L. Rachwa. *Nonlocal quantum gravity: A review*. *Int. J. Mod. Phys. D* **26**.11 (2017) 1730020.

[245] T. Biswas, A. Conroy, A. S. Koshelev, and A. Mazumdar. *Generalized ghost-free quadratic curvature gravity*. *Class. Quant. Grav.* **31** (2014) 015022. Erratum: [285]. [arXiv:1308.2319].

[246] A. Codello. *Polyakov Effective Action from Functional Renormalization Group Equation*. *Ann. Phys.* **325** (2010) 1727. [arXiv:1004.2171].

[247] K. Sravan Kumar, S. Maheshwari, and A. Mazumdar. *Perturbations in higher derivative gravity beyond maximally symmetric spacetimes*. *Phys. Rev.* **D100**.6 (2019) 064022. [arXiv:1905.03227].

[248] J. Borchardt and B. Knorr. *Global solutions of functional fixed point equations via pseudospectral methods*. *Phys. Rev. D* **91**.10 (2015) 105011. Erratum: [286]. [arXiv:1502.07511].

[249] S. Lippoldt. *Spin-base invariance of Fermions in arbitrary dimensions*. *Phys. Rev. D* **91**.10 (2015) 104006. [arXiv:1502.05607].

[250] H. Gies and S. Lippoldt. *Global surpluses of spin-base invariant fermions*. *Phys. Lett. B* **743** (2015) 415. [arXiv:1502.00918].

[251] A. Codello and O. Zanusso. *On the non-local heat kernel expansion*. *J. Math. Phys.* **54** (2013) 013513. [arXiv:1203.2034].

[252] S. Lucat, T. Prokopec, and B. Swiezewska. *Conformal symmetry and the cosmological constant problem*. *Int. J. Mod. Phys.* **D27**.14 (2018) 1847014. [arXiv:1804.00926].

[253] S. Rychkov. *EPFL Lectures on Conformal Field Theory in $D \geq 3$ Dimensions*. SpringerBriefs in Physics. 2016. [arXiv:1601.05000].

[254] D. Simmons-Duffin. *The Conformal Bootstrap*. In: *Proceedings, Theoretical Advanced Study Institute in Elementary Particle Physics: New Frontiers in Fields and Strings (TASI 2015): Boulder, CO, USA, June 1-26, 2015*. 2017, 1. [arXiv:1602.07982].

[255] J. F. Donoghue. *General relativity as an effective field theory: The leading quantum corrections*. *Phys. Rev. D* **50** (1994) 3874. [arXiv:gr-qc/9405057].

[256] A. Akhundov and A. Shiekh. *A Review of Leading Quantum Gravitational Corrections to Newtonian Gravity*. *Electron. J. Theor. Phys.* **5**.17 (2008) 1. [arXiv:gr-qc/0611091].

[257] A. Codello, R. Percacci, L. Rachwal, and A. Tonero. *Computing the Effective Action with the Functional Renormalization Group*. *Eur. Phys. J. C* **76**.4 (2016) 226. [arXiv:1505.03119].

[258] L. Rachwal, A. Codello, and R. Percacci. *One-Loop Effective Action in Quantum Gravitation*. *Springer Proc. Phys.* **170** (2016) 395.

[259] J. F. Donoghue, M. M. Ivanov, and A. Shkerin. *EPFL Lectures on General Relativity as a Quantum Field Theory*. (2017) [arXiv:1702.00319].

[260] A. S. Wightman. *Quantum Field Theory in Terms of Vacuum Expectation Values*. *Phys. Rev.* **101** (1956) 860.

[261] K. Osterwalder and R. Schrader. *Axioms for Euclidean Green's functions*. *Commun. Math. Phys.* **31** (1973) 83.

[262] K. Osterwalder and R. Schrader. *Axioms for Euclidean Green's Functions. 2*. *Commun. Math. Phys.* **42** (1975) 281.

[263] J. Glimm and A. M. Jaffe. *Quantum Physics. A Functional Integral Point of View*. New York: Springer, 1987.

[264] A. Jaffe and G. Ritter. *Reflection Positivity and Monotonicity*. *J. Math. Phys.* **49** (2008) 052301. [arXiv:0705.0712].

[265] R. Trinchero. *Examples of reflection positive field theories*. *Int. J. Geom. Methods Mod. Phys.* **15**.02 (2017) 1850022. [arXiv:1703.07735].

[266] V. A. Zorich. *Mathematical Analysis I*. Springer, 2015.

[267] G. Grubb. *Distributions and Operators*. Springer, 2009.

[268] R. S. Strichartz. *A Guide to Distribution Theory and Fourier Transforms*. World Scientific Publishing Company, 2003.

[269] J. Glimm and A. M. Jaffe. *A note on reflection positivity*. *Lett. Math. Phys.* **3** (1979) 377.

[270] A. Jaffe and G. Ritter. *Quantum field theory on curved backgrounds. I. The Euclidean functional integral*. *Commun. Math. Phys.* **270** (2007) 545. [arXiv:hep-th/0609003].

[271] A. Jaffe and G. Ritter. *Quantum field theory on curved backgrounds. II. Spacetime symmetries*. (2007) [arXiv:0704.0052].

[272] A. H. Chamseddine, A. Connes, and M. Marcolli. *Gravity and the standard model with neutrino mixing*. *Adv. Theor. Math. Phys.* **11**.6 (2007) 991. [arXiv:hep-th/0610241].

[273] B. Iochum, C. Levy, and D. Vassilevich. *Spectral action beyond the weak-field approximation*. *Commun. Math. Phys.* **316** (2012) 595. [arXiv:1108.3749].

[274] W. D. van Suijlekom. *Renormalization of the asymptotically expanded Yang-Mills spectral action*. *Commun. Math. Phys.* **312** (2012) 883. [arXiv:1104.5199].

[275] C. M. Bender and P. D. Mannheim. *No-ghost theorem for the fourth-order derivative Pais-Uhlenbeck oscillator model*. *Phys. Rev. Lett.* **100** (2008) 110402. [arXiv:0706.0207].

[276] M. Niedermaier. *A quantum cure for the Ostrogradski instability*. *Ann. Phys.* **327**.2 (2012) 329.

[277] A. S. Koshelev, K. Sravan Kumar, and A. A. Starobinsky. *R^2 inflation to probe non-perturbative quantum gravity*. *JHEP* **03** (2018) 071. [arXiv:1711.08864].

[278] T. Chiba. *1/R gravity and scalar-tensor gravity*. *Phys. Lett. B* **575** (2003) 1. [arXiv:astro-ph/0307338].

[279] R. Ooijer. *A complete cosmic history from Asymptotic Safety*. MA thesis. Nijmegen: Radboud University, 2018.

[280] D. F. Litim. *Optimization of the exact renormalization group*. *Phys. Lett. B* **486** (2000) 92. [arXiv:hep-th/0005245].

[281] J. F. Donoghue and B. K. El-Menoufi. *Covariant non-local action for massless QED and the curvature expansion*. *J. High Energy Phys.* **10** (2015) 044. [arXiv:1507.06321].

[282] D. Benedetti and F. Caravelli. *Erratum: The local potential approximation in quantum gravity*. *J. High Energy Phys.* **2012**.10 (2012) 157.

[283] P. Donà, A. Eichhorn, P. Labus, and R. Percacci. *Erratum: Asymptotic safety in an interacting system of gravity and scalar matter*. *Phys. Rev. D* **93**.12 (2016) 129904.

[284] A. D. Bond and D. F. Litim. *Erratum to: Theorems for asymptotic safety of gauge theories*. *Eur. Phys. J. C* **77**.8 (2017) 525.

[285] T. Biswas, A. Conroy, A. S. Koshelev, and A. Mazumdar. *Corrigendum: Generalized ghost-free quadratic curvature gravity (2014 Class. Quantum Grav. 31 015022)*. *Classical Quantum Gravity* **31**.15 (2014) 159501.

[286] J. Borchardt and B. Knorr. *Erratum: Global solutions of functional fixed point equations via pseudospectral methods [Phys. Rev. D 91, 105011 (2015)]*. *Phys. Rev. D* **93**.8 (2016) 089904.

ACKNOWLEDGEMENTS

This thesis is the result of four years of PhD research. And it has been some four years! I would never have guessed how many blood, sweat, tears and Mathematica-kernels there would be in the book that you have just finished.

This thesis could not have been written without the help of several fantastic people. I have had the privilege to collaborate with them, to have deep scientific discussions in front of the blackboard, or just to have a cup of coffee in front of the much-loved watering hole in front of the office. Either way, all these people have been essential in creating this thesis and I hereby would like to thank them.

First and foremost, I am deeply grateful to my copromotor Frank Saueressig. Only with an infinite-dimensional parameter space I can describe how much I have learnt from Frank. Both on scientific and on a personal level, Frank has been a fixed point for me as a starting researcher. Whatever singularity in formulas, equations, RG flows, PhD planning or future career paths showed up, you had the right strategy ready to smoothen it out. Frank, thank you for being an inspiration to continue in the academic world.

Secondly, I would like to thank my promotor Renate Loll, under whose supervision on the organizational side of this PhD, this thesis has come to a successful end. I would also like to thank Renate for the Friday Quantum Gravity Seminar, which has given me a glimpse of the huge landscape of Quantum Gravity theories.

Thirdly, this is the place to thank my other collaborators, who have given me a diverse view of Asymptotic Safety, Quantum Gravity and theoretical physics in general. Thank you Daniel Becker for showing me the ropes in the world of functional RG. Already on the first day of my PhD it was clear that you are an amazing teacher, giving me the best start I could have hoped for. Also many thanks to Francesca Arici and Walter van Suijlekom, who taught me a lot about mathematical rigor in choosing the right functional spaces. Another thank you goes to Tom Draper, who was always ready for another challenge during his bachelor internship. Thank you also Giulia Gubitosi and Robin Ooijer, who have shown me the wealth of information to be found in the CMB, the vast literature on cosmological models and for patiently integrating out orders of magnitude along an RG flow. And finally I would like to express my deepest gratidude towards Benjamin Knorr for showing me what's calculable in the RG universe and for all the crazy discussions

about anything and everything at our usual hangout-spot.

All this scientific work could not have been done without a solid social structure present at the High Energy Physics department. Centered around the coffee machine, the lunch table or elsewhere, several people have made PhD life for me a great time: thank you very much Jian, Amir, Marcus, Alicia, Luis, Joren, Nilas, Giulio, Jan, Timothy, Lisa, Jimmy, Jeff, Luca, Reiko, Merce, Sean, Fleur, Arthur, Jesse, Lando, Wim, Marrit, Bob, David, Berend, Renz, Nadia, Clara, Jeremy, Lieke, Charles, Cristina, Anamika, Rob, Sascha, Jeroen, Ronald, Annelies, Gemma, Marjo and Gertie and everybody else at the HEP department for drinking a cup of coffee with me, having a chat in the kitchen, and all the other nice moments we had together.

A special thanks goes to Natália Alkofer and Melissa van Beekveld, for being the best neighbors I could wish for, both in the office as well as at home.

Furthermore, I would like to thank Abel, Jordy, Veronica and PROBE for the work that we did together for the well-being of PhDs. You guys have shown me that doing a PhD is more than just about doing research.

Also outside the HEP department and the university, uncountably many people been of invaluable support: dank je wel Daan, Laura, Stijn, Tobias, Ragnar, Anton, Sandra en voor de Eten Bijs, Aftertentamenstapfilmavonden en andere avonturen, Wouter, Freek en Bram voor de onvergetelijke USA-roadtrip, de Nimma Boys & Girls Erik, Stan, Nicole, Jan-Willem, Remco, Sophie, Tijl, Jorn, Roel, Ben, Tim en Maarten voor de weekeindjes weg, de avonden uit en de laatste opmerkelijke nieuwtjes, en de Bosschenaren Tijn, Rosa, Rosalie, Vesko, Boris, Coen, Imre en Iris voor al die jaren dat we elkaar nu al kennen en die nog gaan komen. Verder wil ik graag Kees, Jeanine, Jan-Willem, Matthijs en Floor bedanken voor het warme welkom in jullie familie.

Ten slotte een dank je wel uit het diepste van mijn hart aan mijn familie voor de onvoorwaardelijke steun tijdens, voor en na deze promotieperiode. Dank je wel pap en mam, Renée en Bart, en Lise en Jos. Jullie staan altijd voor mij klaar en zonder jullie had ik dit niet gekund.

De allerlaatste regels van dit proefschrift zijn voor jou, Agnieke. Je bent mijn steun en toeverlaat en ik hou van je. Jij bent het mooiste dat ik uit mijn promotietraject mee naar de toekomst mag nemen. Jij bent de grootste ontdekking van deze promotie.

CR, March 2020

CURRICULUM VITAE

Chris Ripken was born on March 31st, 1993 in Drunen, the Netherlands. After attending the Stedelijk Gymnasium in 's-Hertogenbosch, he started studying Physics and Astronomy at the Radboud Universiteit Nijmegen in 2010. In 2015, he there obtained his master's degree cum laude in Physics and Astronomy. His master's thesis was entitled "Curvature on the noncommutative tangent bundle," written under the supervision of prof. dr. R. Kleiss and prof. dr. W. Beenakker. In addition, he obtained a bachelor's degree in Mathematics (cum laude) and took part in the Radboud Honours Academy.

Between 2015 and 2019, Chris was a PhD candidate under the supervision of dr. F. Saueressig and prof. dr. R. Loll at Radboud University. During this period, Chris has studied various aspects of asymptotically safe quantum gravity. The results of this work are presented in this thesis.

During his PhD, Chris has been the PhD representative in the board of the Institute of Mathematics, Astrophysics and Particle Physics (IMAPP), as well as the IMAPP representative in PROBE, the PhD council for the Faculty of Science. He also taught several tutorial classes, for which he received honorable mentions of the Education Programme Committee (OLC) of Physics and Astronomy.

Starting from 2020, Chris Ripken is a researcher at the Johannes Gutenberg-Universität in Mainz.